AD-A085 479 ROYAL AIRCRAFT ESTABLISHMENT FARNBOROUGH (ENGLAND) F/G 17/7
CONTRIBUTIONS TO THE UK MICROWAVE LANDING SYSTEM RESEARCH AND D--ETC(U)
MAY 79 J M JONES
UNCLASSIFIED RAE-TR-79052-VOL-2 DRIC-BR-73762 NL

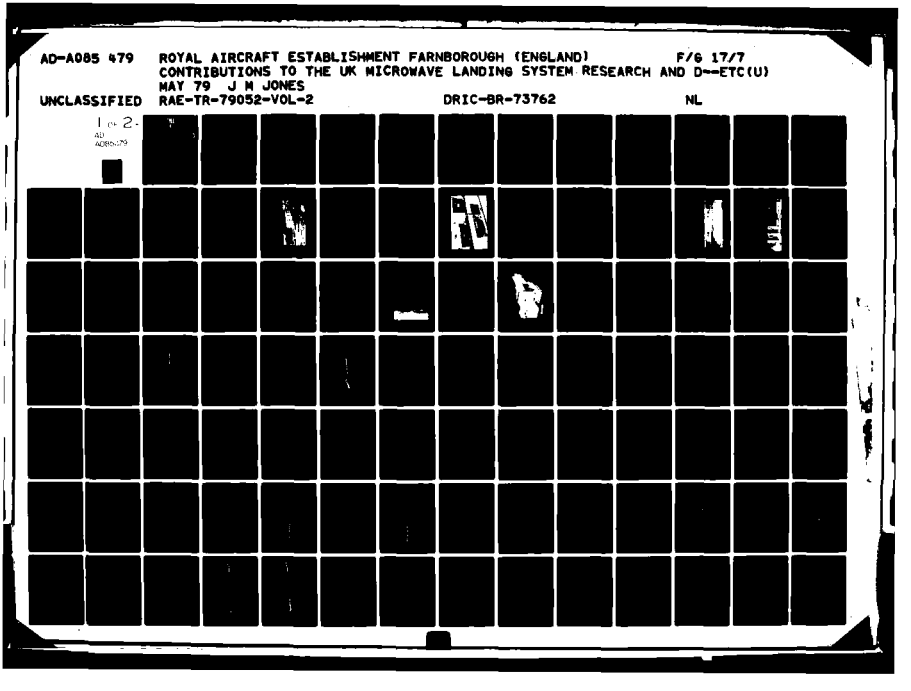

LEVEL II

ROYAL AIRCRAFT ESTABLISHMENT

*

(9) Technical Report 79052

(11) May 1979

(6) # CONTRIBUTIONS TO THE UK MICROWAVE LANDING SYSTEM RESEARCH AND DEVELOPMENT PROGRAMME 1974 TO 1978.

Volume 2.

by

(12) 68

(10) J.M. Jones

(18) DRIC

(19) BR-73762

VOLUME 2

*

(14) RAE-TR-79052-Vol-2

Procurement Executive, Ministry of Defence
Farnborough, Hants

JOB

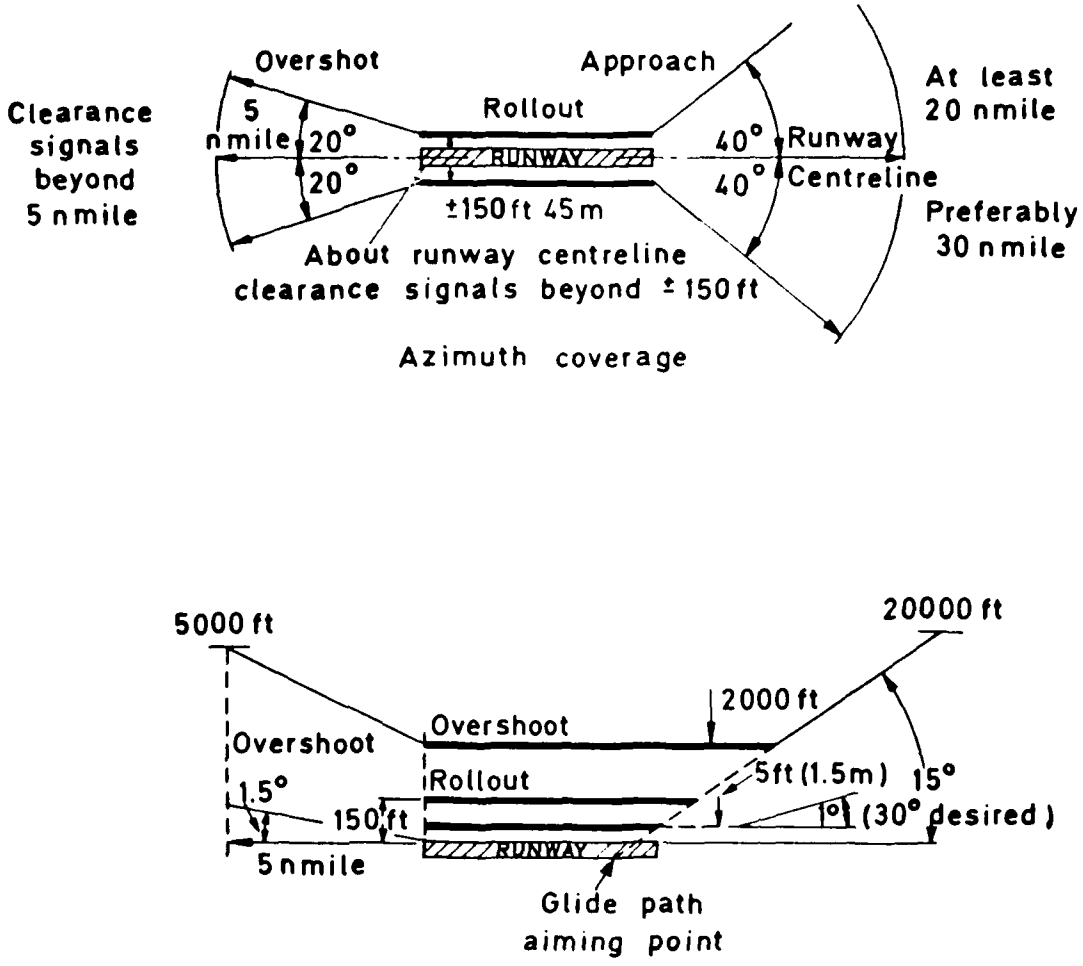

TR 79052

Fig 1.1 Coverage requirements for MLS

Fig 2.1

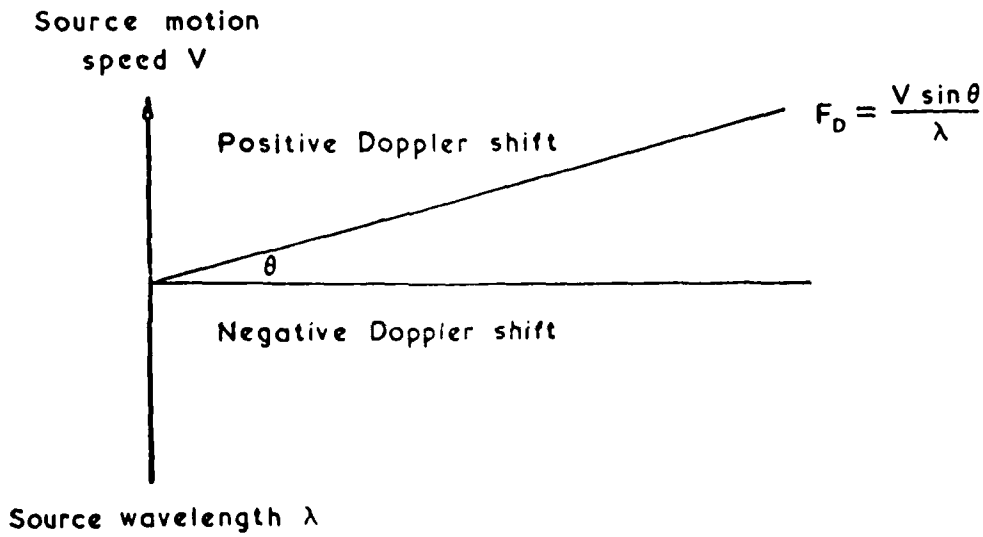

Fig 2.1 Doppler effect

TR 79052

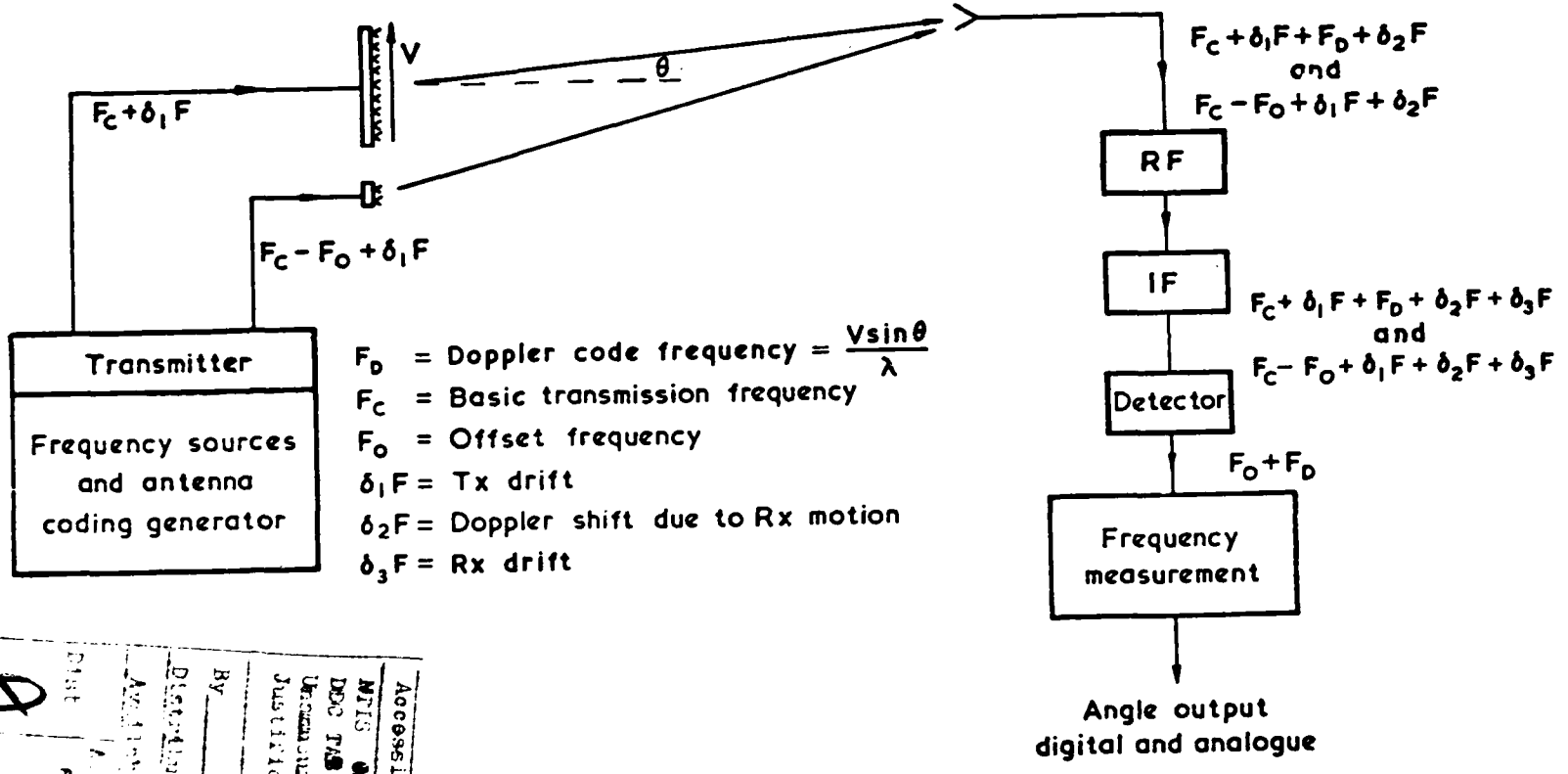

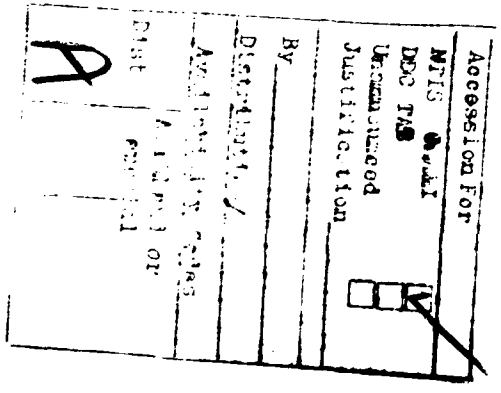

Fig 2.2 Basic system — block diagram

Fig 2.2

Fig 2.3

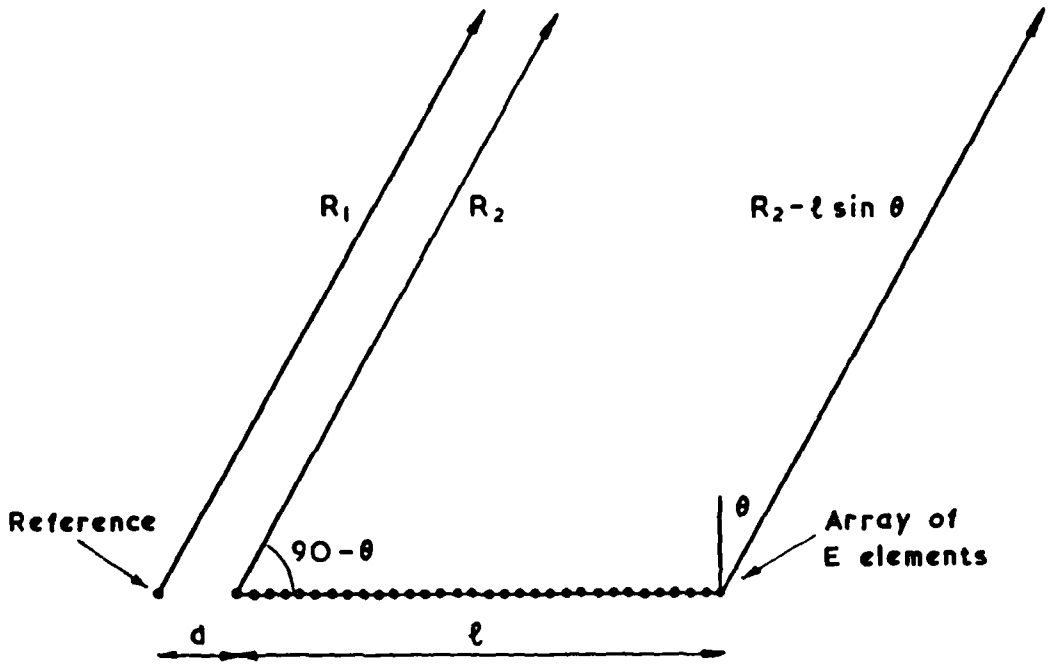

$d = D\lambda \quad \ell = L\lambda$

Reference transmission $\exp j\omega_R t$

Array signal 'left to right' $\exp j(\omega_{A_1} t + \alpha)$

Array signal 'right to left' $\exp j(\omega_{A_2} t + \beta)$

Fig 2.3 Propagation geometry

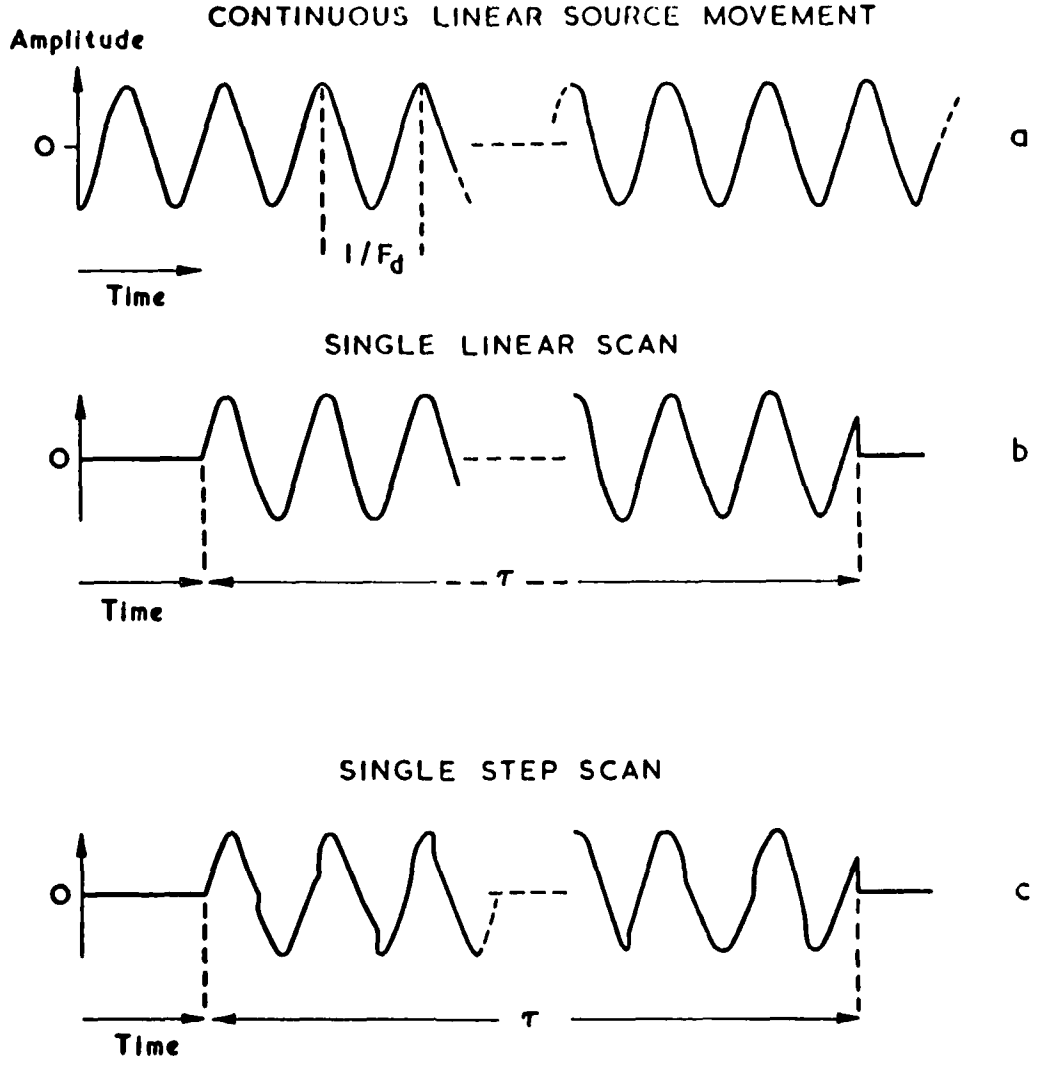

TR 79052

Fig 2.4 Doppler signal waveforms

Fig 2.5

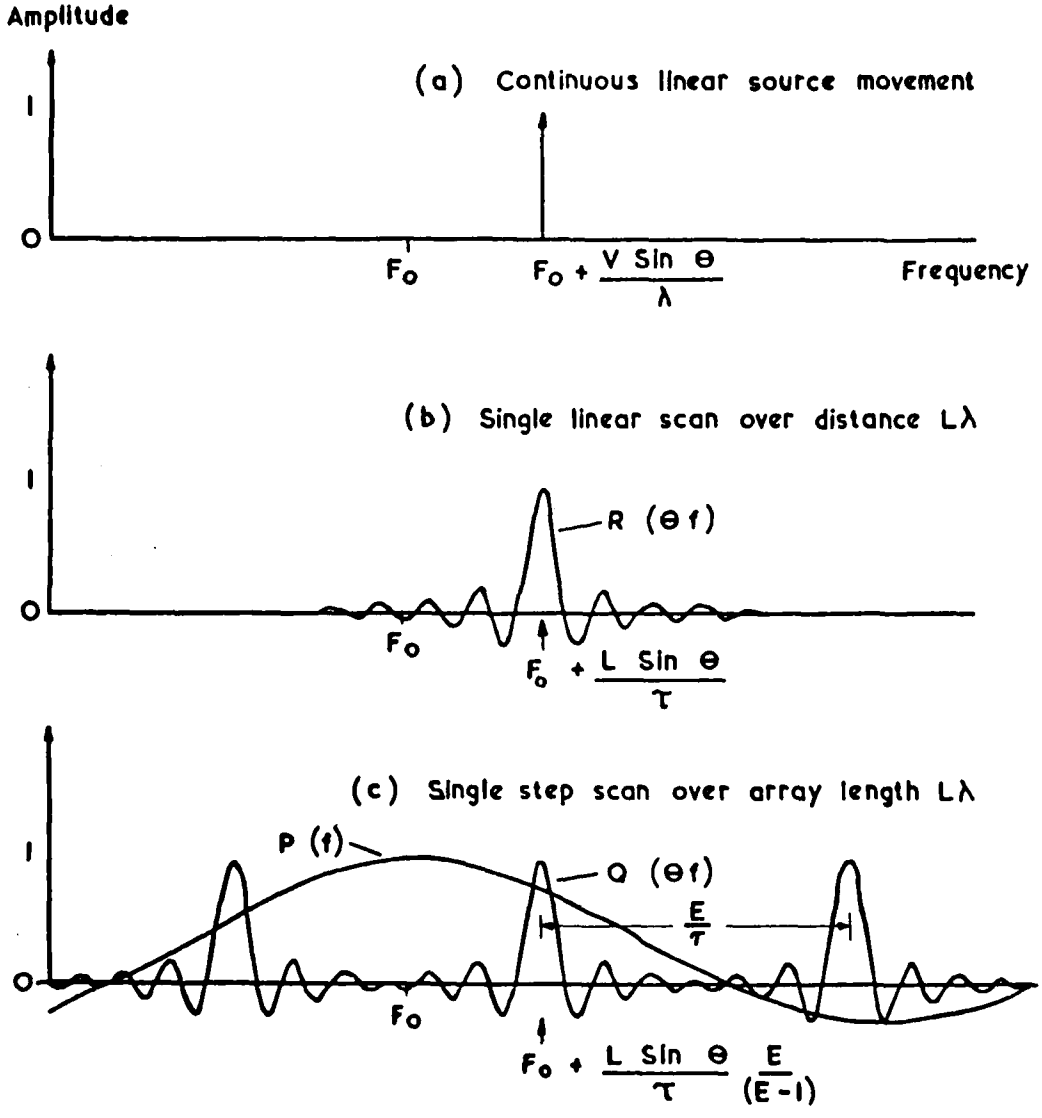

TR 79052

Fig 2.5 Doppler signal spectra

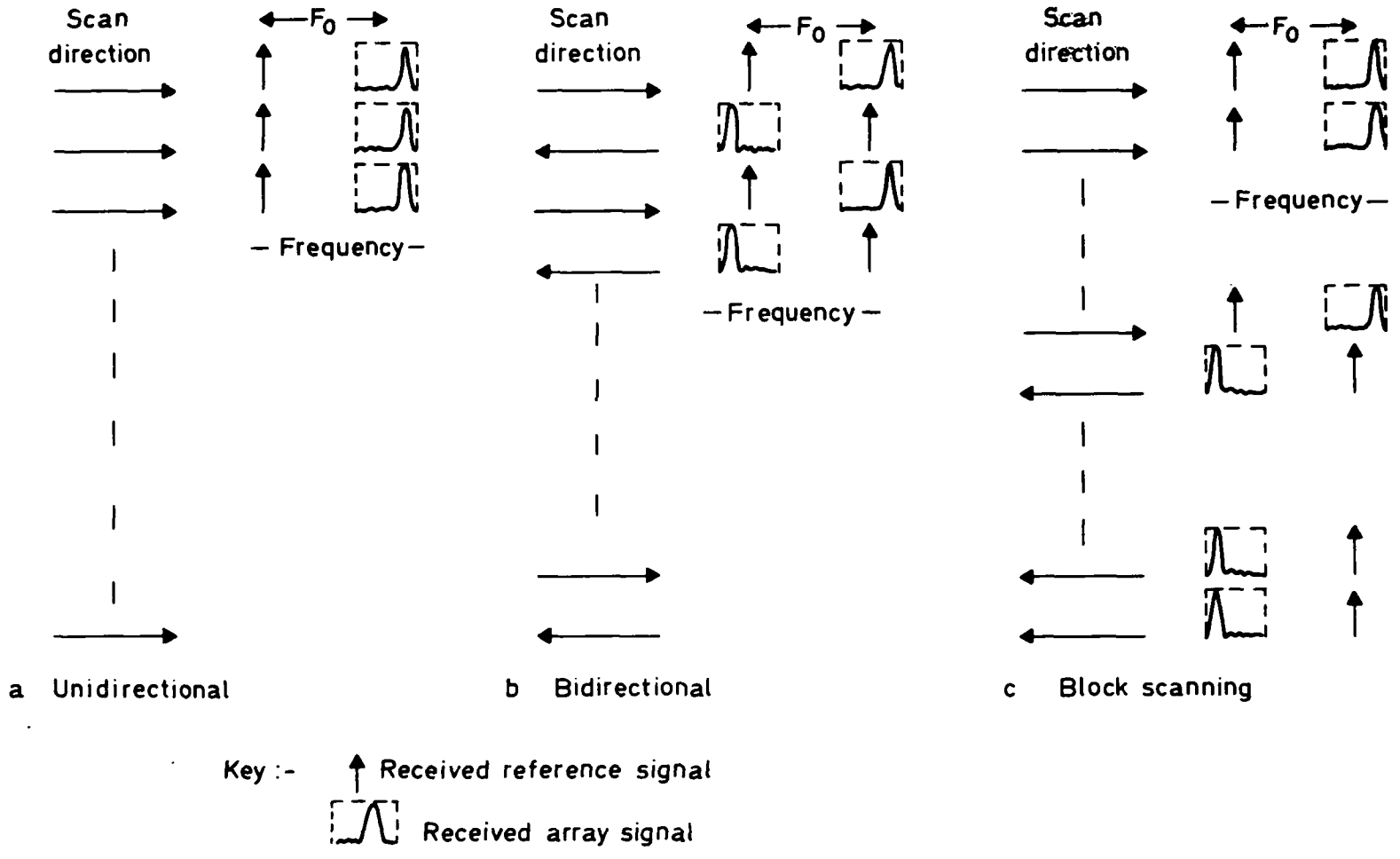

Fig 2.6 Typical angle transmission formats

Fig 2.6

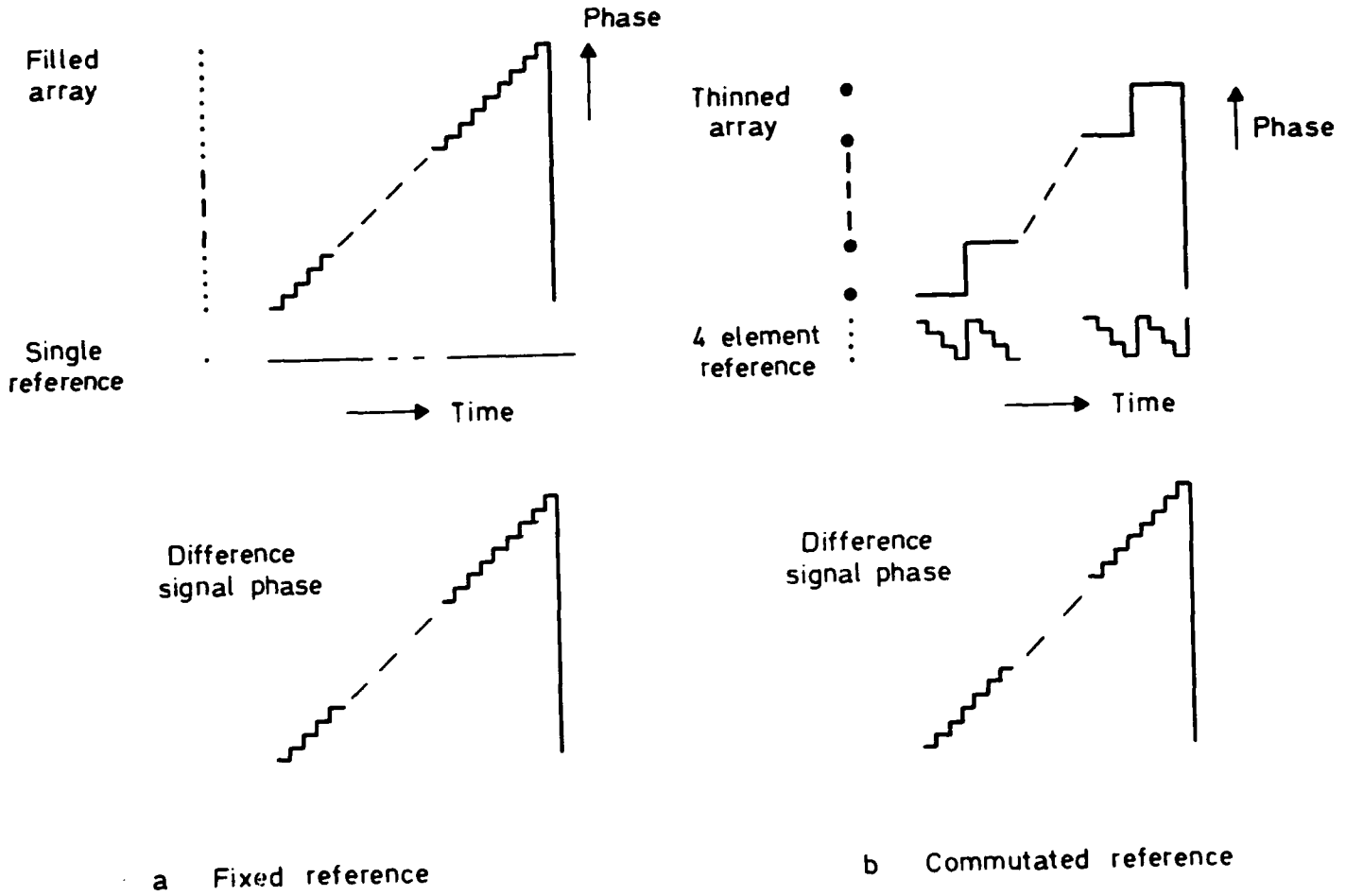

Fig 2.7 Fixed and commutated reference systems

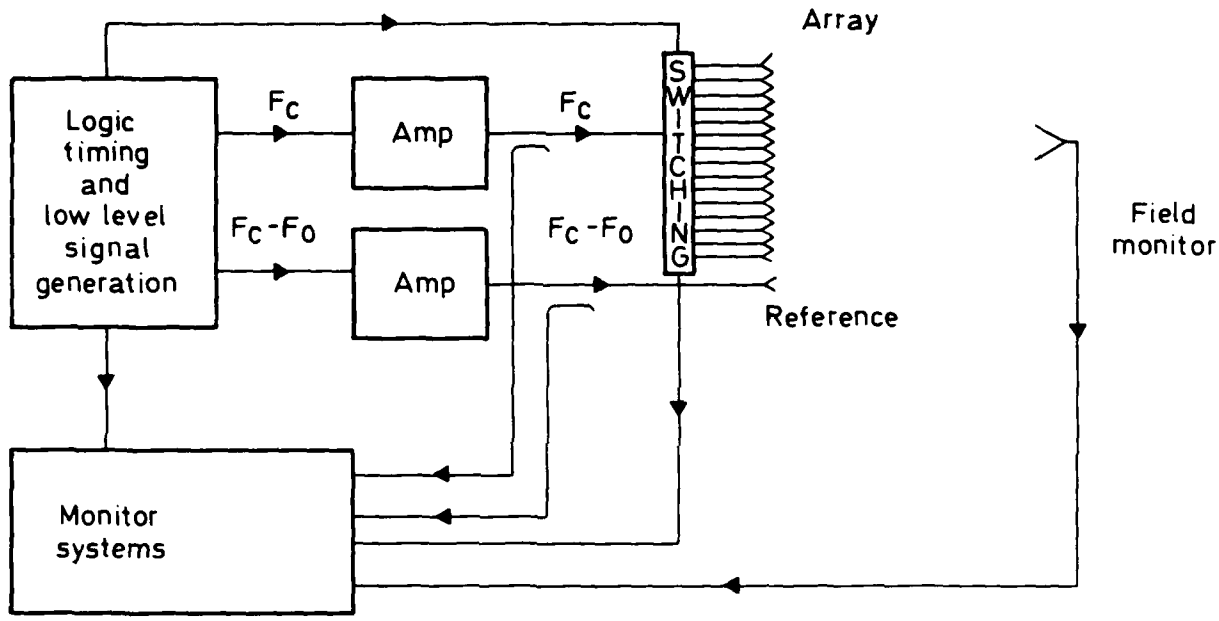

TR 79052

Fig 2.8 The basic DMLS ground system

Fig 2.9a&b

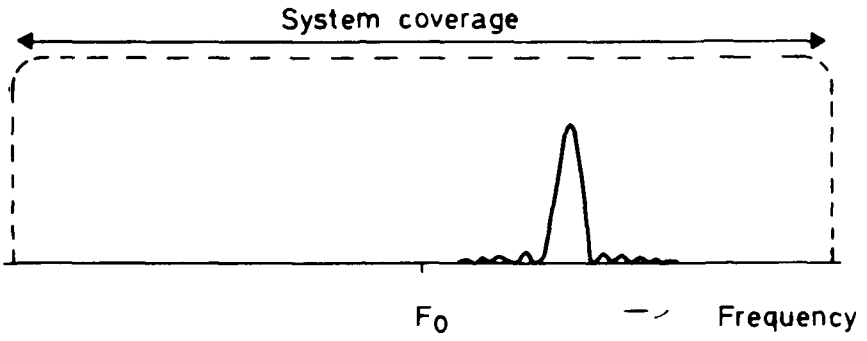

2.9a Azimuth system

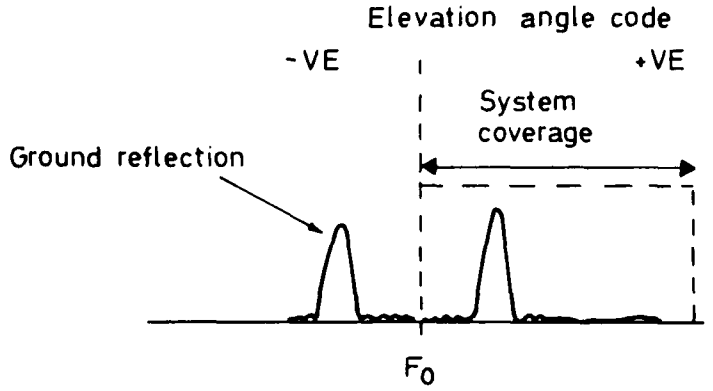

2.9b Elevation system

TR 79052

Fig 2.9a&b Received difference signal spectra

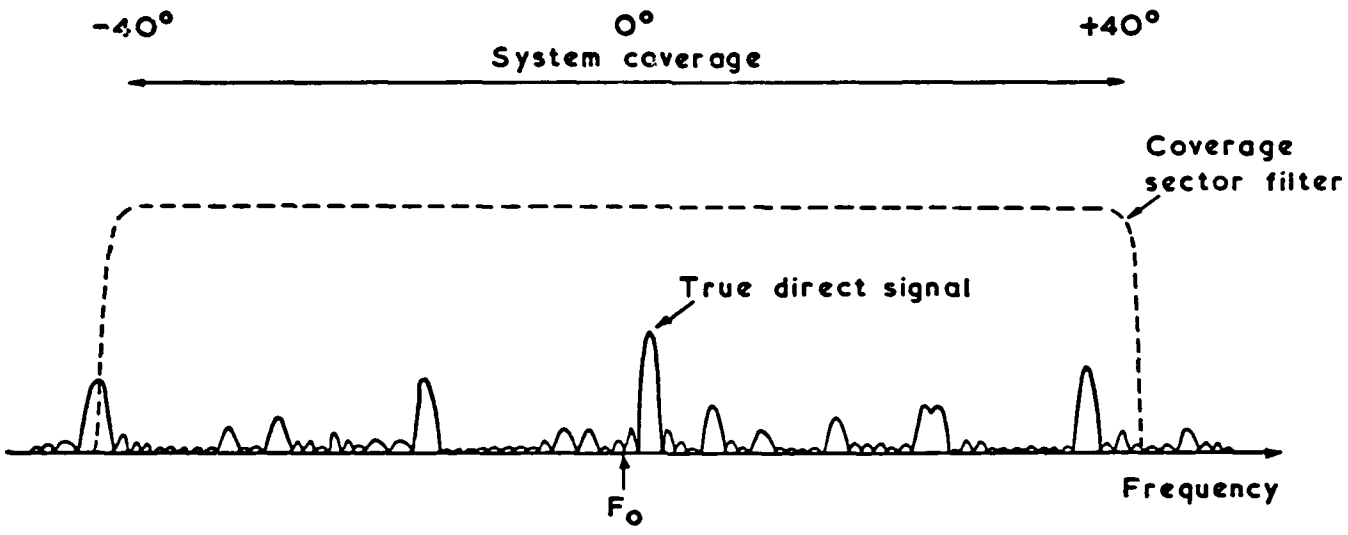

Fig 2.10 Doppler signal with multipath

Fig 2.10

Fig 2.11

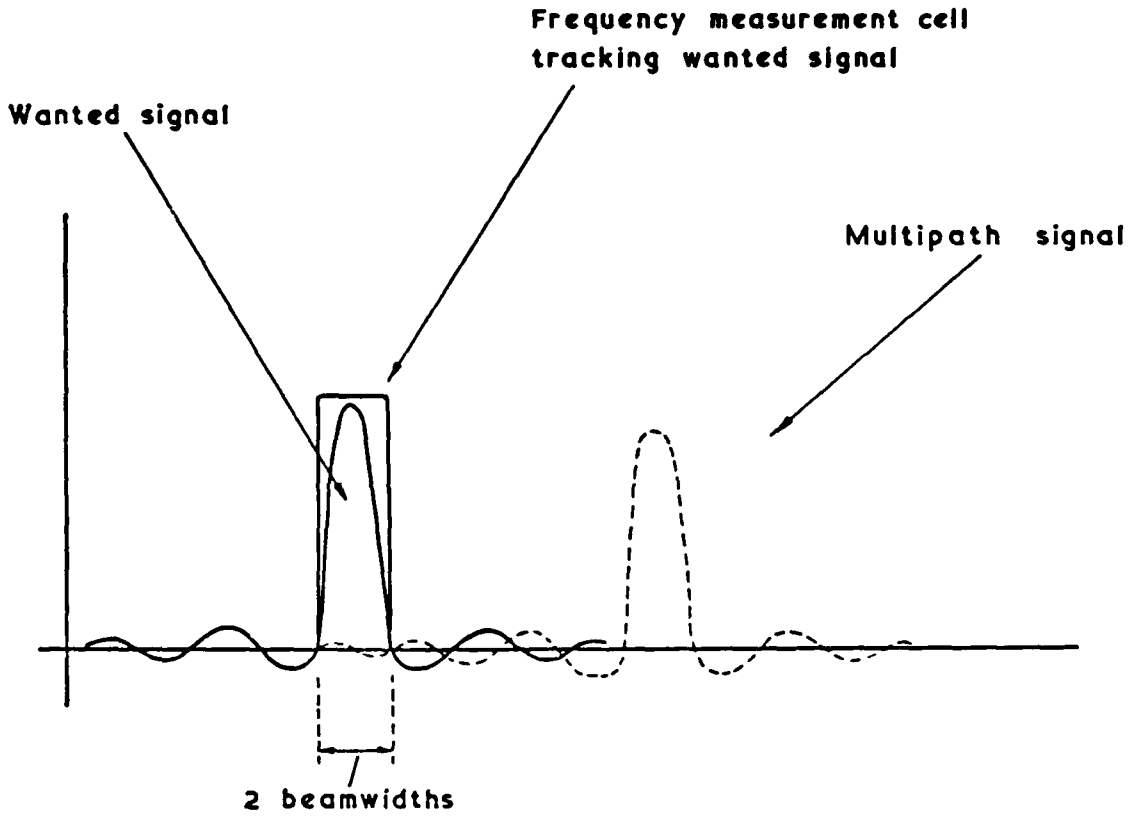

Fig 2.11 Separation of wanted signal using frequency cell

TR 79052

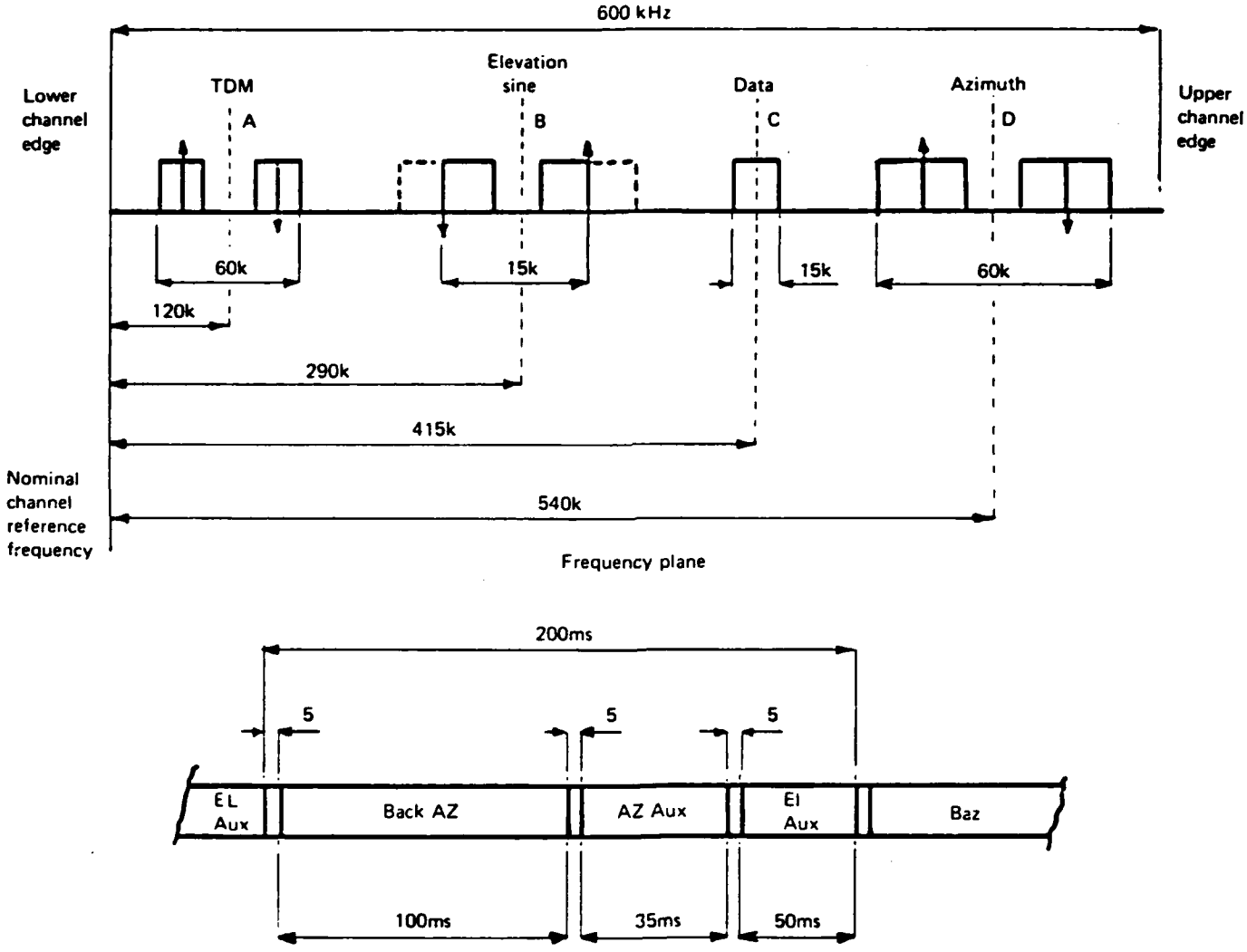

Fig 3.1 Hybrid format

Fig 3.1

Fig 3.2

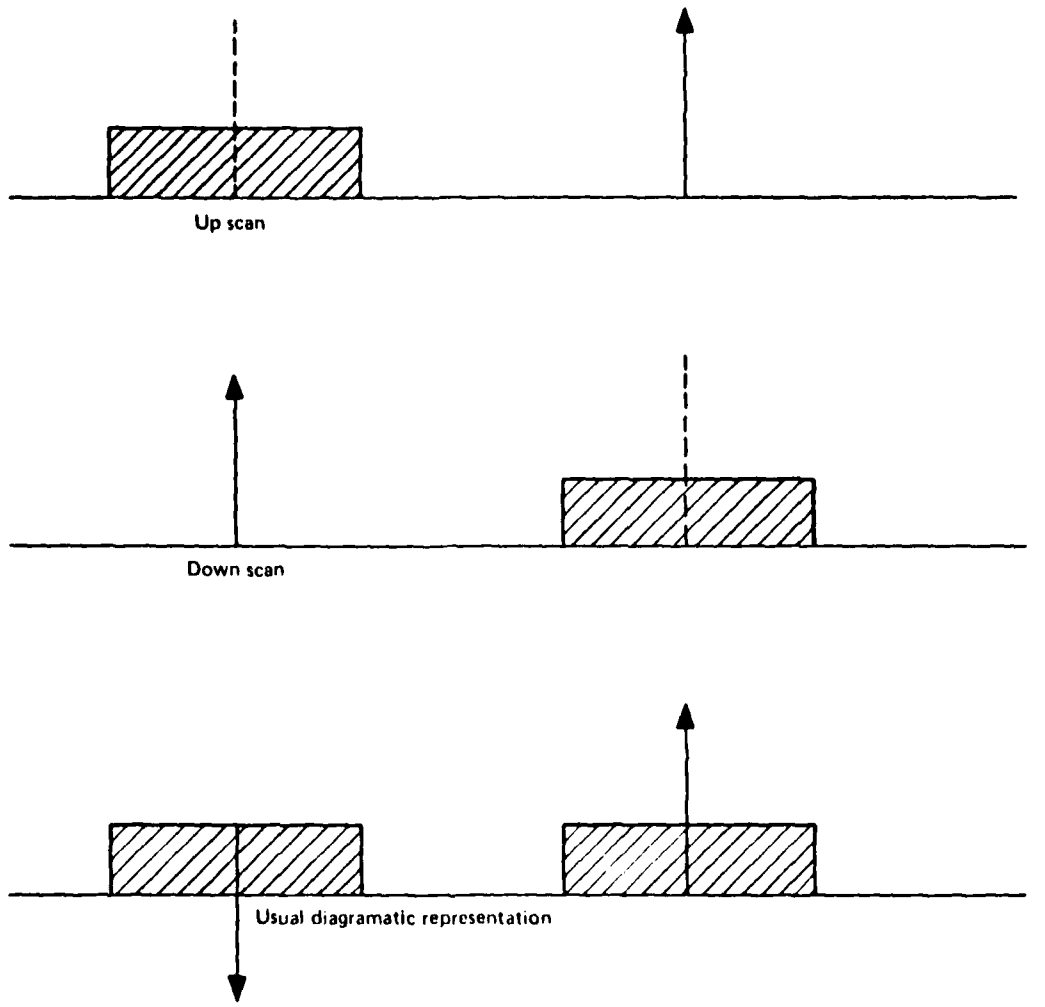

Key:

Frequency band occupied by all possible received commutated frequencies.

Commutated array feed frequency

Reference frequency

TR 79052

Fig 3.2 Frequency interchange method of providing offset frequency

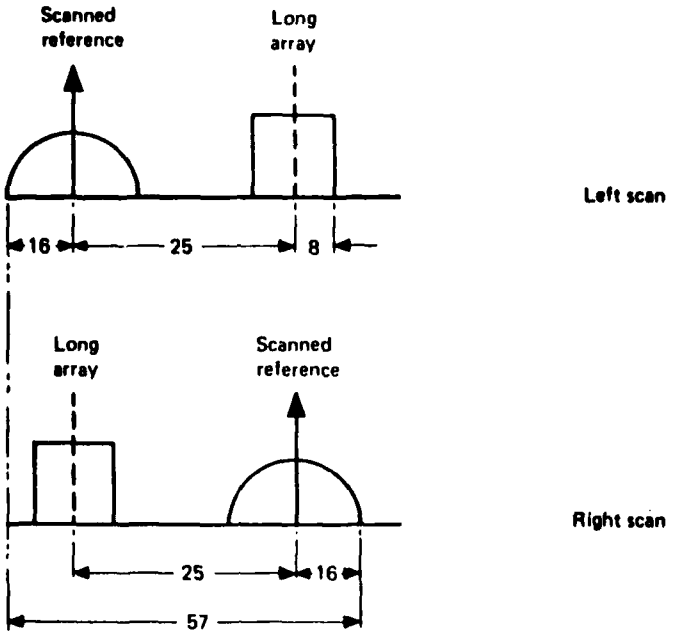

Fig 3.3 Azimuth sub-channel frequencies (kHz)

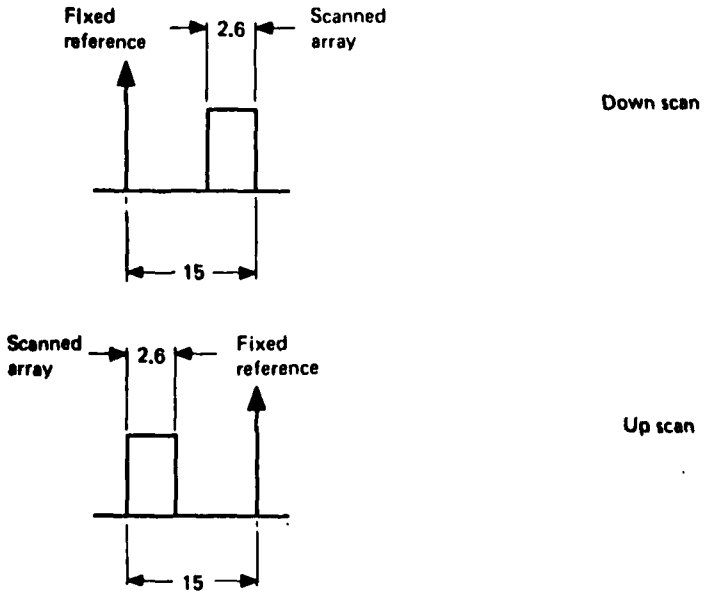

Fig 3.4 Elevation sub-channel frequencies (kHz)

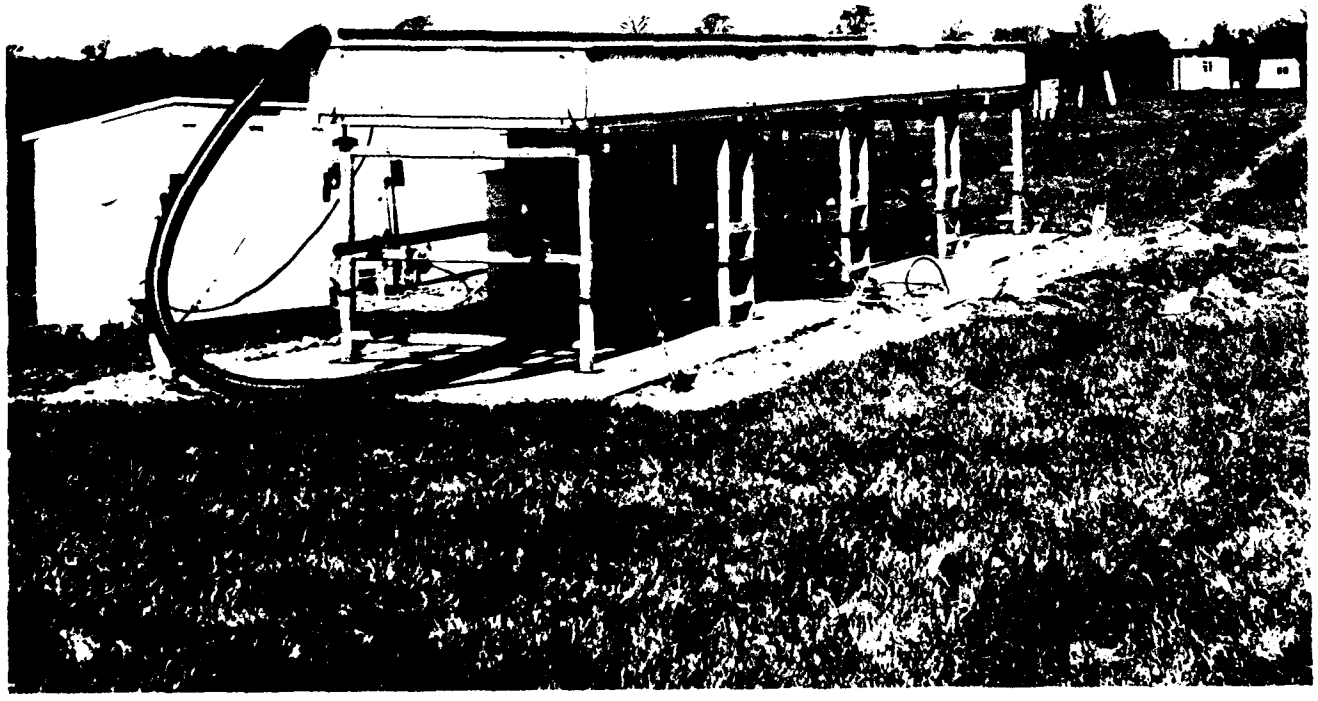

Fig 3.5 120 wavelength azimuth antenna

Fig 3.6

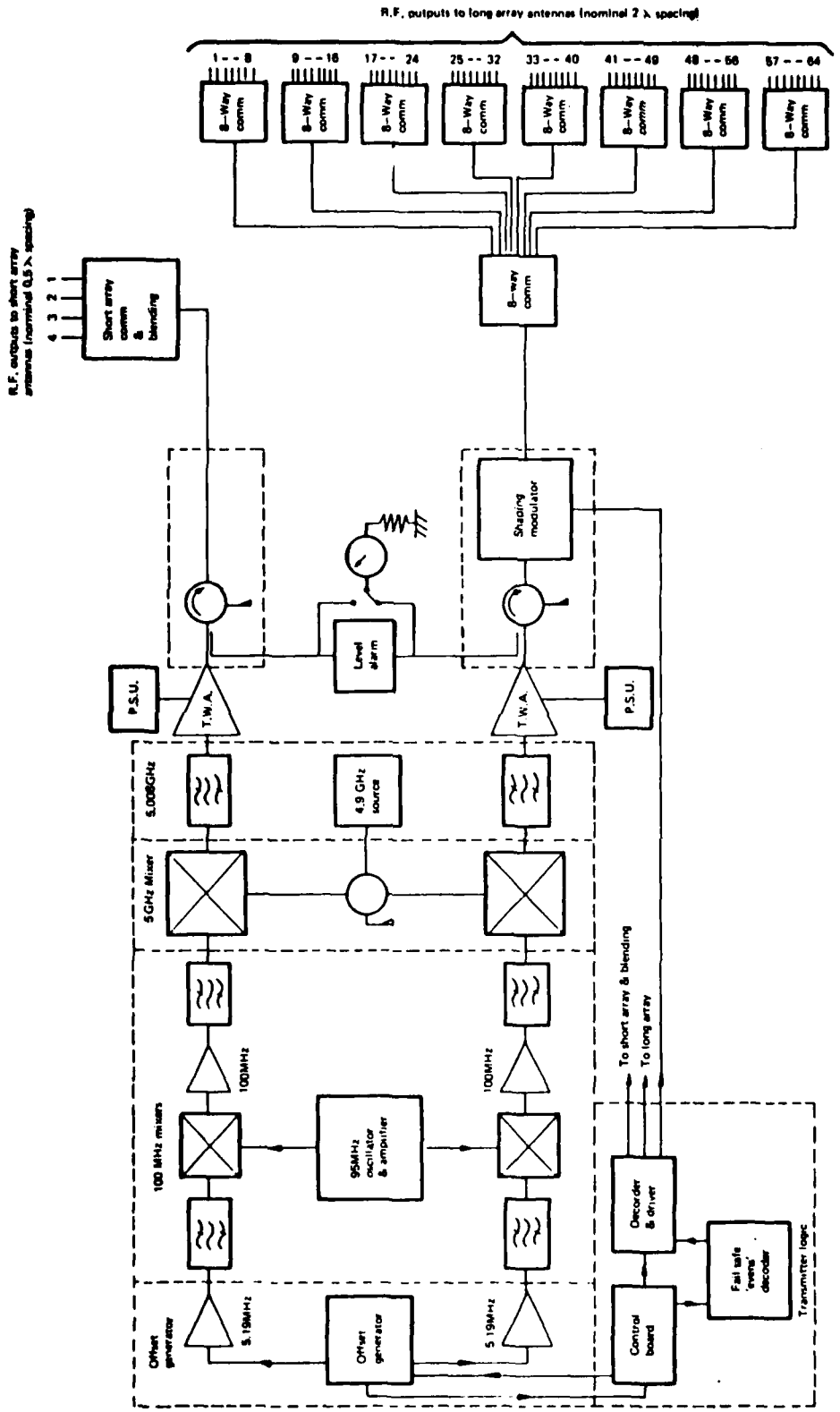

Fig 3.6 Azimuth transmitter block diagram

TR 79052

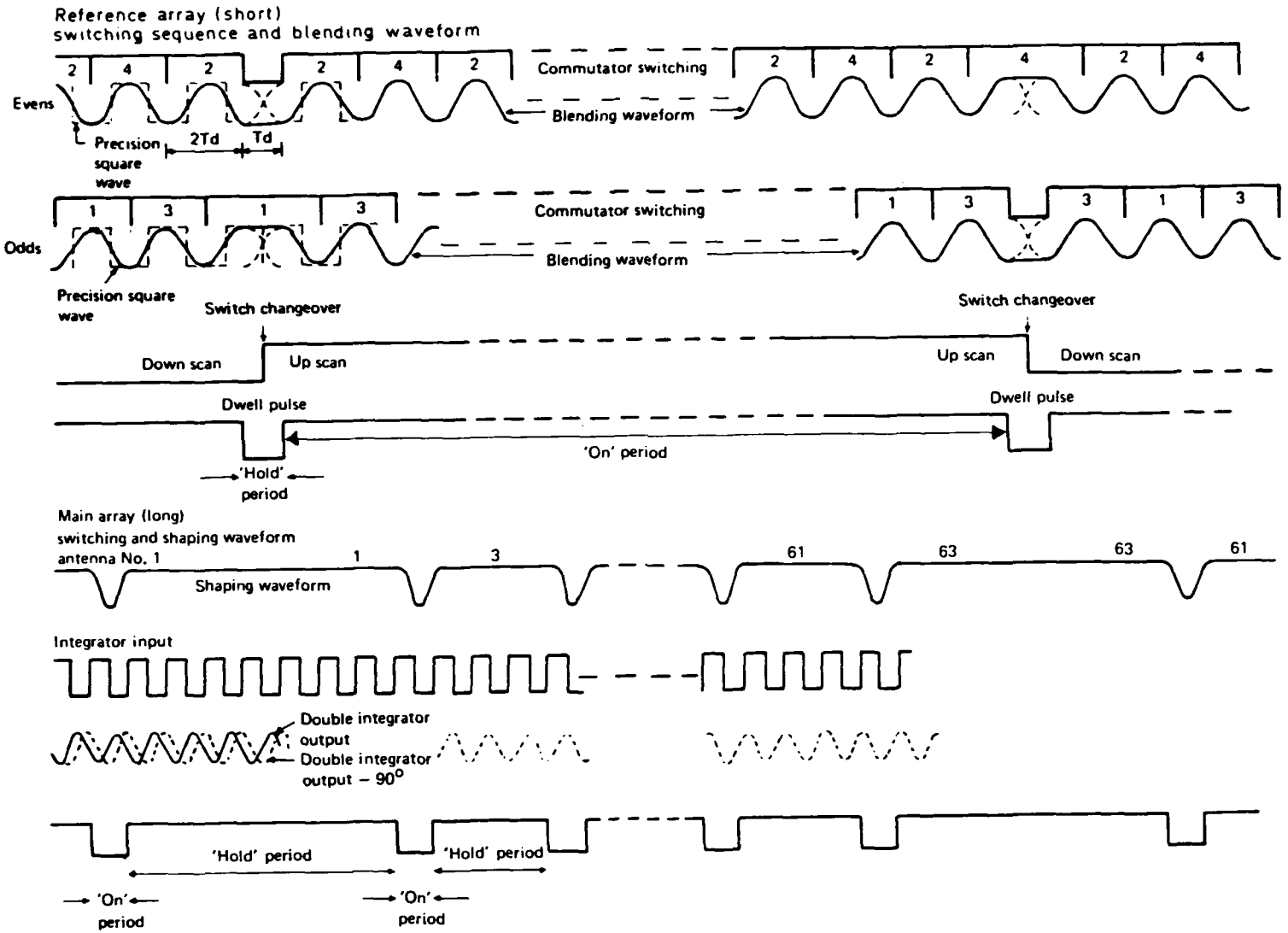

Fig 3.7 Azimuth facilities blending and shaping

Fig 3.7

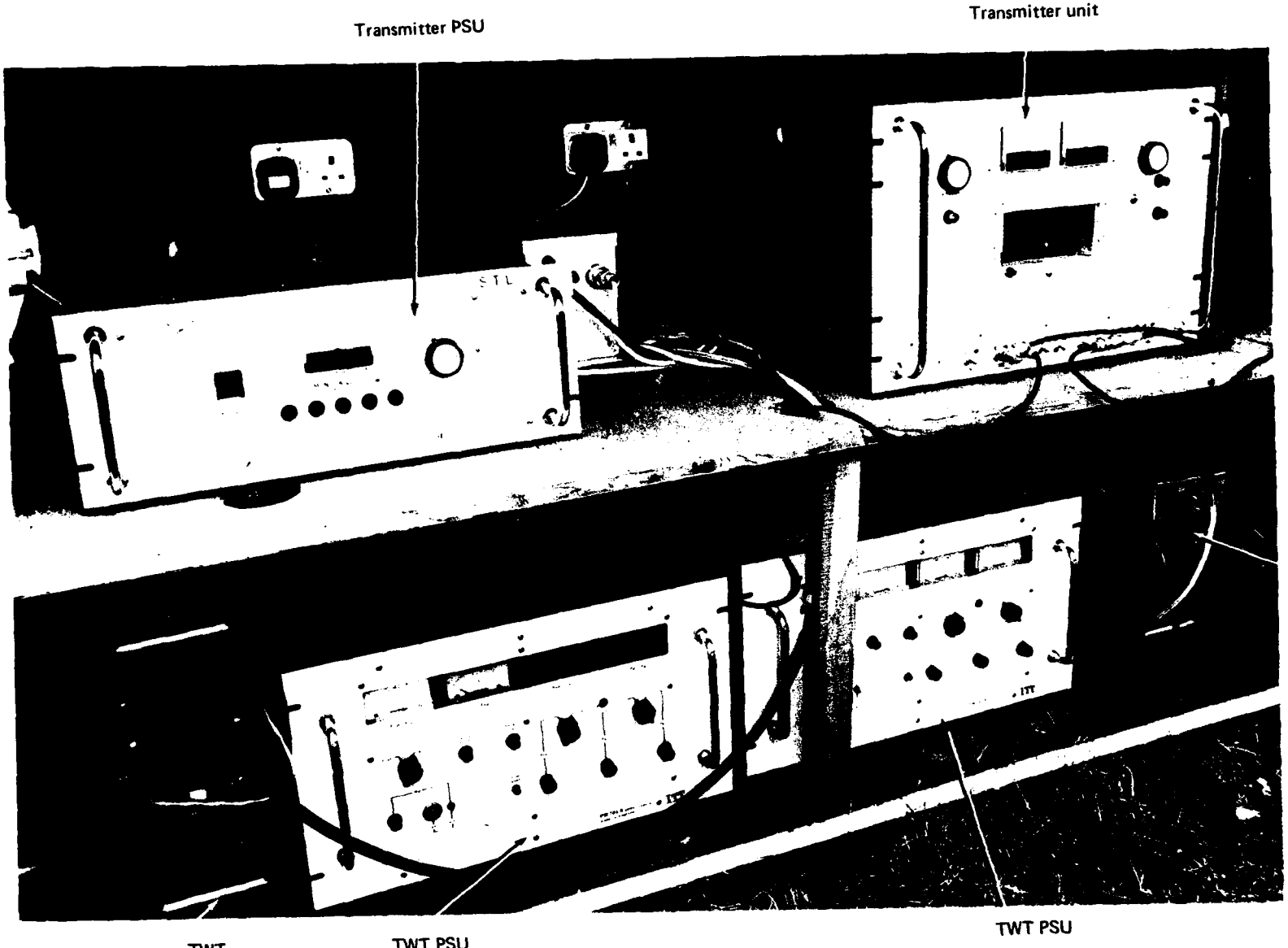

Fig 3.8 Azimuth transmitter

Fig 3.8

Fig 3.9

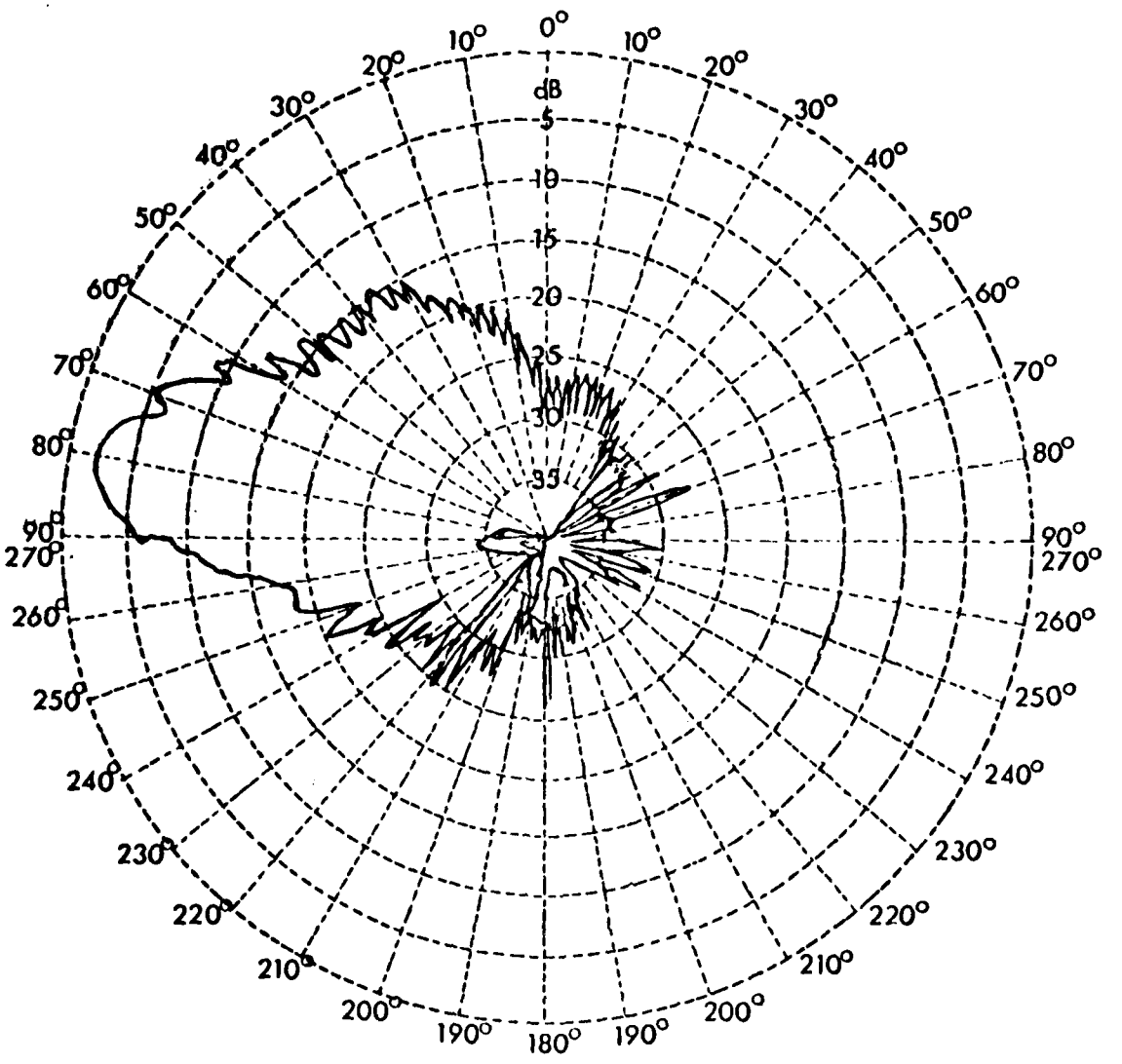

TR 79052

Fig 3.9 Monopole on 3 ft counterpoise (vertical pattern)

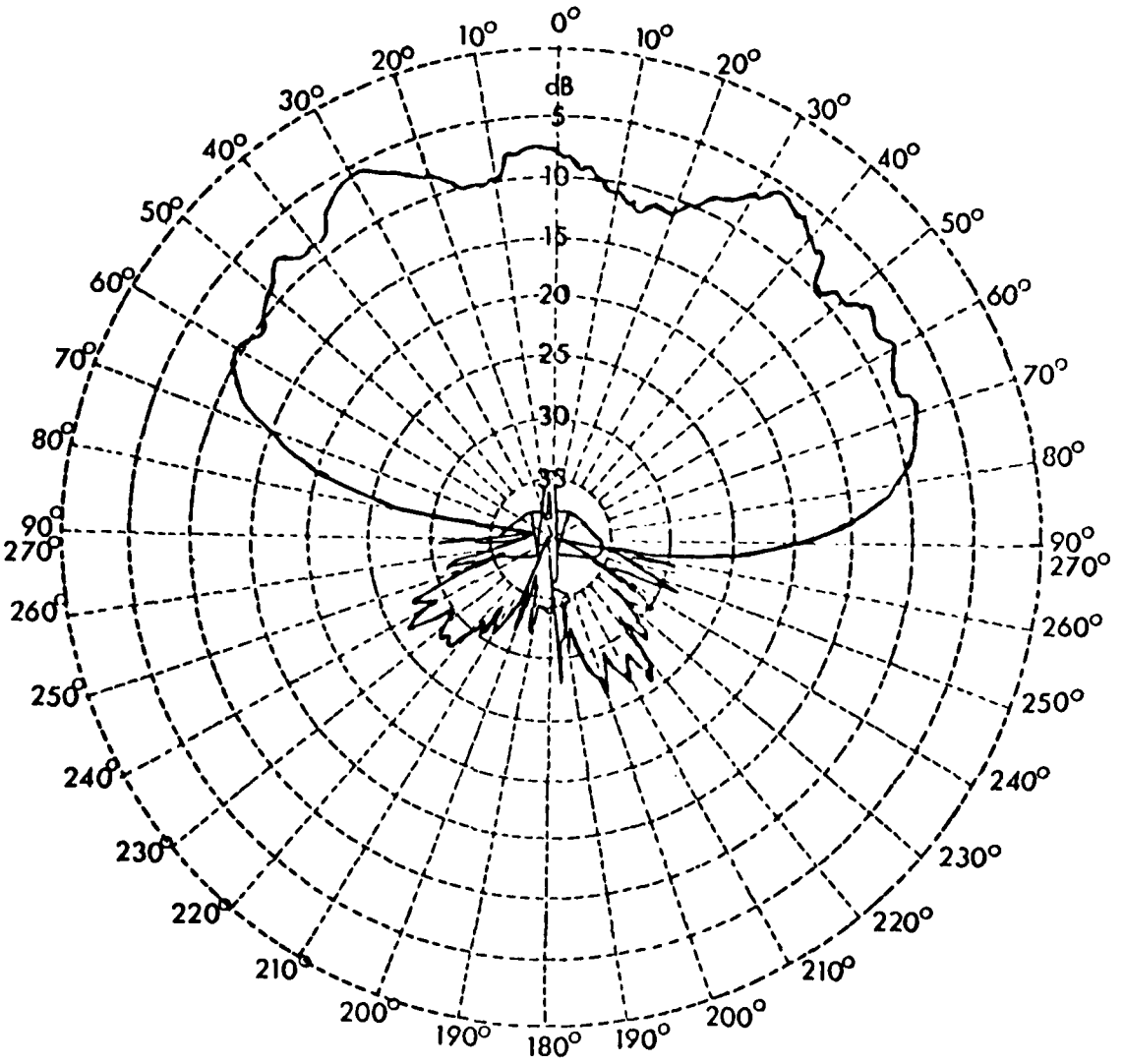

TR 79082

Fig 3.10 Monopole on 3 ft counterpoise (horizontal pattern)

Fig 3.11

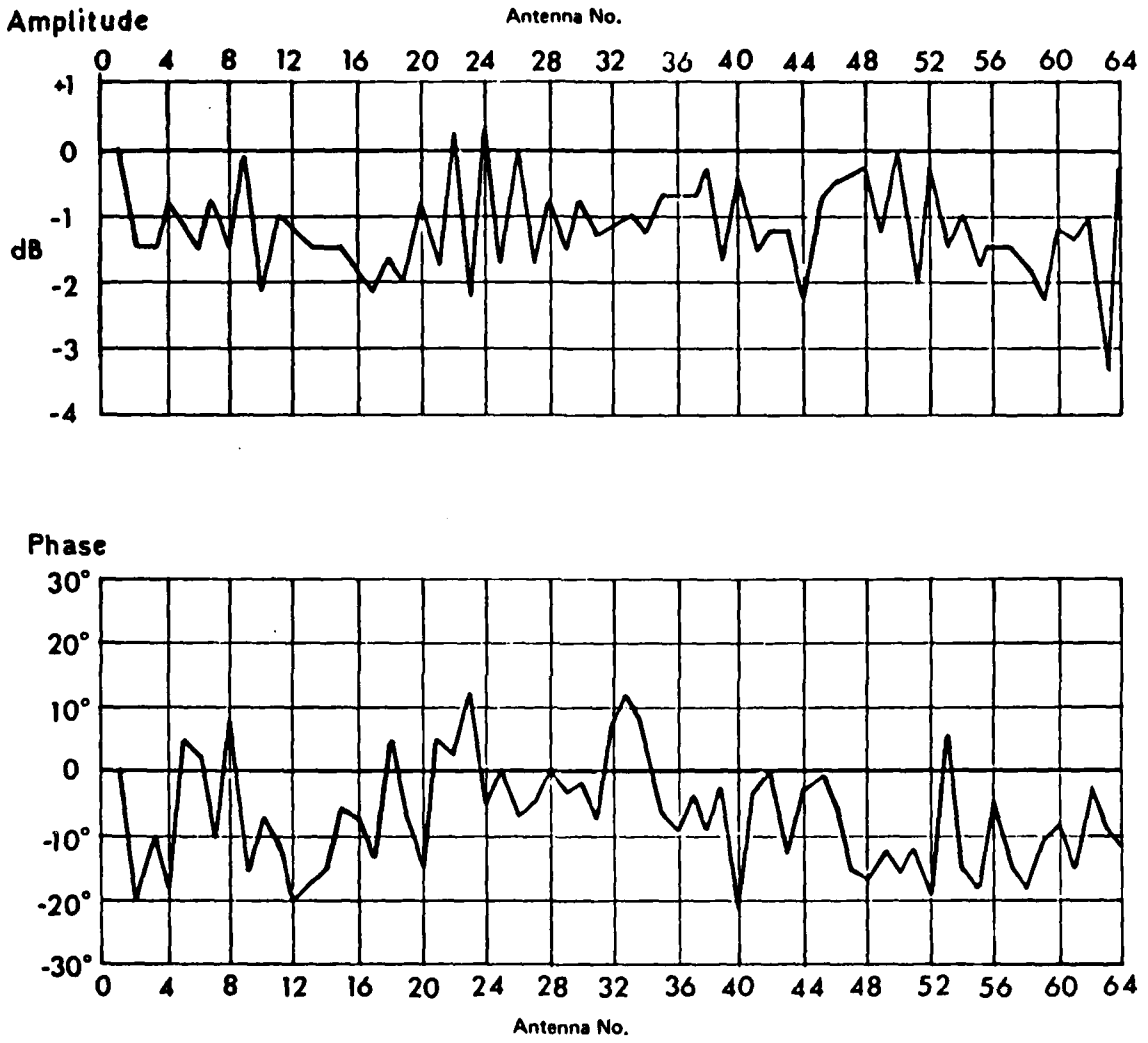

Fig 3.11 Transmitted signal phase and amplitude spread (approach azimuth)

TR 79062

Fig 3.12 Missed approach azimuth

Fig 3.12

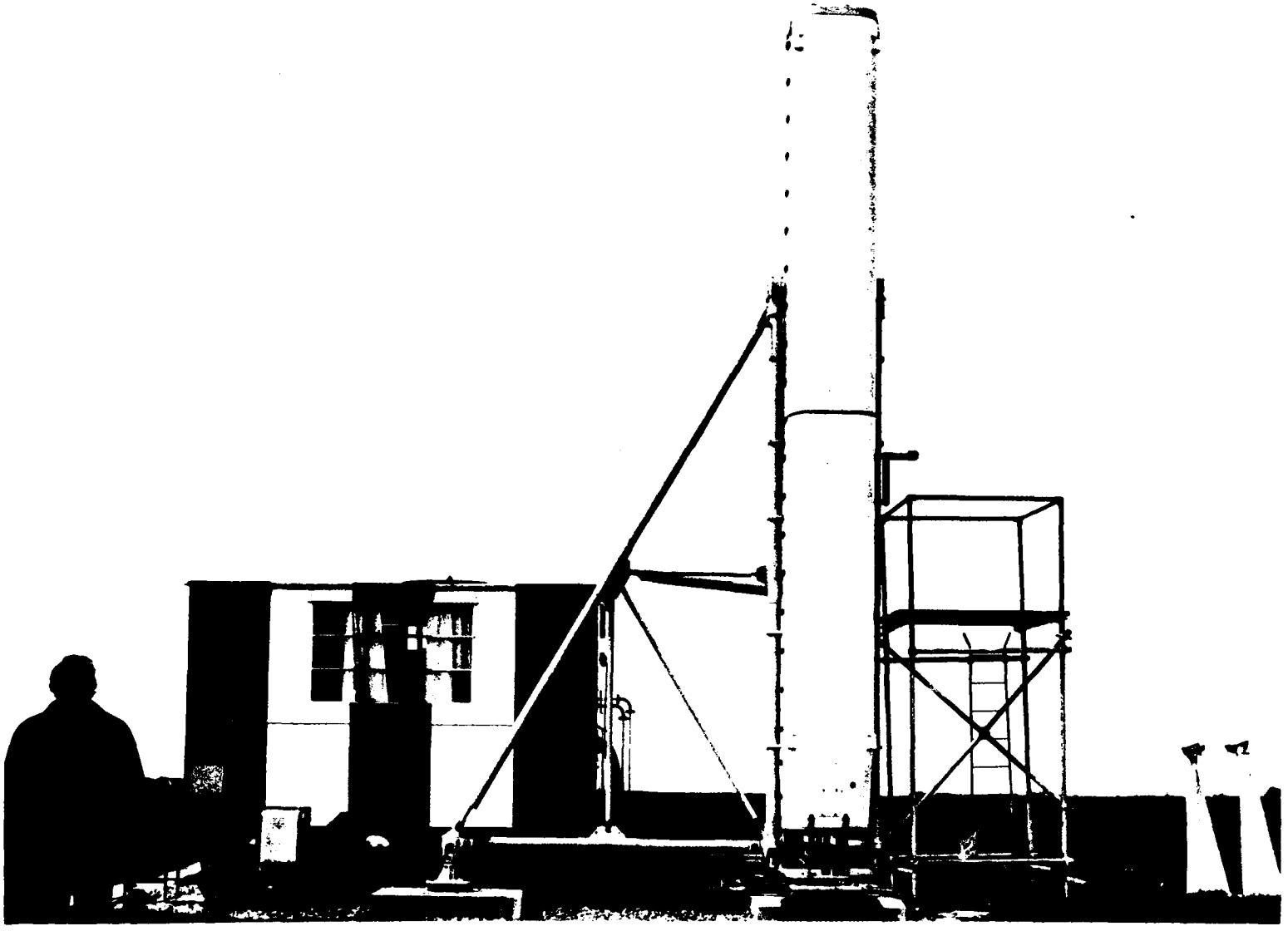

Fig 3.13 90 wavelength elevation array

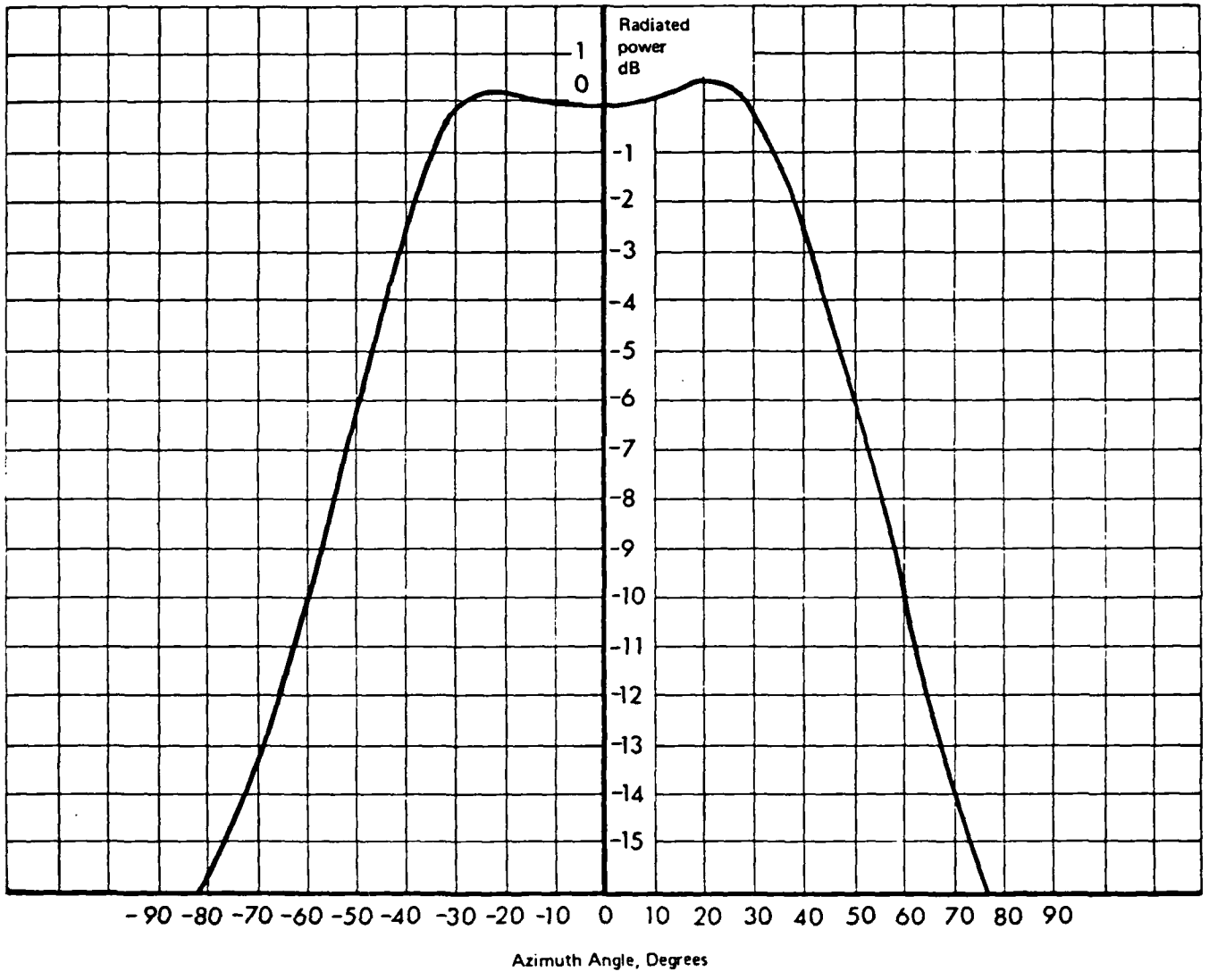

Fig 3.14 Array element azimuth radiation pattern

Fig 3.15

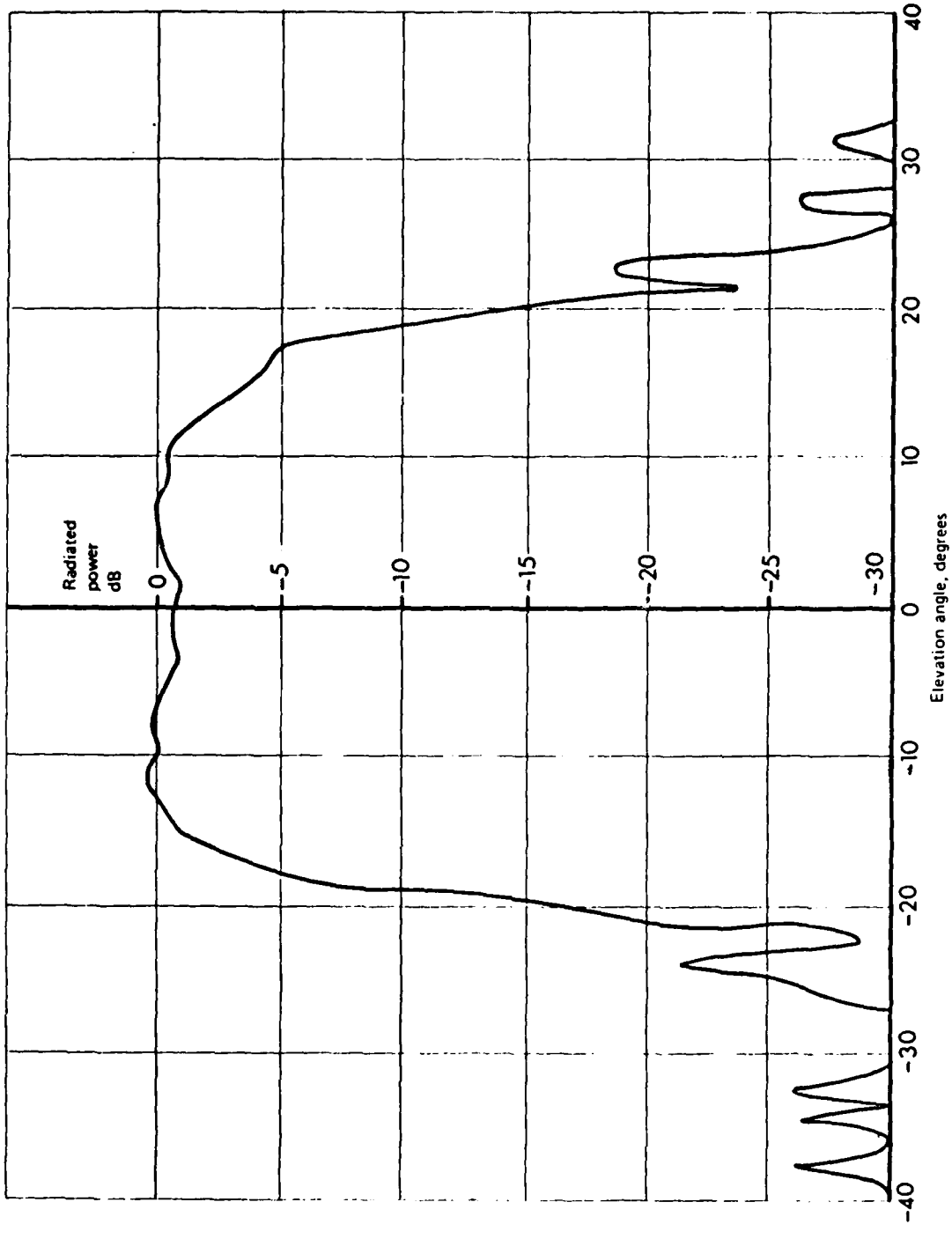

Fig 3.15 Array element elevation radiation pattern

TR 79052

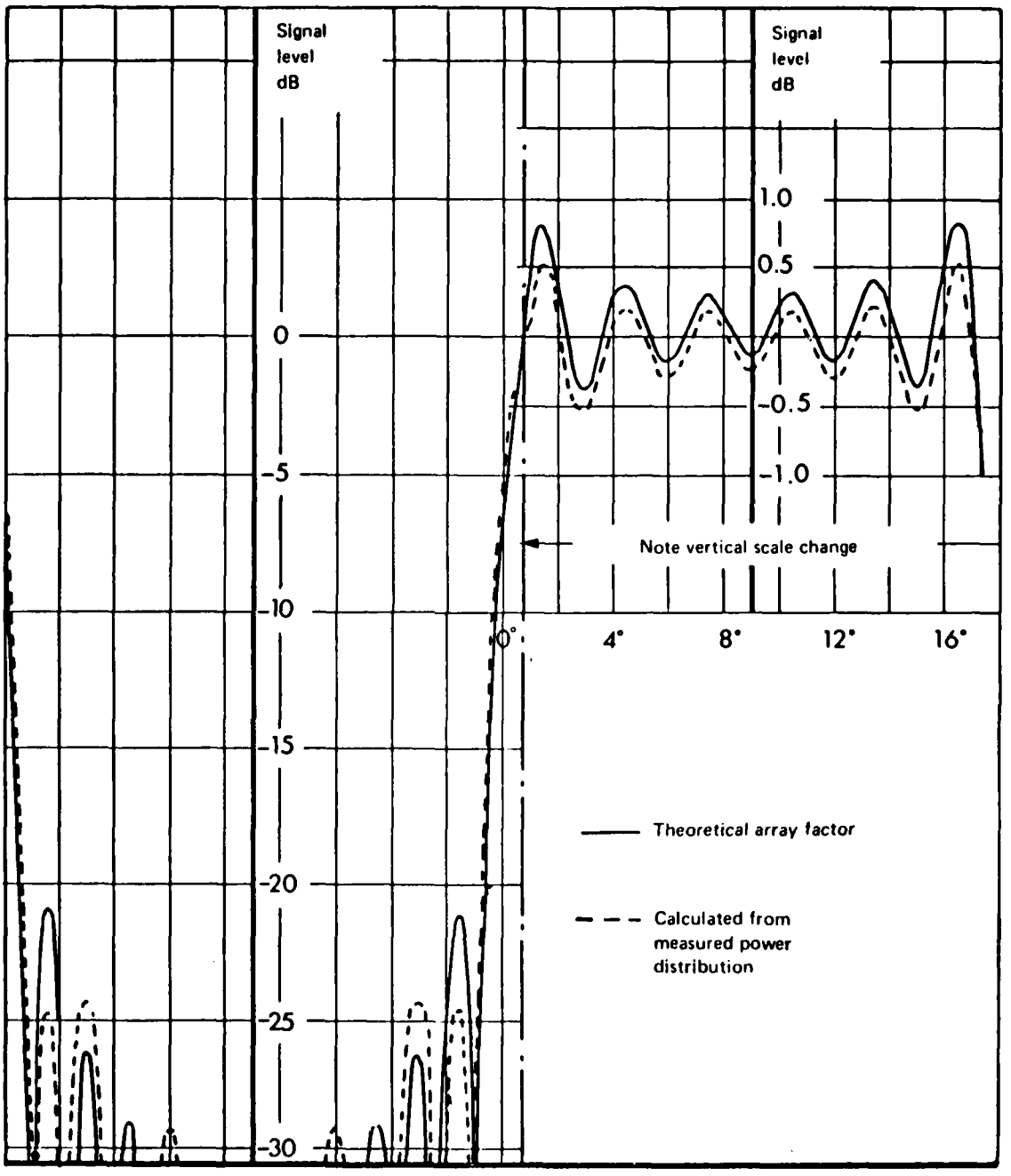

TR 79052

Fig 3.16 Reference antenna array factors

Fig 3.17

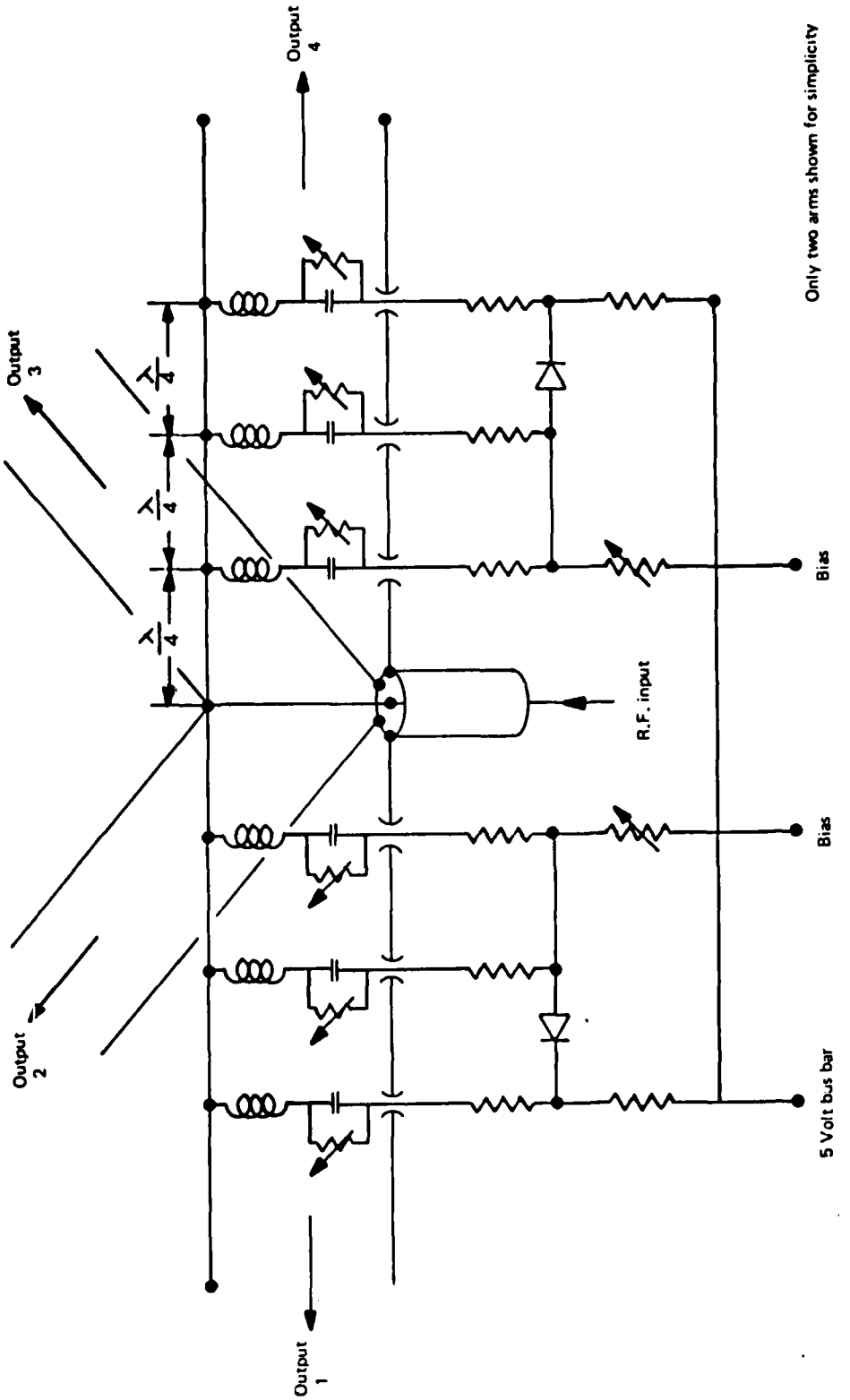

Fig 3.17 Resonant switch and biassing circuit

TR 79052

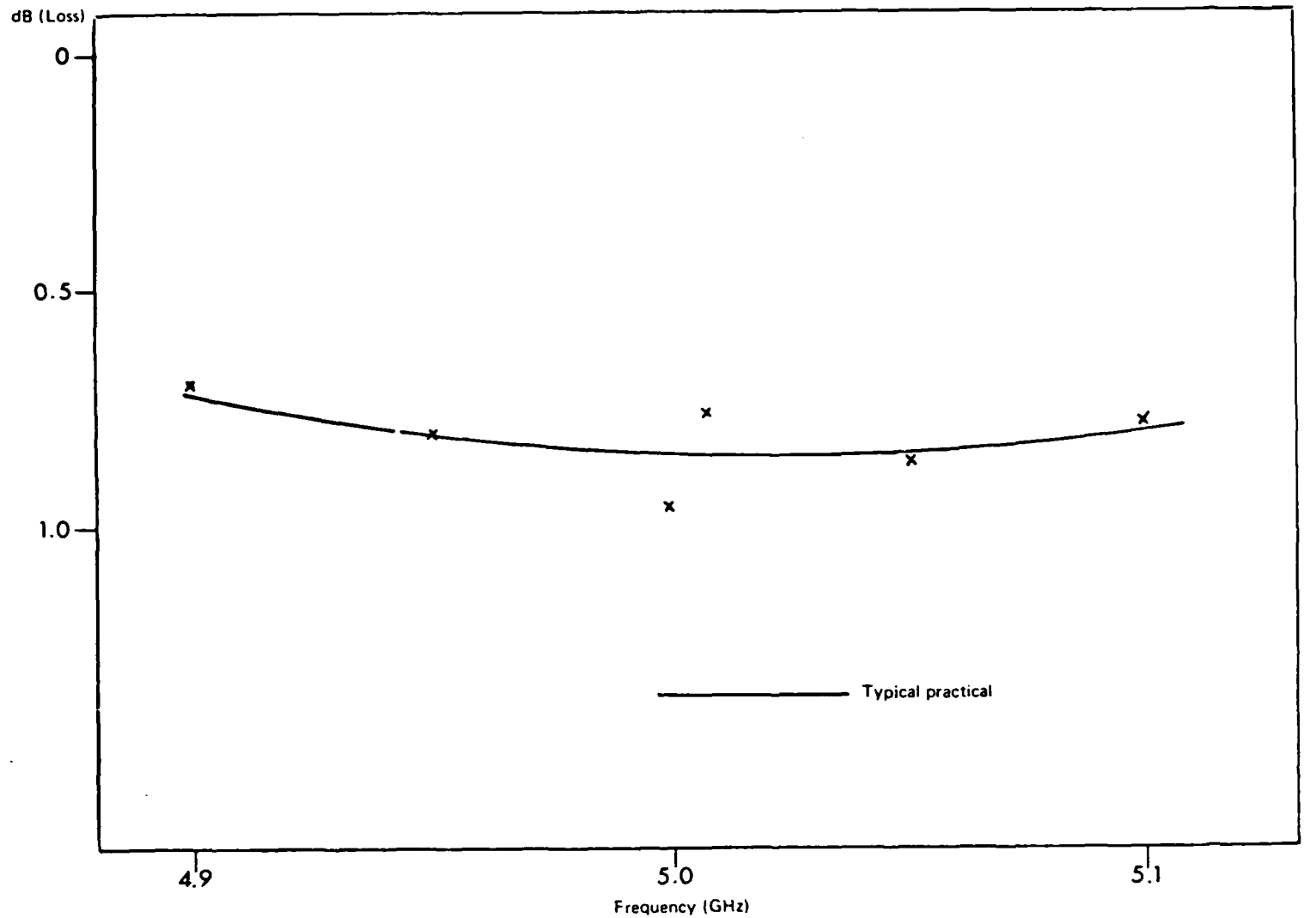

Fig 3.18 Curve of insertion loss for 4-way switching module

Fig 3.18

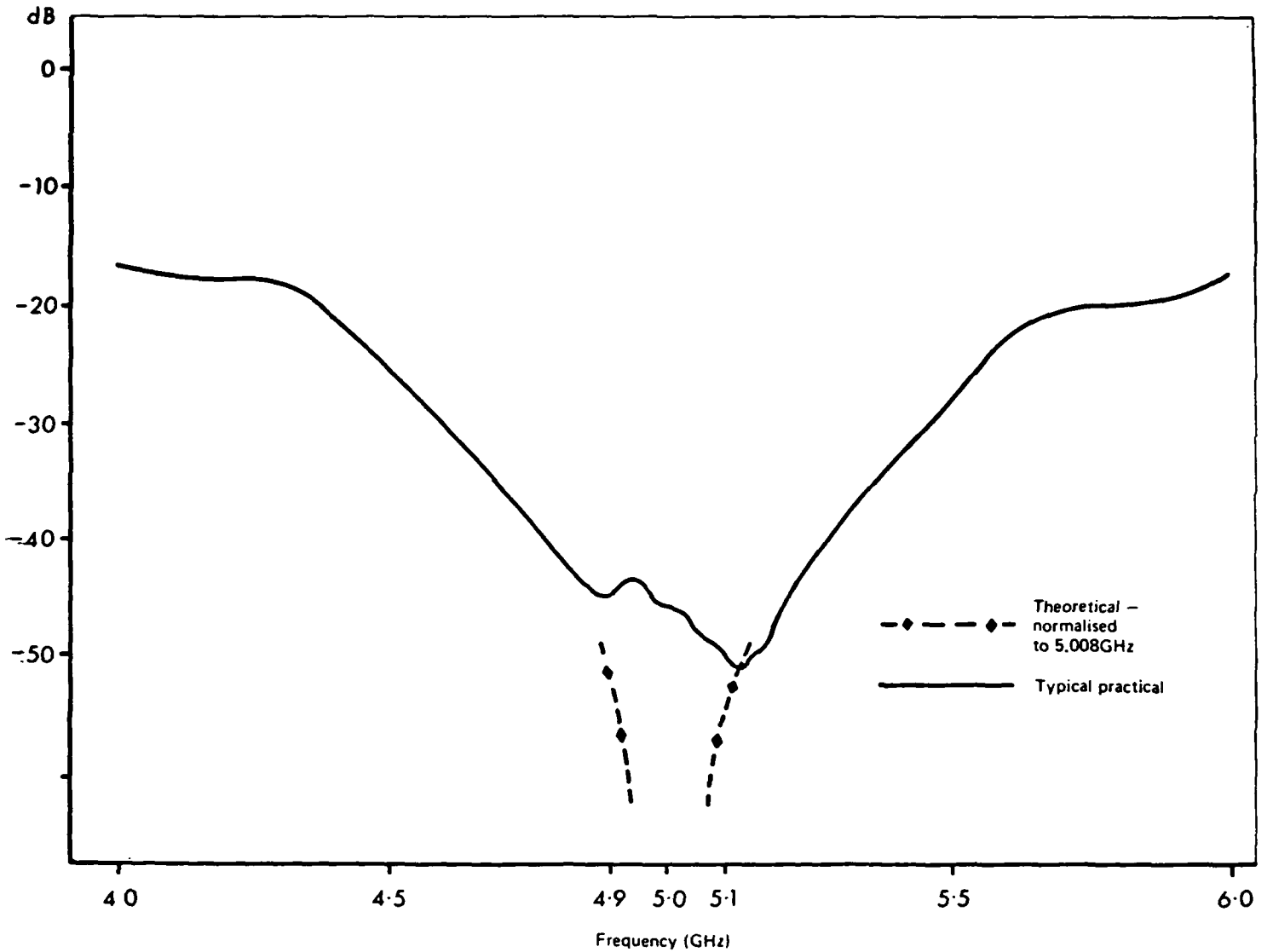

Fig 3.19 Theoretical and practical curves of isolation for 4-way switching module

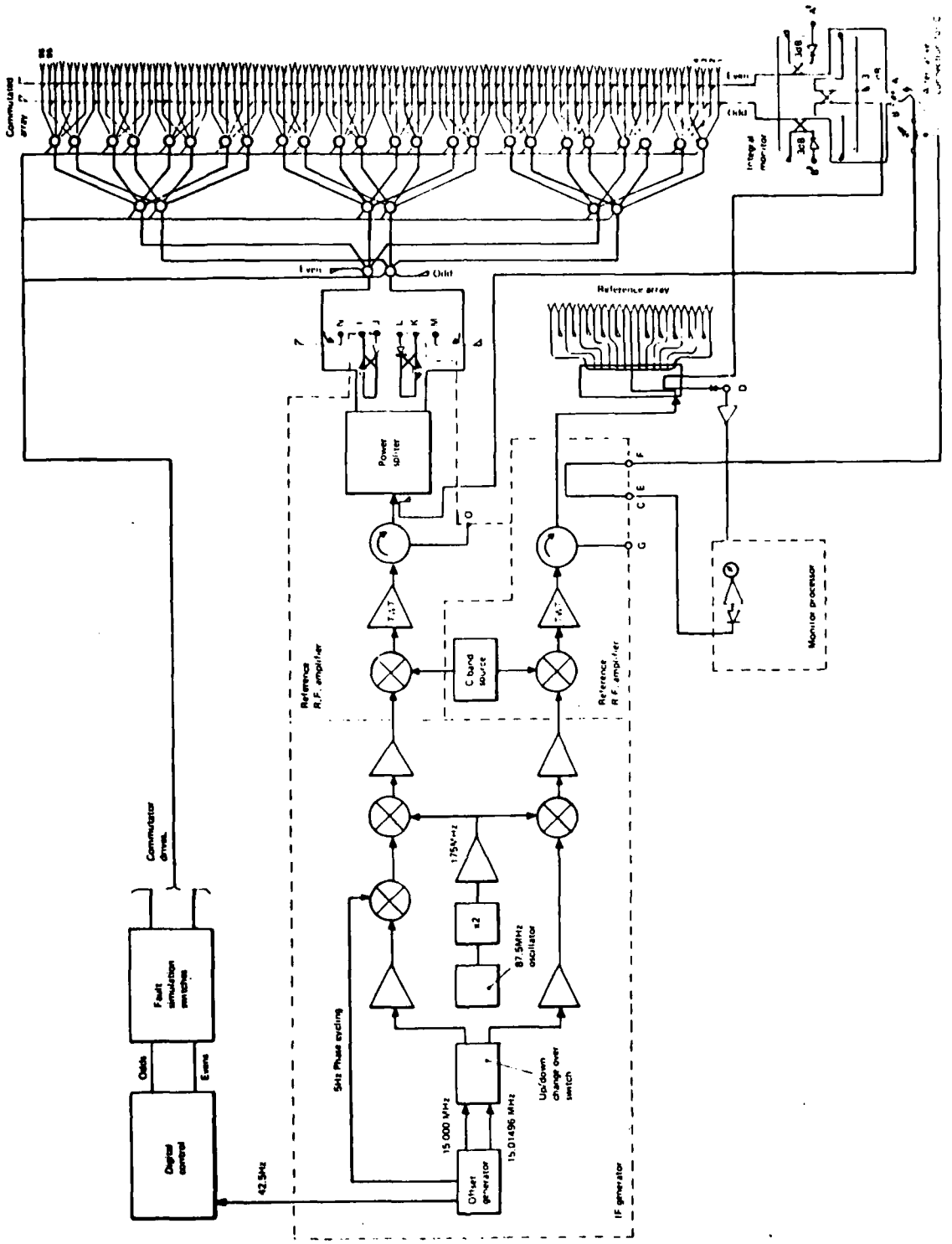

Fig 3.20 Elevation ground system

TR 79062

Fig 3.21

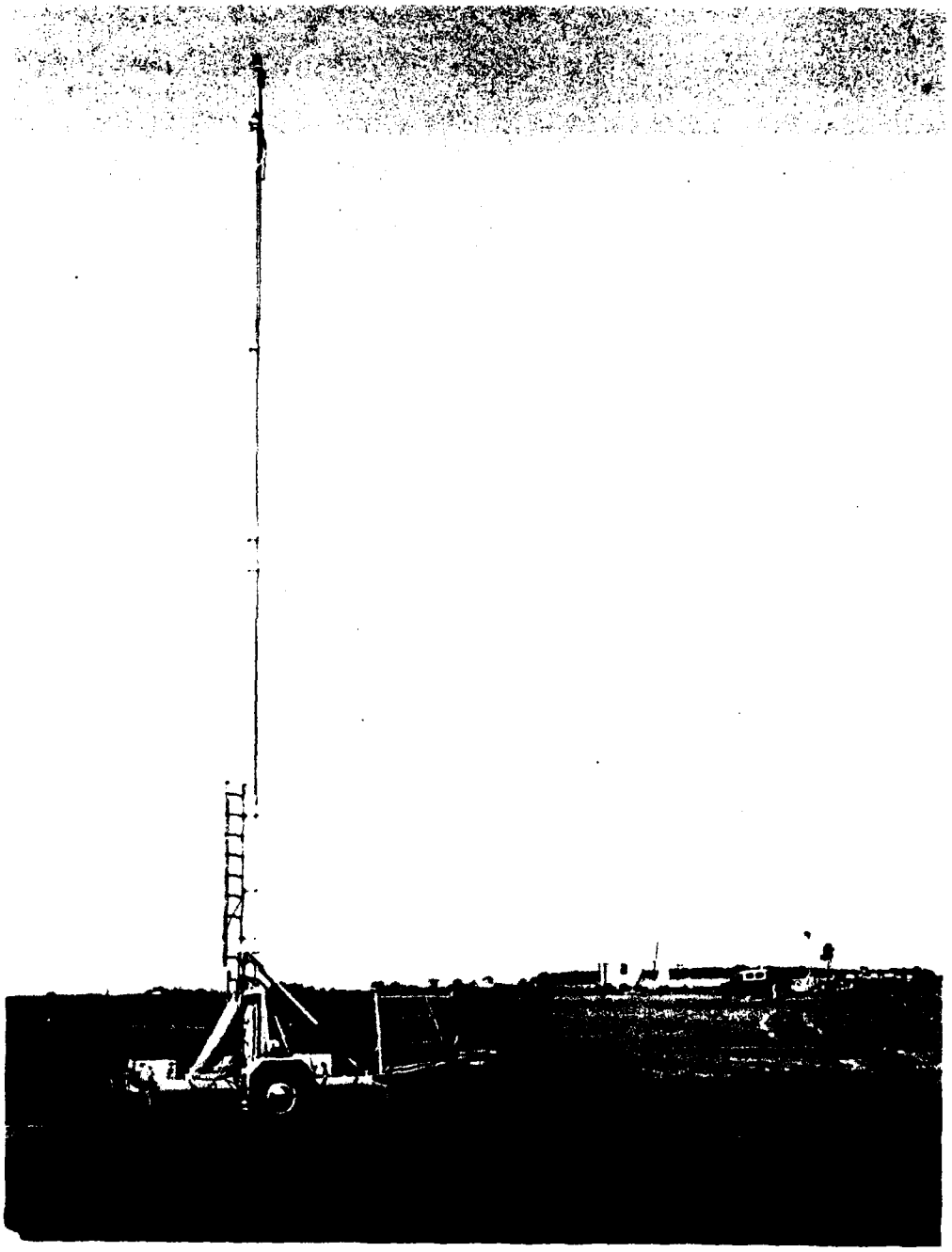

Fig 3.21 Elevation field monitor mounting

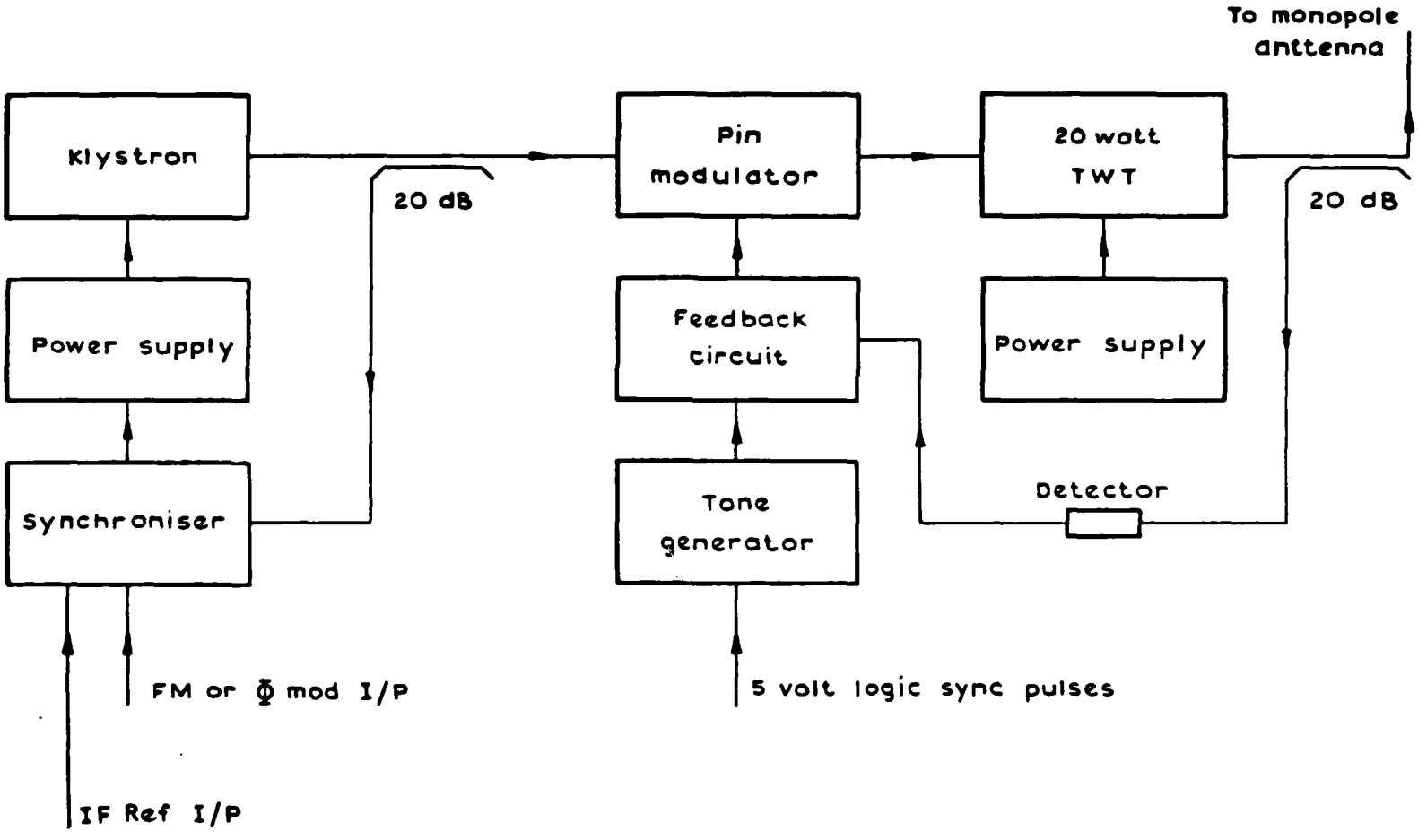

Fig 3.22 Data transmitter block diagram

Fig 3.22

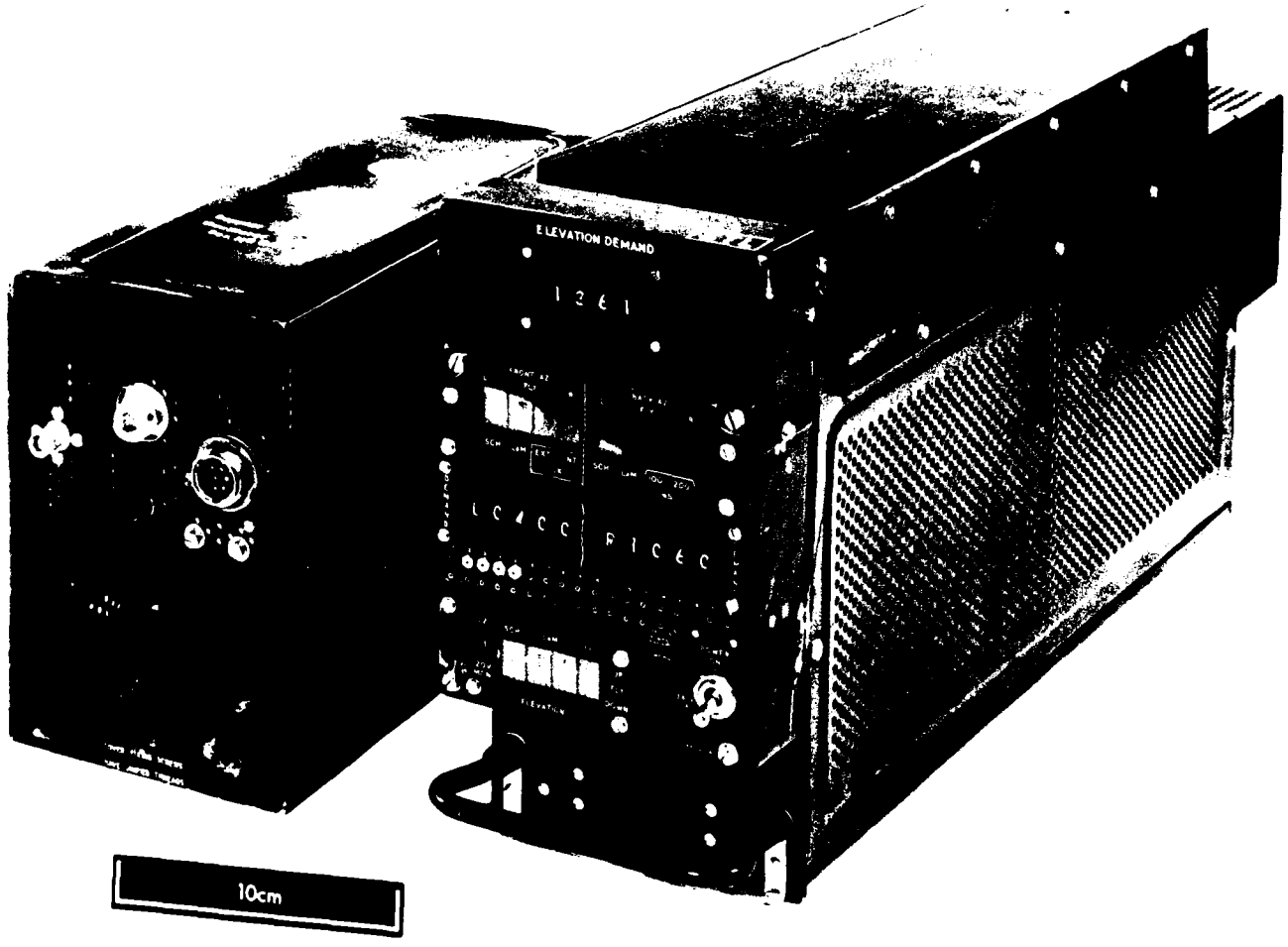

Fig 3.23 S type receiver system

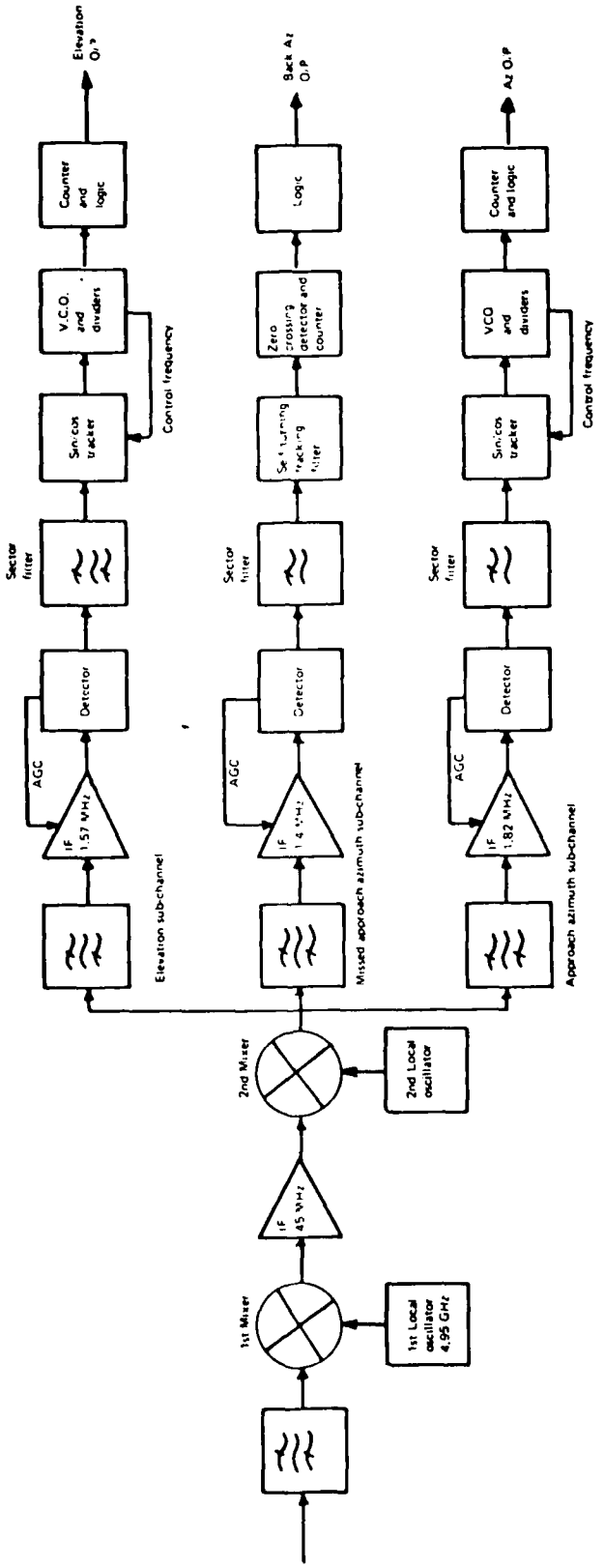

Fig 3.24 Outline block diagram of type S receiver

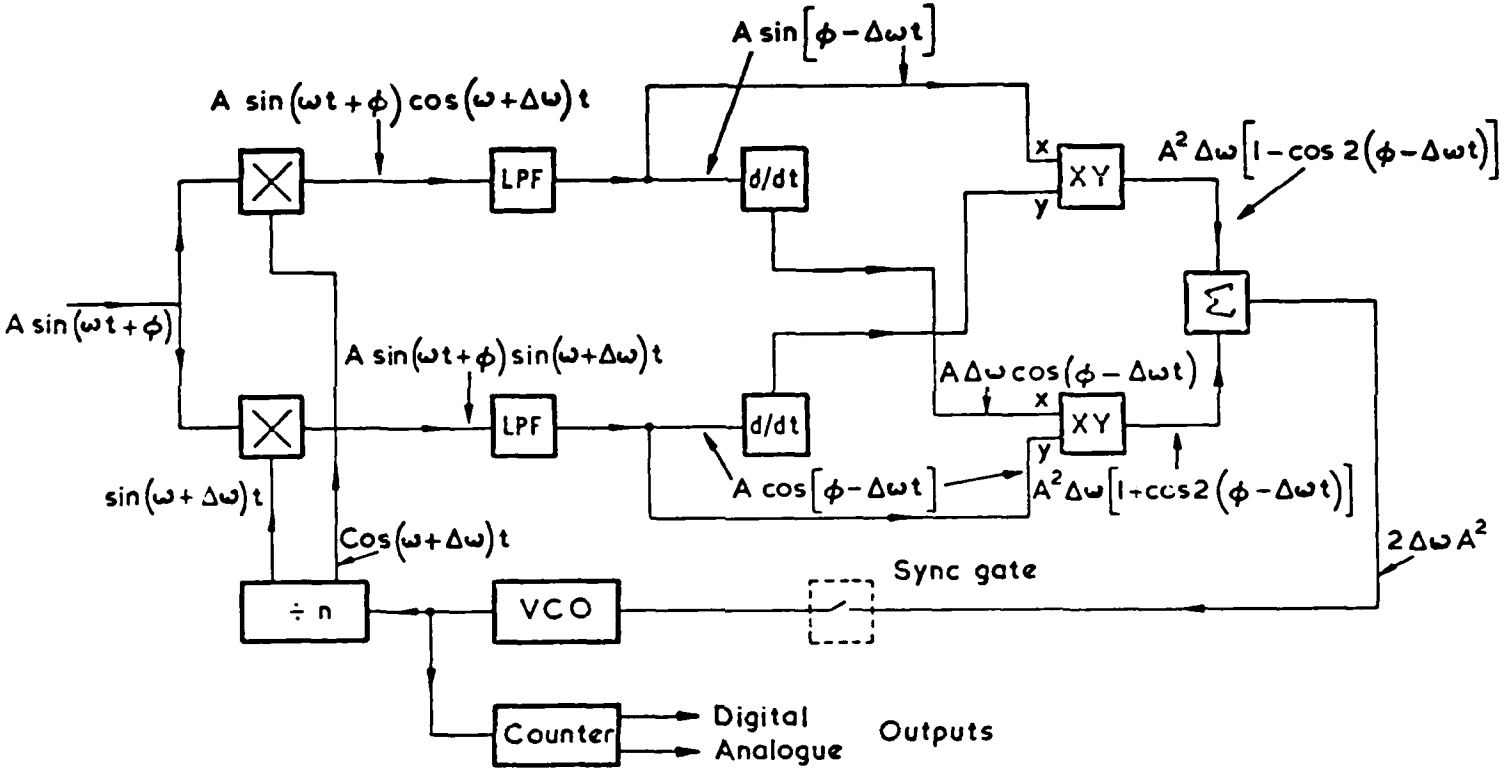

Fig 3.25 Sine/cosine tracker system detail diagram

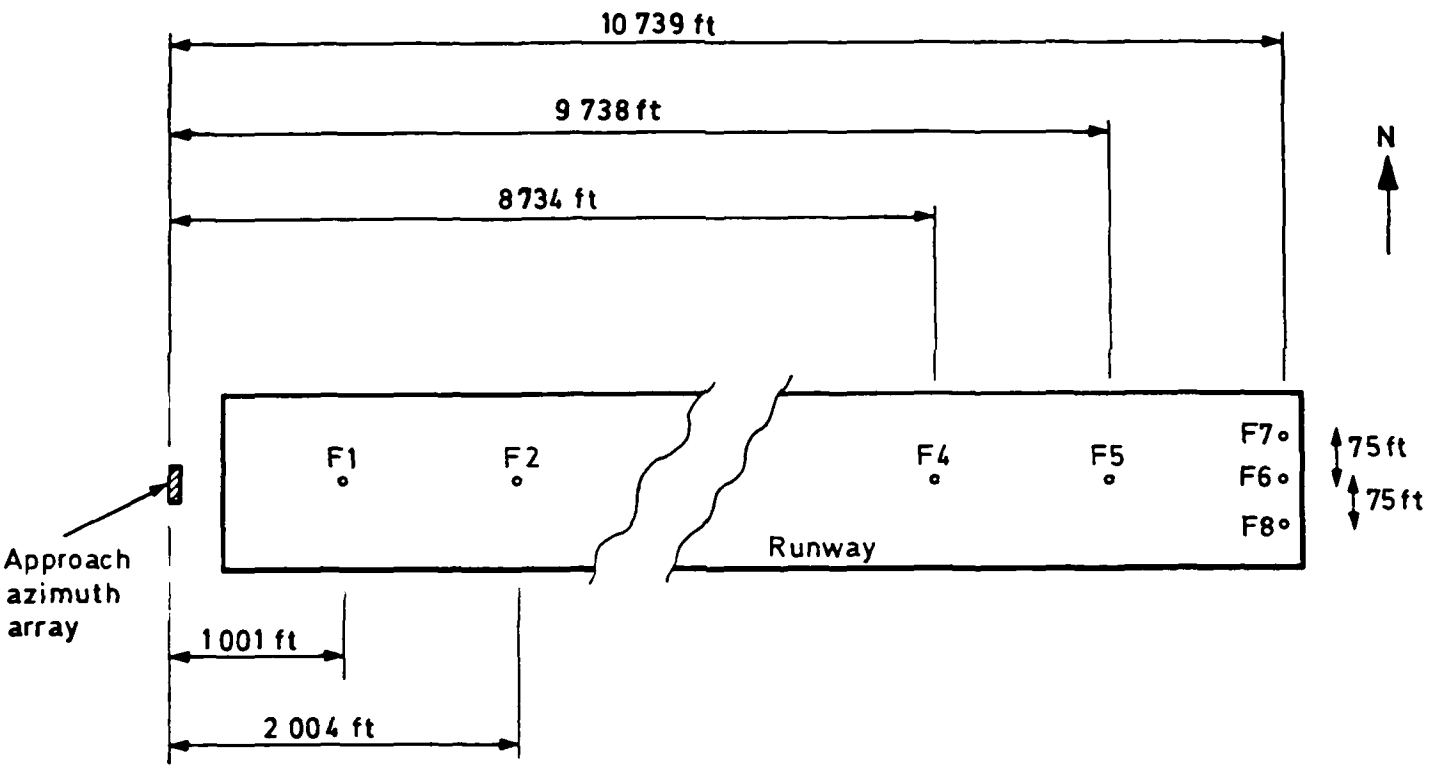

Fig 4.1a Close and long range approach azimuth test points

Fig 4.1b

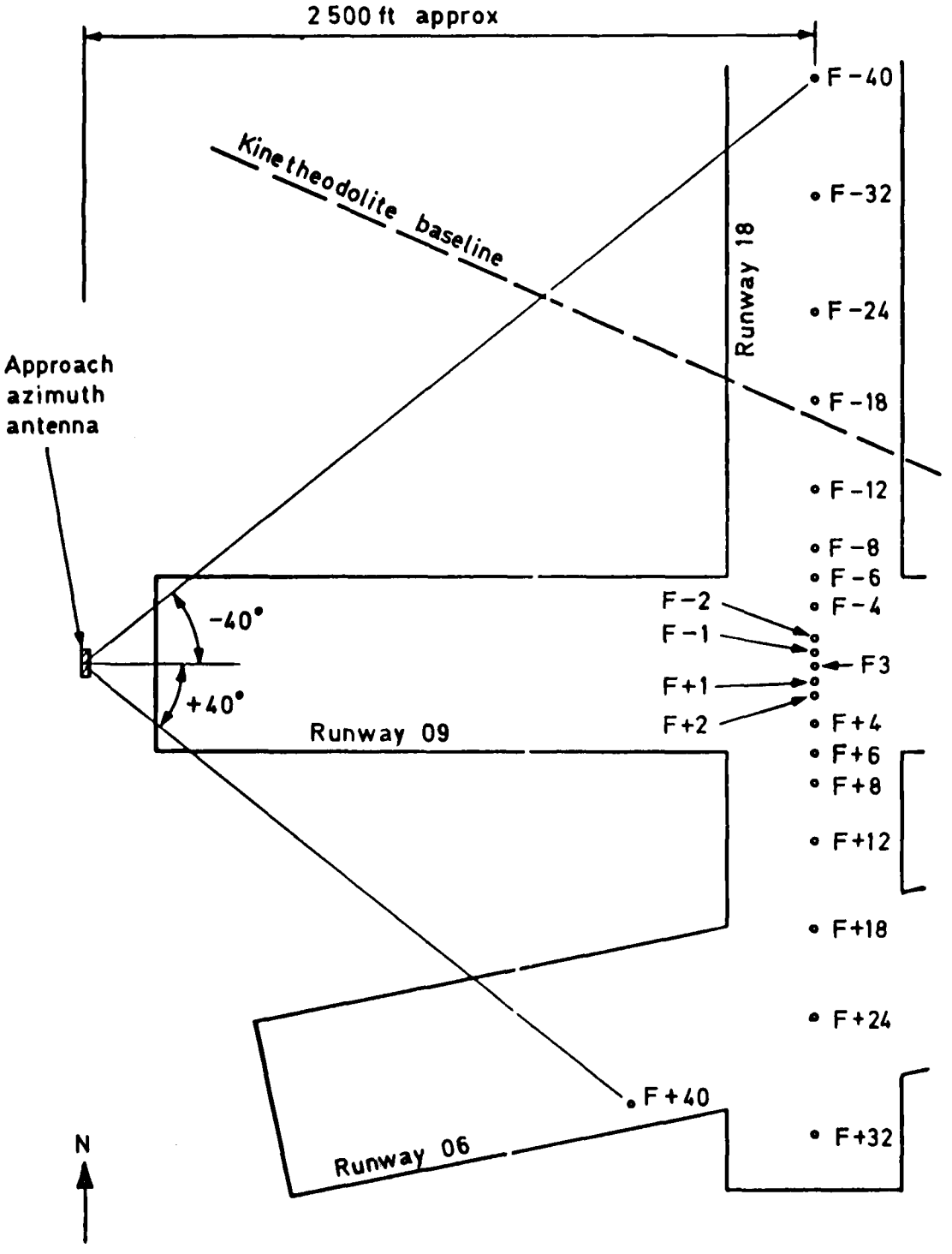

TR 79052

Fig 4.1b Cross runway approach azimuth test points

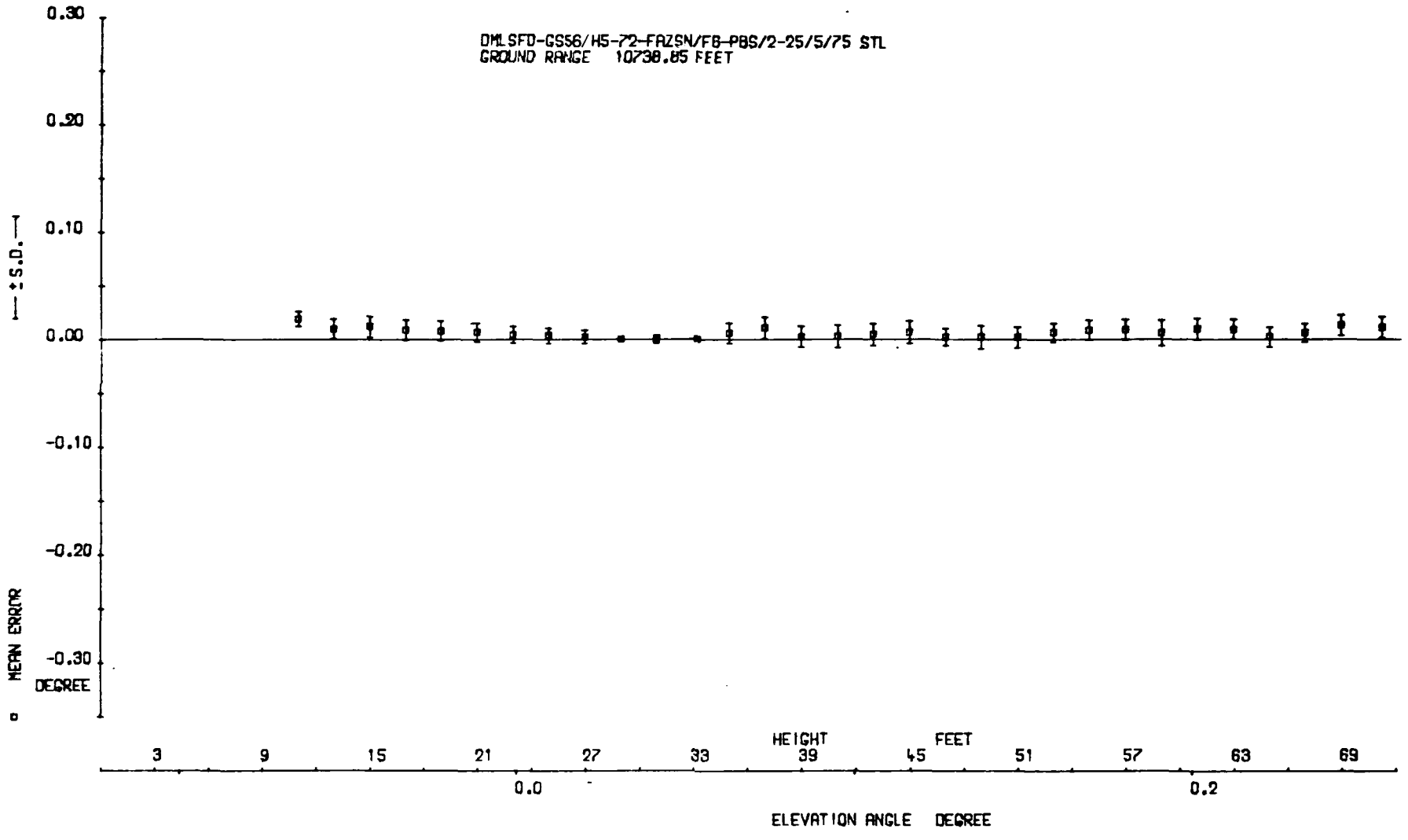

Fig 4.2 Approach azimuth static test GS56, position F6

Fig 4.2

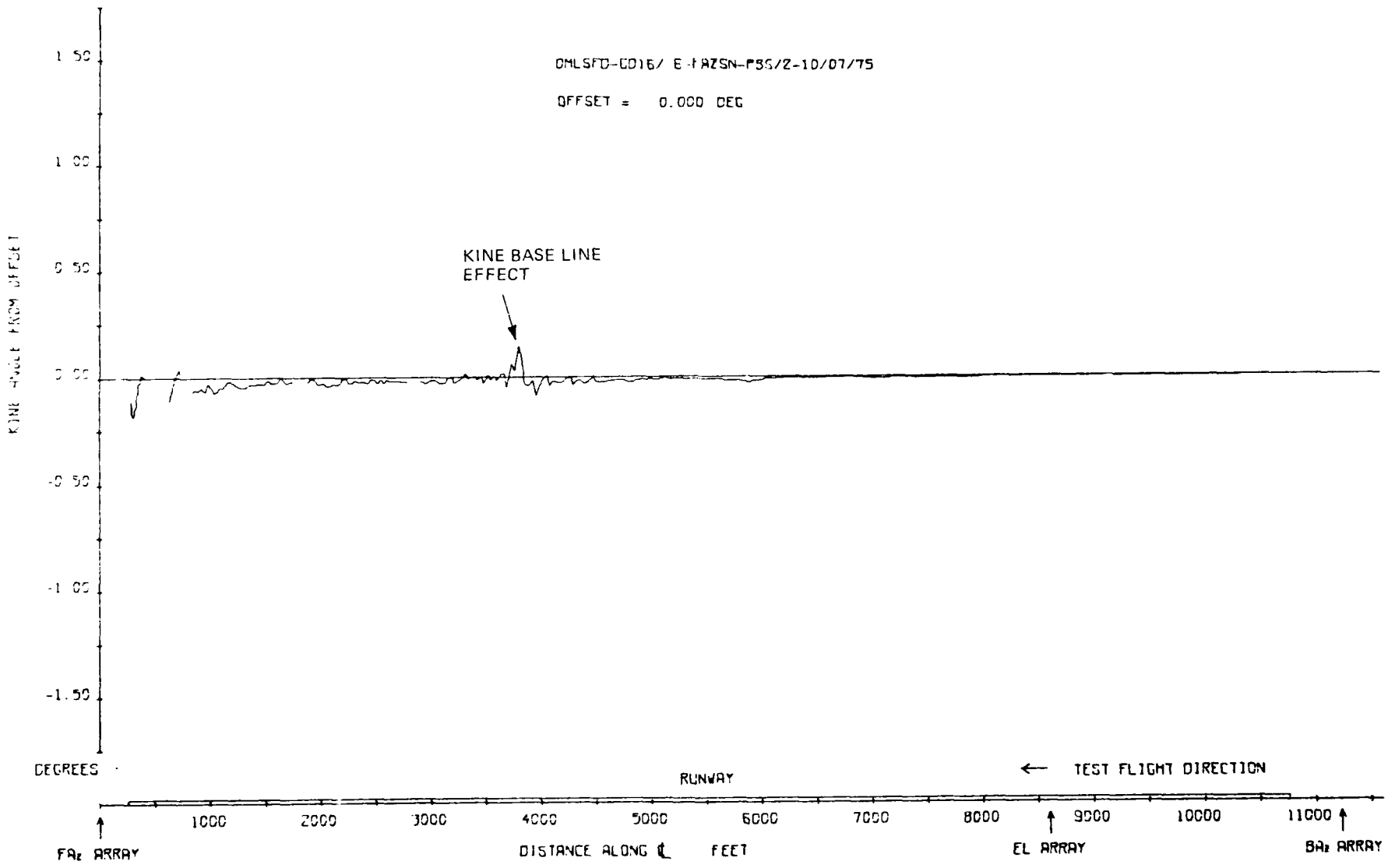

Fig 4.3a

Fig 4.3a Approach azimuth. Vehicle run along test runway centre line. Mast height 20 ft

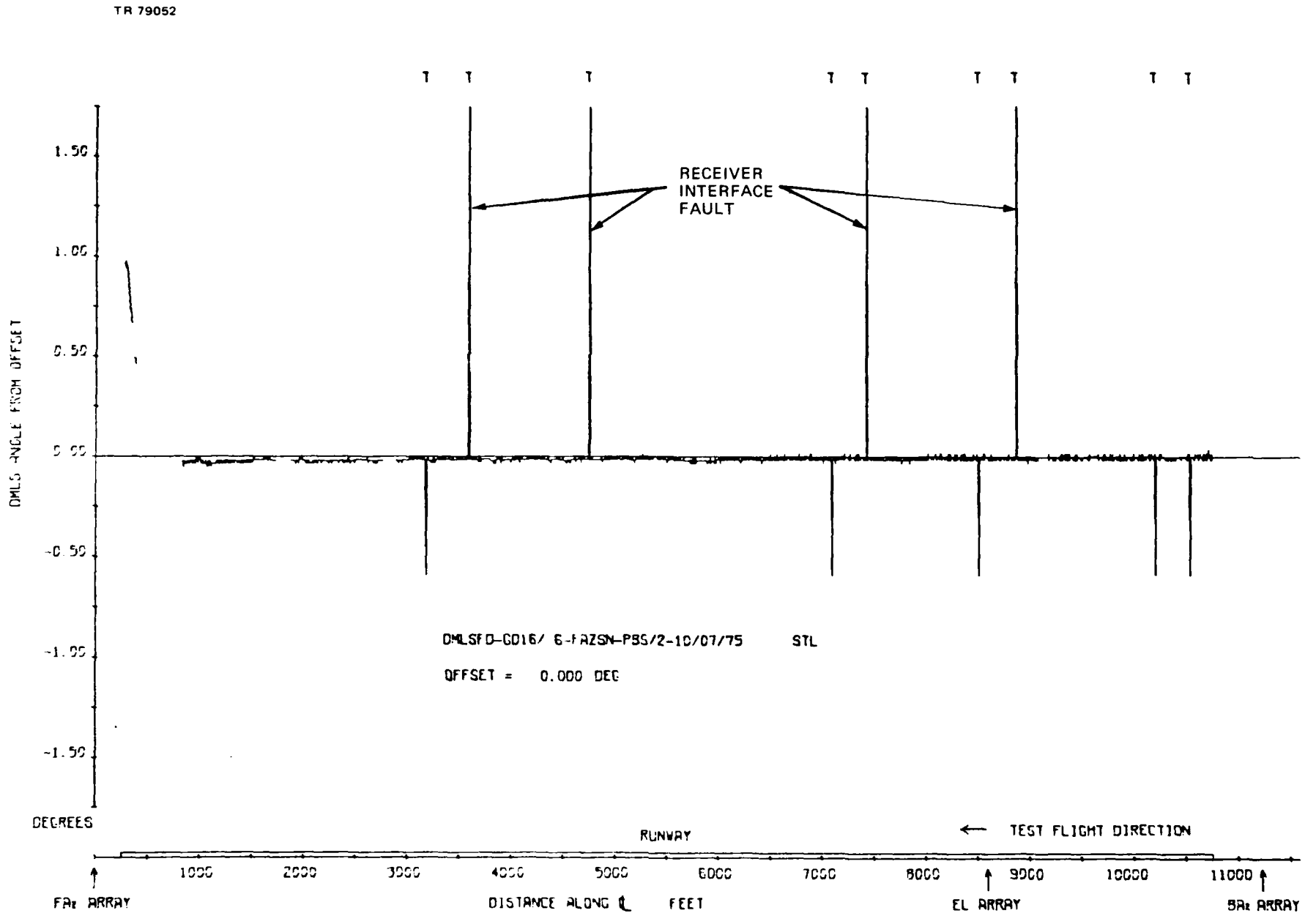

Fig 4.3b

Fig 4.3b Approach azimuth. Vehicle run along test runway centre line. Mast height 20 ft

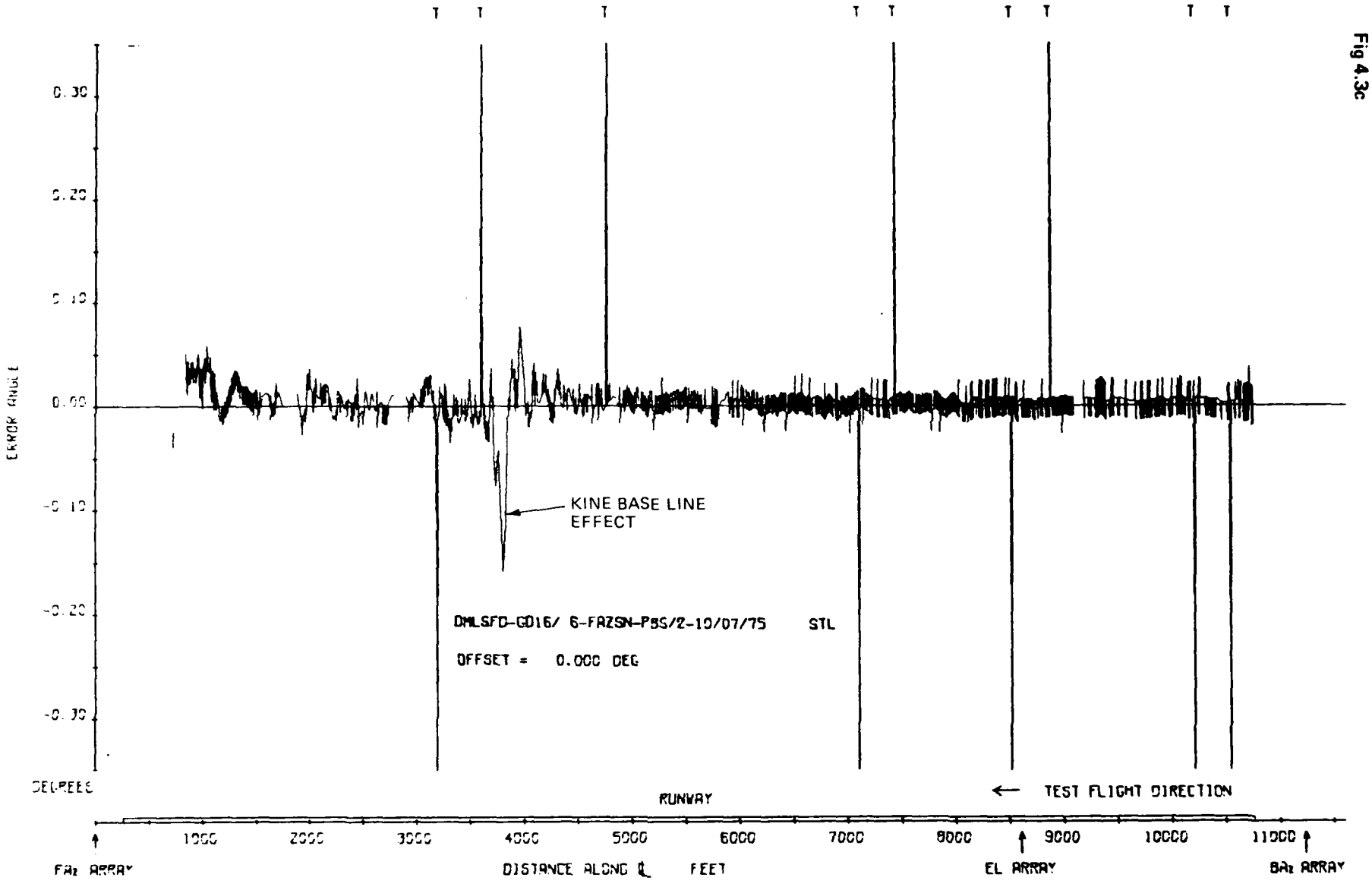

Fig 4.3c

Fig 4.3c Approach azimuth. Vehicle run along test runway centre line. Mast height 20 ft

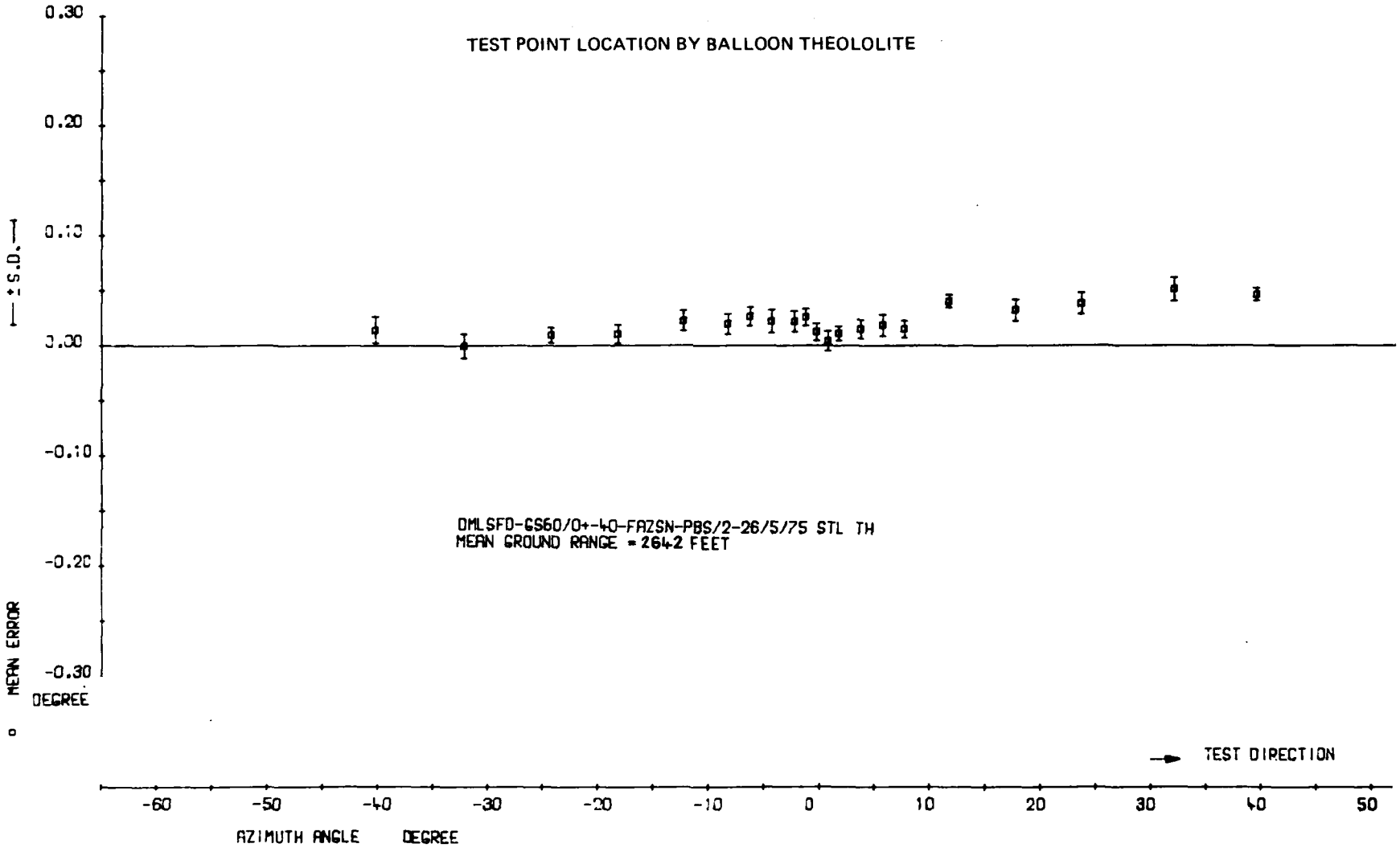

Fig 4.4 Approach azimuth cross runway test GS60

Fig 4.4

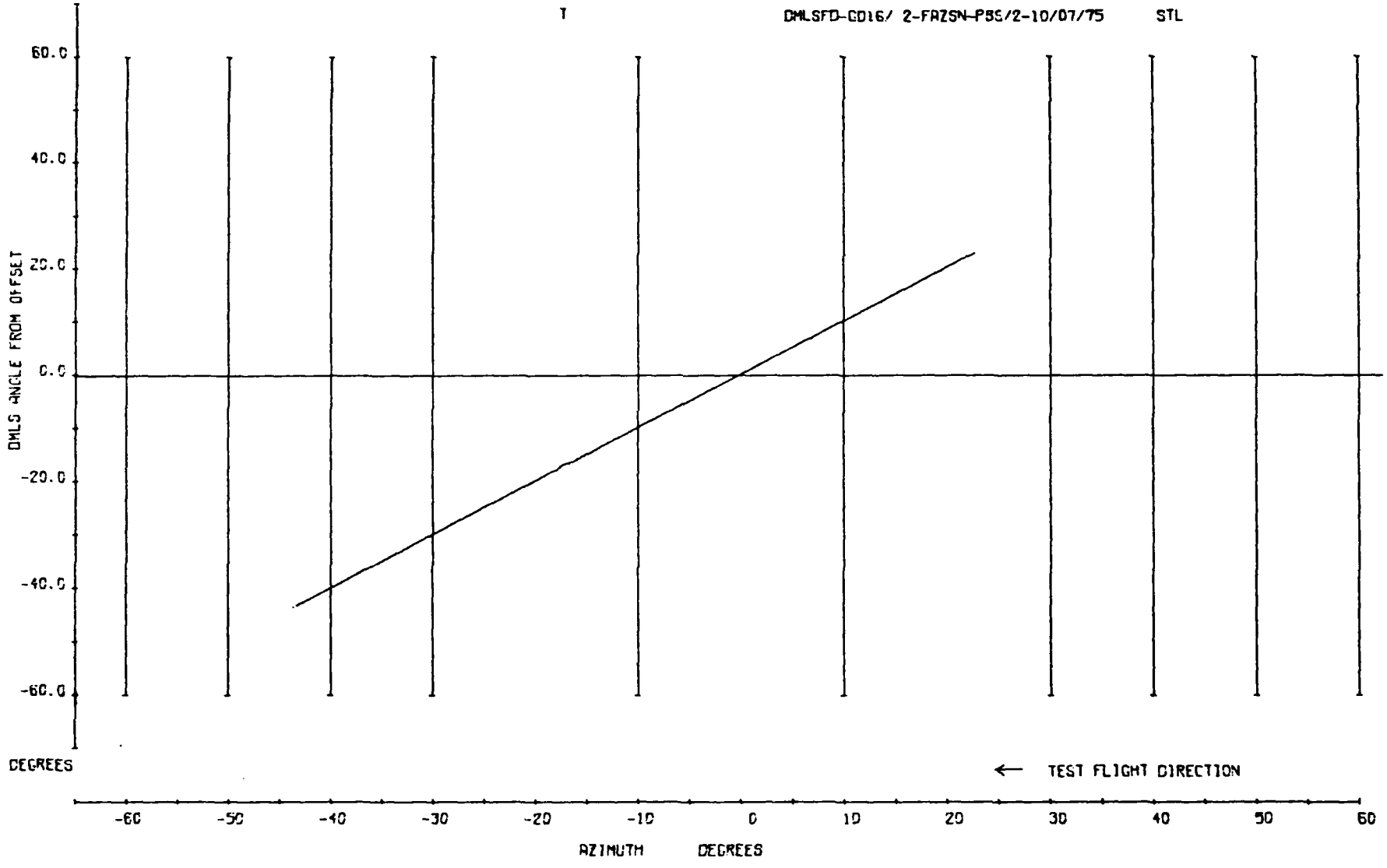

Fig 4.5a

Fig 4.5a Approach azimuth. Vehicle run along N–S runway. Mast height 20 ft

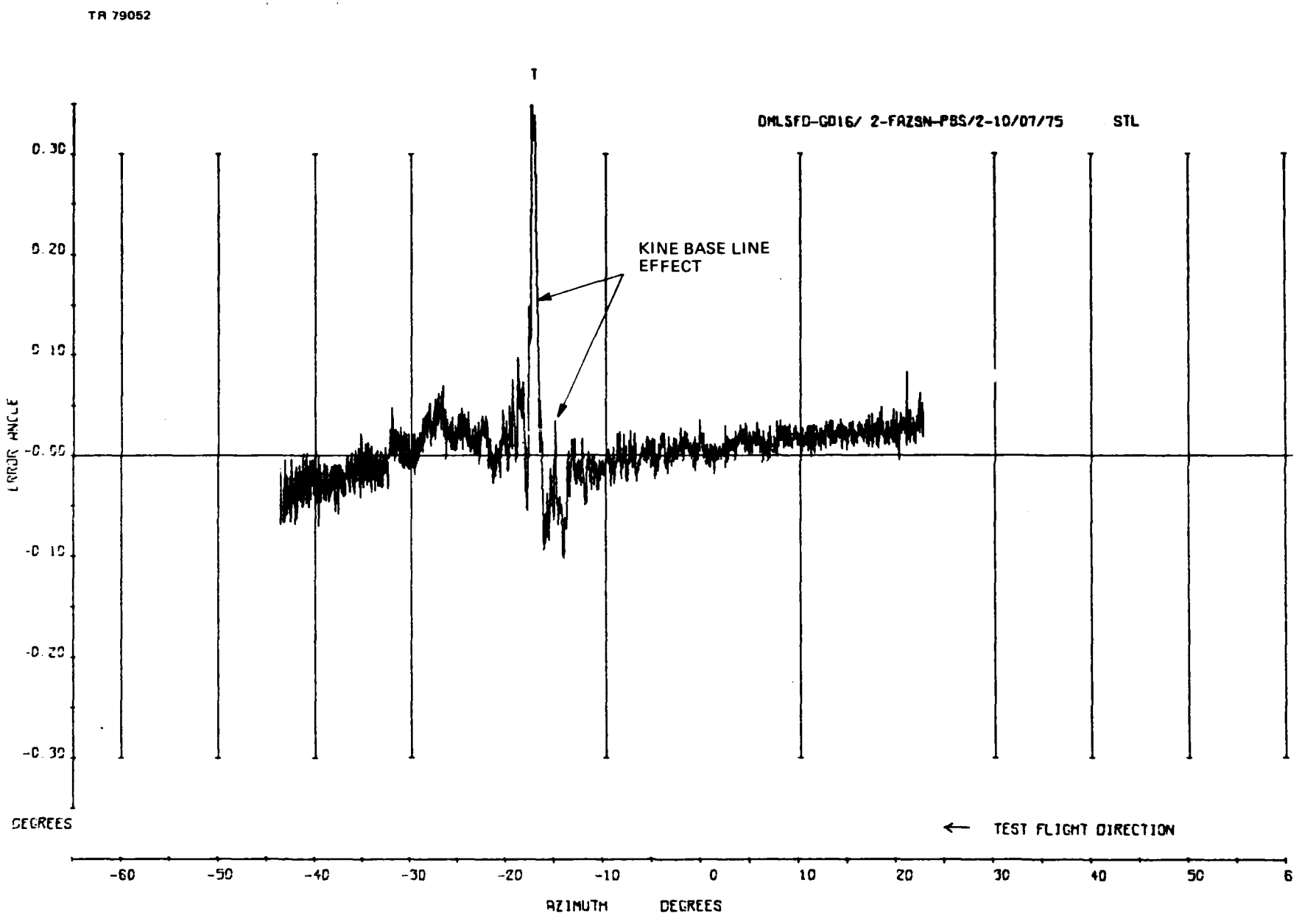

Fig 4.5b Approach azimuth. Vehicle run along N–S runway. Mast height 20 ft

Fig 4.5b

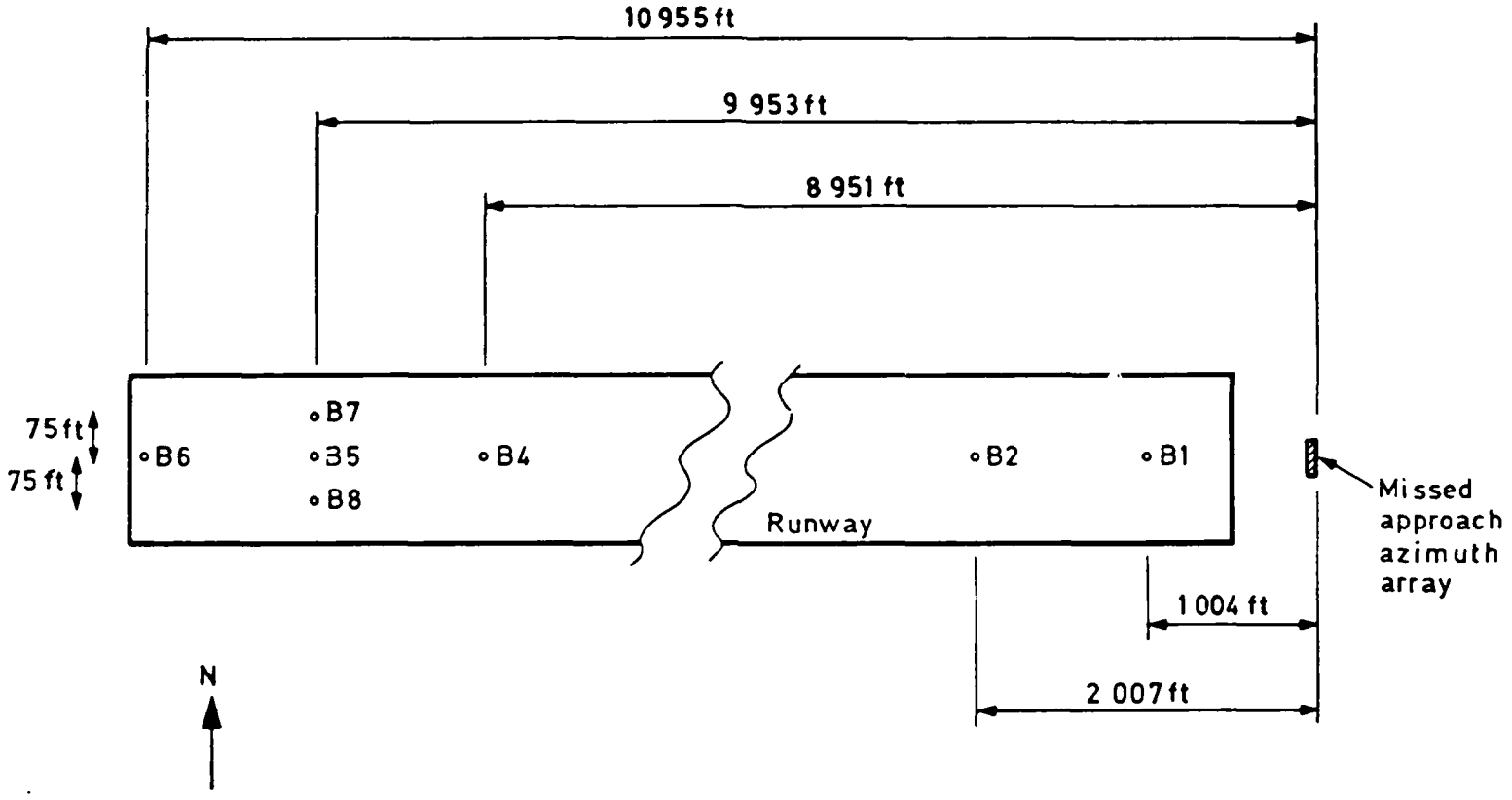

Fig 4.6a Close and long range missed approach azimuth test points

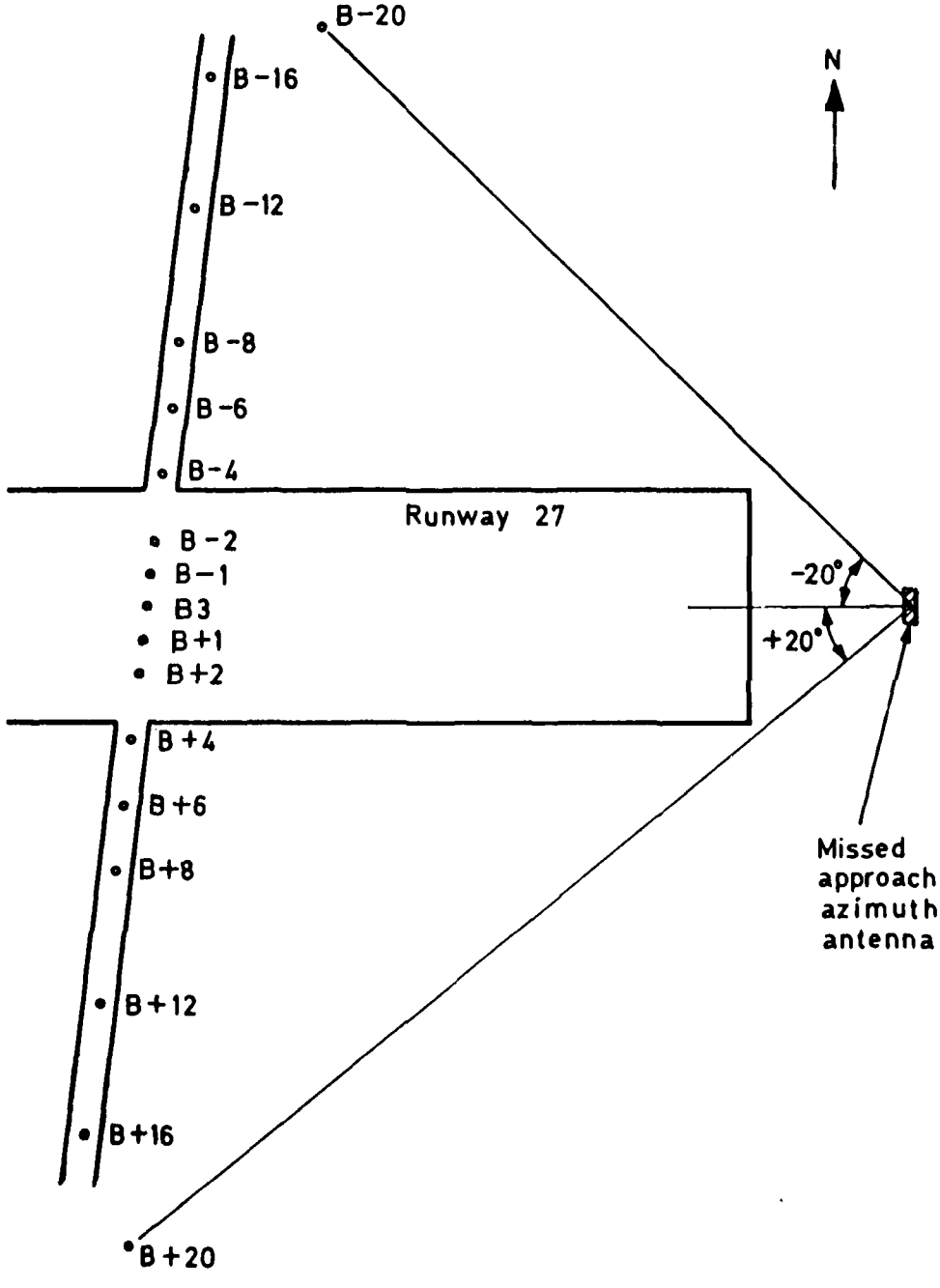

TR 79052

Fig 4.6b Cross runway missed approach azimuth test points

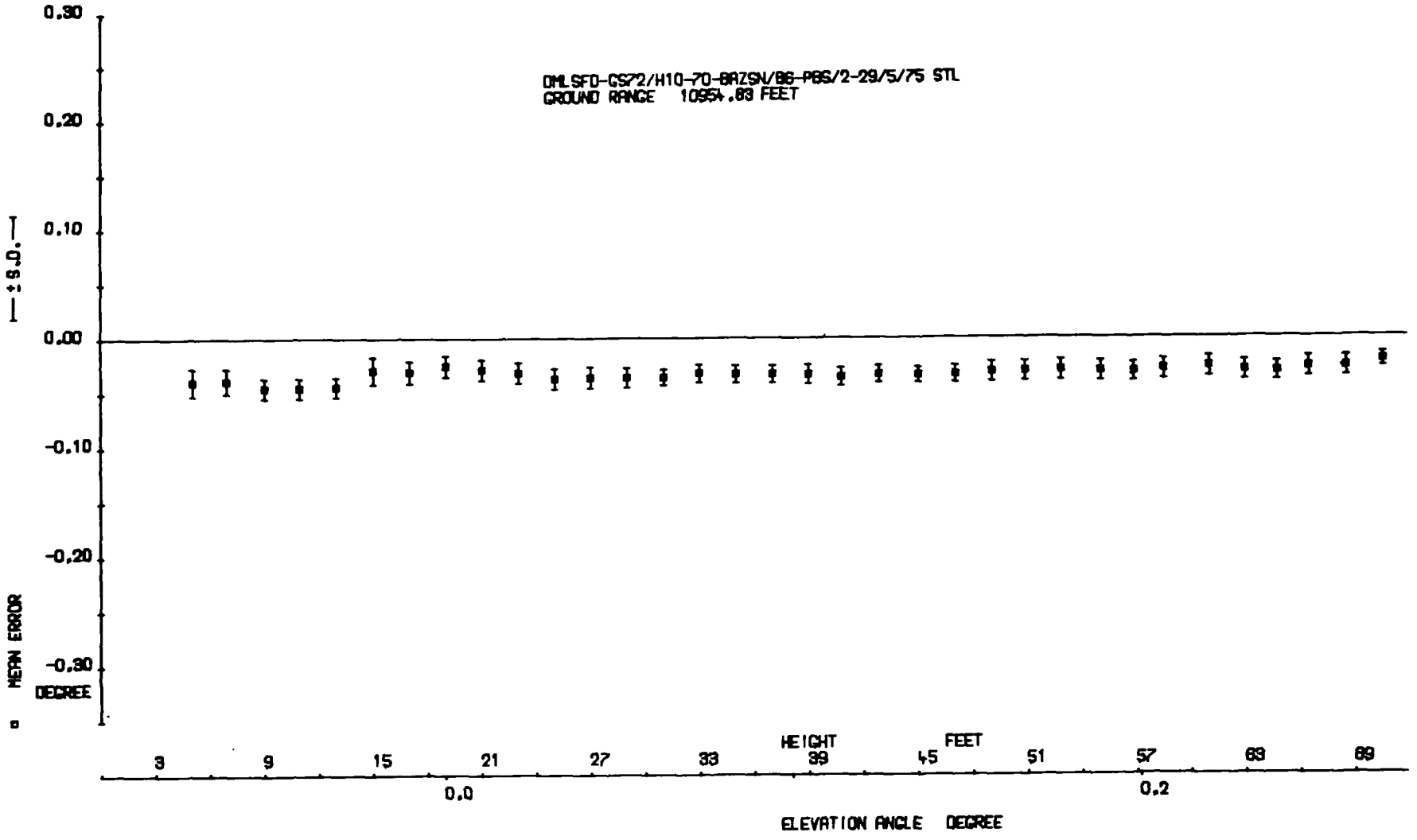

Fig 4.7 Missed approach azimuth static test GS72, position B6

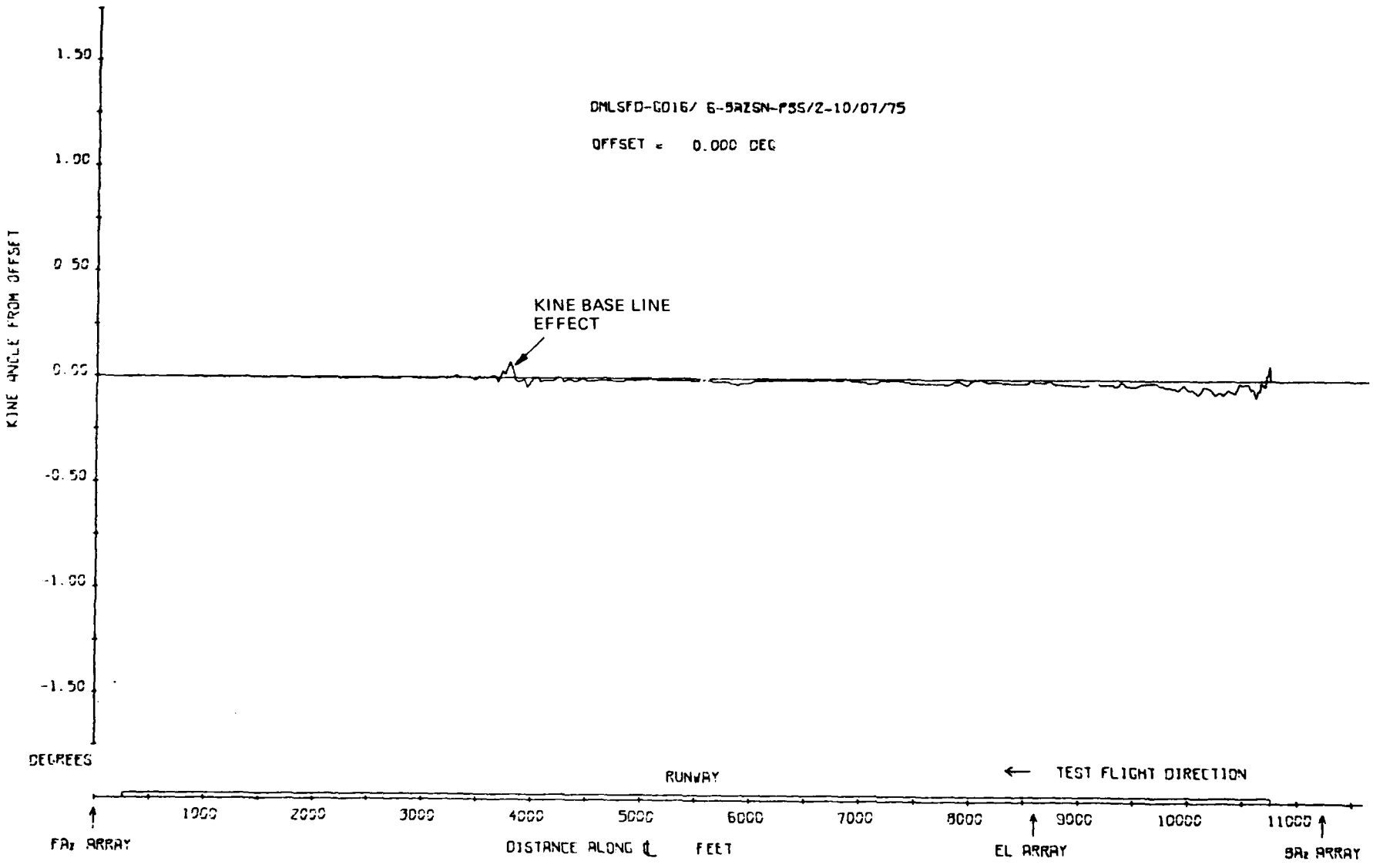

Fig 4.8a

Fig 4.8a Missed approach azimuth. Run along test runway centre line. Mast at 20 ft

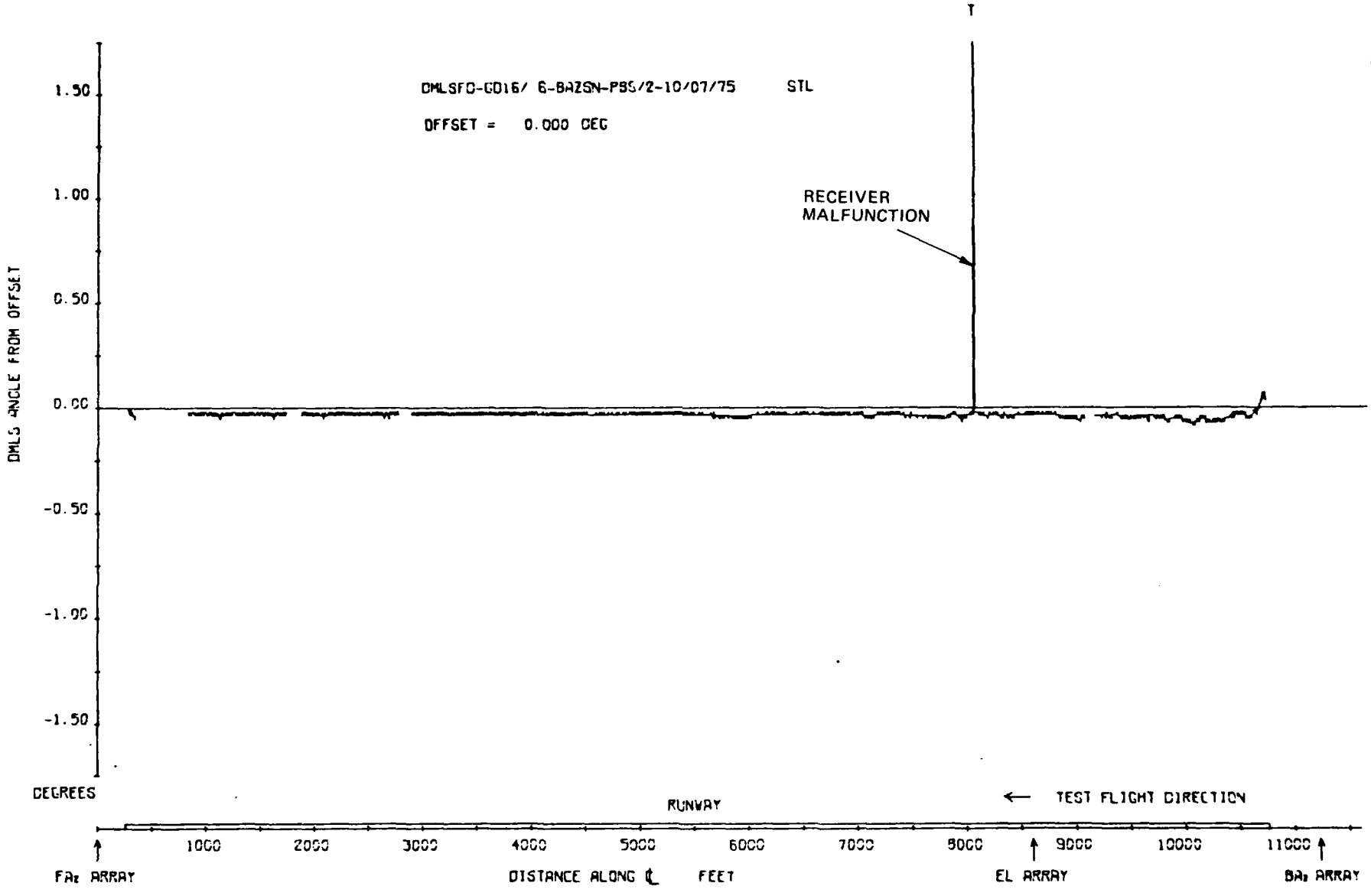

Fig 4.8b

Fig 4.8b Missed approach azimuth. Run along test runway centre line. Mast at 20 ft

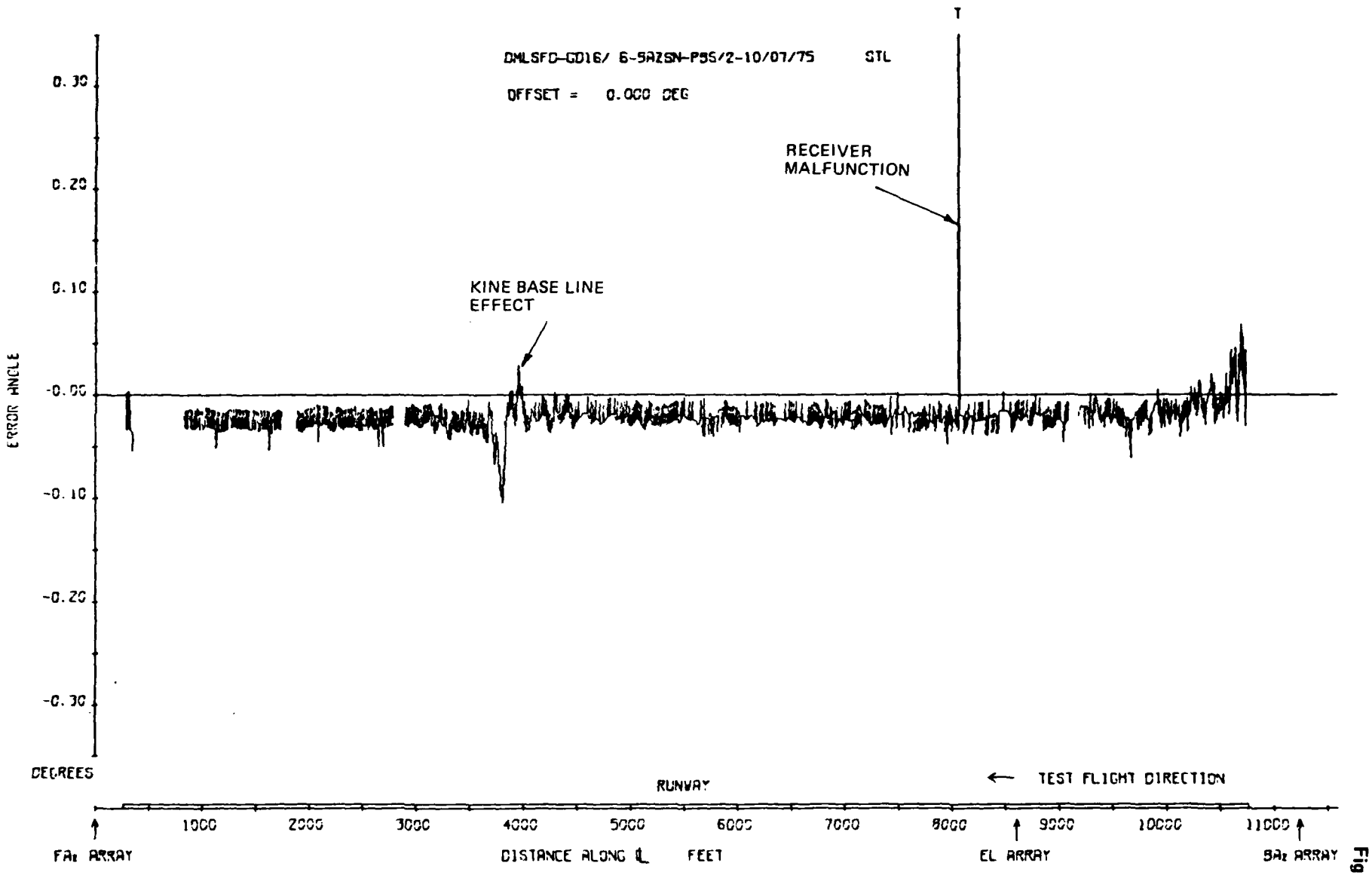

Fig 4.8c

Fig 4.8c Missed approach azimuth. Run along test runway centre line. Mast at 20 ft

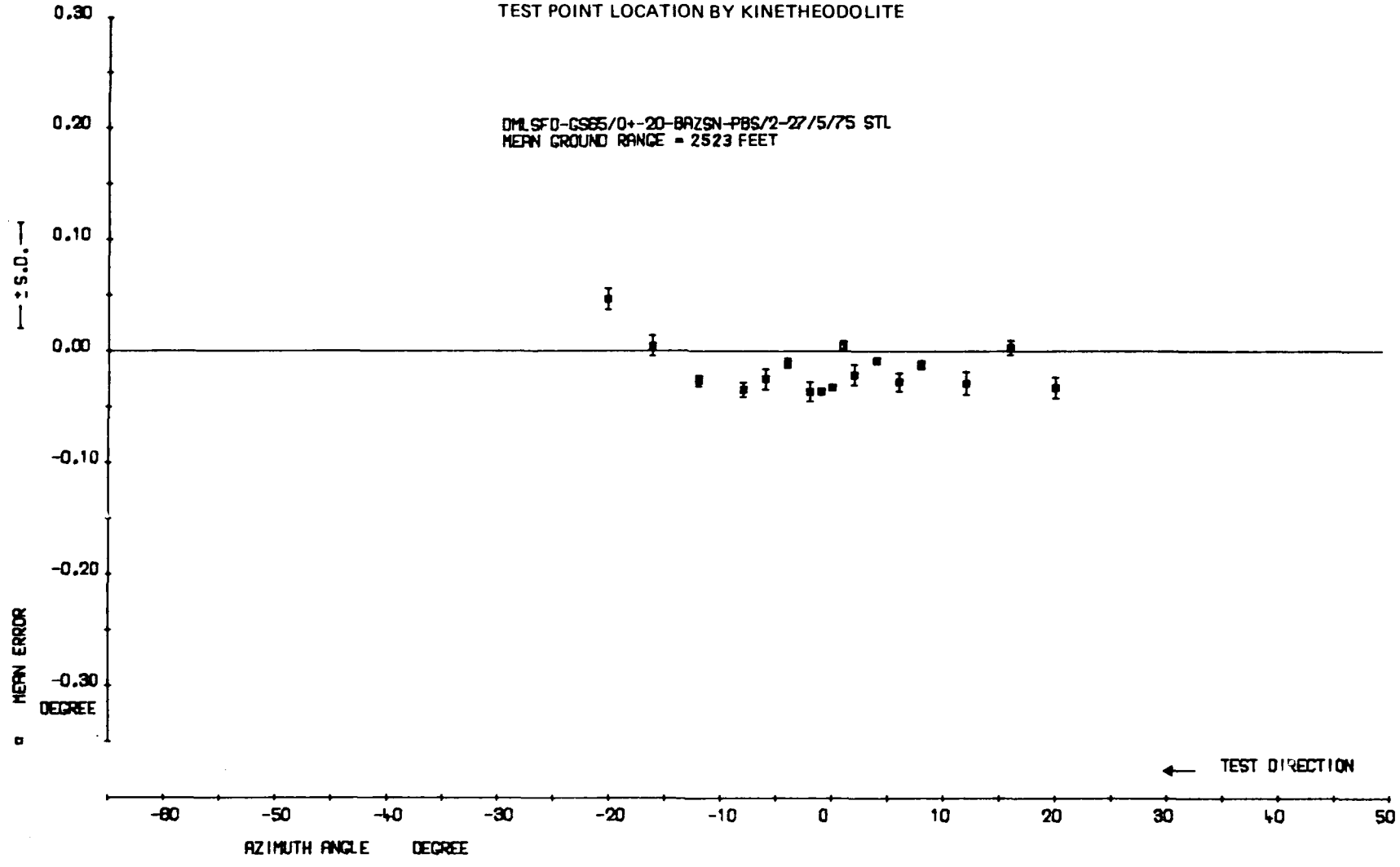

Fig 4.9 Missed approach azimuth cross runway test GS65

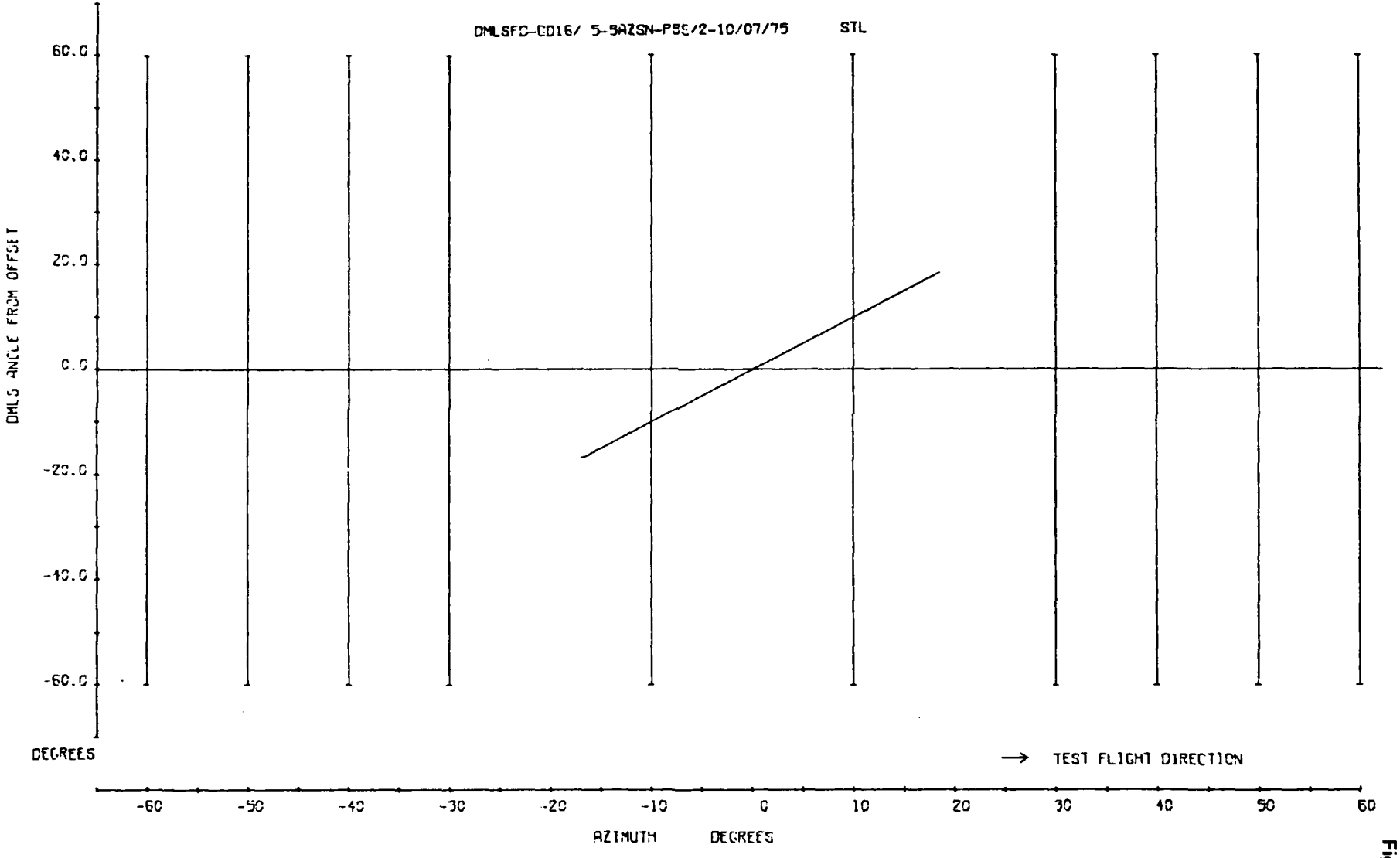

Fig 4.10a Missed approach azimuth. Vehicle run along cross road. Mast height 20 ft

Fig 4.10a

Fig 4.10b

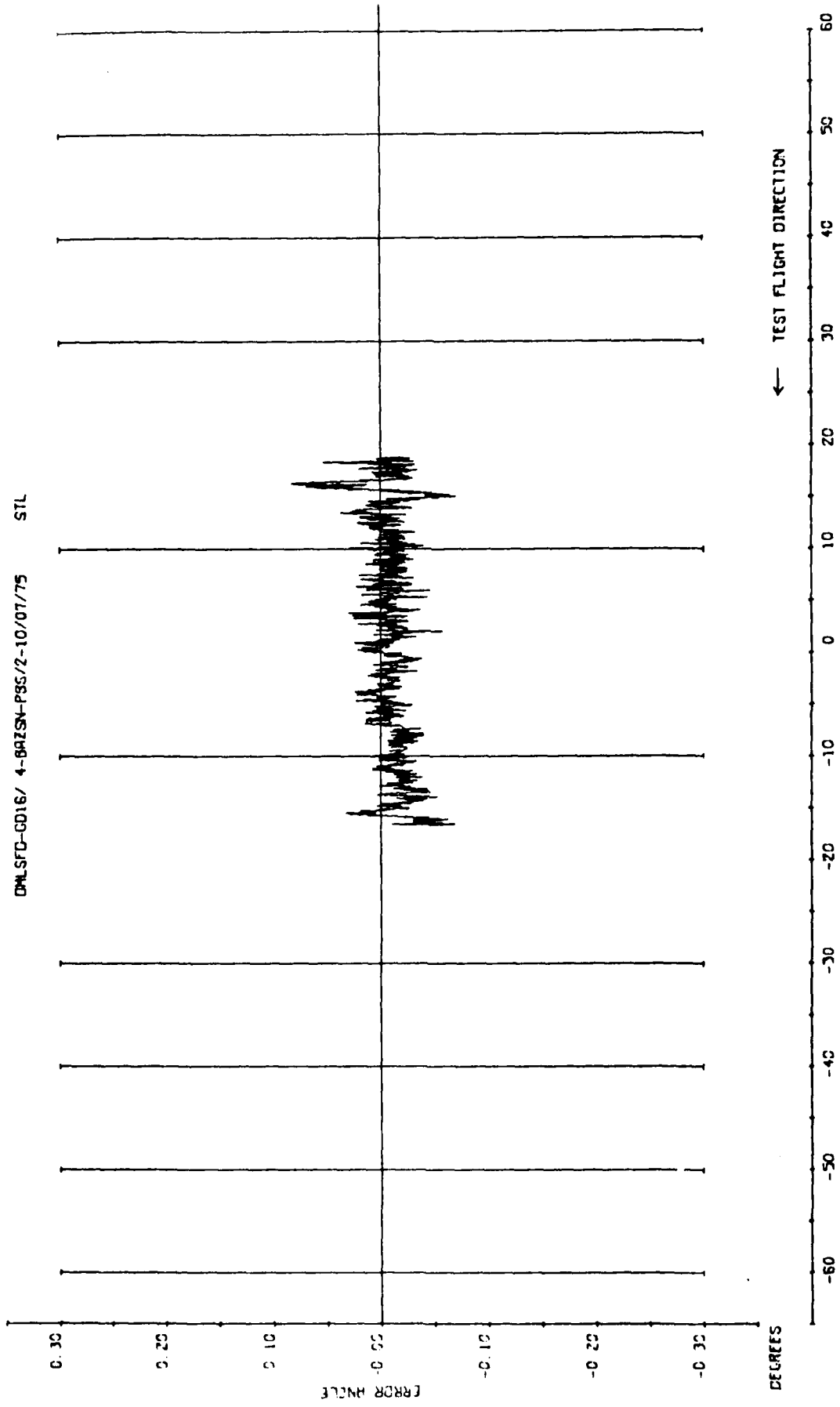

Fig 4.10b Missed approach azimuth. Vehicle run along cross road. Mast height 30 ft

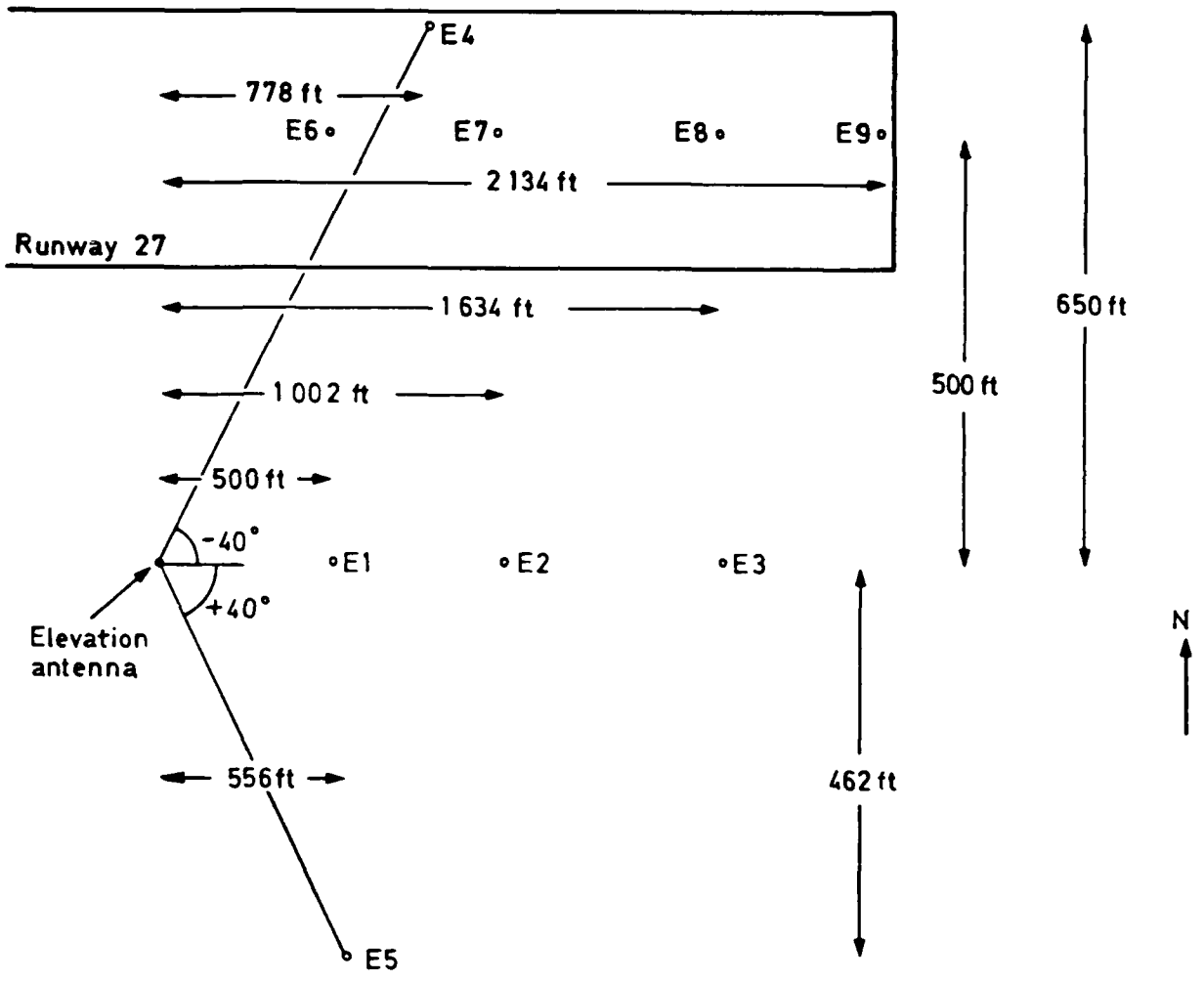

Fig 4.11 Elevation test points

Fig 4.11

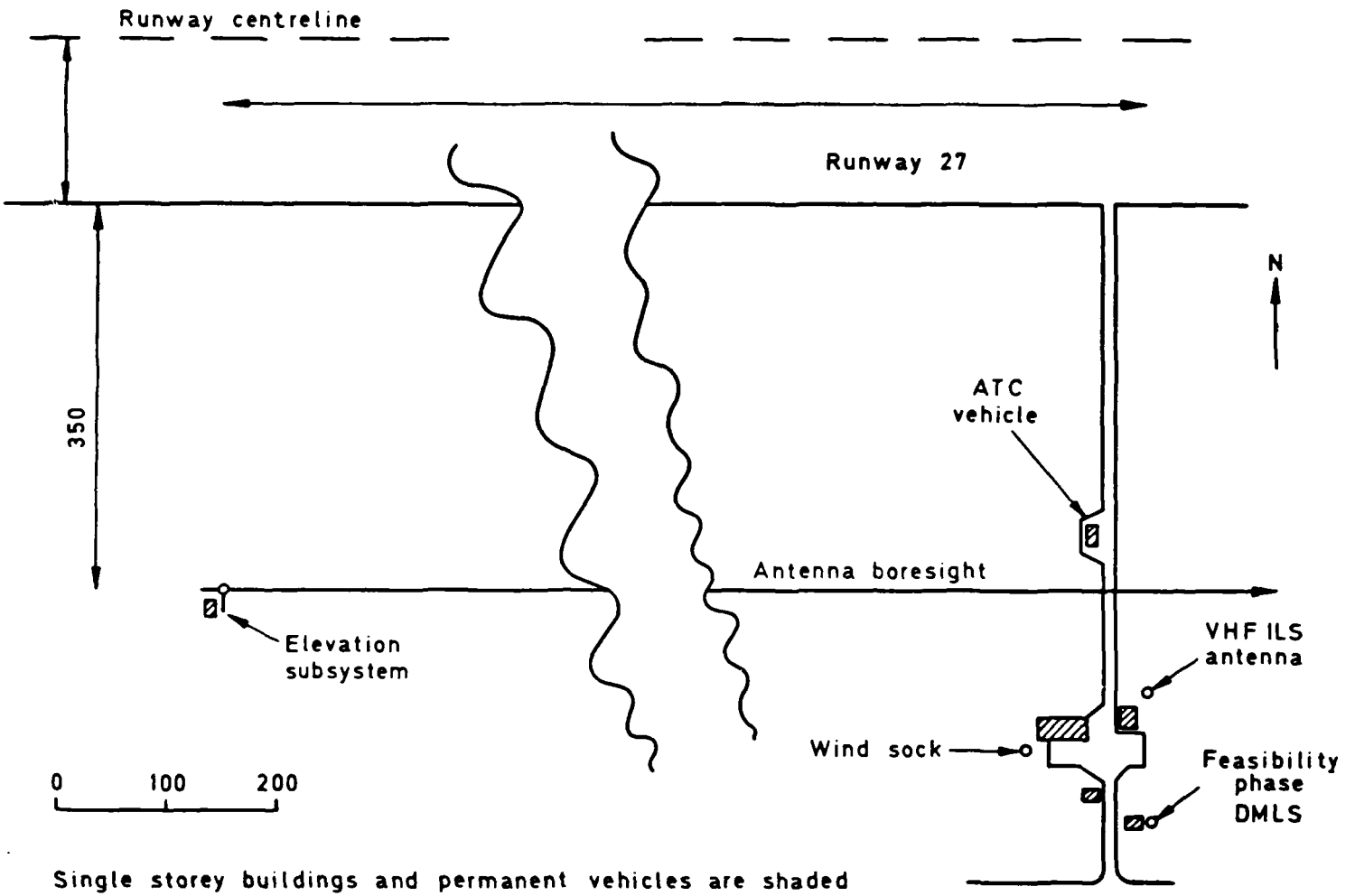

Fig 4.12 Elevation sub-system installation

Fig 4.12

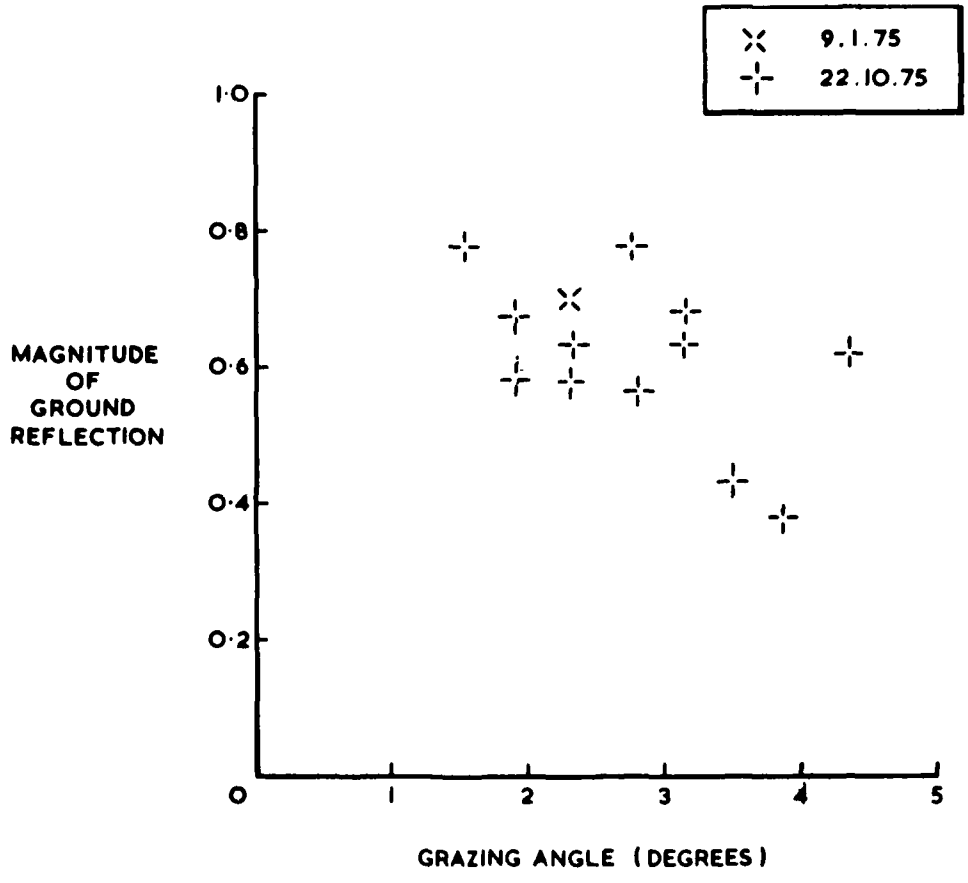

Fig 4.13 Magnitude of ground reflection in front of elevation transmitter. Range 1000 ft

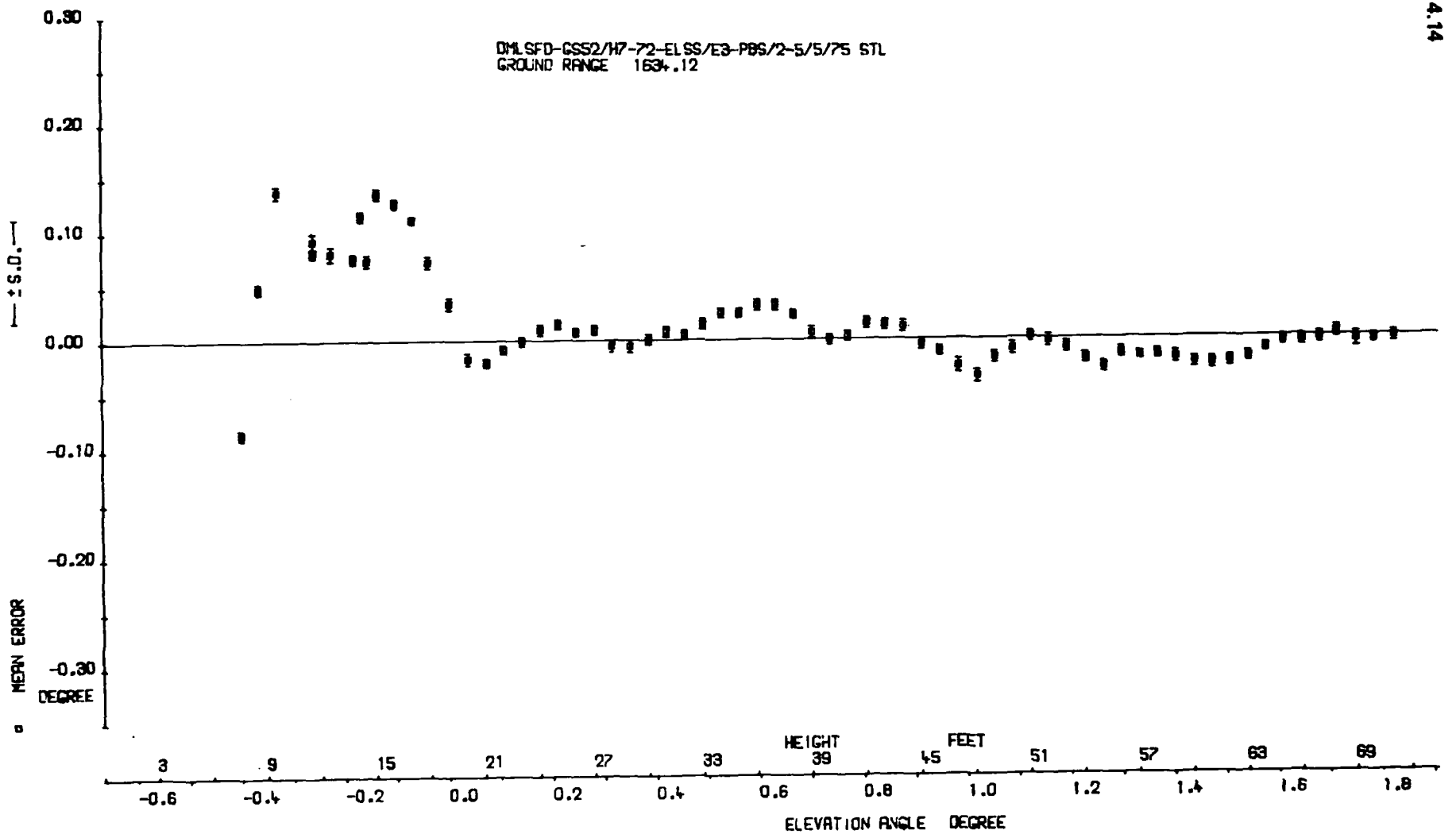

Fig 4.14 Elevation static test GS52, position E3

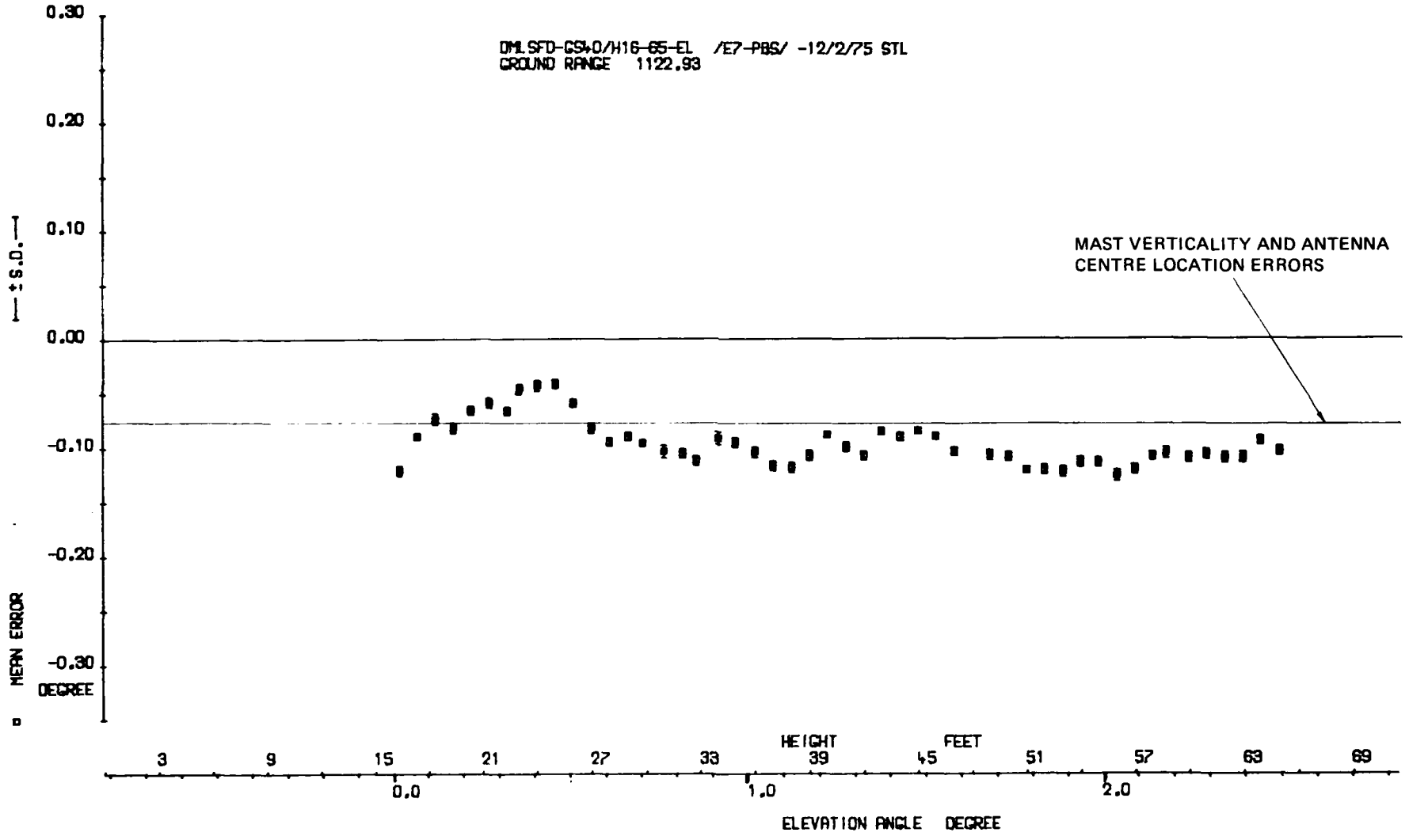

Fig 4.15a Elevation static test GS40, position E7

Fig 4.15a

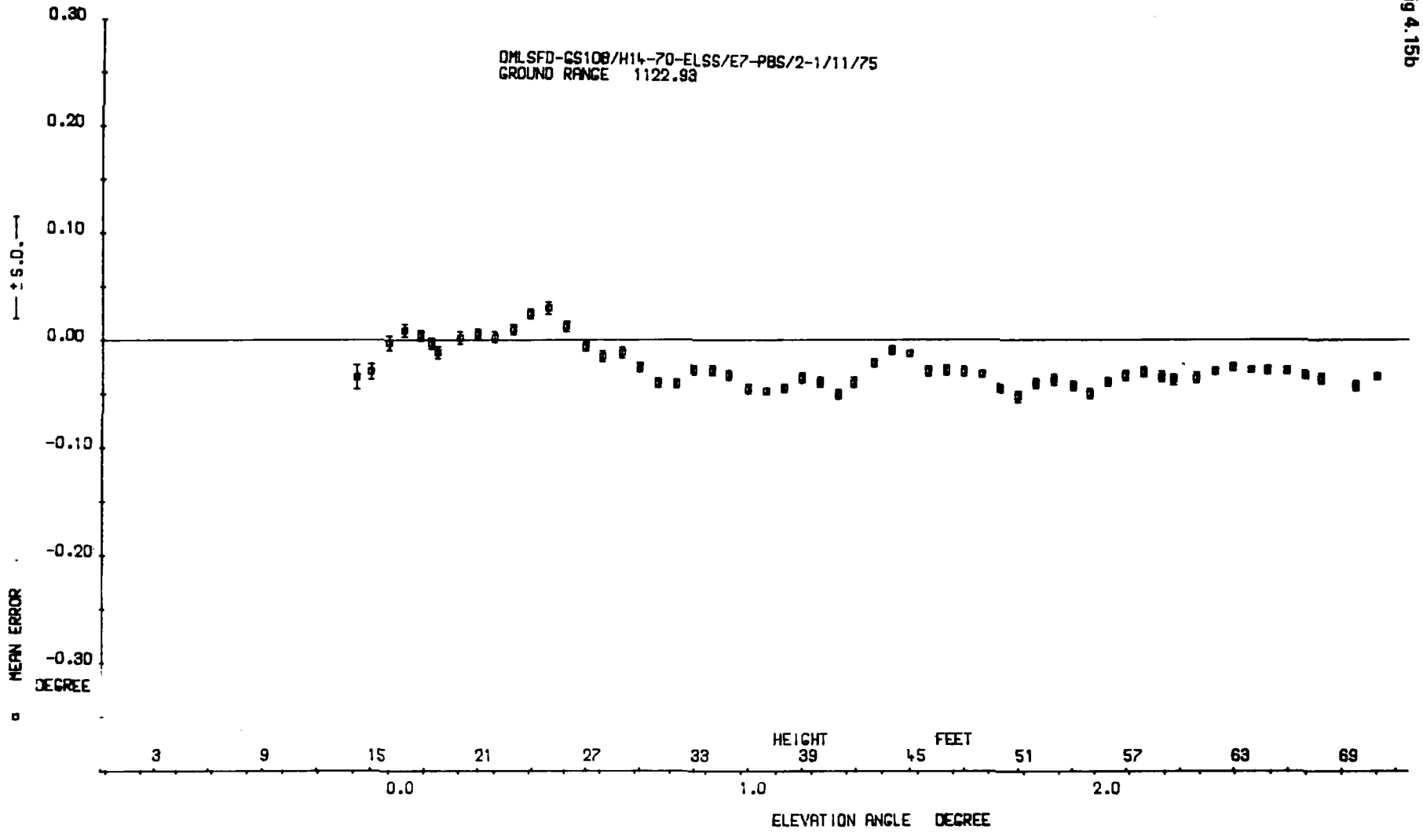

Fig 4.15b

Fig 4.15b Elevation static test GS108, position E7

TR 79052

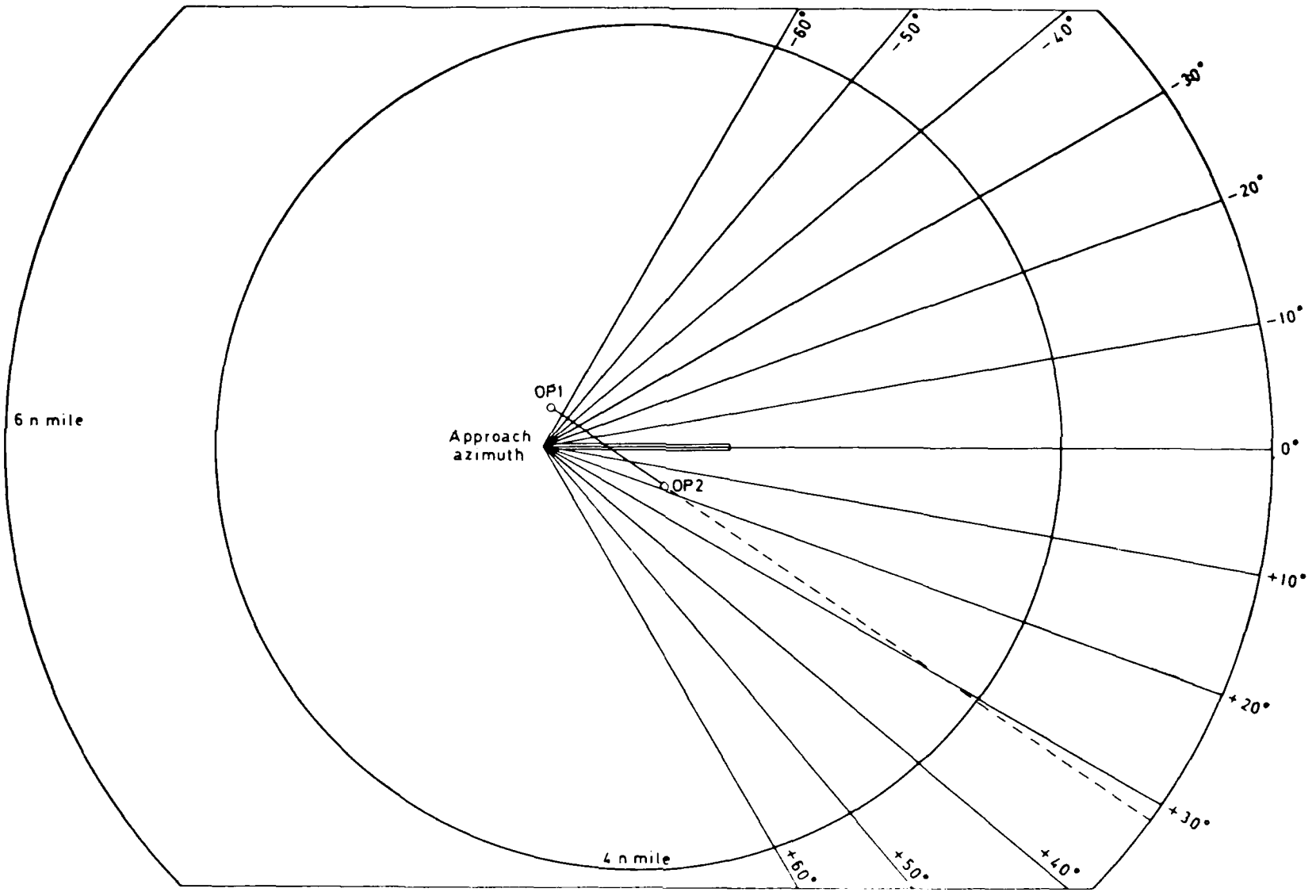

Fig 4.16a Kine base line in relation to approach azimuth flight paths

Fig 4.16a

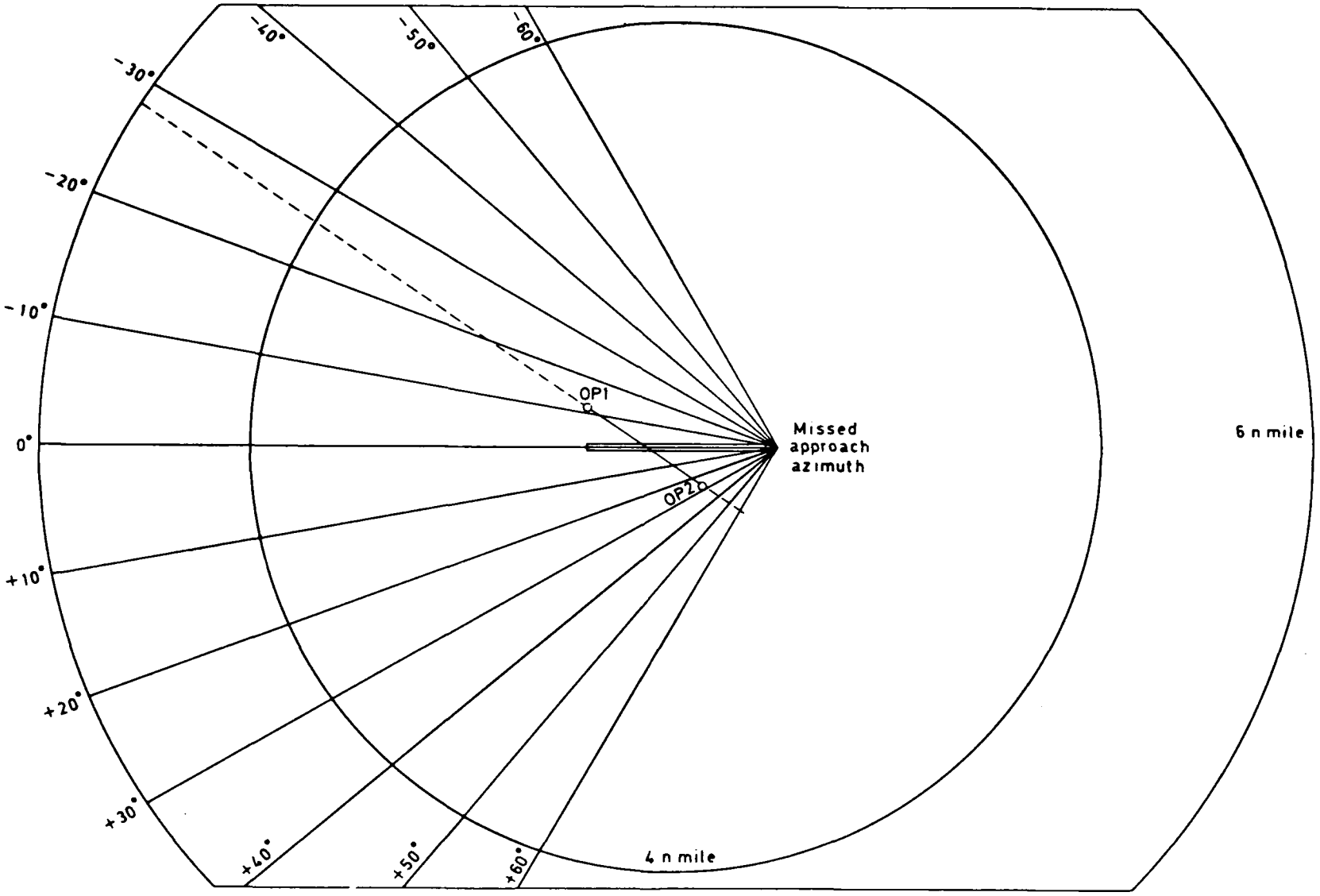

Fig 4.16b

Fig 4.16b Kine base line in relation to missed approach azimuth flight paths

TR 79052

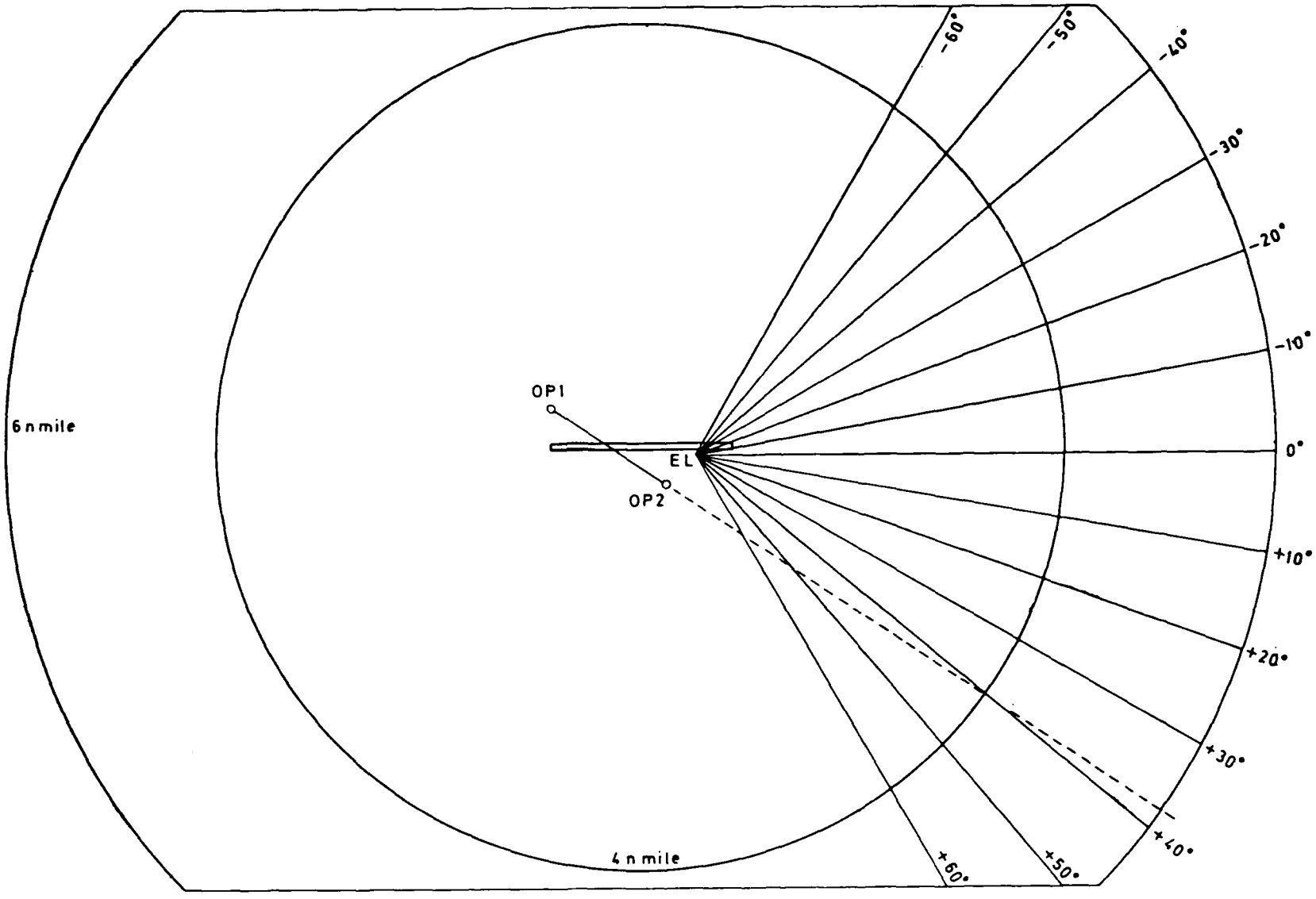

Fig 4.16c Kine base line in relation to elevation flight paths

Fig 4.16c

Fig 4.17

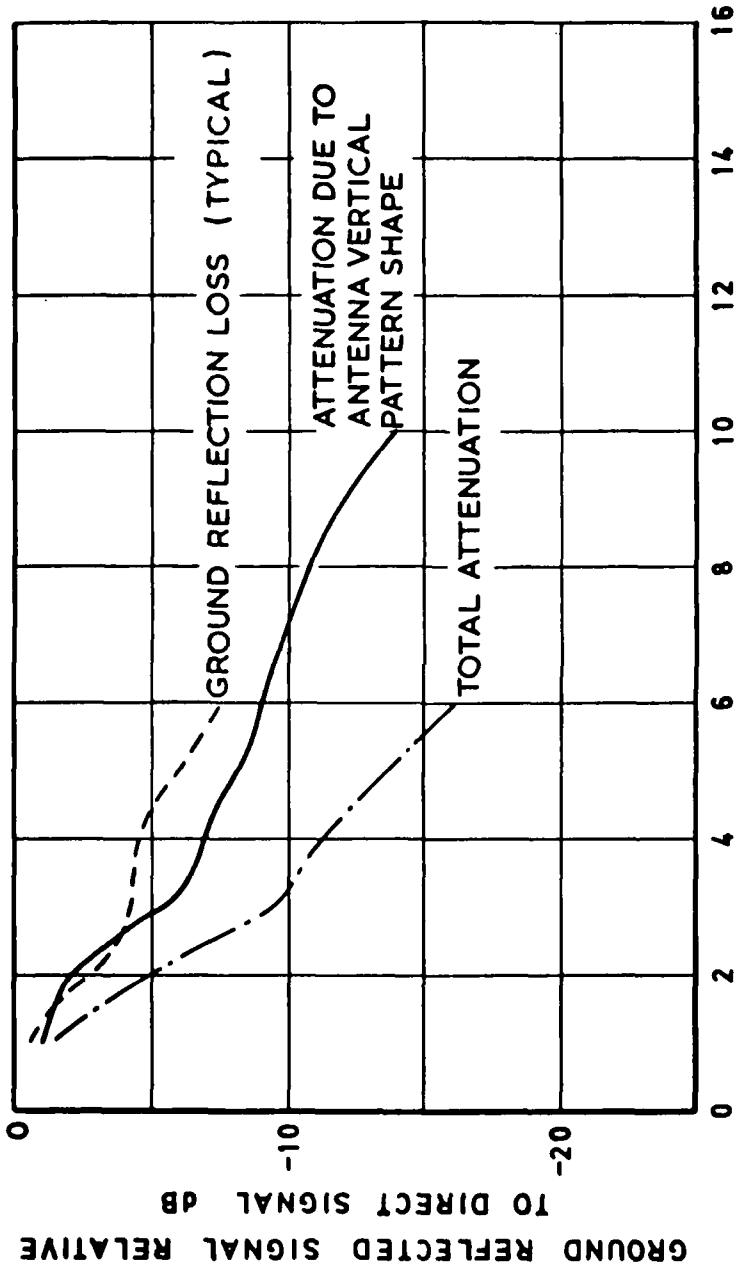

Fig 4.17 Estimated ground reflected signal for azimuth ground plane antenna

TR 79052

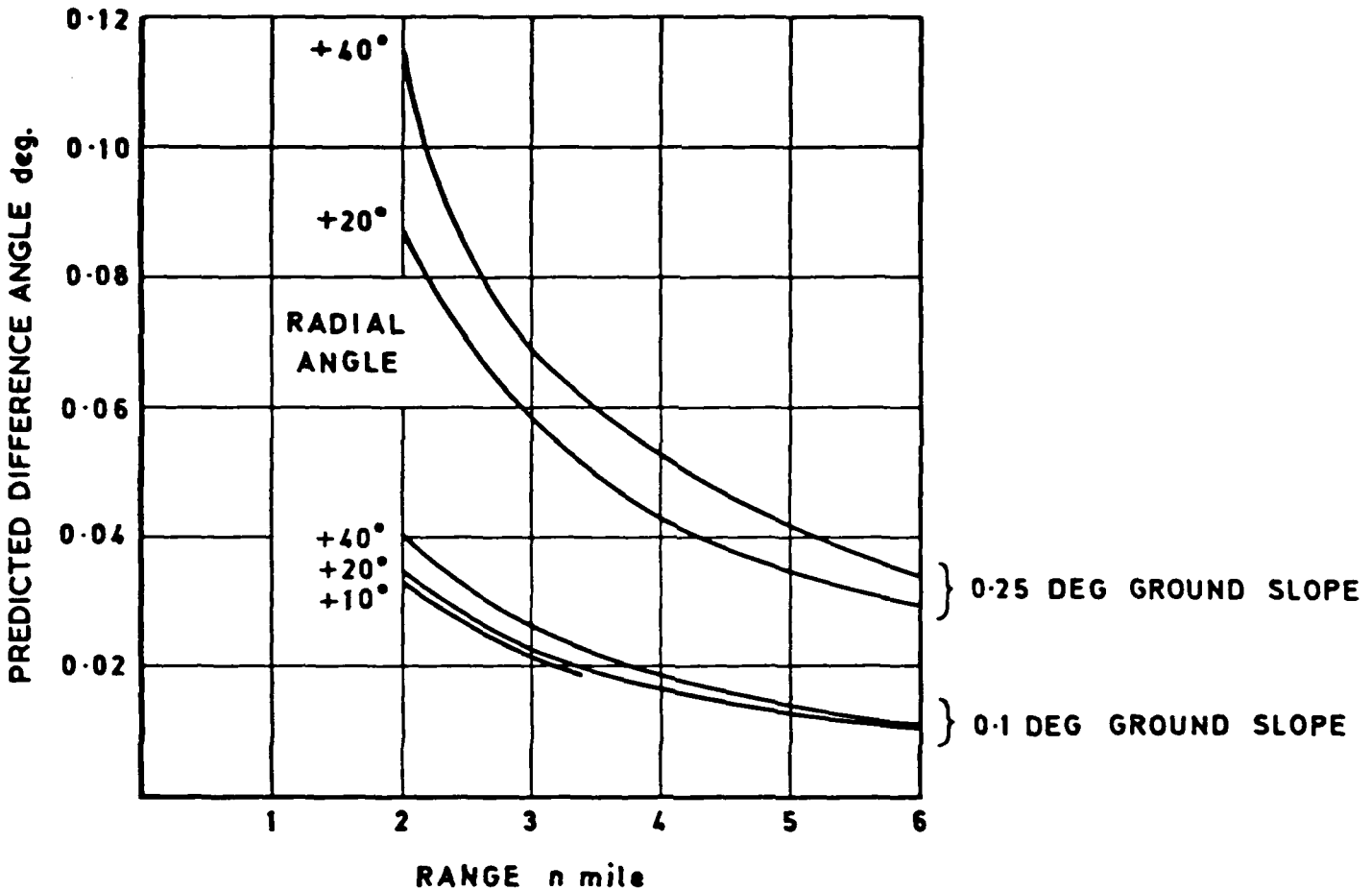

Fig 4.18 Predicted code angle difference between direct and ground reflected signal for 0.1 and 0.25 degree lateral slope during 2000 ft constant height radials

Fig 4.18

Fig 4.19

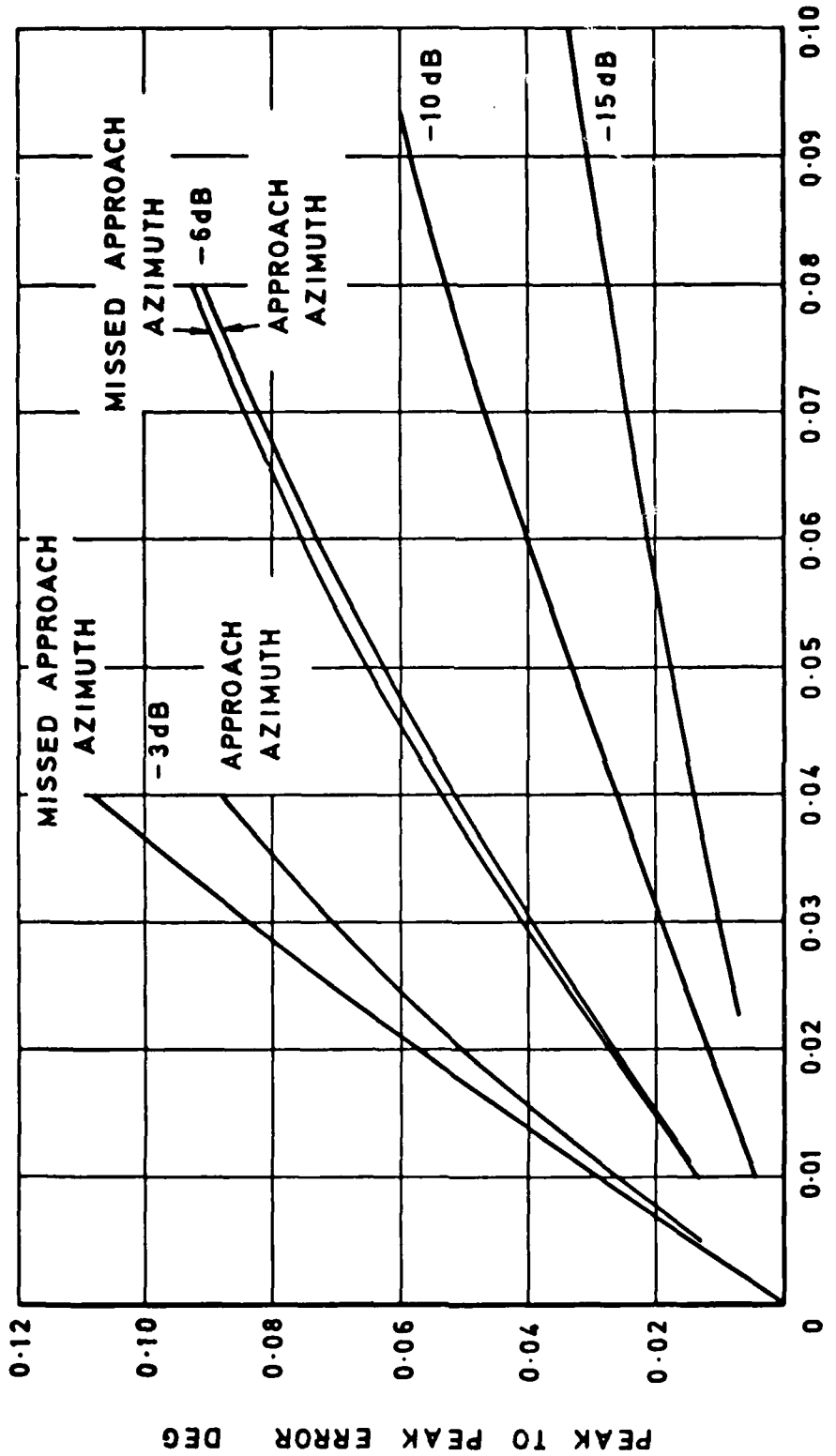

Fig 4.19 Calculated peak to peak error as a function of offset angle between direct and interfering signal

TR 79052

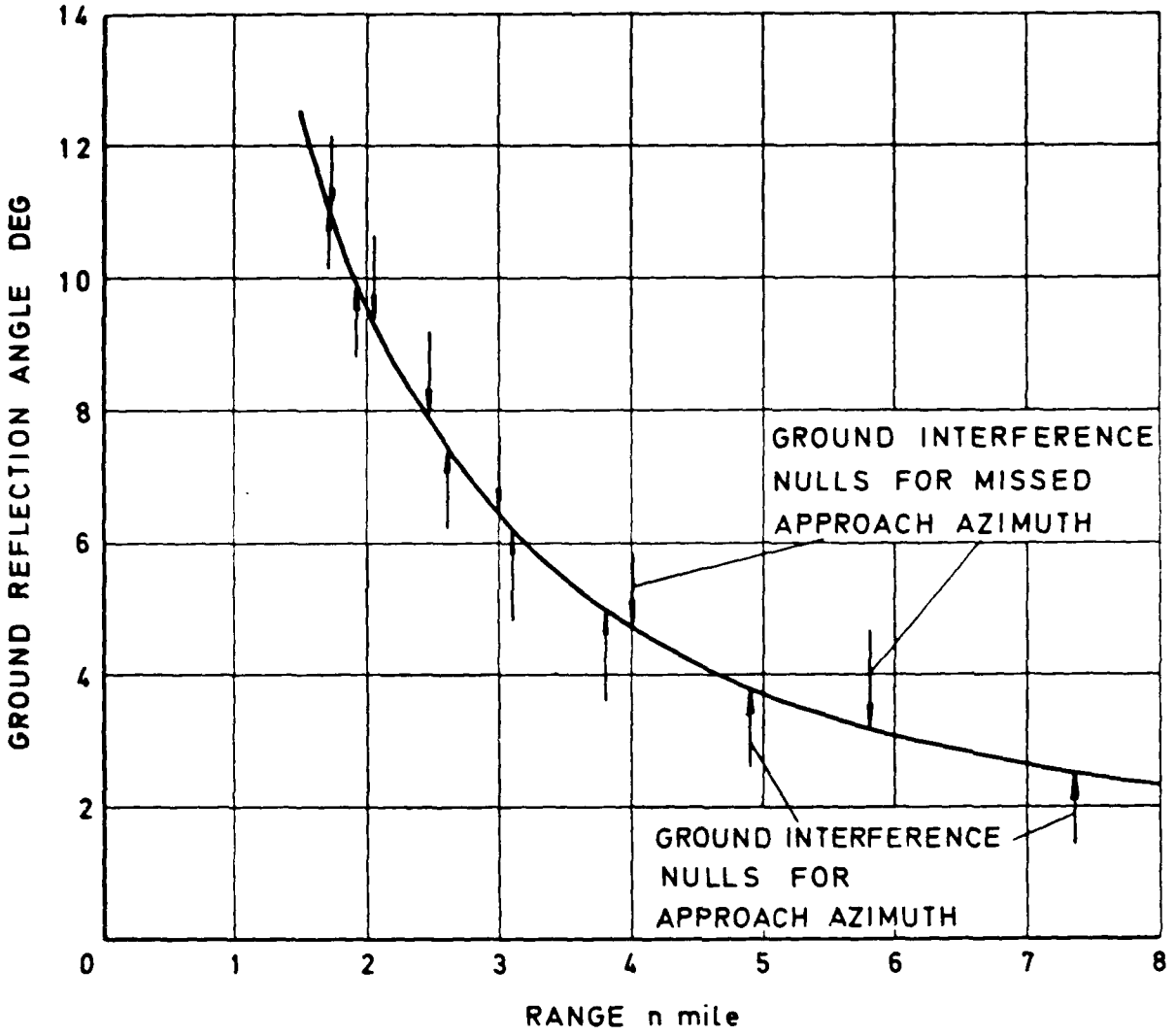

TR 79052

Fig 4.20 Elevation angle and ground interference nulls for 2000 ft constant height radials

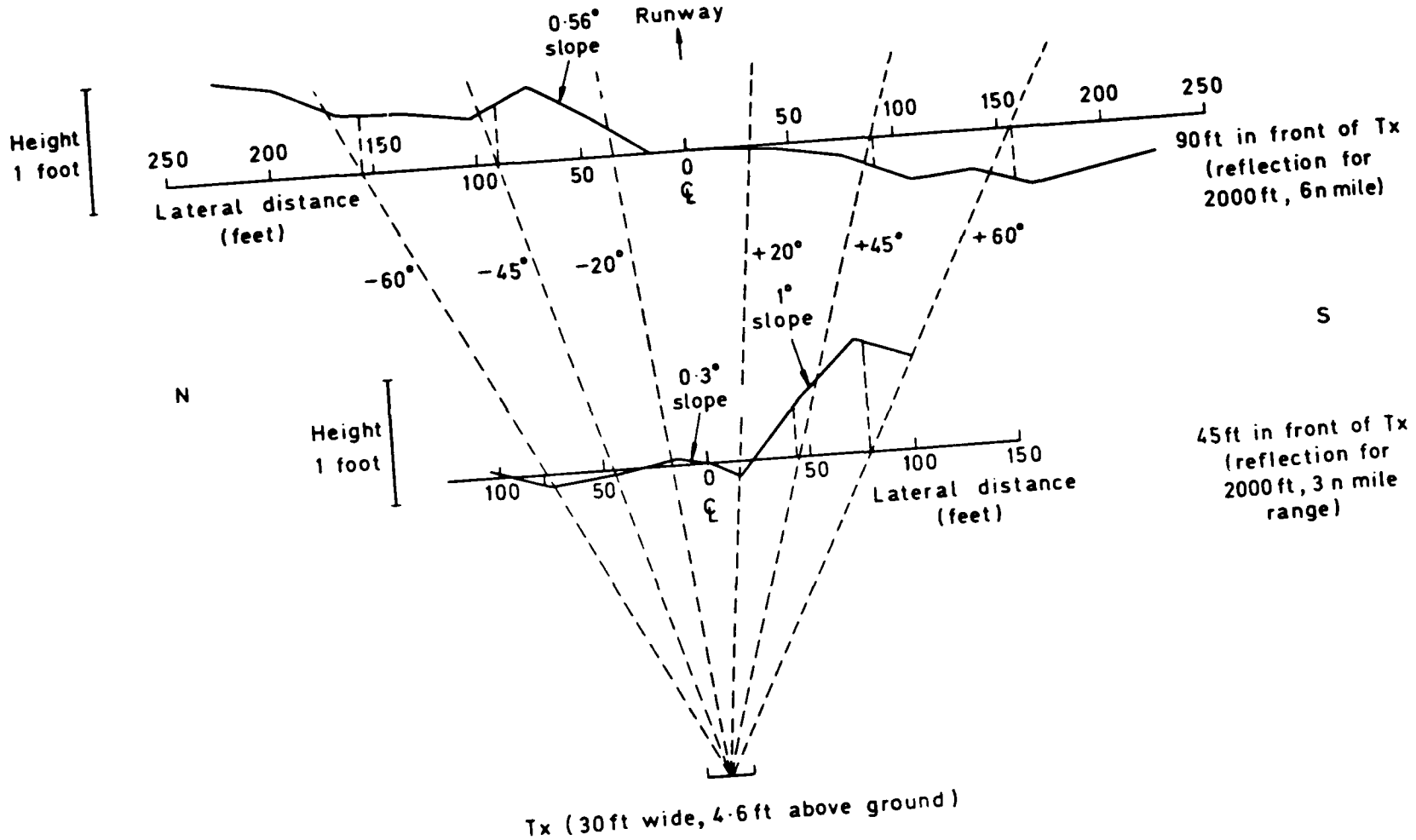

Fig 4.21a Lateral ground slope in front of approach azimuth transmitter

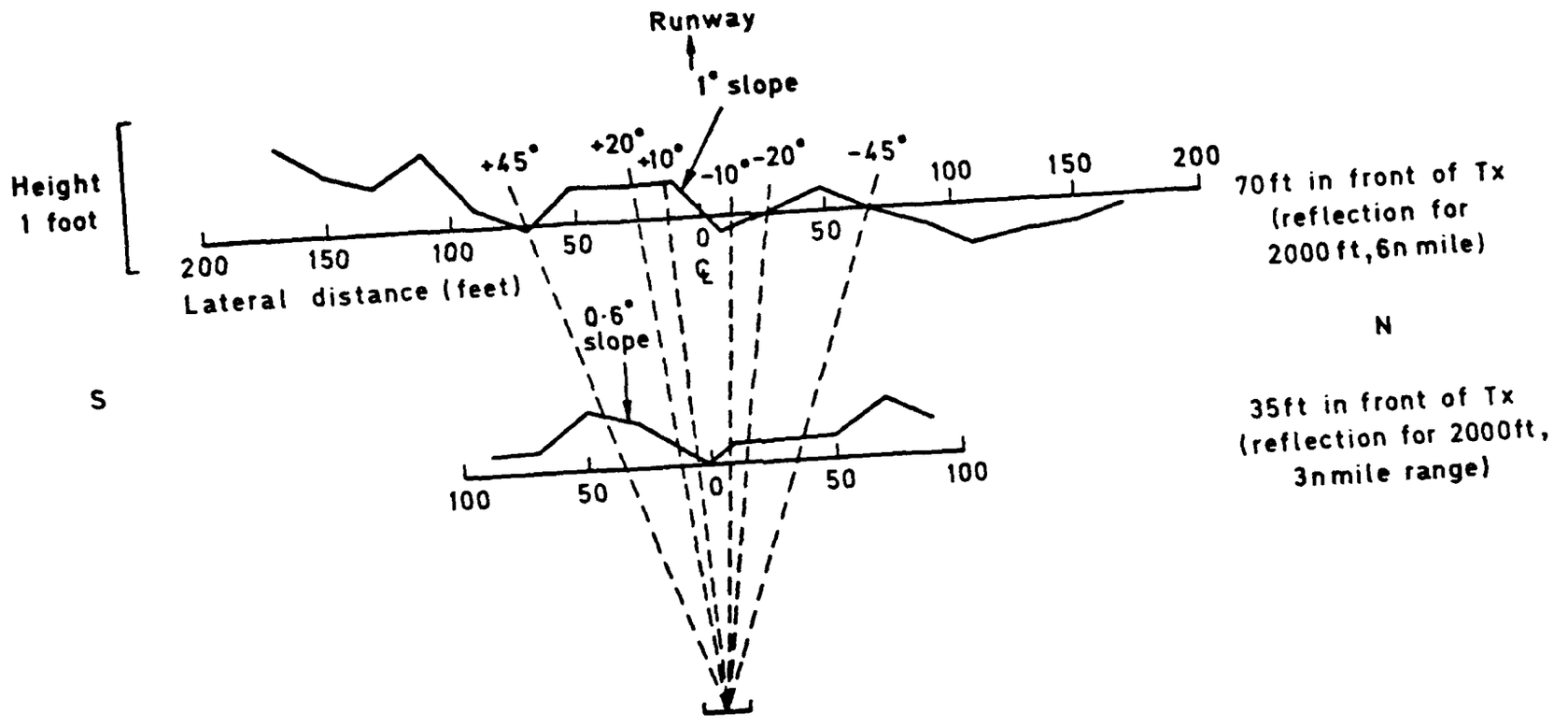

Fig 4.21b Lateral ground slope in front of missed approach azimuth transmitter

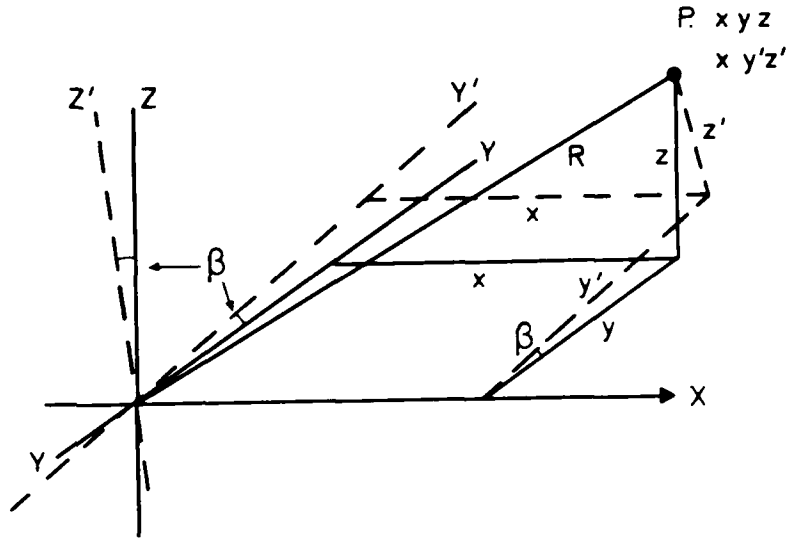

True azimuth code angle = ϕ

$\cos \phi = \frac{y}{R}$

Tilted array axis is $Y'Y'$

Array code angle = ϕ'

$$\cos \phi' = \frac{y'}{R} = \frac{1}{R}\left[\frac{y}{\cos\beta} + (Z - y\tan\beta)\sin\beta\right]$$

$$= \frac{1}{R}\left[Z\sin\beta + y\left(\frac{1-\sin^2\beta}{\cos\beta}\right)\right]$$

$$= \frac{1}{R}(Z\sin\beta + y\cos\beta)$$

$$= \sin\theta\sin\beta + \cos\phi\cos\beta$$

Fig 4.22 Azimuth antenna tilt errors

TR 79052

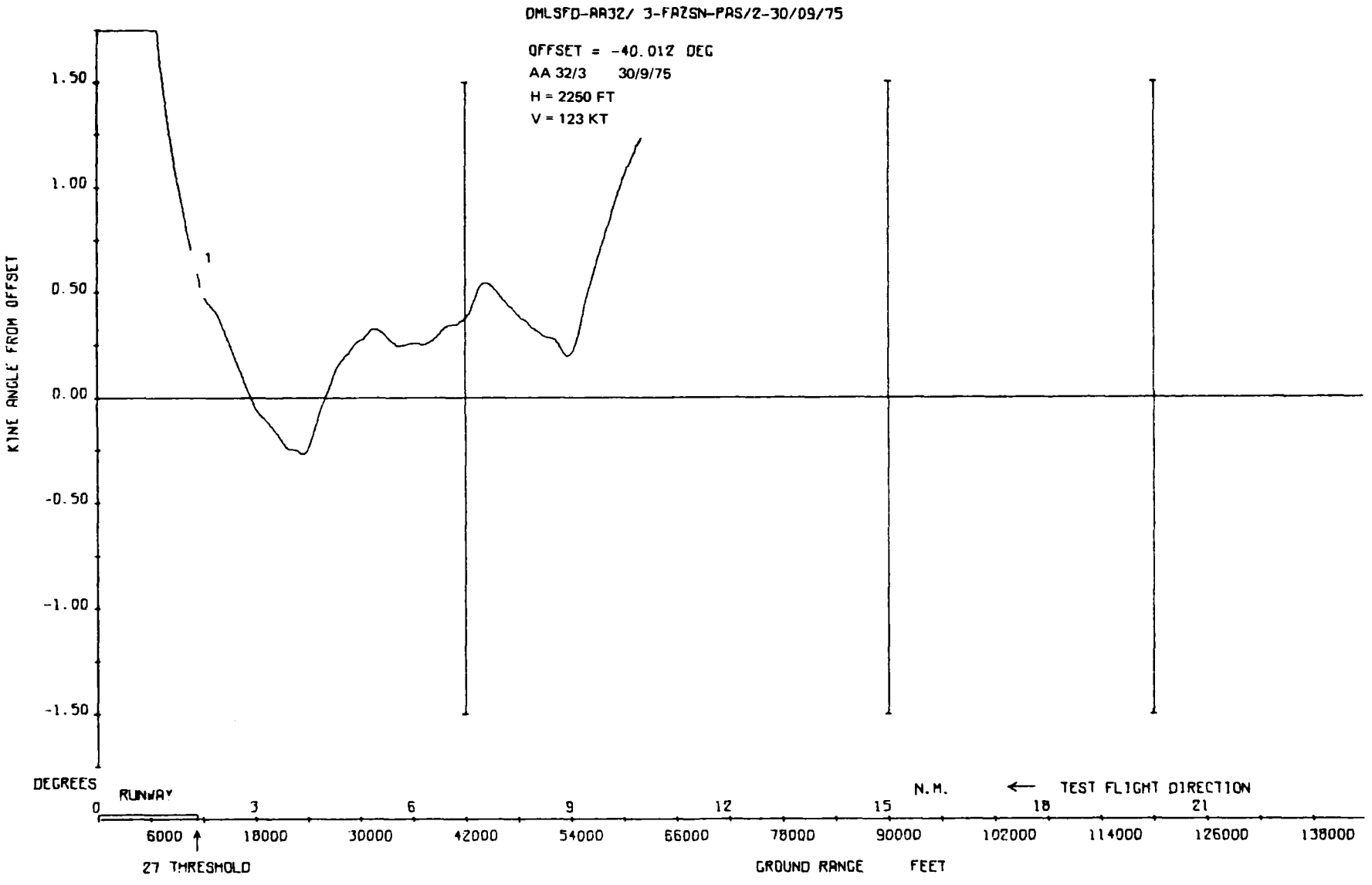

Fig 4.23a Approach azimuth radial at —40 degrees

Fig 4.23a

Fig 4.23c

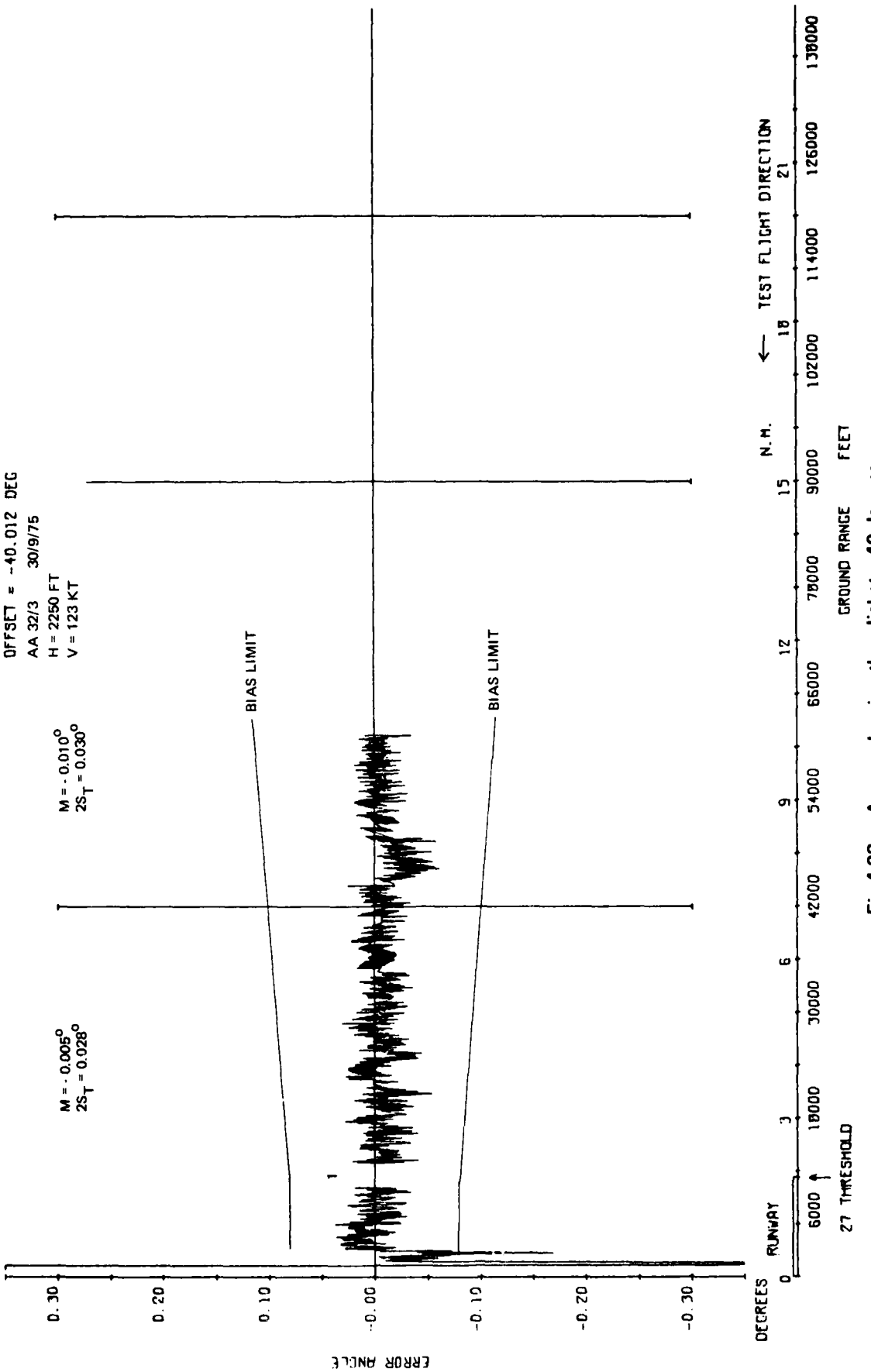

Fig 4.23c Approach azimuth radial at —40 degrees

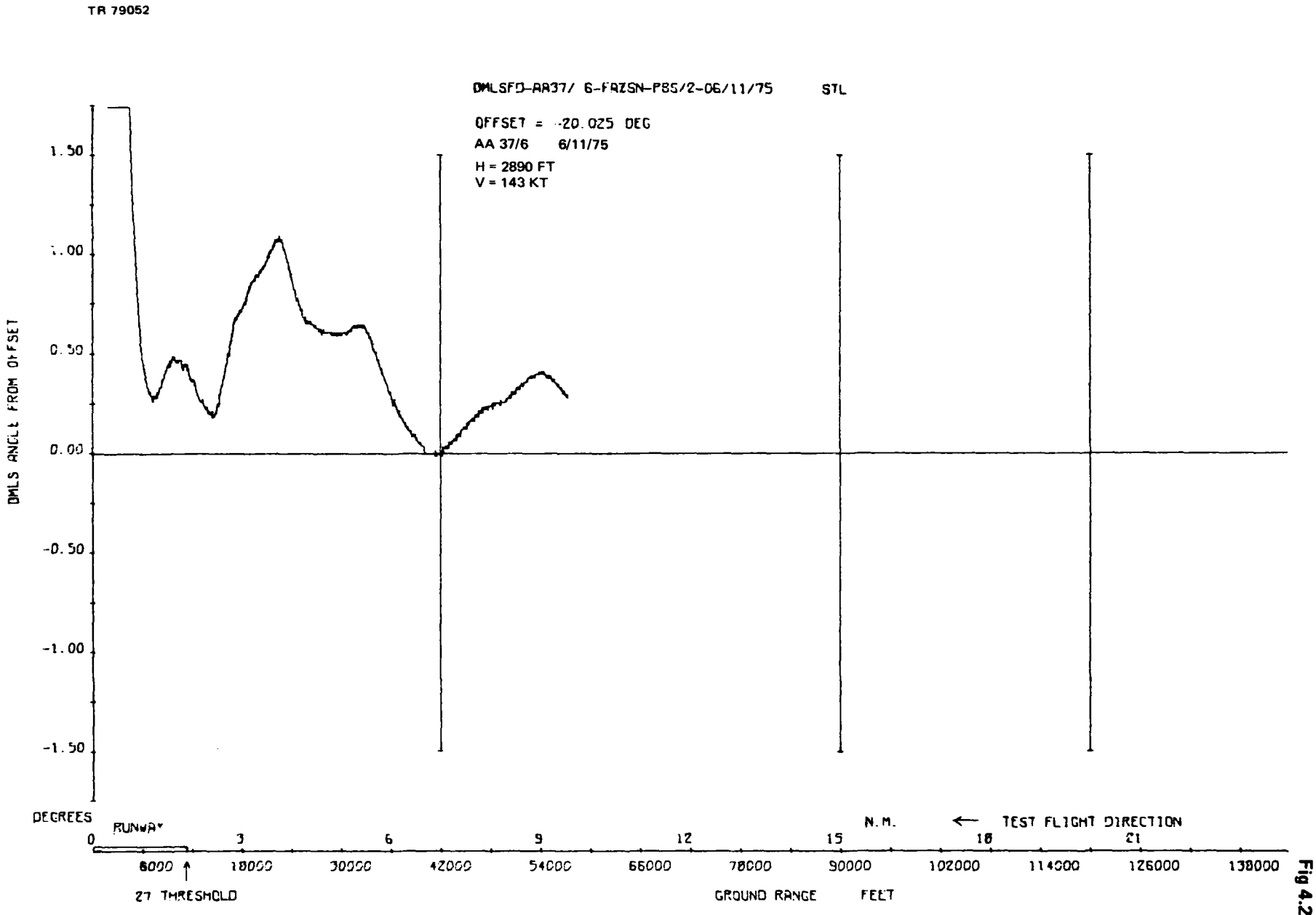

Fig 4.24b

Fig 4.24b Approach azimuth radial at –20 degrees

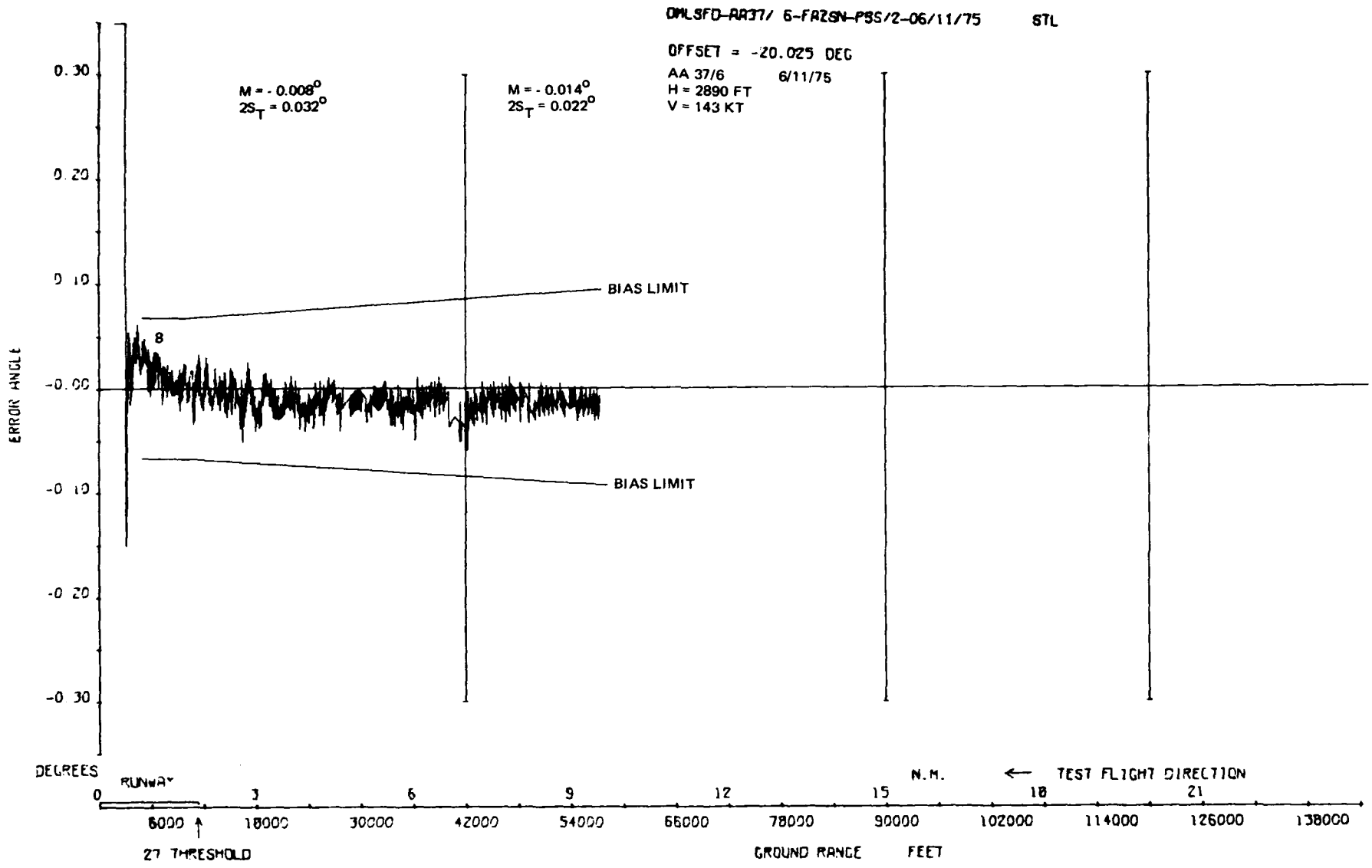

Fig 4.24c

Fig 4.24c Approach azimuth radial at −20 degrees

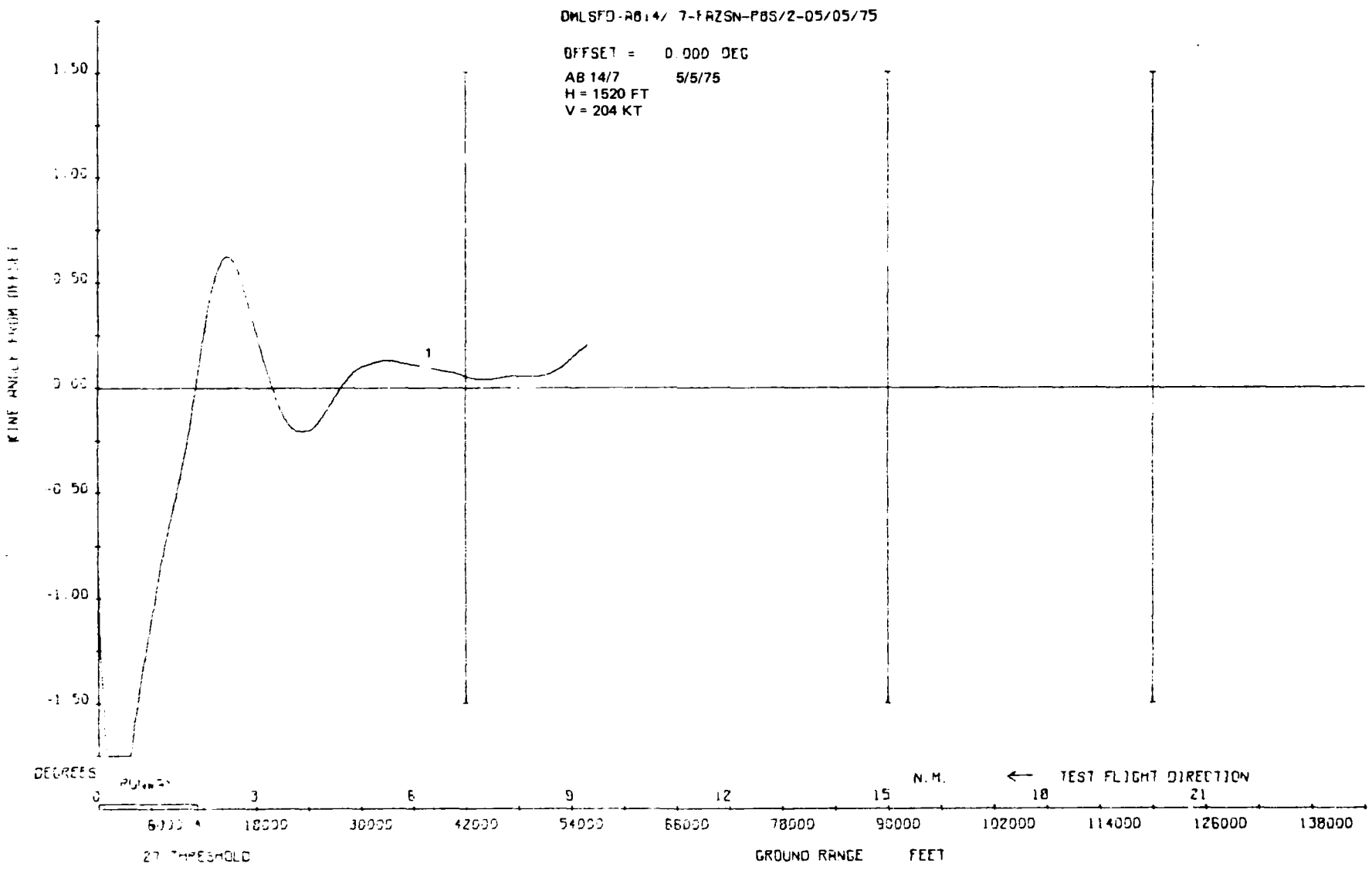

Fig 4.25a

Fig 4.25a Approach azimuth radial at 0 degree

Fig 4.25c

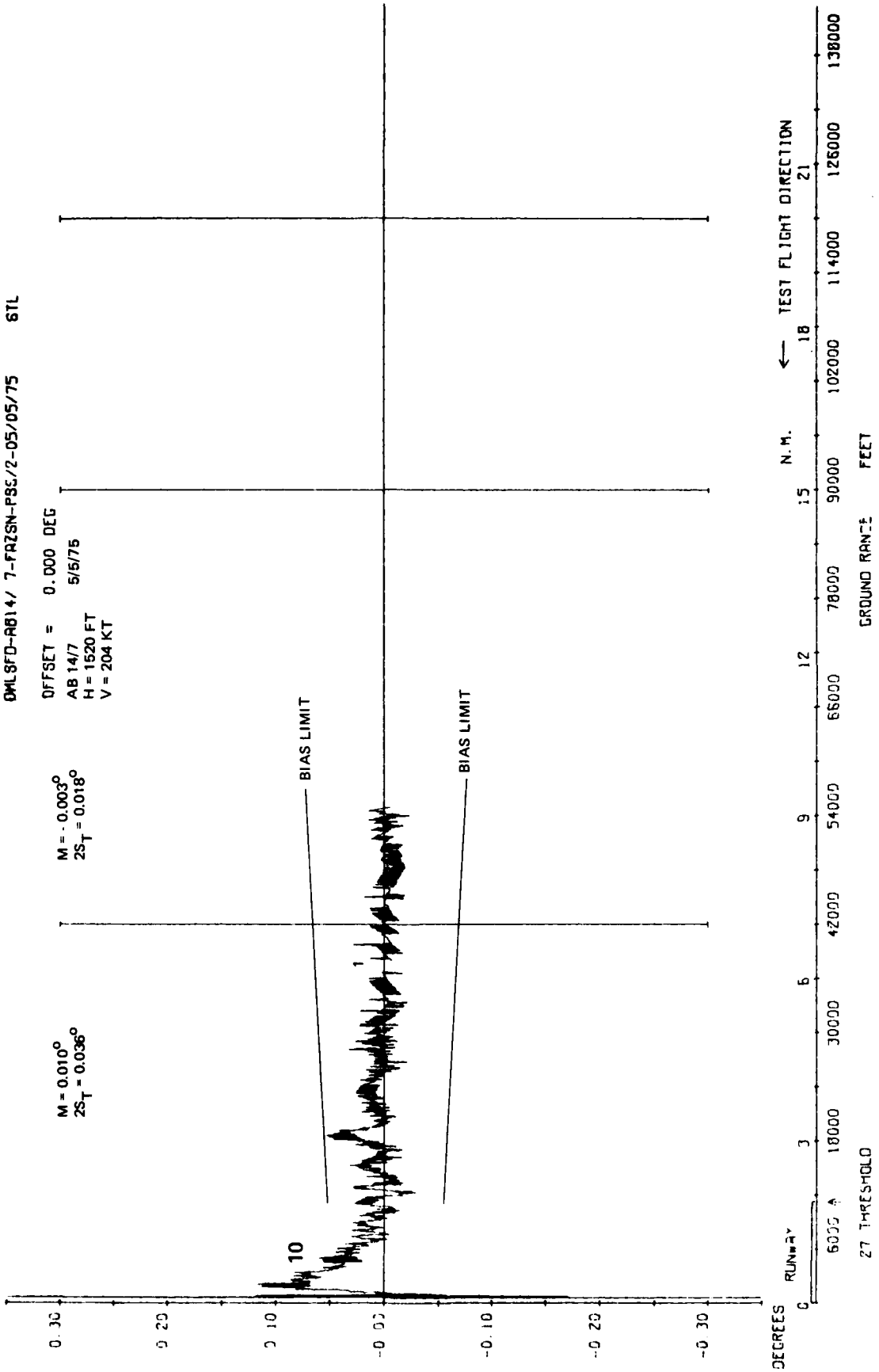

Fig 4.25c Approach azimuth radial at 0 degree

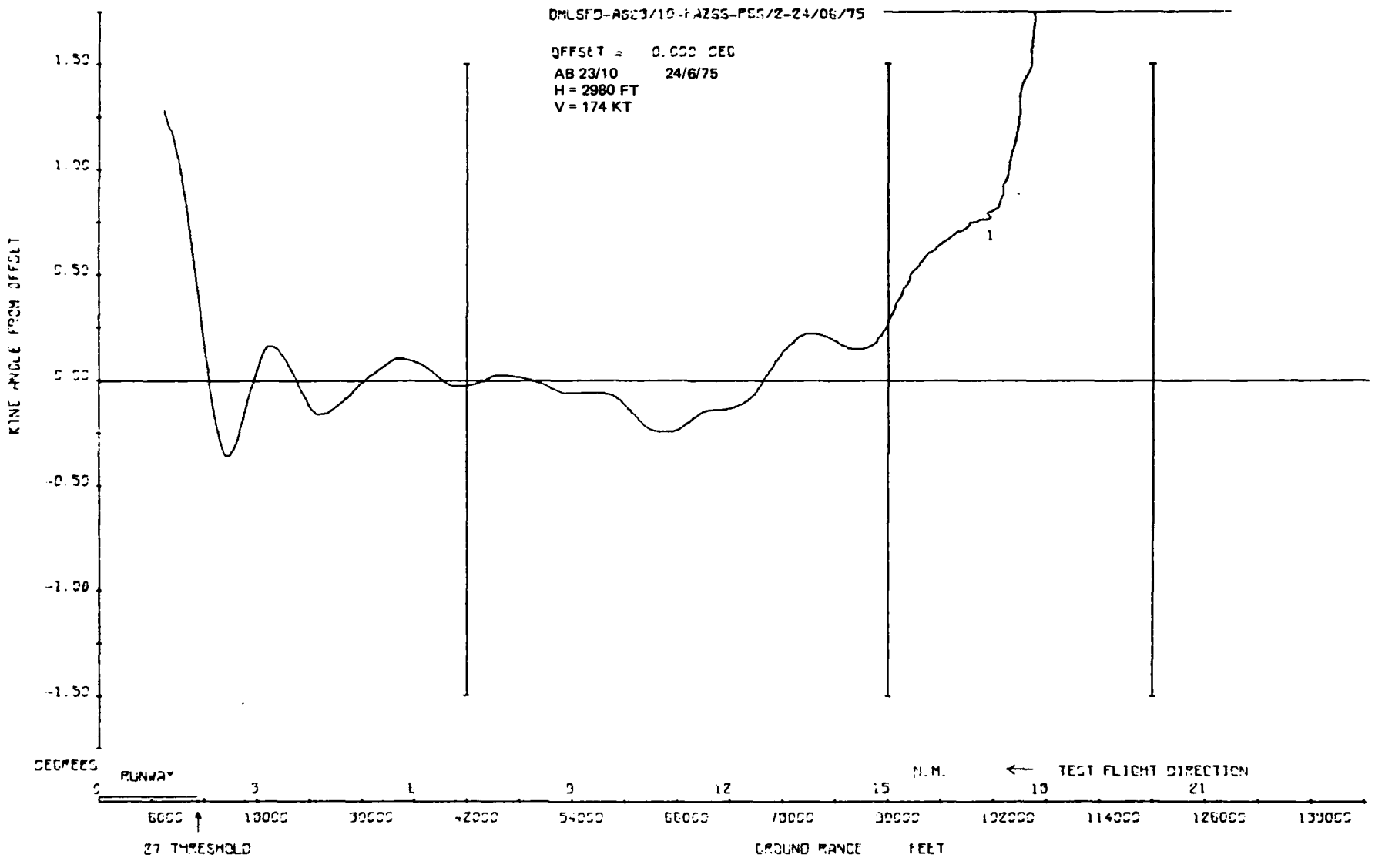

Fig 4.26a

Fig 4.26a Approach azimuth radial at 0 degree

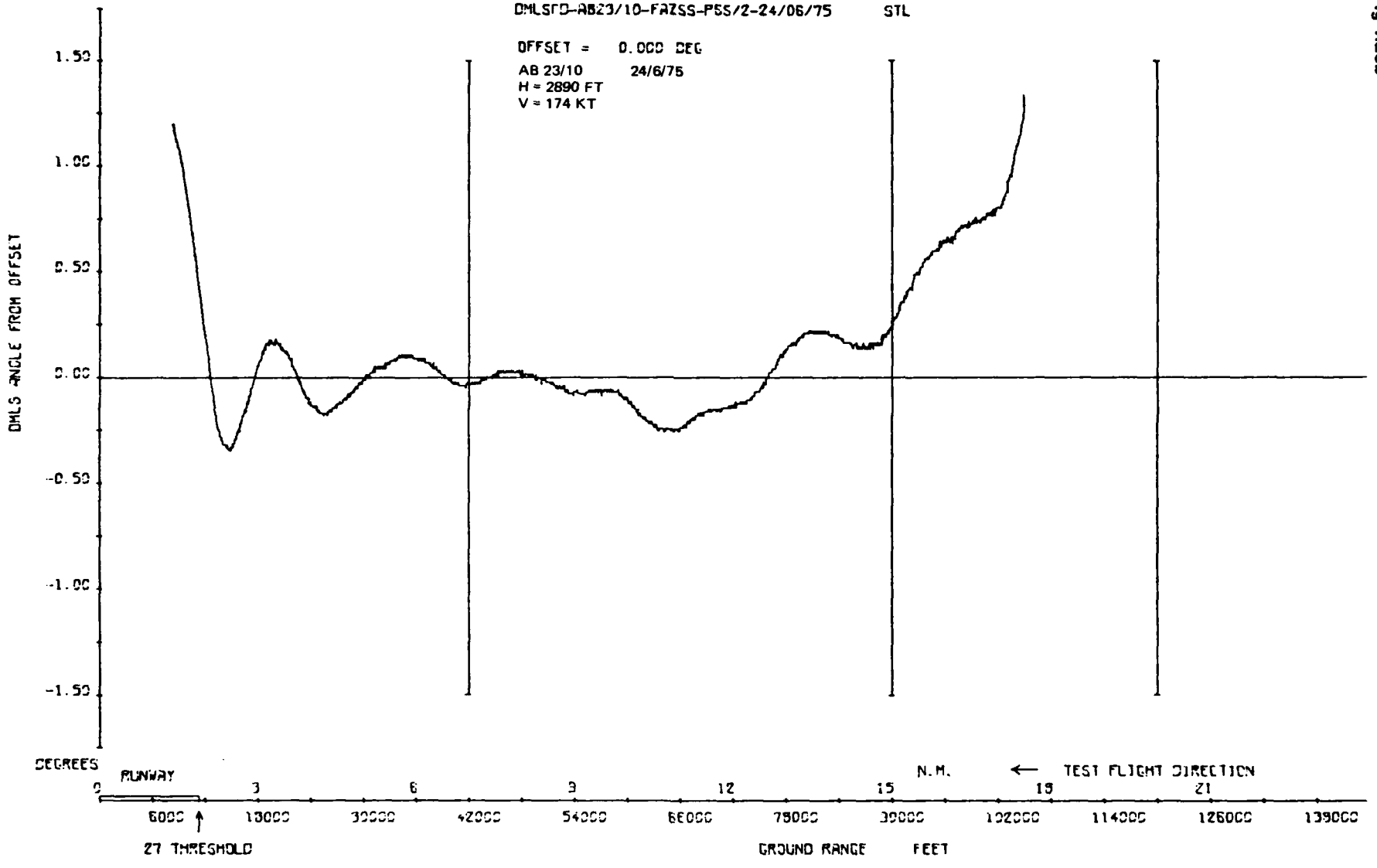

Fig 4.26b

Fig 4.26b Approach azimuth radial at 0 degree

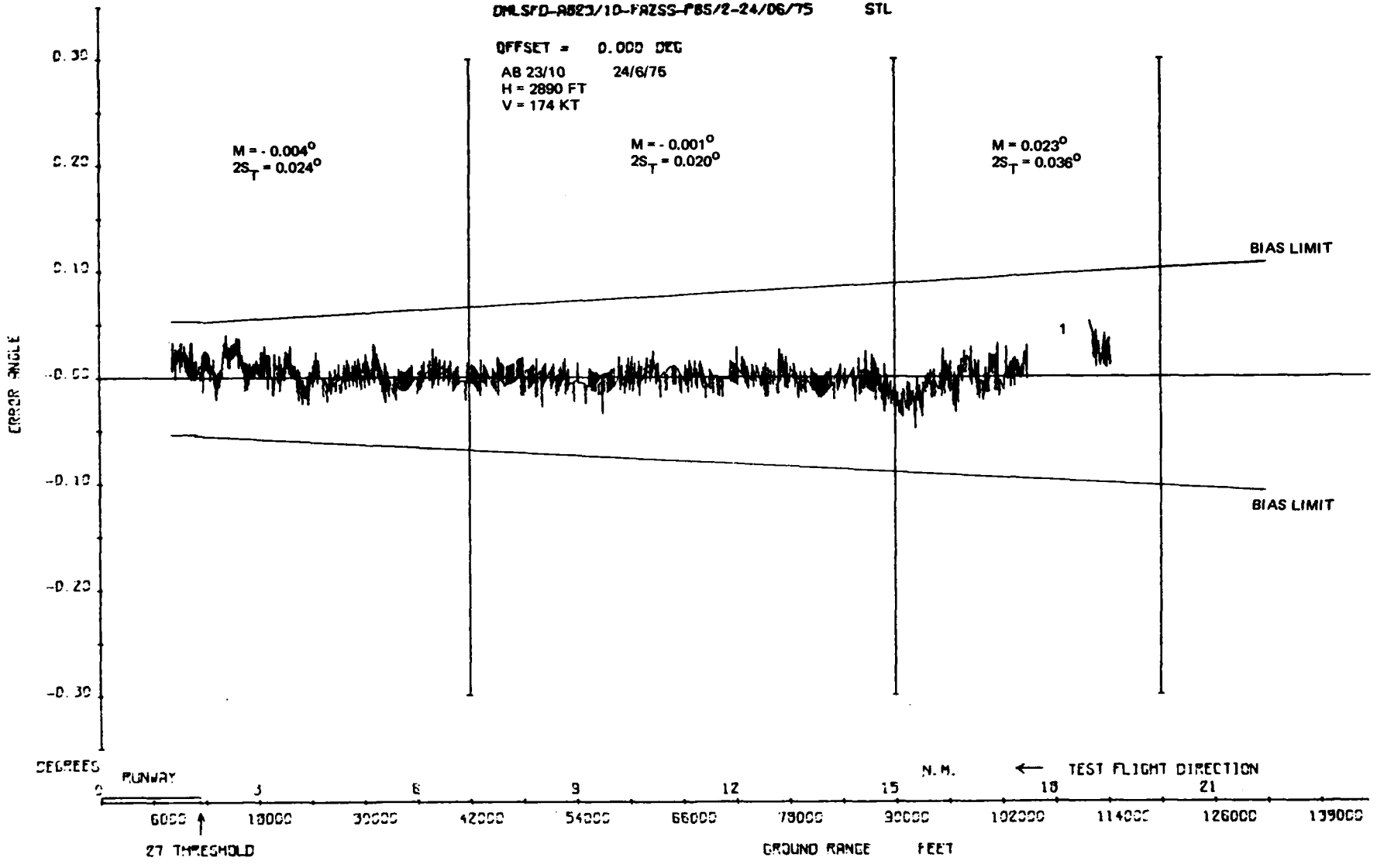

Fig 4.26c Approach azimuth radial at 0 degree

Fig 4.26c

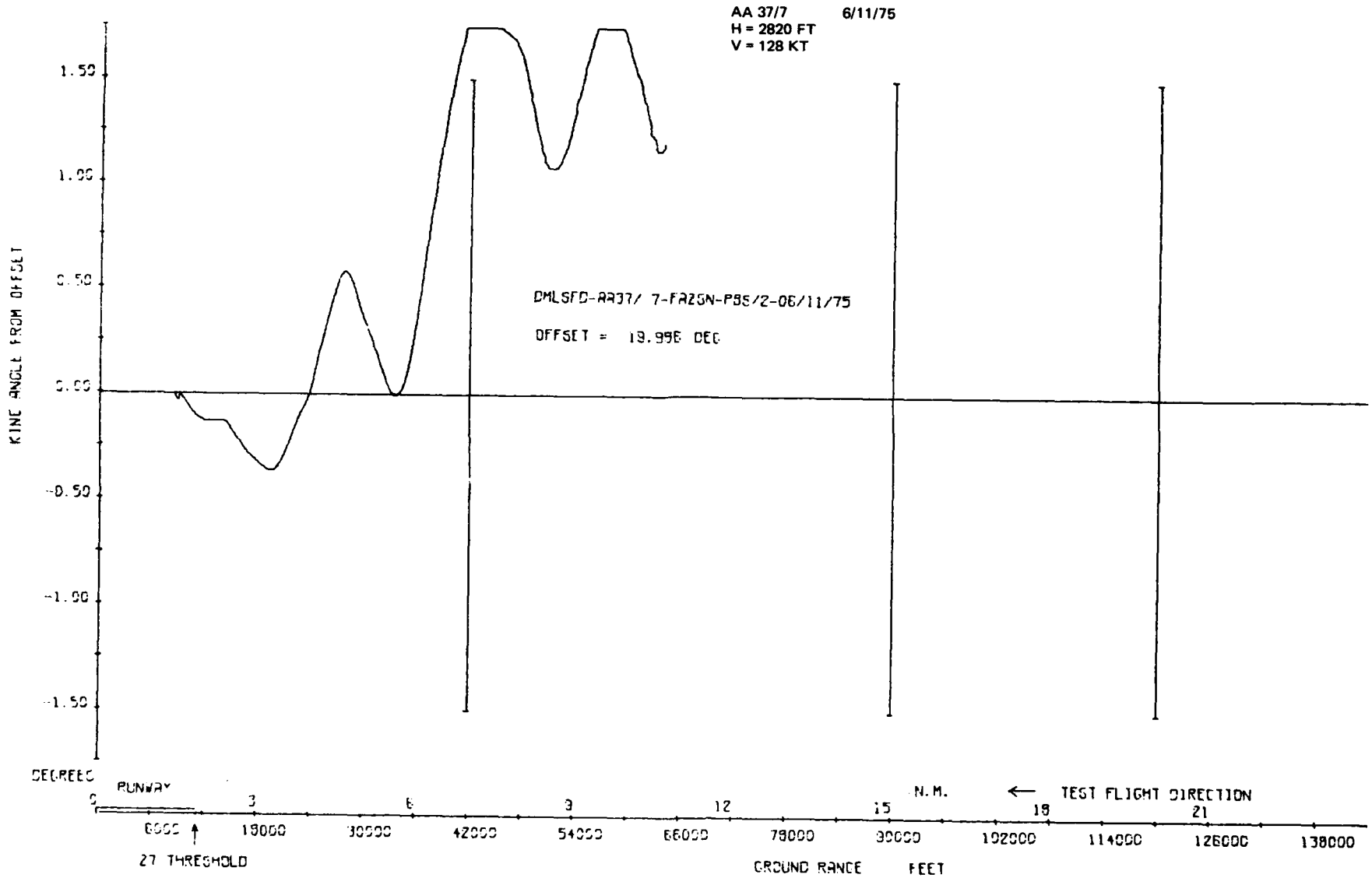

Fig 4.27a

Fig 4.27a Approach azimuth radial at +20 degrees

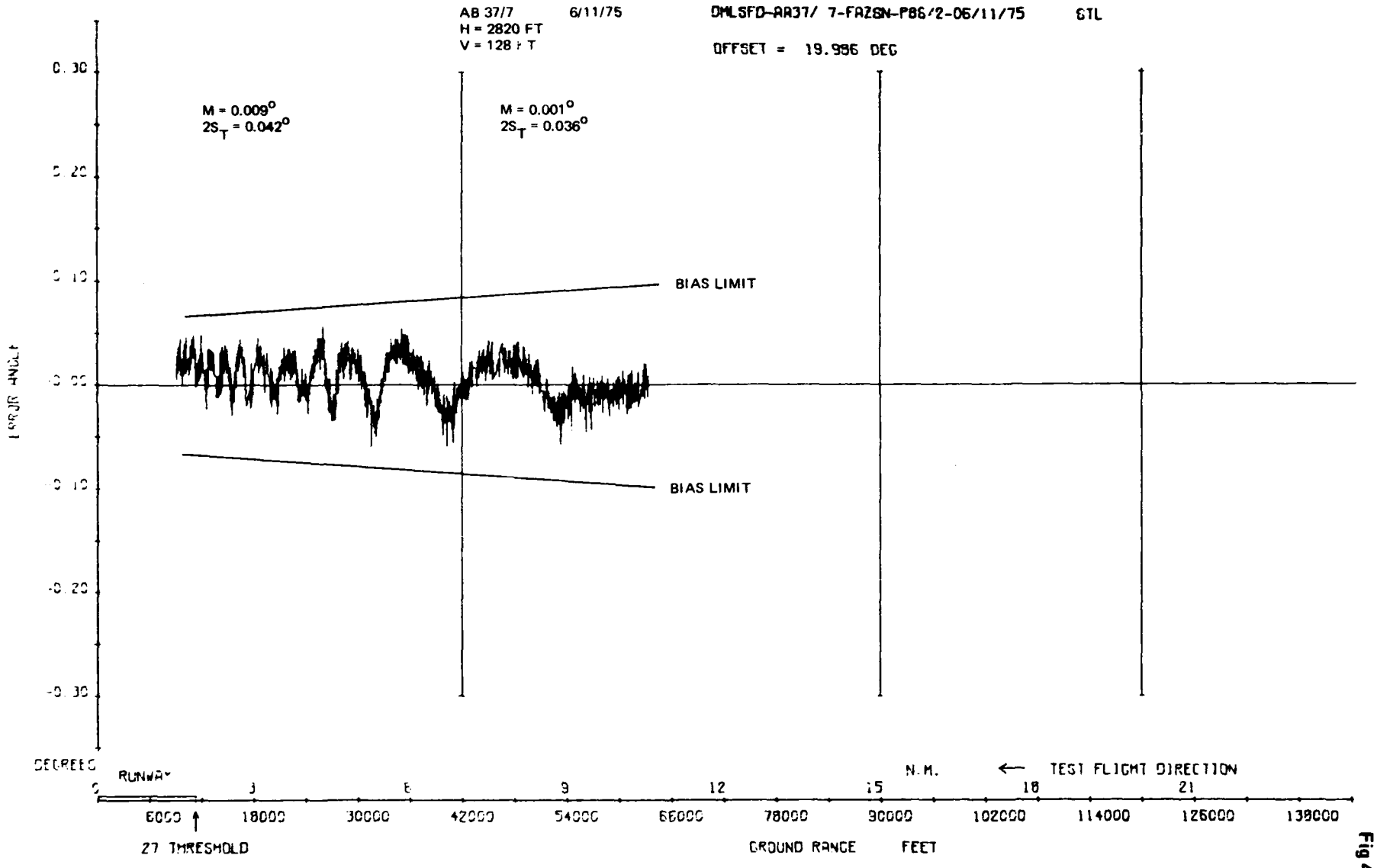

Fig 4.27c Approach azimuth radial at +20 degrees

Fig 4.27c

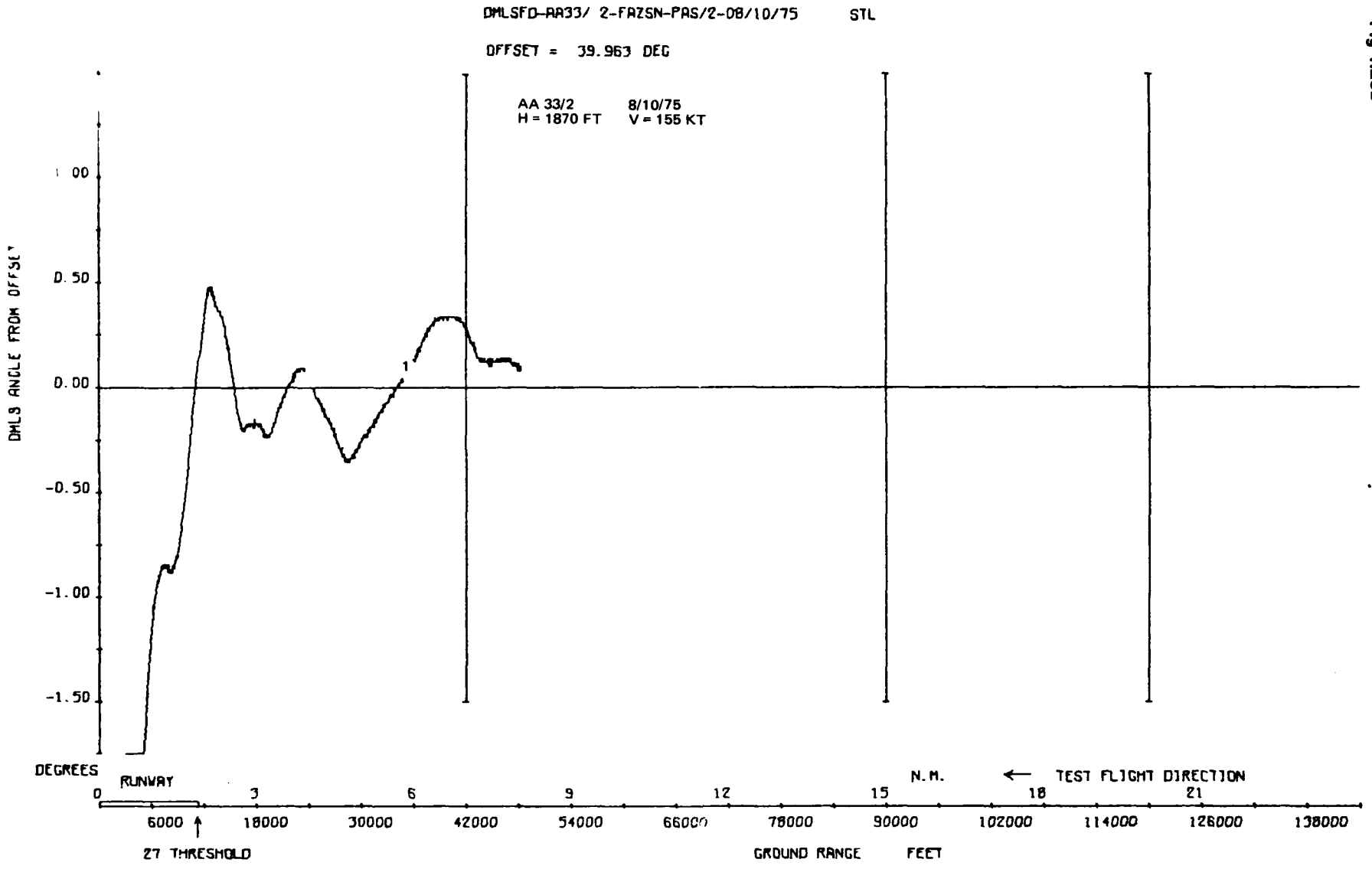

Fig 4.28b

Fig 4.28b Approach azimuth radial at +40 degrees

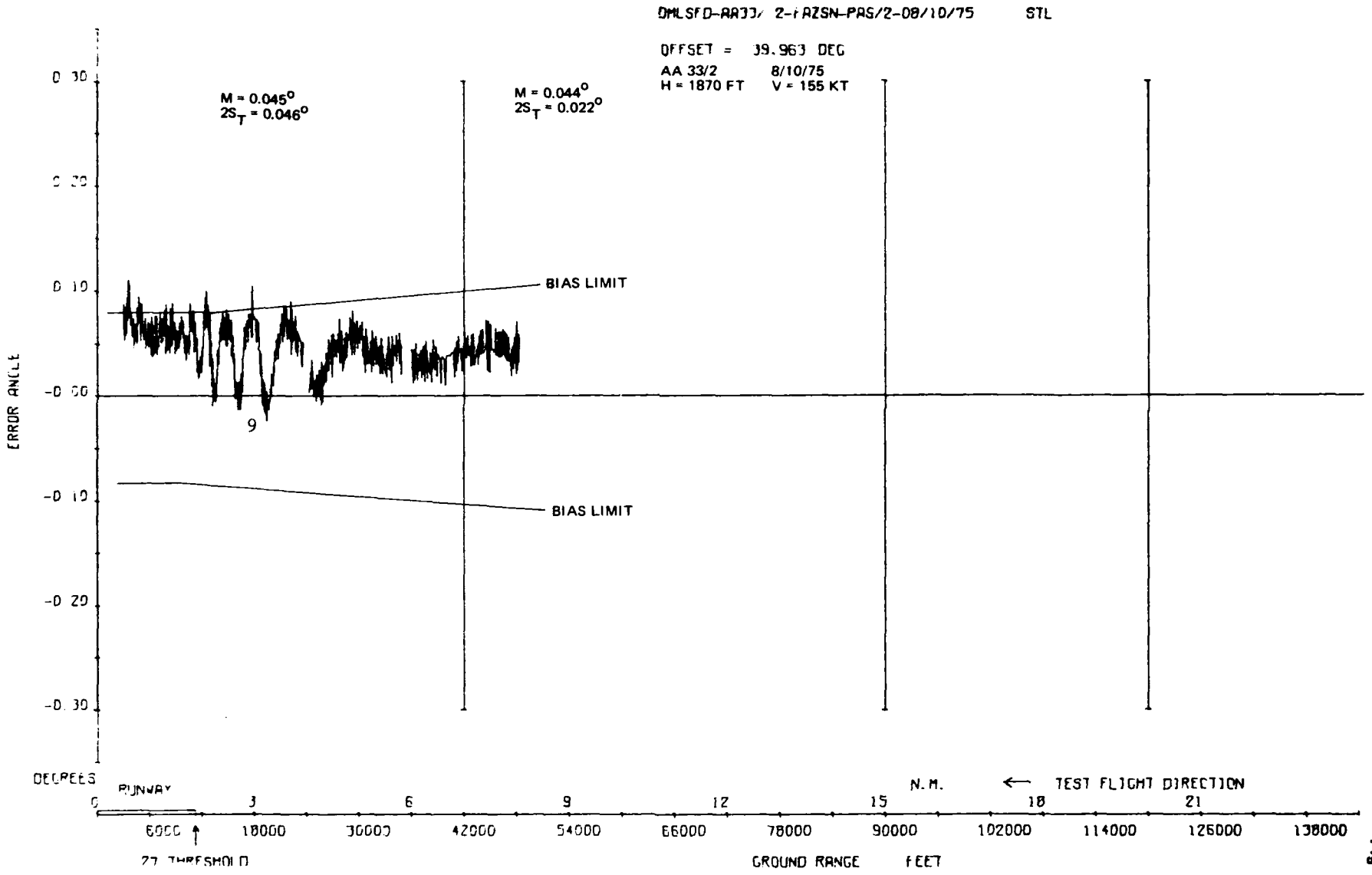

Fig 4.28c Approach azimuth radial at +40 degrees

Fig 4.28c

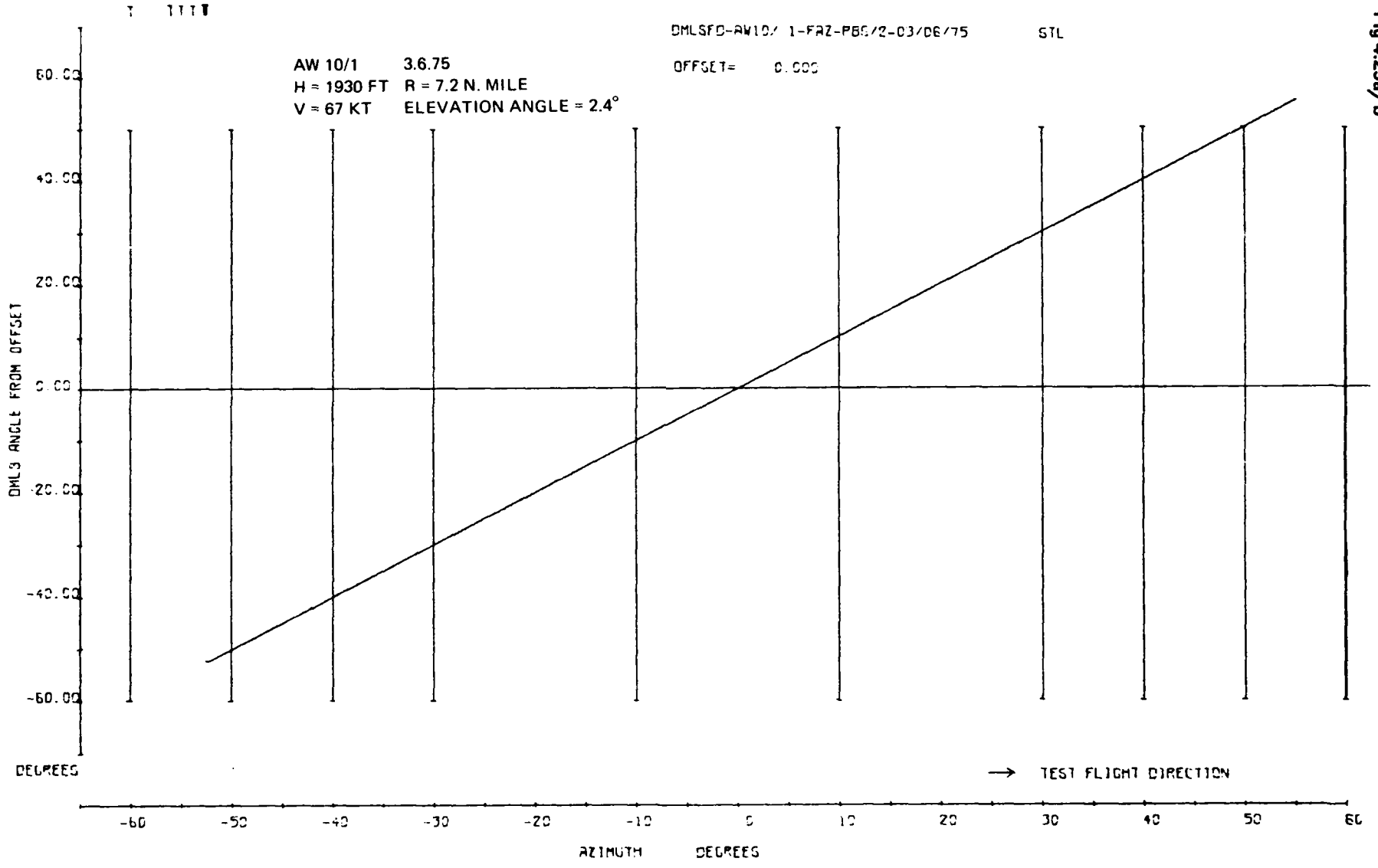

Fig 4.29a/b

Fig 4.29a/b Approach azimuth orbital flight

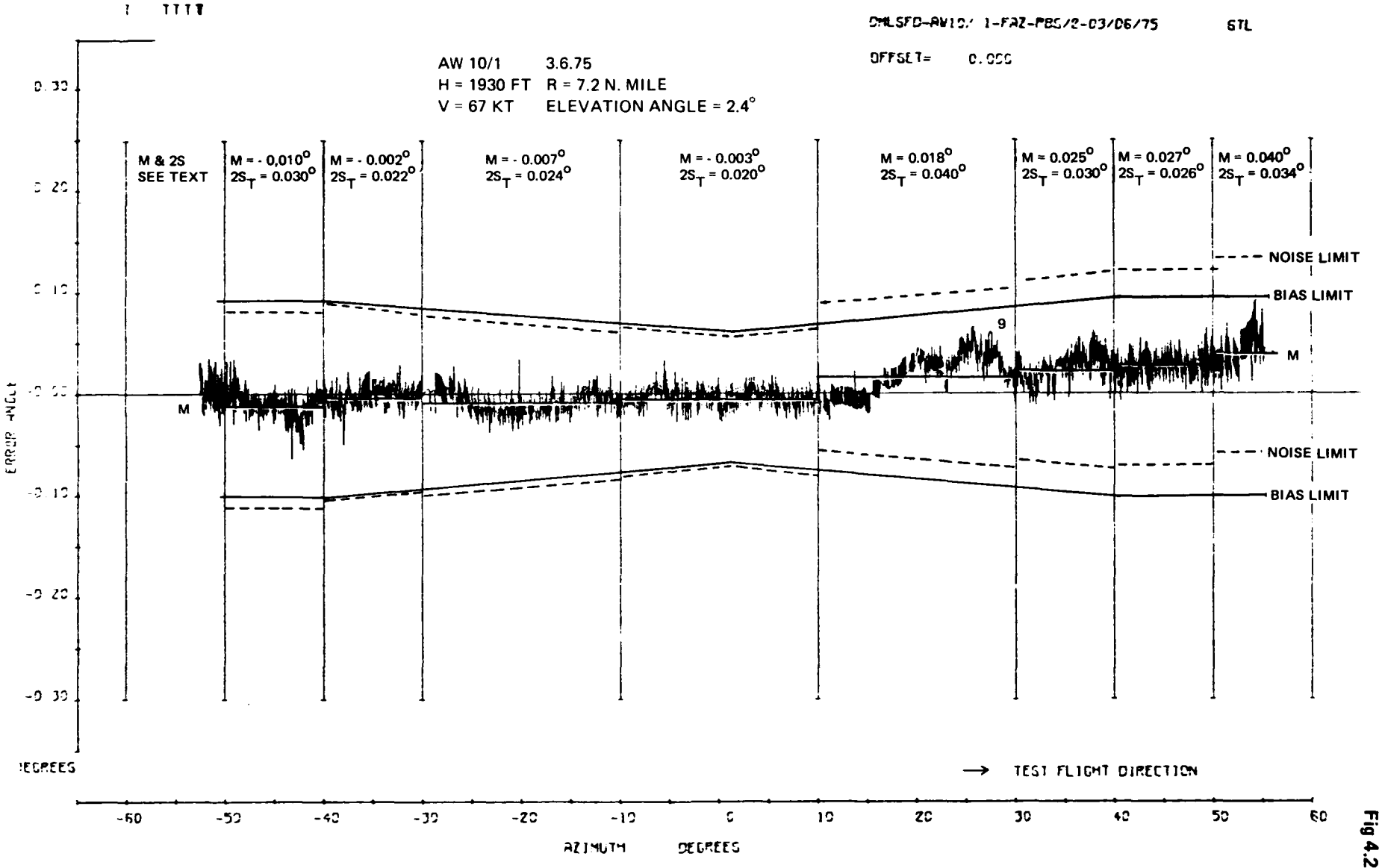

Fig 4.29c

Fig 4.29c Approach azimuth orbital flight

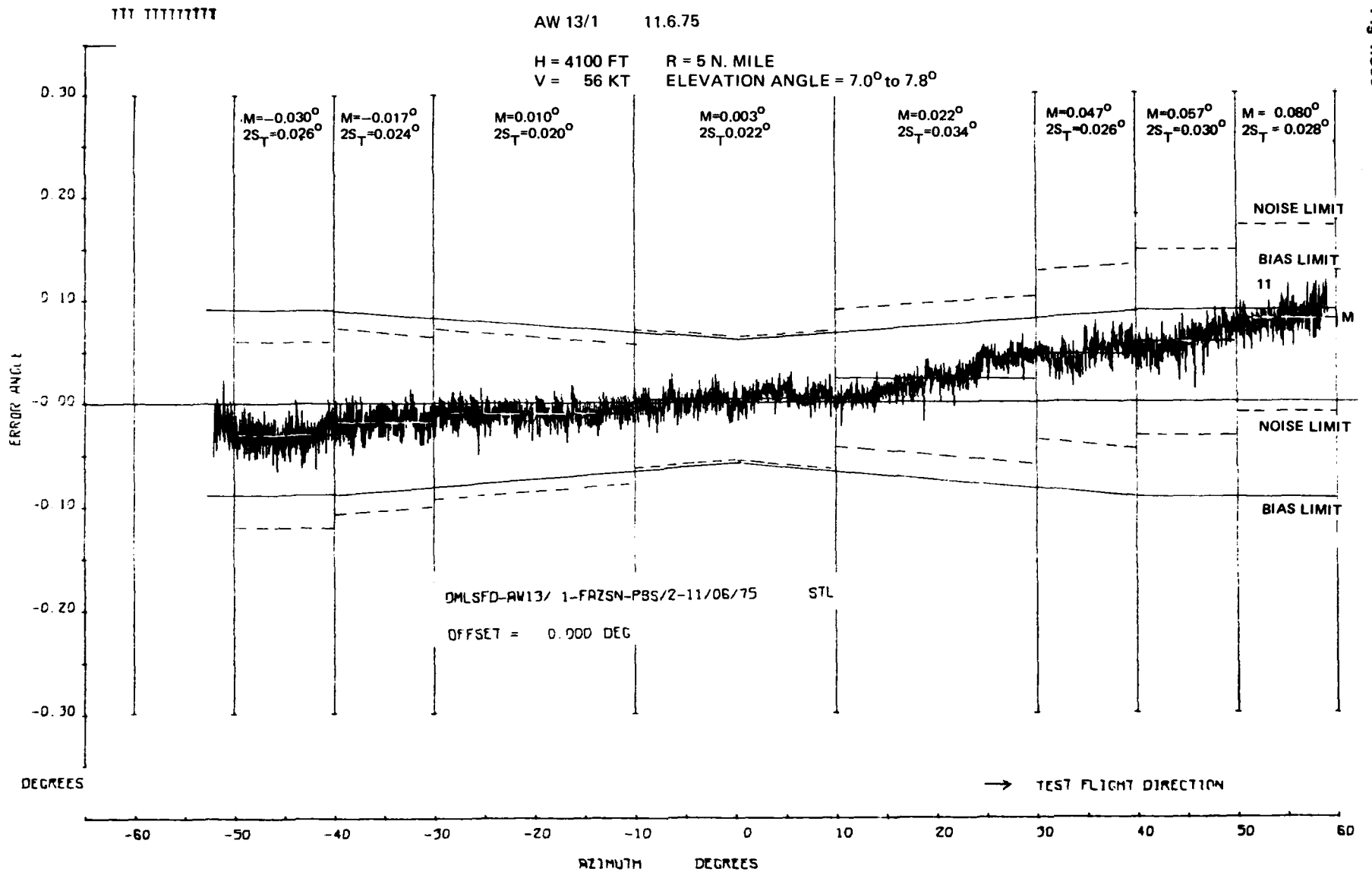

Fig 4.30c

Fig 4.30c Approach azimuth orbital flight at 4100 ft. 5 n mile radius

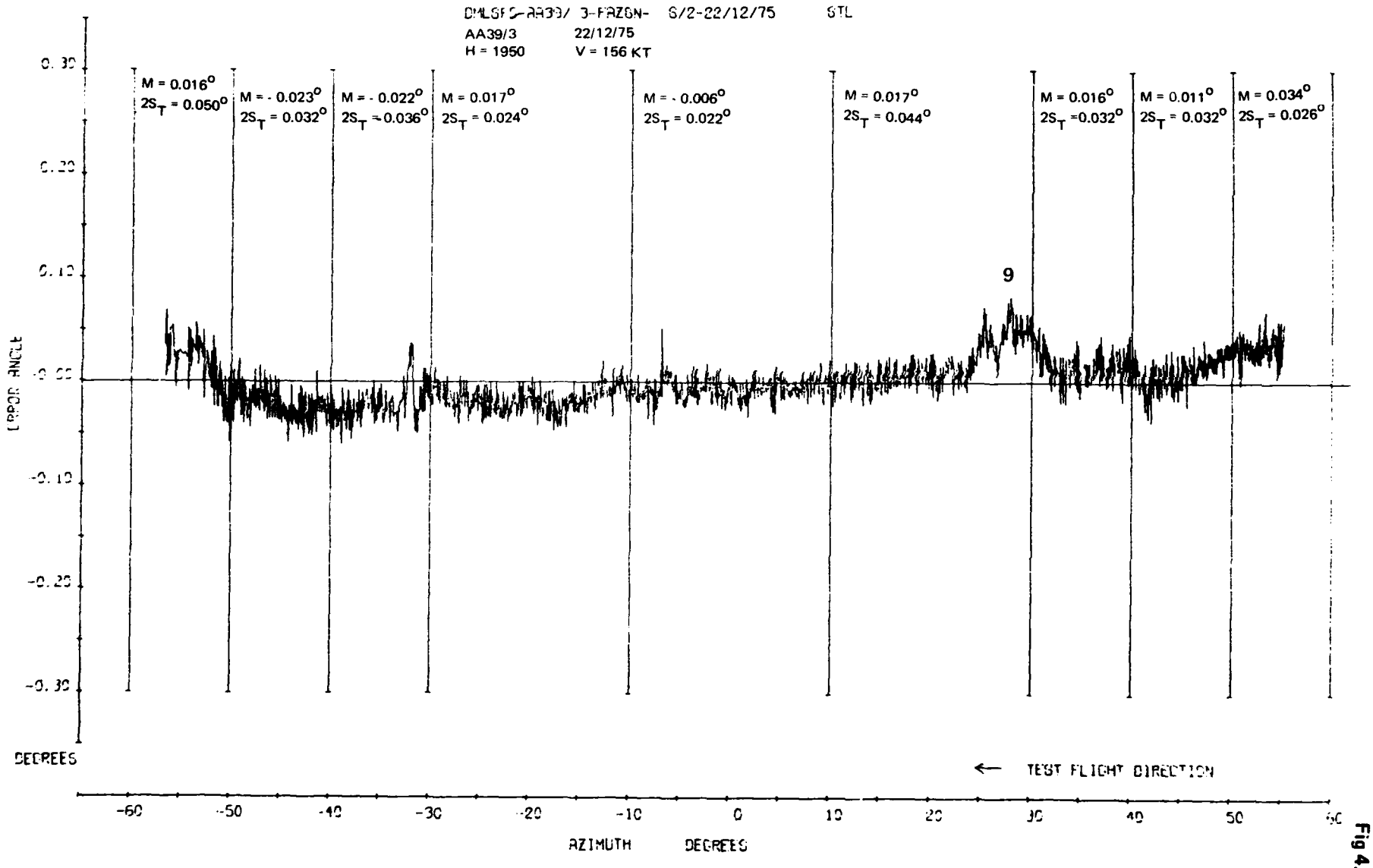

Fig 4.31c

Fig 4.31c Approach azimuth orbital flight at 1950 ft. 6 n mile radius

Fig 4.32a

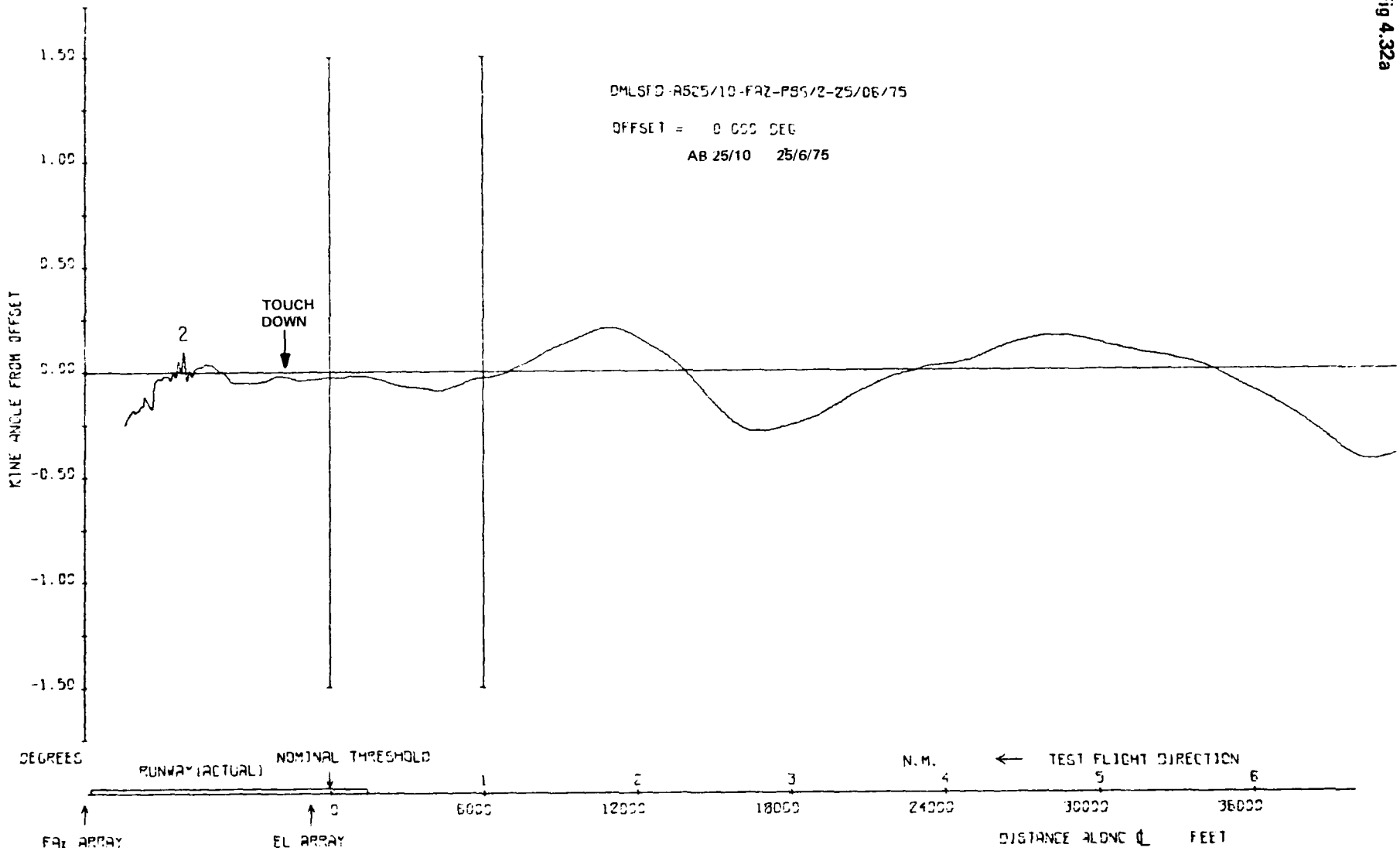

Fig 4.32a Approach azimuth accuracy. 3 degree approach to land and roll out

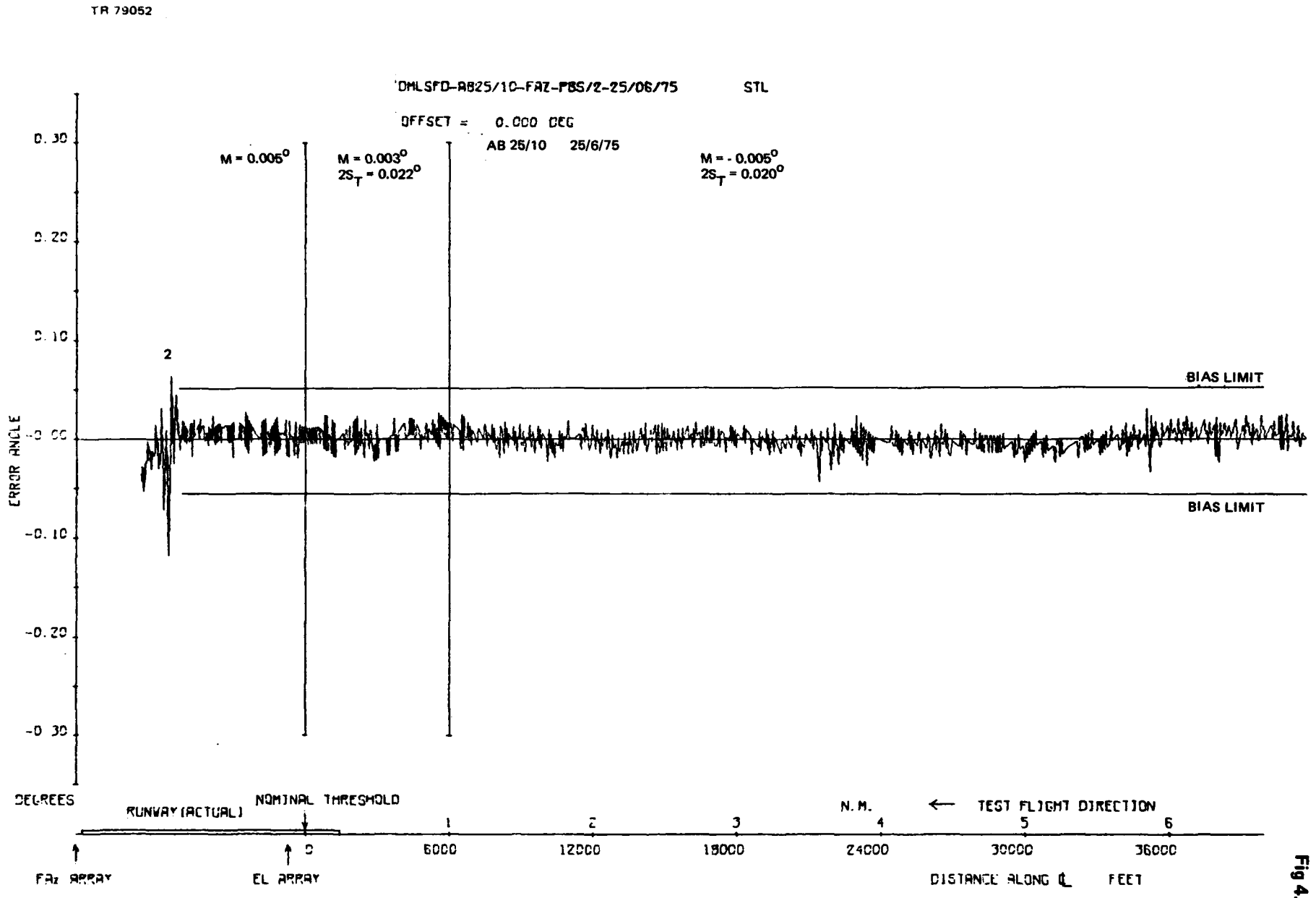

Fig 4.32c

Fig 4.32c Approach azimuth accuracy. 3 degree approach to land and roll out

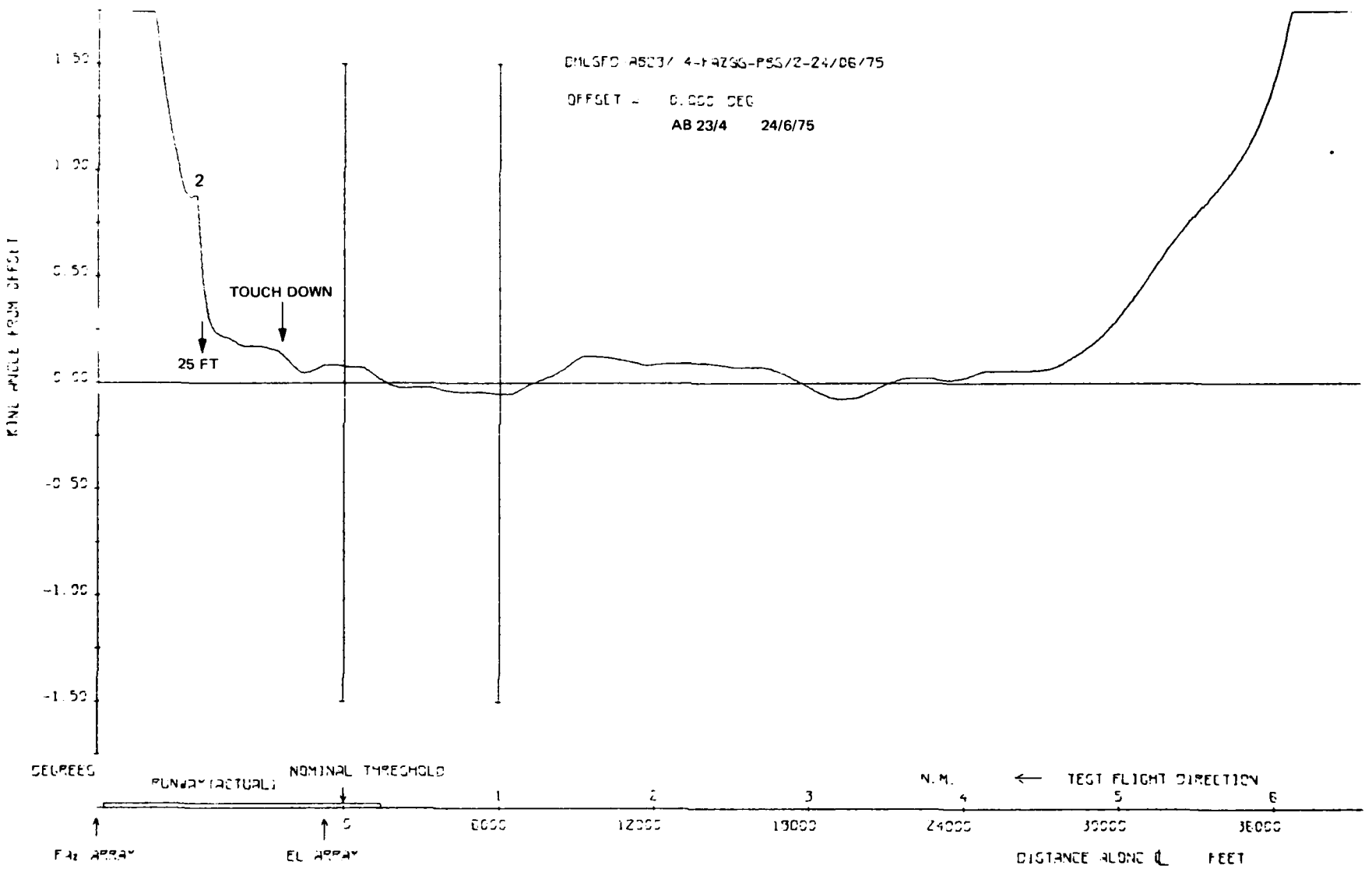

Fig 4.33a

Fig 4.33a Approach azimuth accuracy. 3 degree approach to touch and go

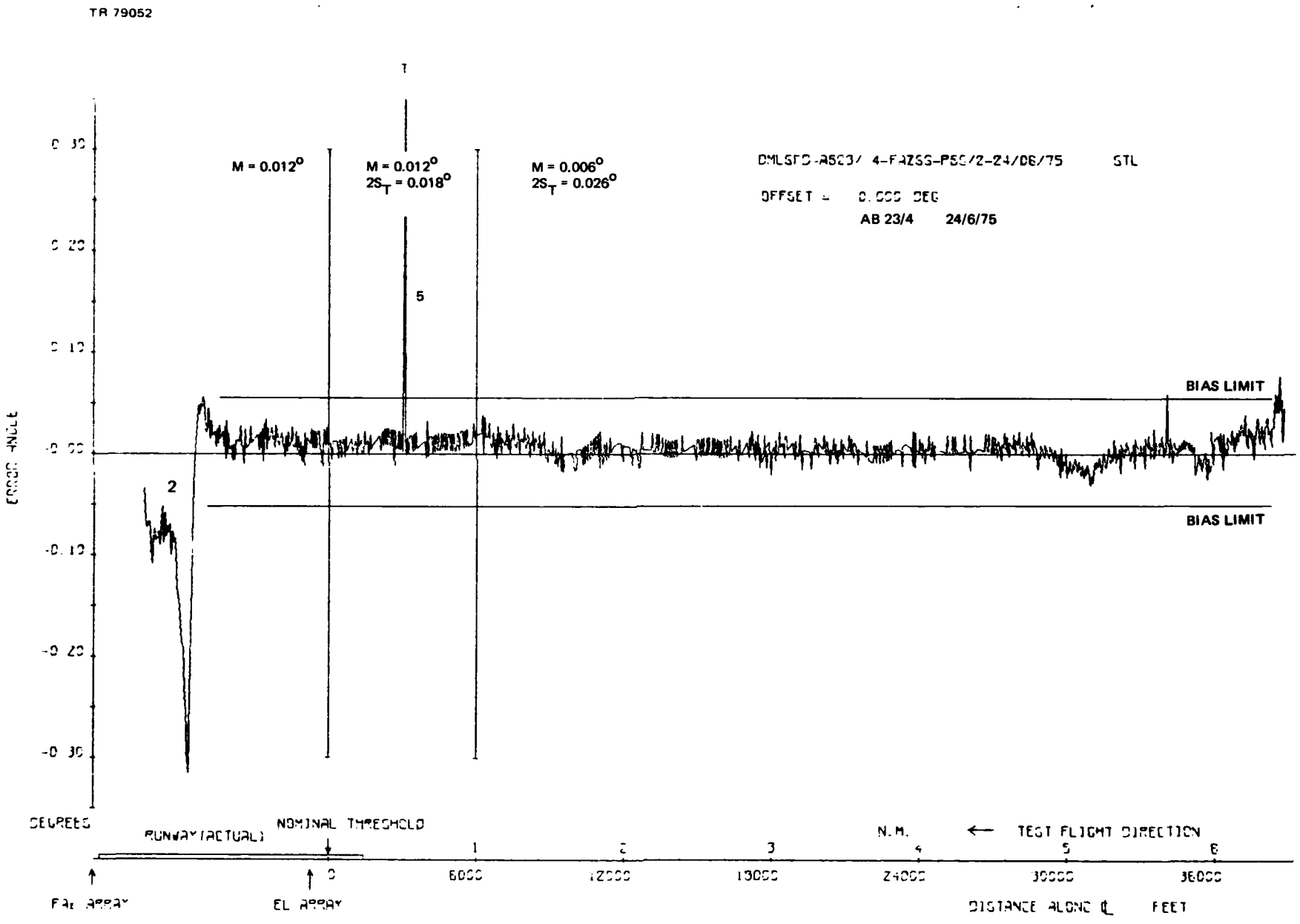

Fig 4.33c Approach azimuth accuracy. 3 degree approach to touch and go

Fig 4.33c

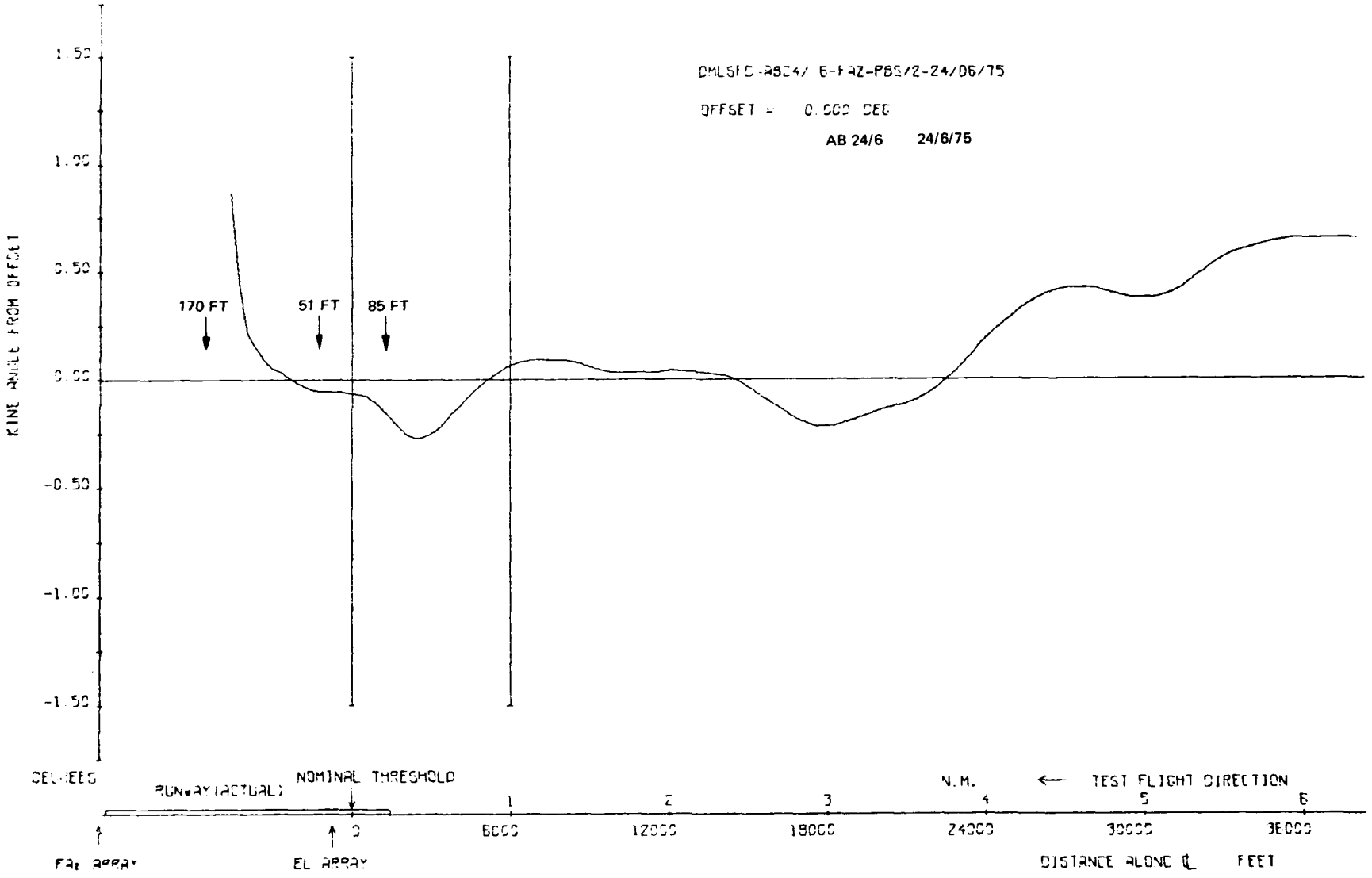

Fig 4.34a

Fig 4.34a Approach azimuth accuracy. 3 degree approach to low overfly

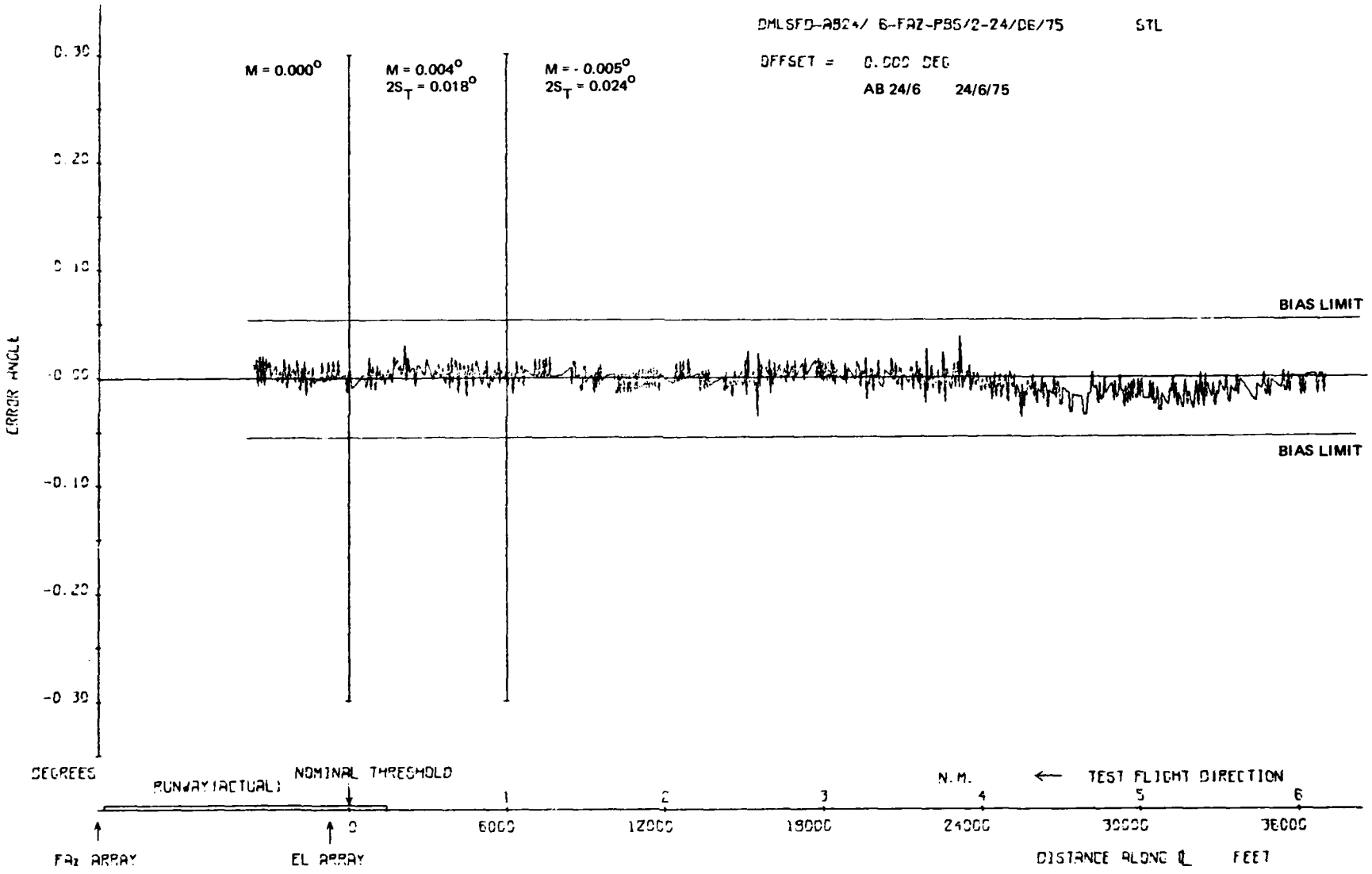

Fig 4.34c Approach azimuth accuracy. 3 degree approach to low overfly

Fig 4.34c

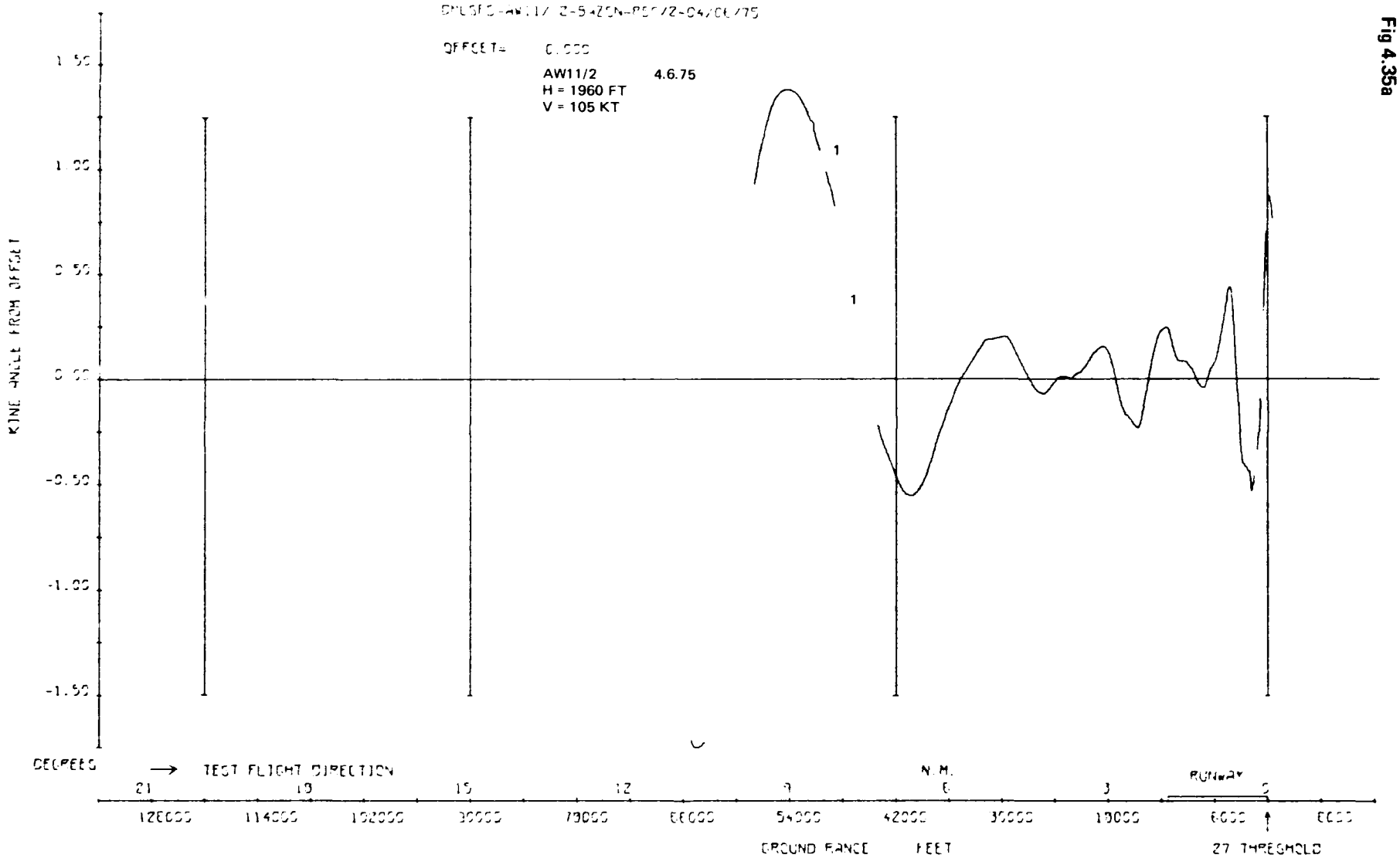

Fig 4.35a

Fig 4.35a Missed approach azimuth radial flight on centre line

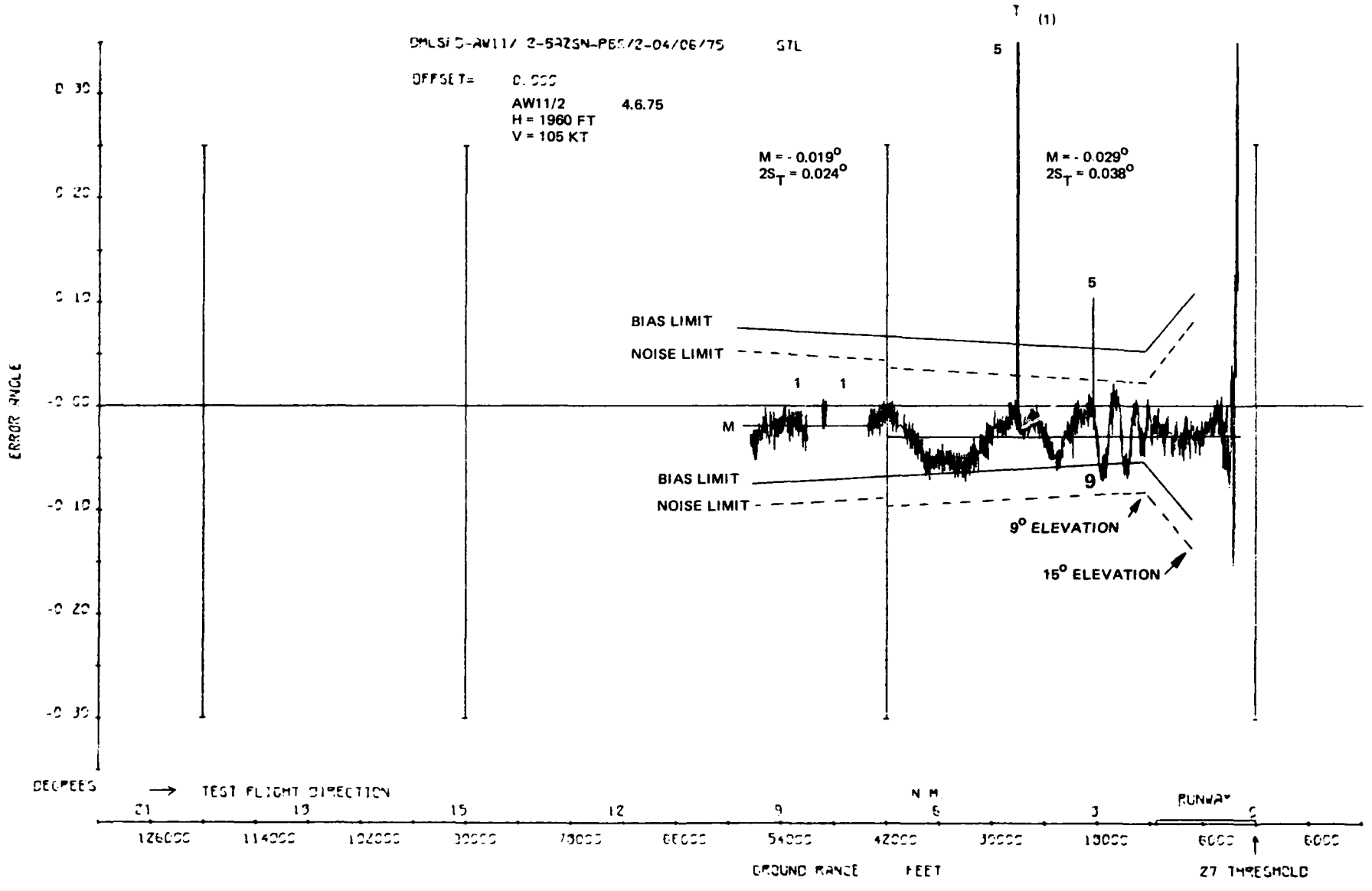

Fig 4.35c

Fig 4.35c Missed approach azimuth radial flight on centre line

AD-A085 479 ROYAL AIRCRAFT ESTABLISHMENT FARNBOROUGH (ENGLAND) F/G 17/7
CONTRIBUTIONS TO THE UK MICROWAVE LANDING SYSTEM RESEARCH AND D--ETC(U)
MAY 79 J M JONES
UNCLASSIFIED RAE-TR-79052-VOL-2 DRIC-BR-73762 NL

2 OF 2
AD A085479

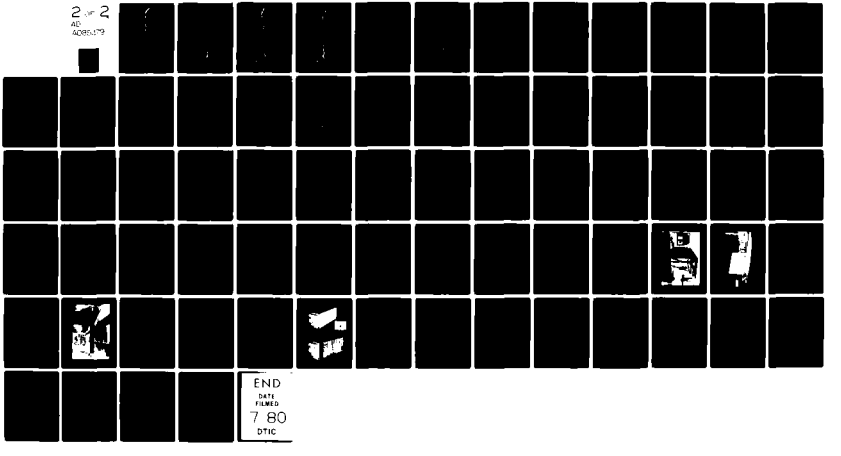

END
DATE FILMED
7 80
DTIC

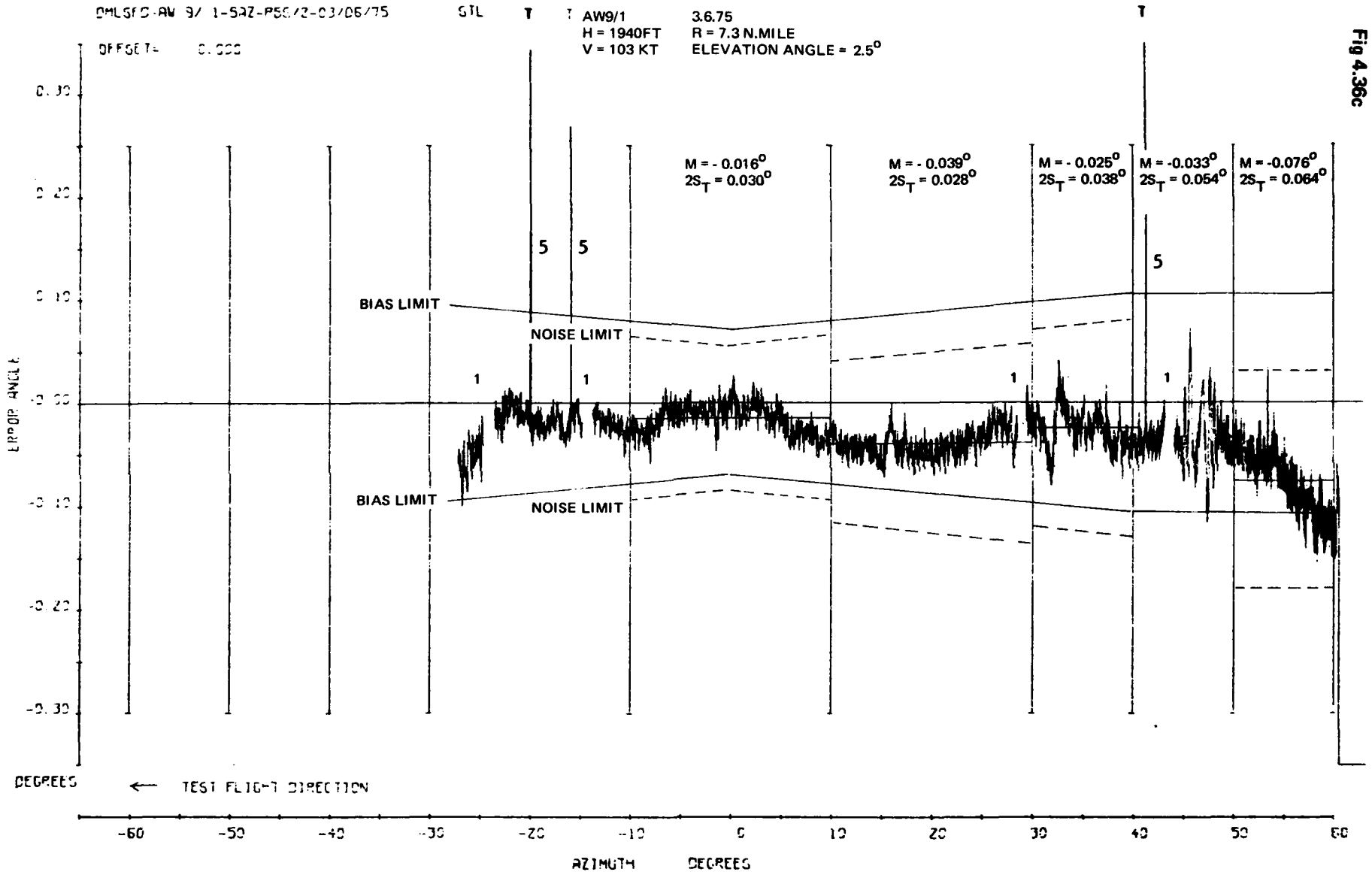

Fig 4.36c

Fig 4.36c Missed approach azimuth orbital flight at 1940 ft and 7.3 n mile radius

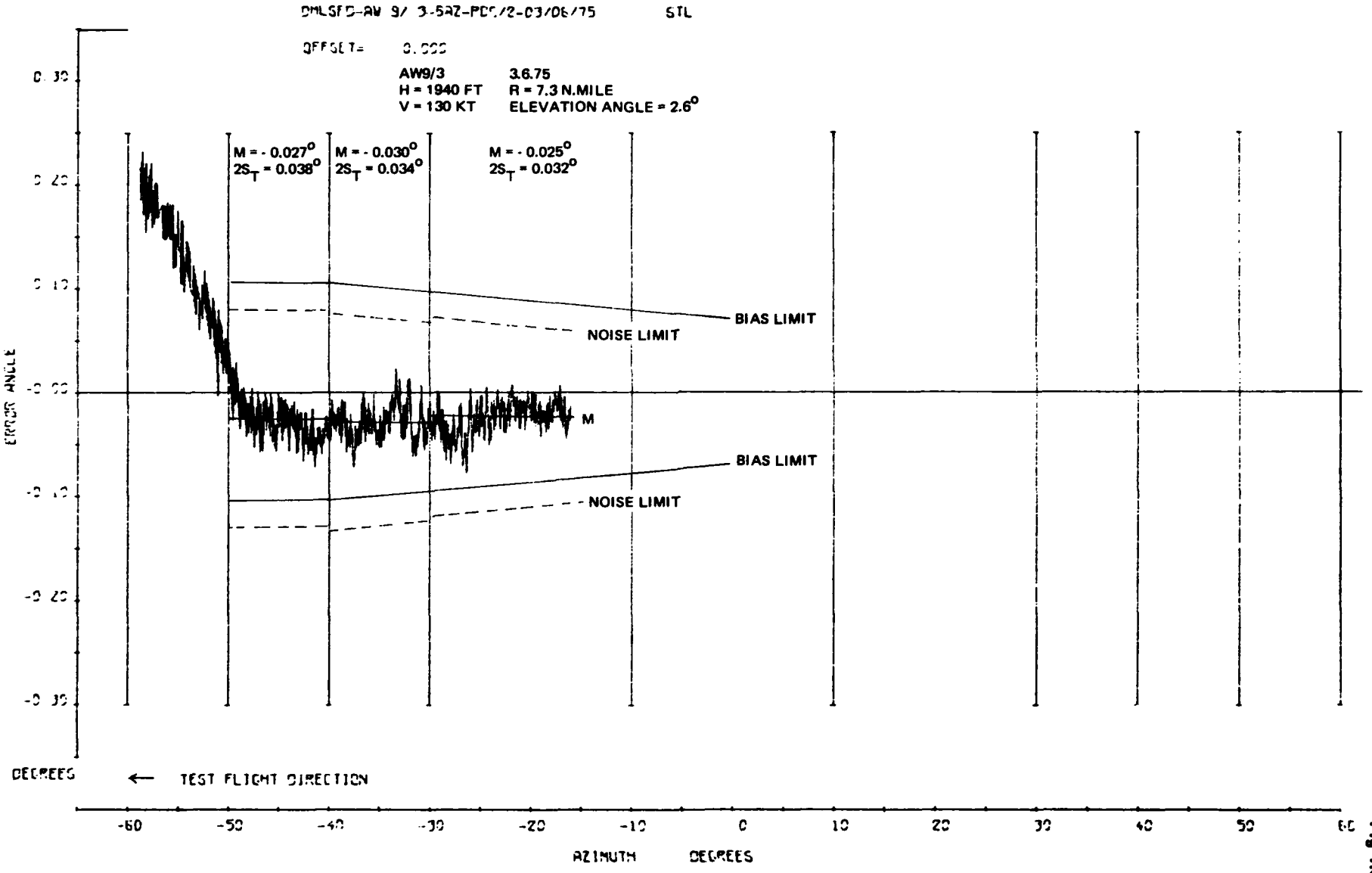

Fig 4.37c

Fig 4.37c Missed approach orbital flight at 1940 ft and 7.3 n mile radius

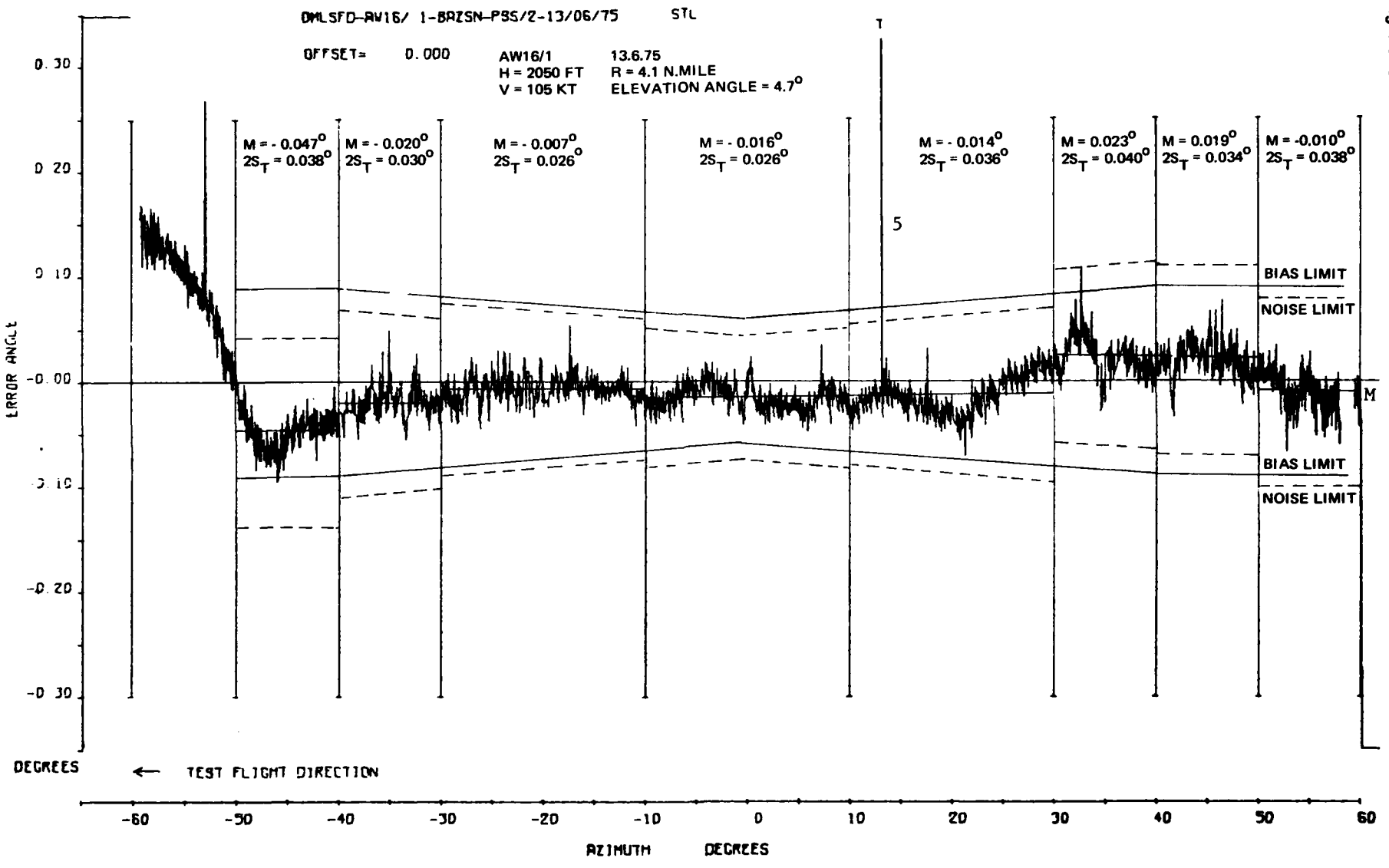

Fig 4.38c

Fig 4.38c Missed approach orbital flight at 2050 ft and 4.1 n mile radius

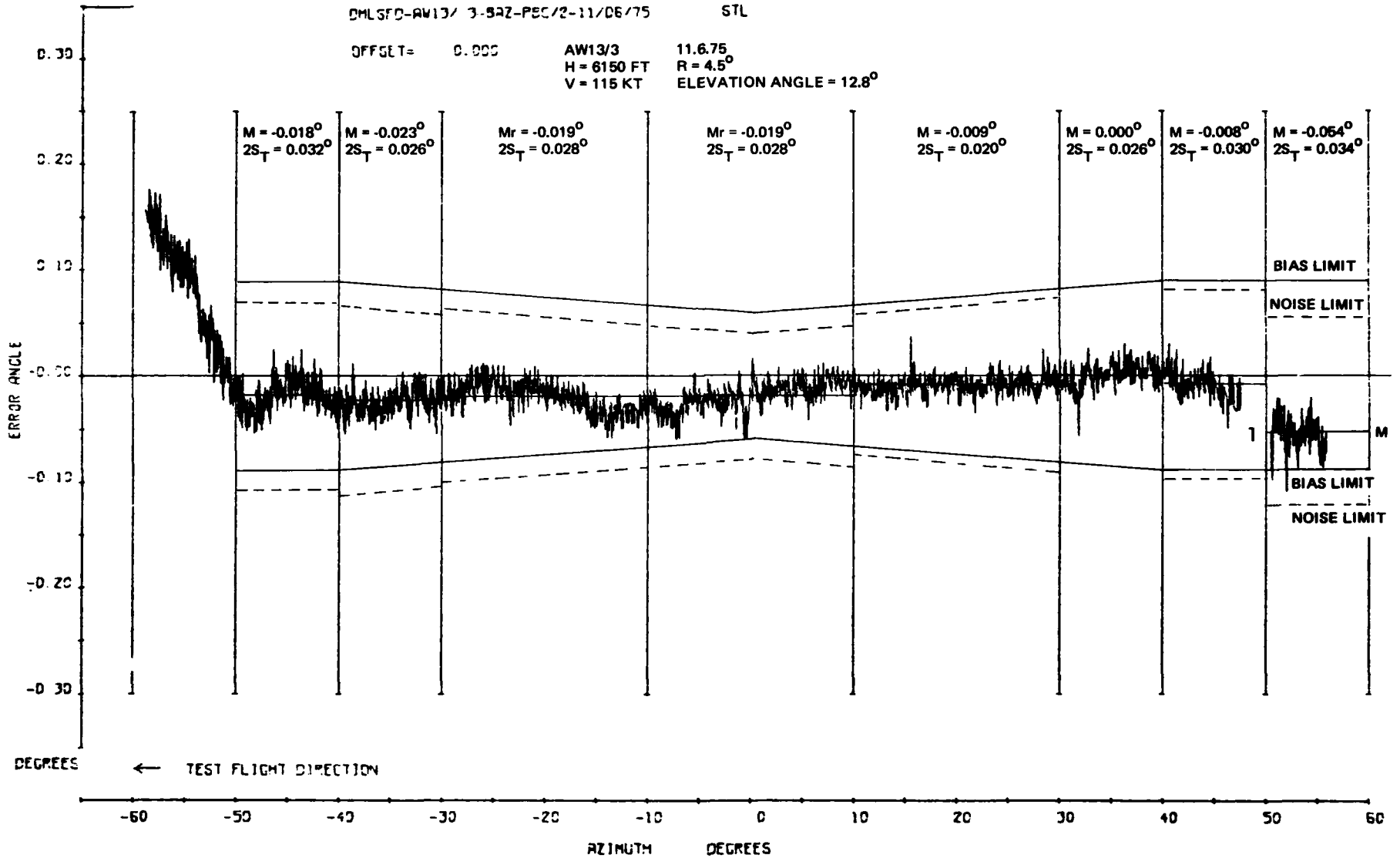

Fig 4.39c

Fig 4.39c Missed approach azimuth orbital flight at 6150 ft and 4.5 n mile radius

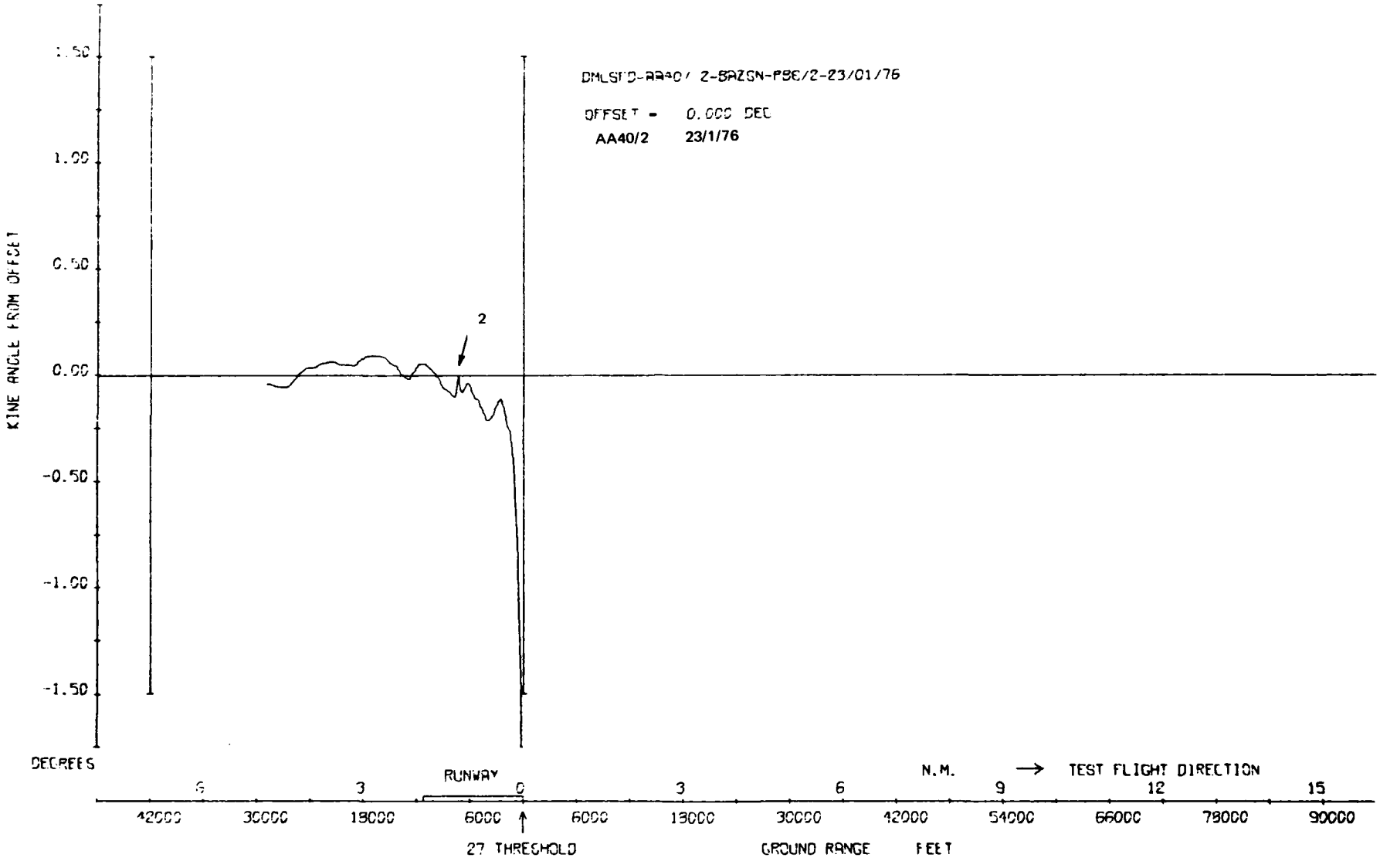

Fig 4.40a 3 degree approach using 60λ array missed approach guidance to low overshoot

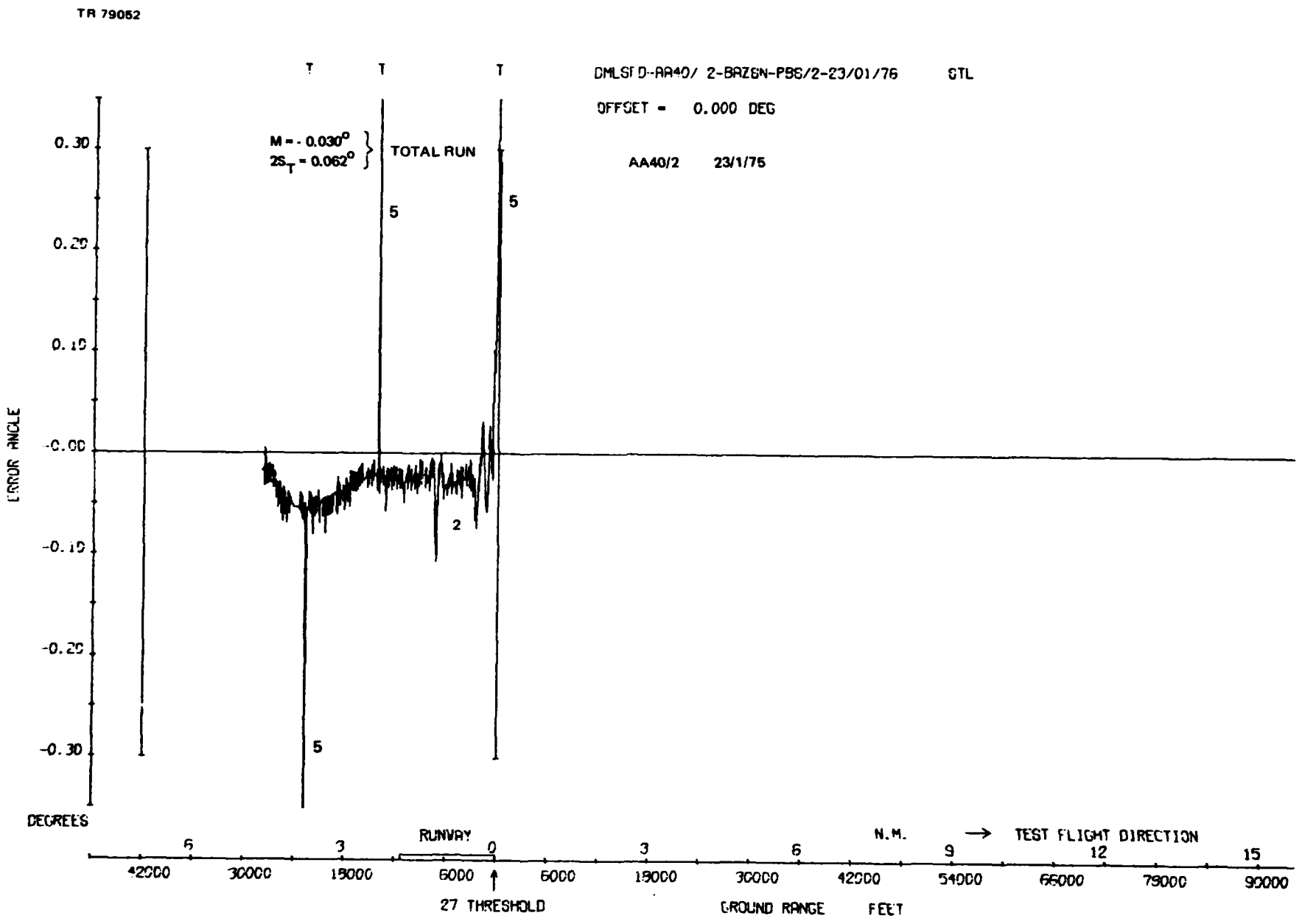

Fig 4.40c 3 degree approach using 60λ array missed approach guidance to low overshoot

Fig 4.40c

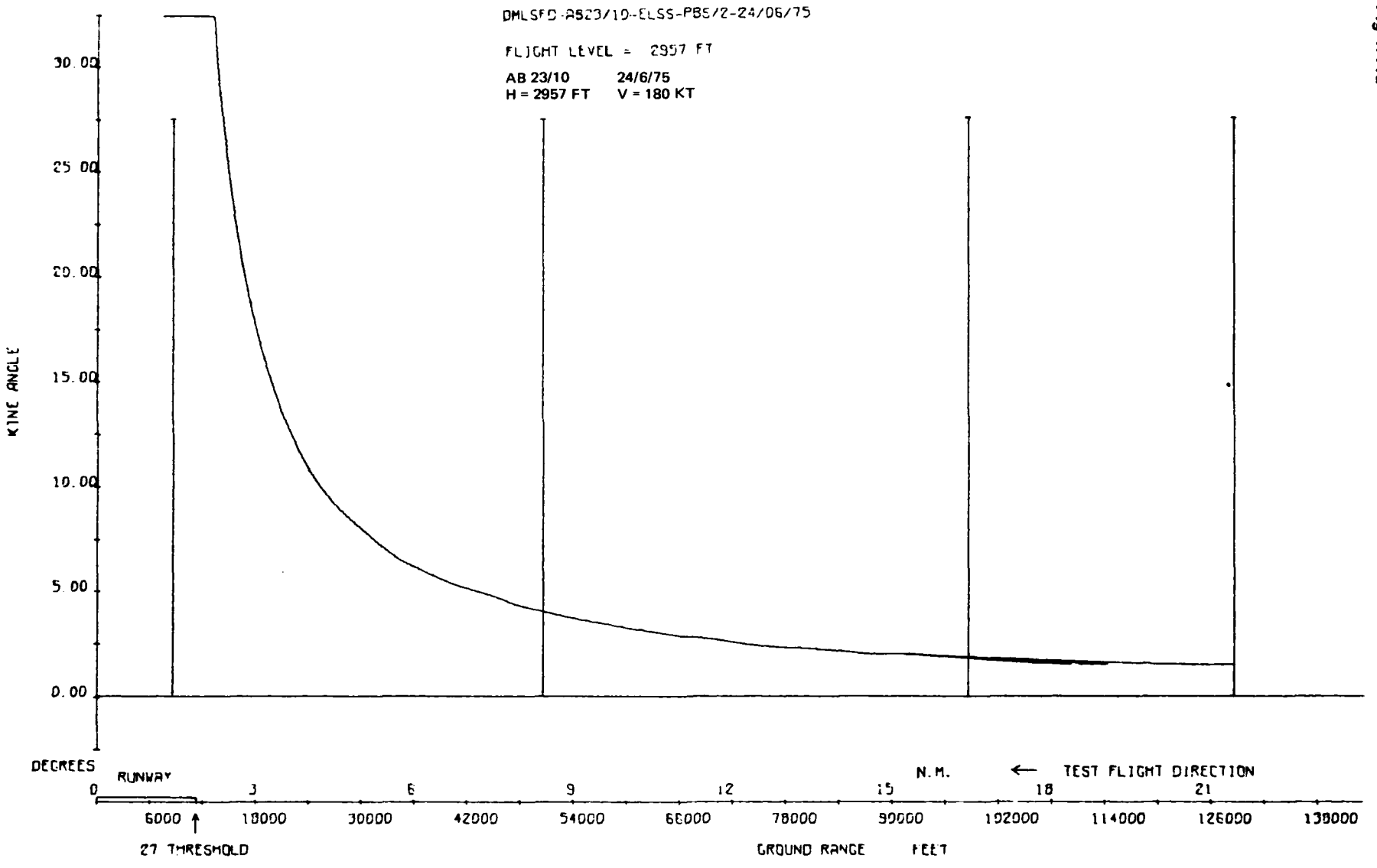

Fig 4.41a

Fig 4.41a Elevation accuracy. Radial flight at 2957 ft and 0 degree

TR 79052

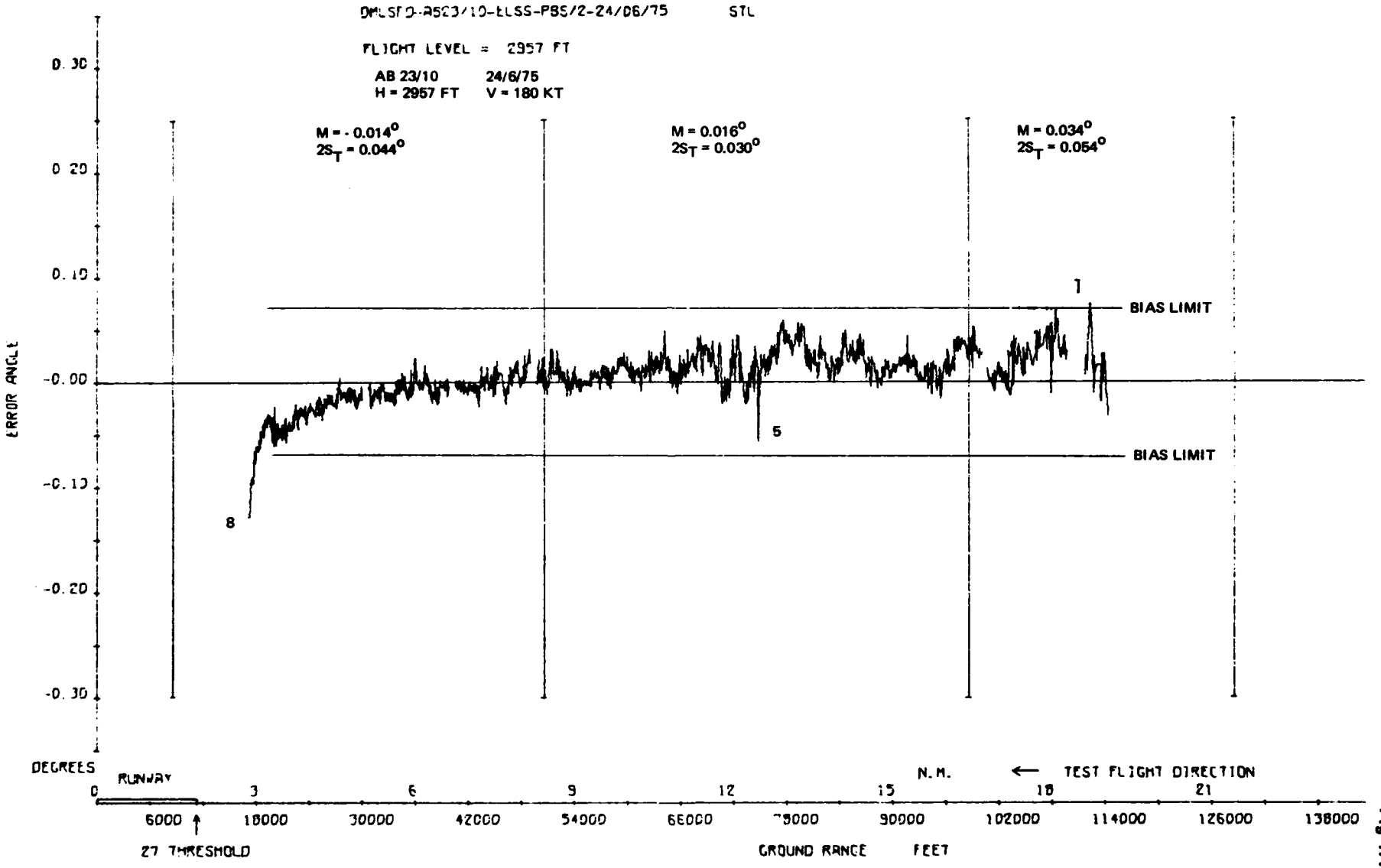

Fig 4.41c

Fig 4.41c Elevation accuracy. Radial flight at 2957 ft and 0 degree

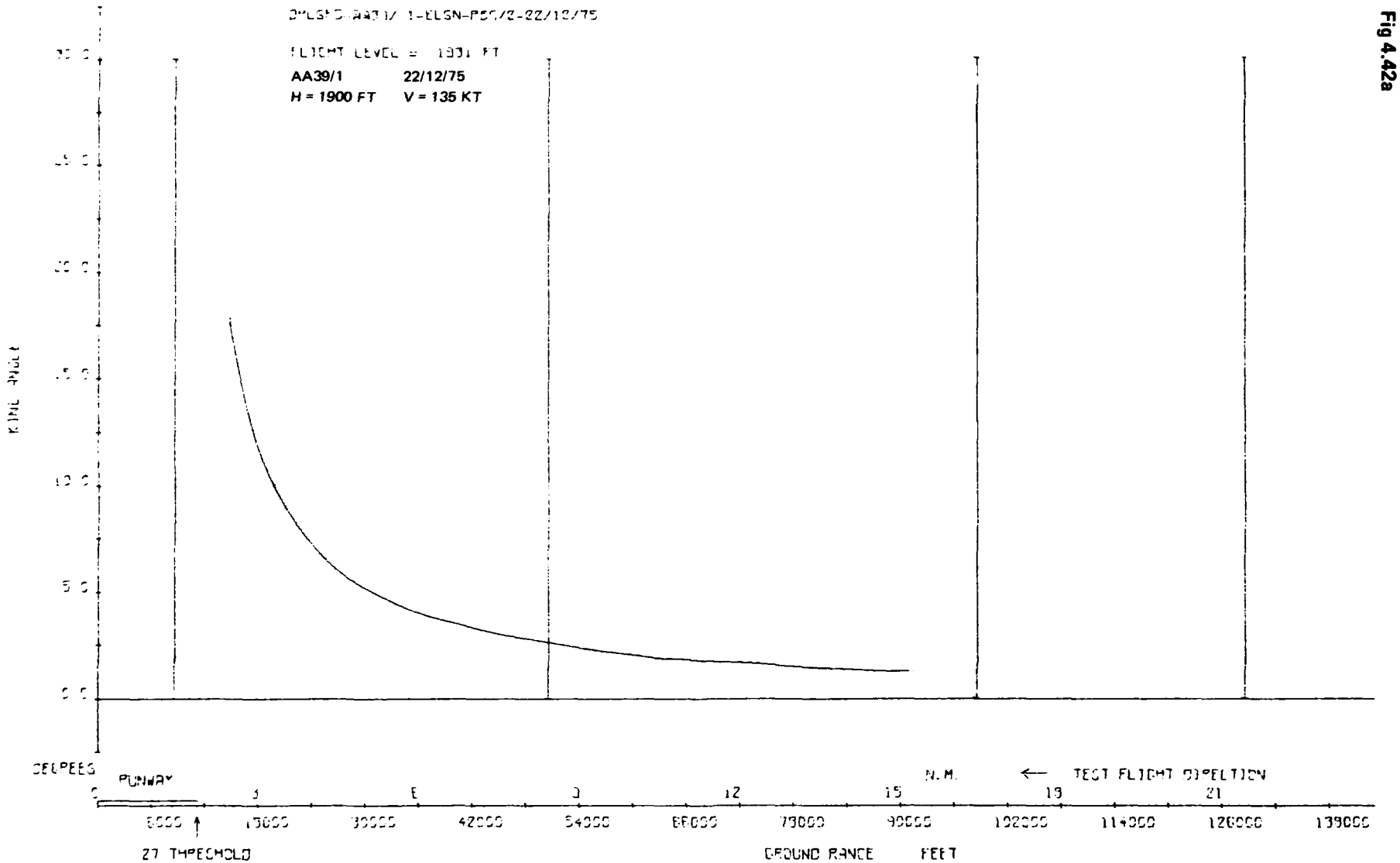

Fig 4.42a

Fig 4.42a Elevation accuracy radial flight at 1900 ft and on —44 degrees radial

TR 79052

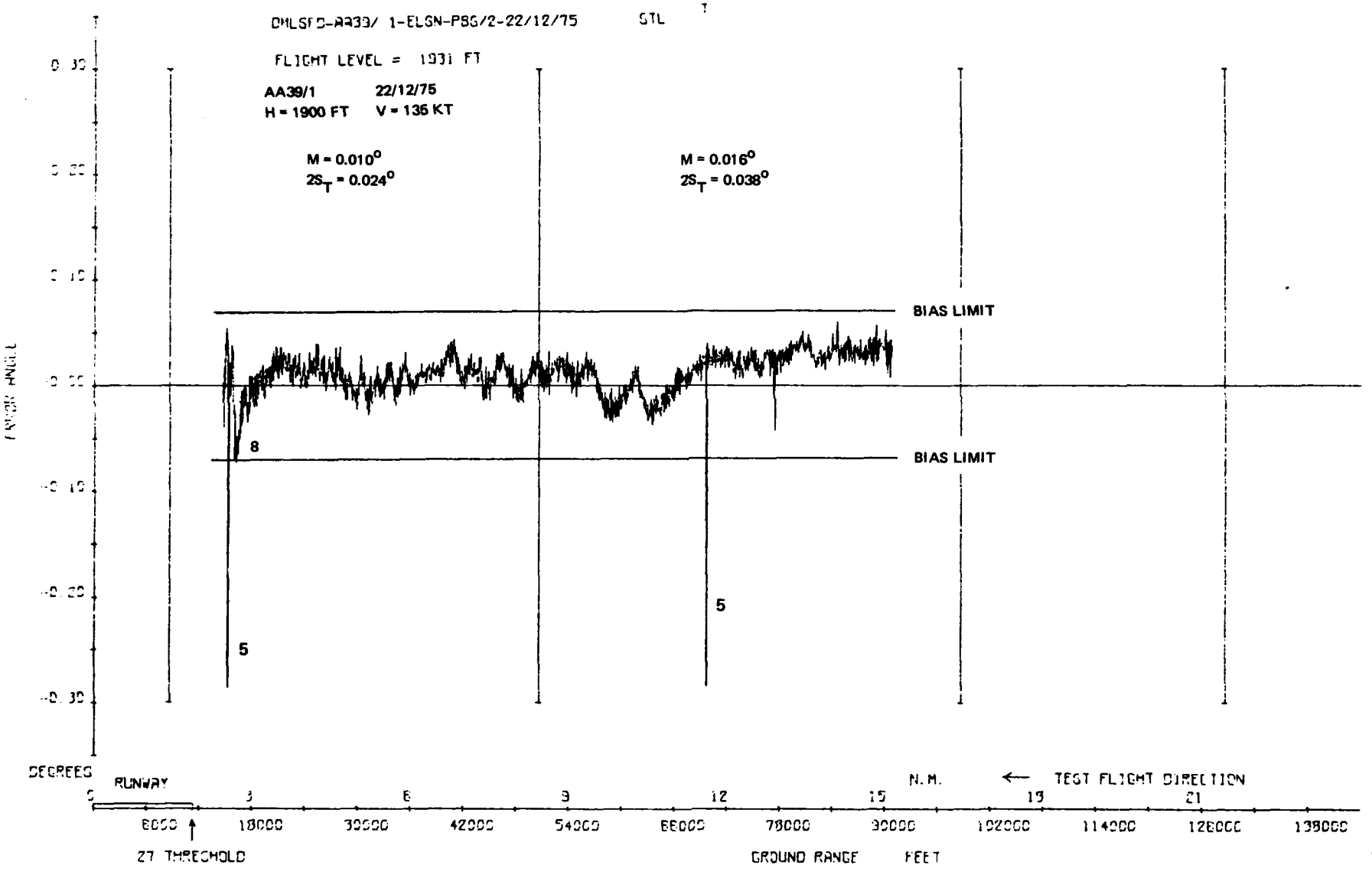

Fig 4.42c

Fig 4.42c Elevation accuracy radial flight at 1900 ft and on –44 degrees radial

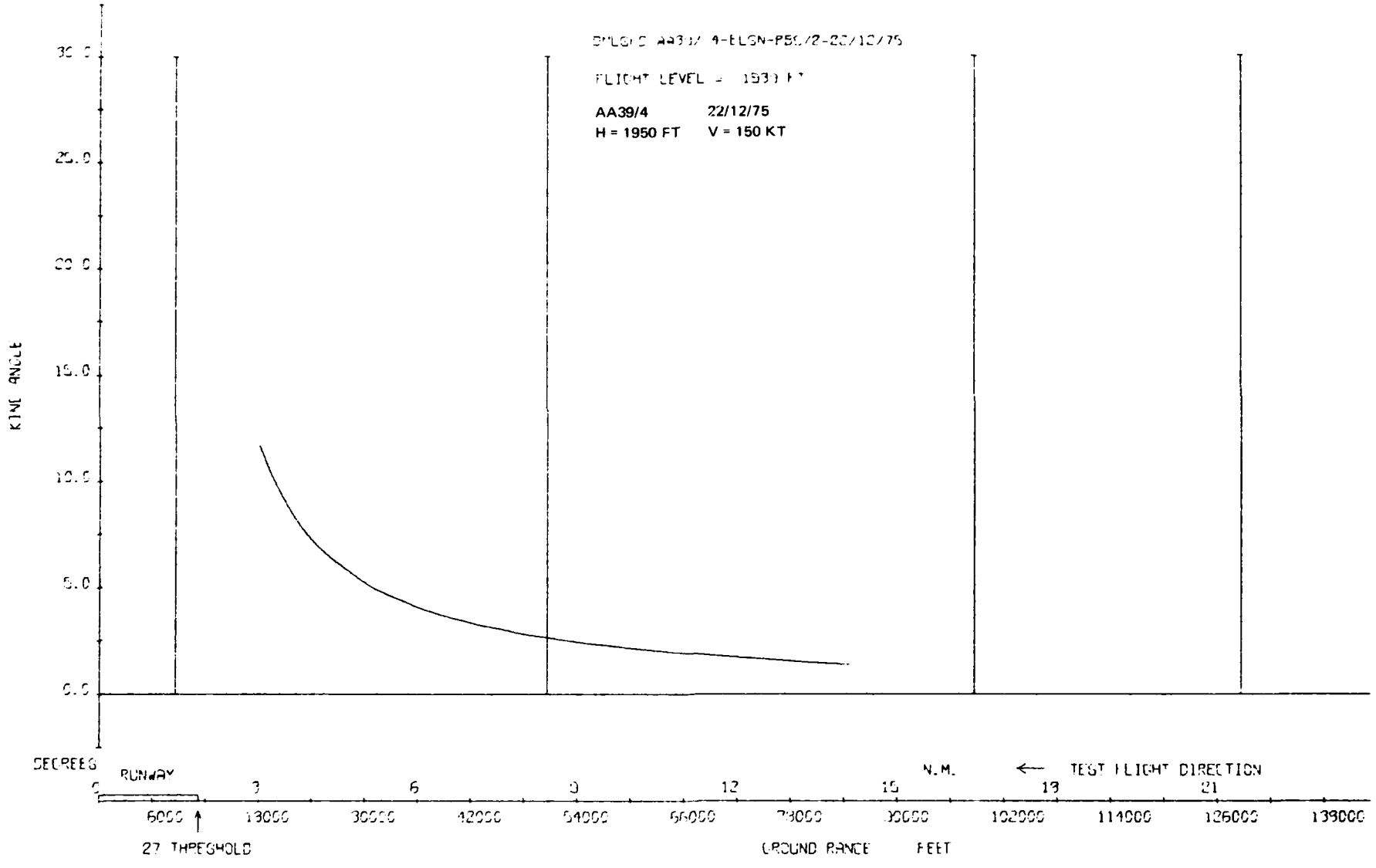

Fig 4.43a Elevation accuracy radial flight at 1950 ft and on +51 degrees radial

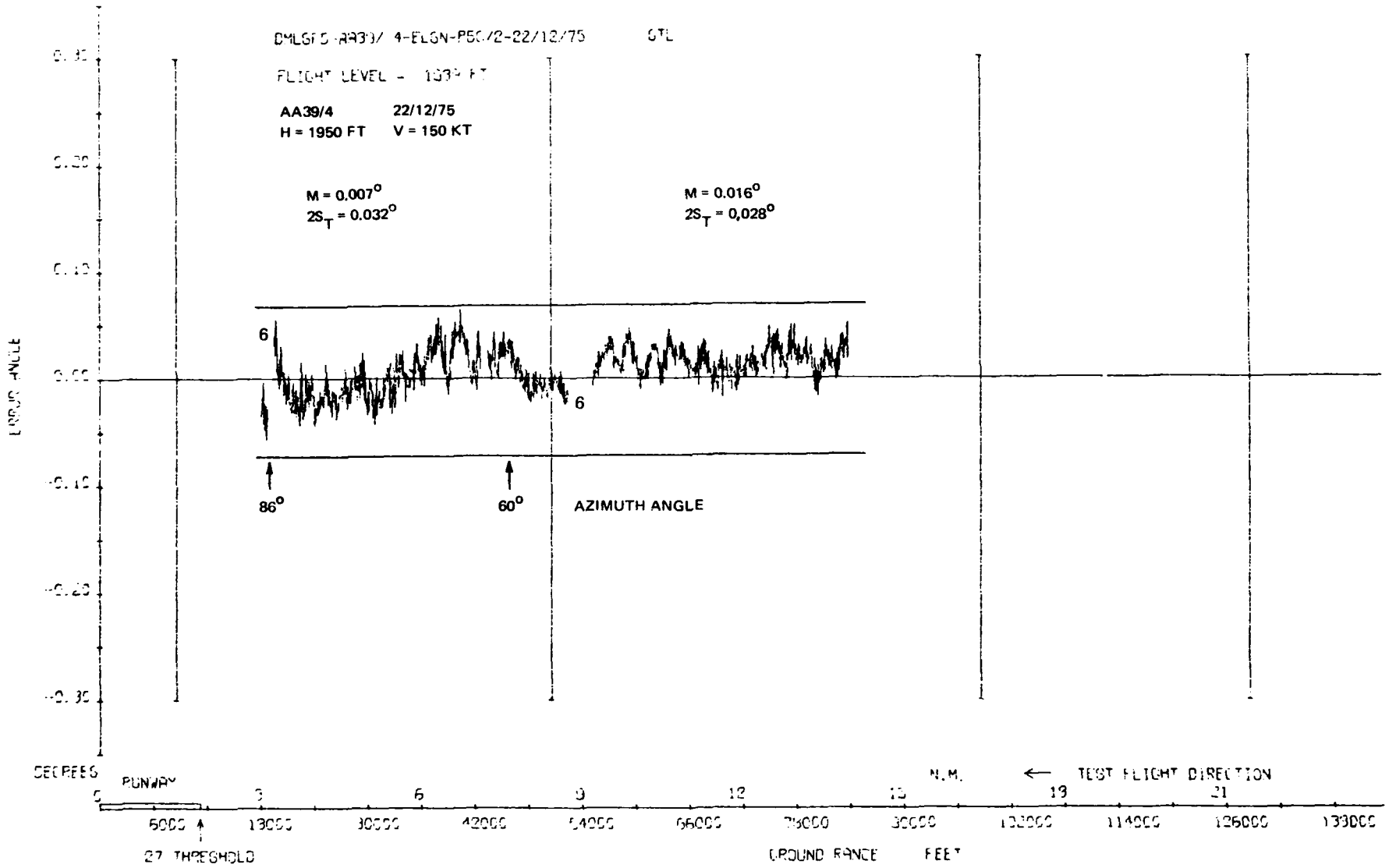

Fig 4.43c

Fig 4.43c Elevation accuracy radial flight at 1950 ft and on +51 degrees radial

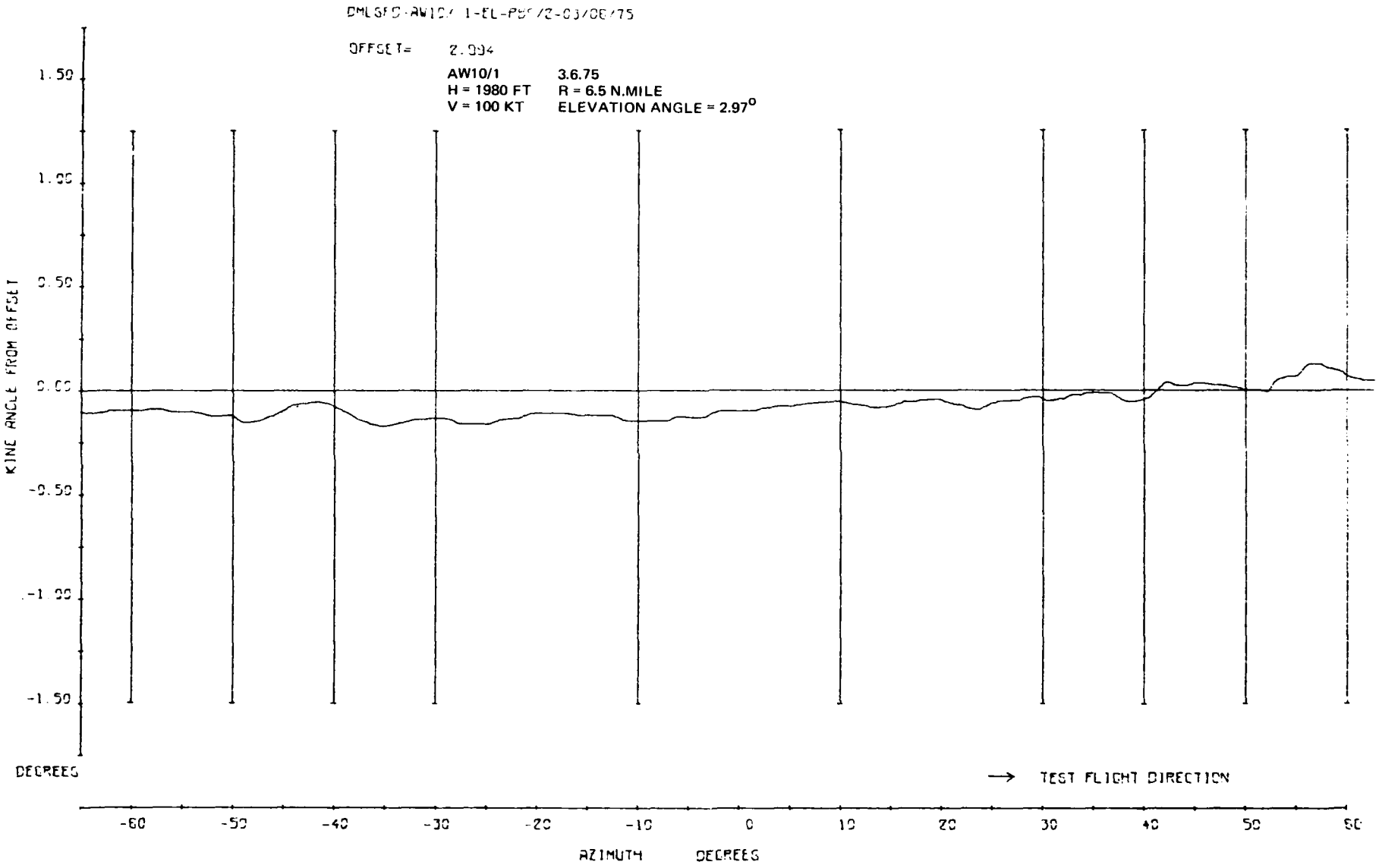

Fig 4.44a

Fig 4.44a Elevation orbital flight at 1980 ft and 6.5 n mile radius

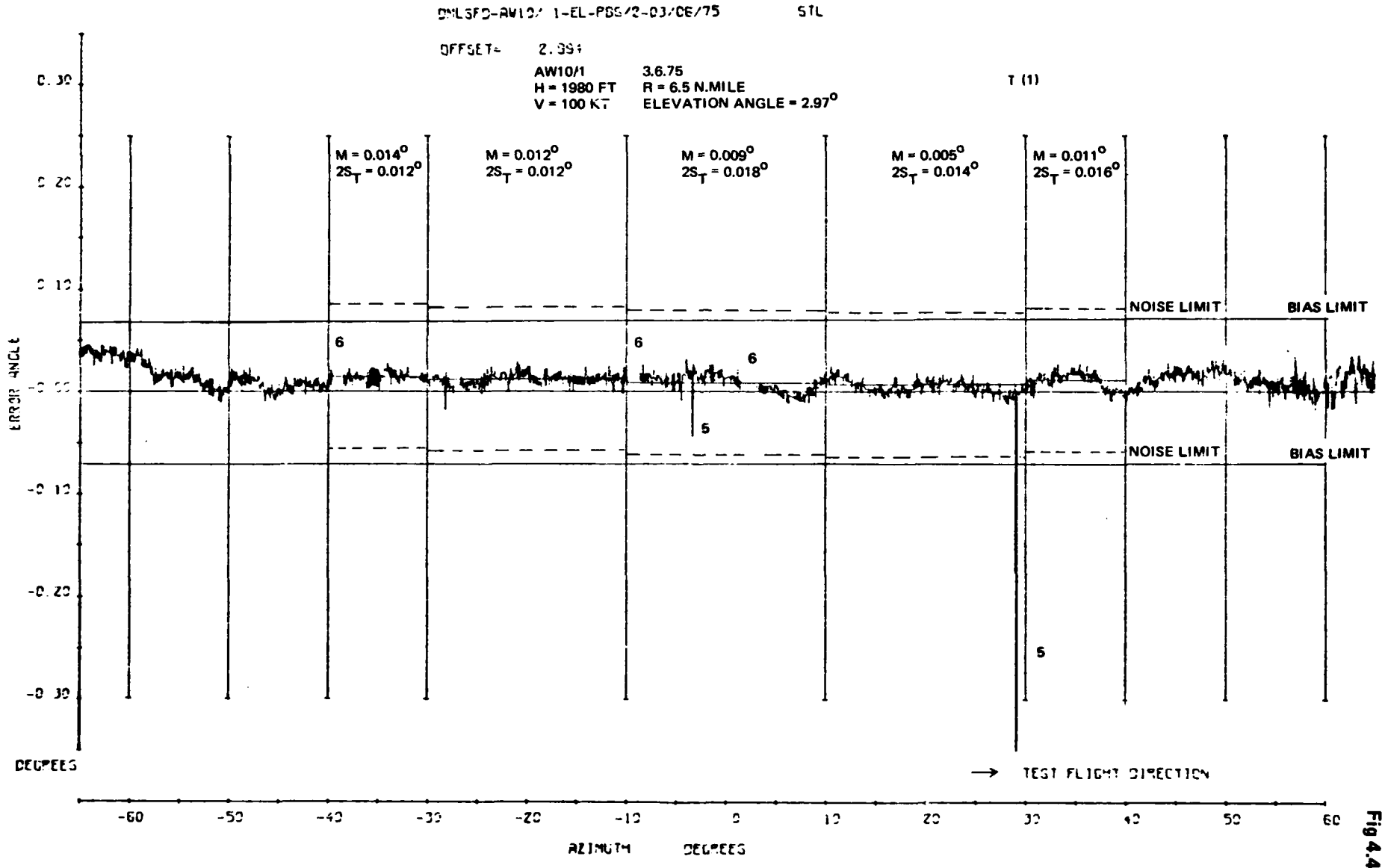

Fig 4.44c Elevation orbital flight at 1980 ft and 6.5 n mile radius

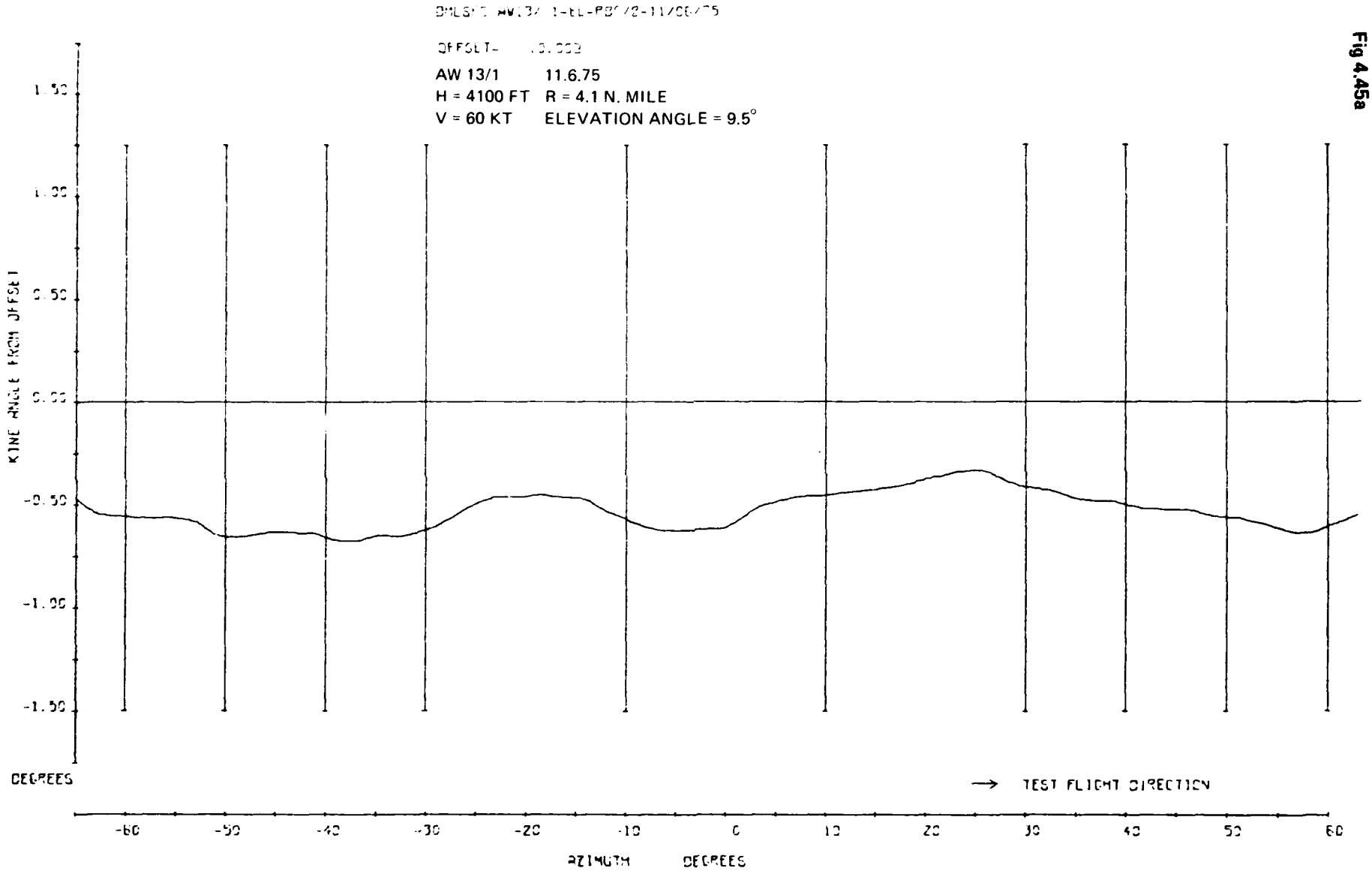

Fig 4.45a

Fig 4.45a Elevation orbital flight at 4100 ft and 4.1 n mile radius

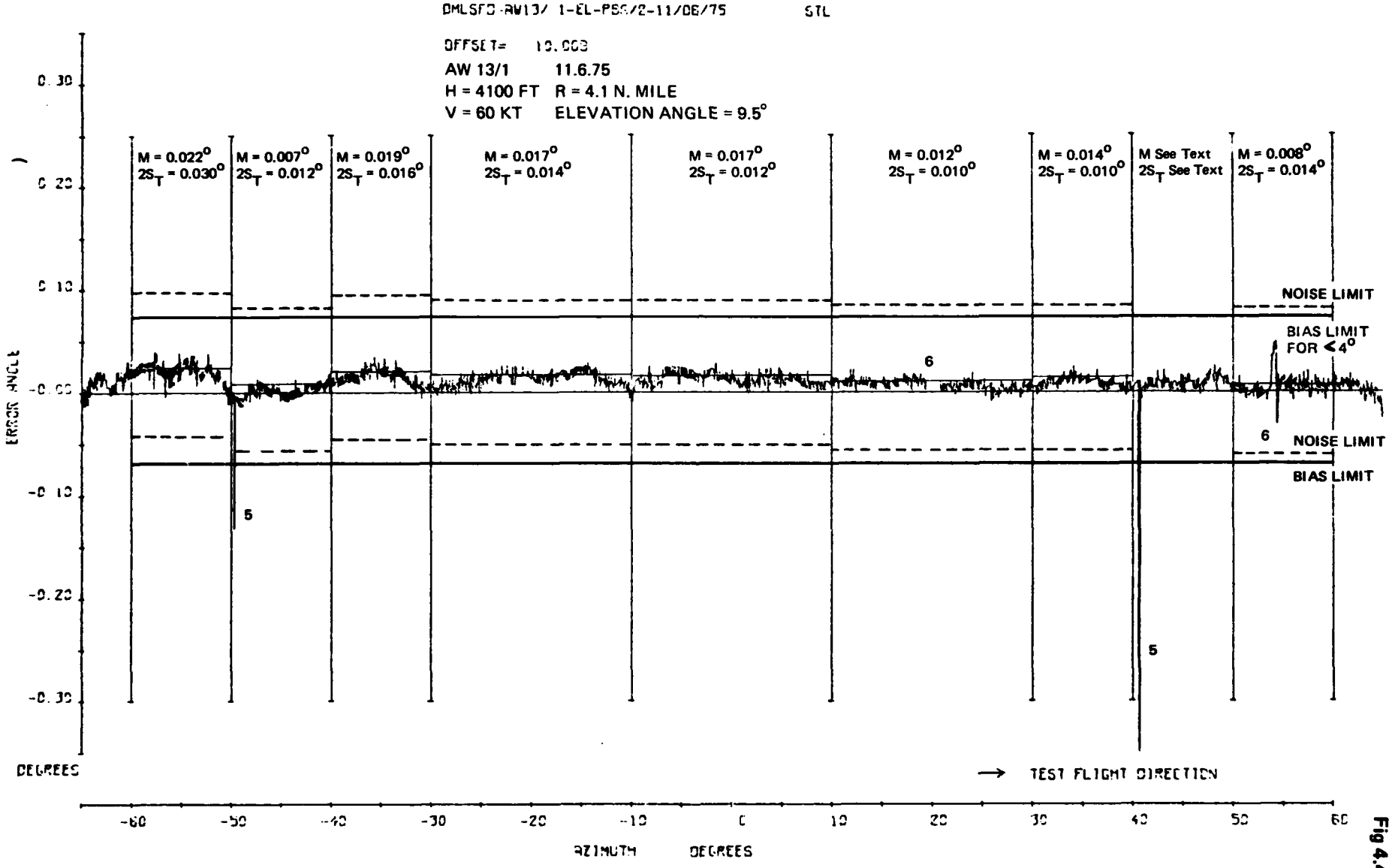

Fig 4.45c

Fig 4.45c Elevation orbital flight at 4100 ft and 4.1 mile radius

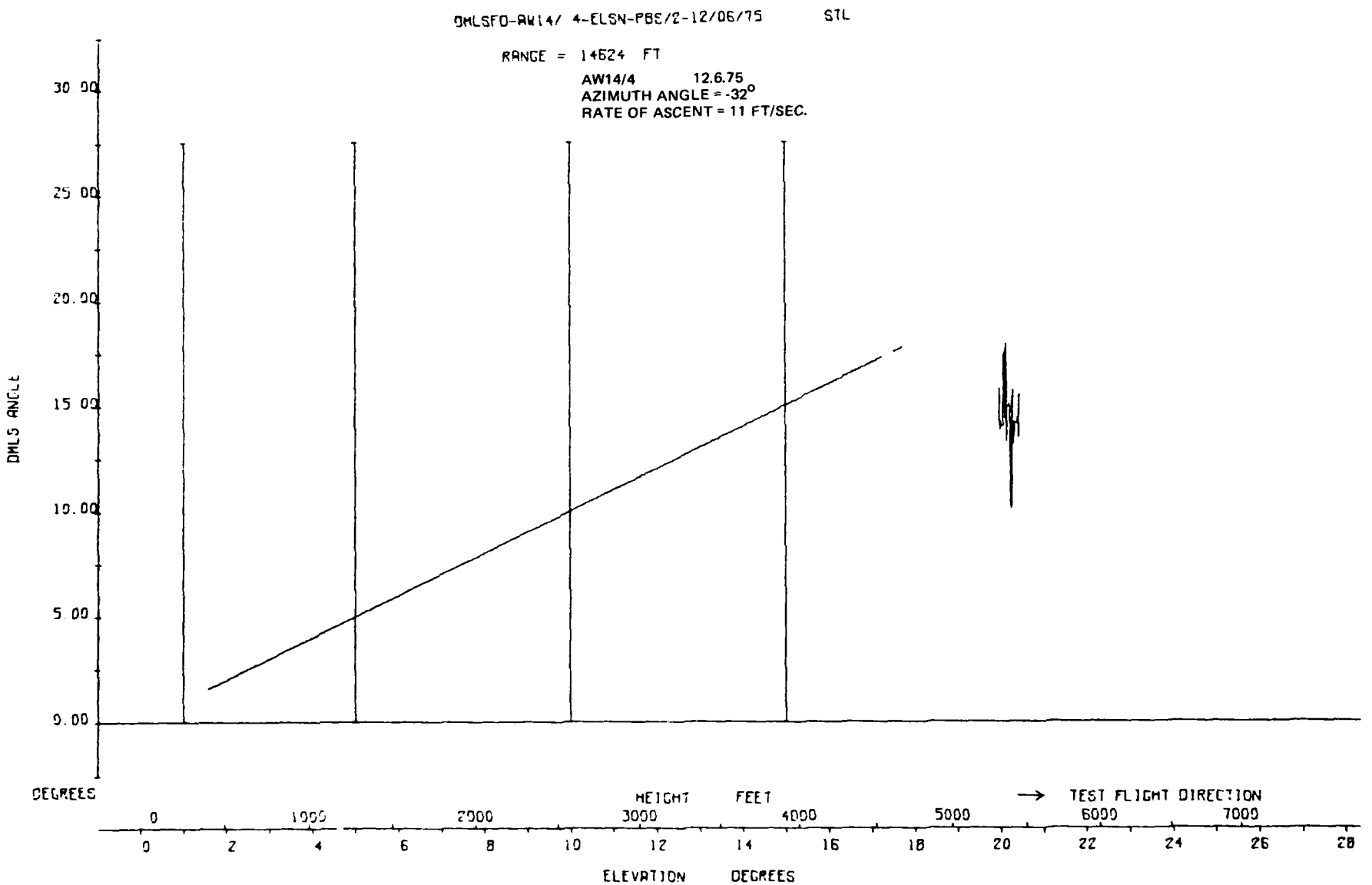

Fig 4.46a/b

Fig 4.46a/b Elevation vertical ascent

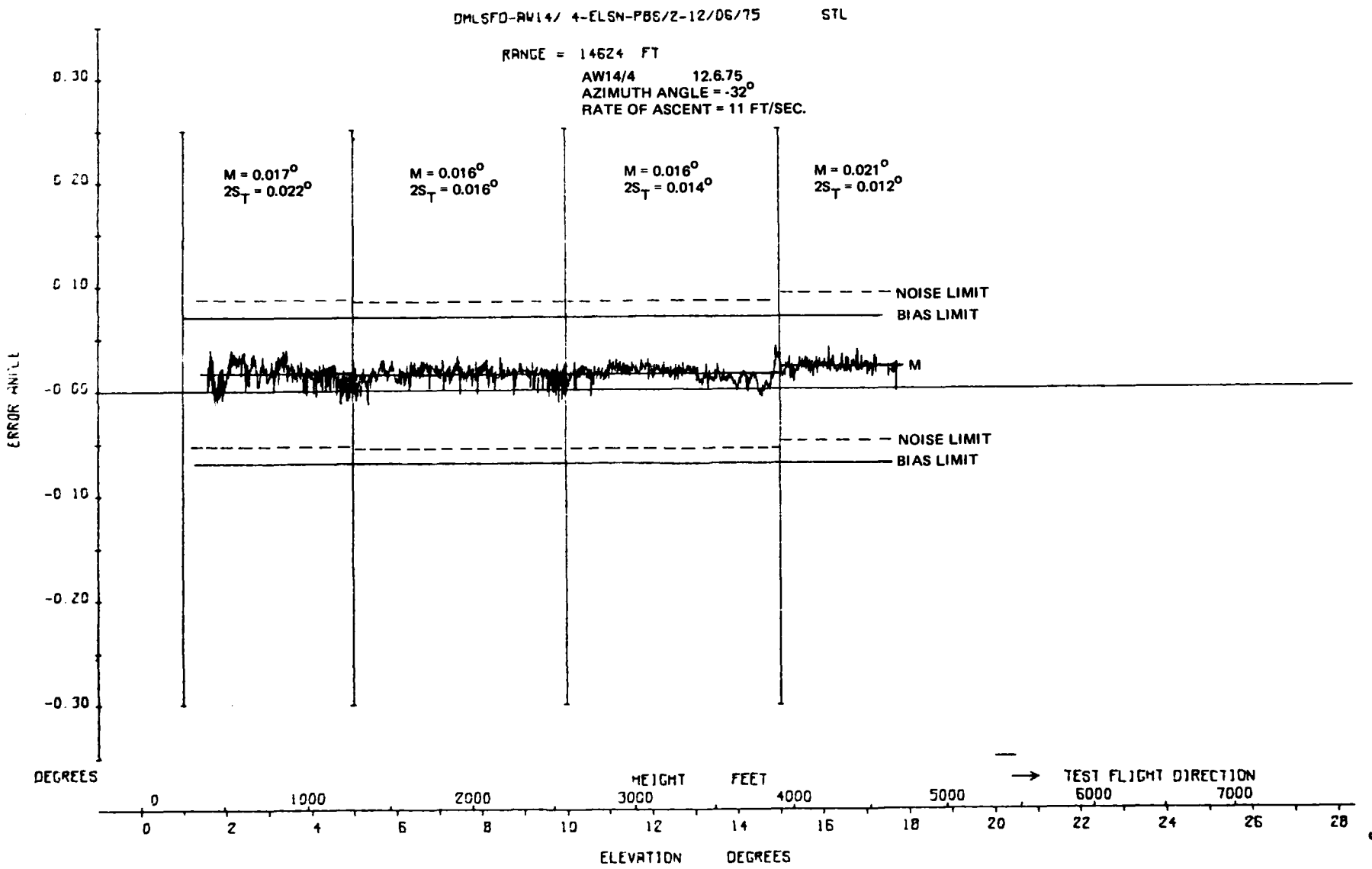

Fig 4.46c

Fig 4.46c Elevation vertical ascent

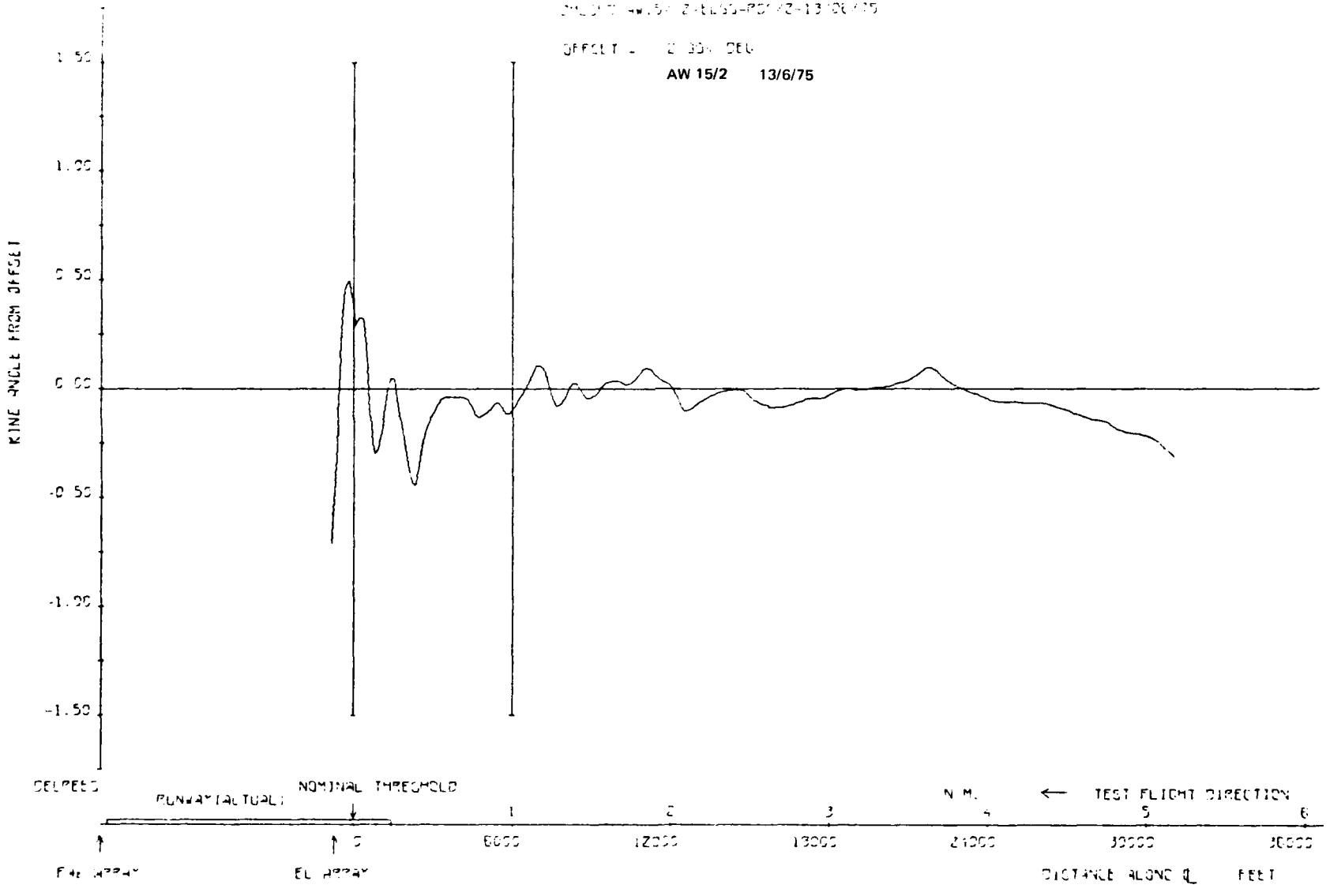

Fig 4.47a

Fig 4.47a Elevation accuracy. 3 degree approach to touchdown

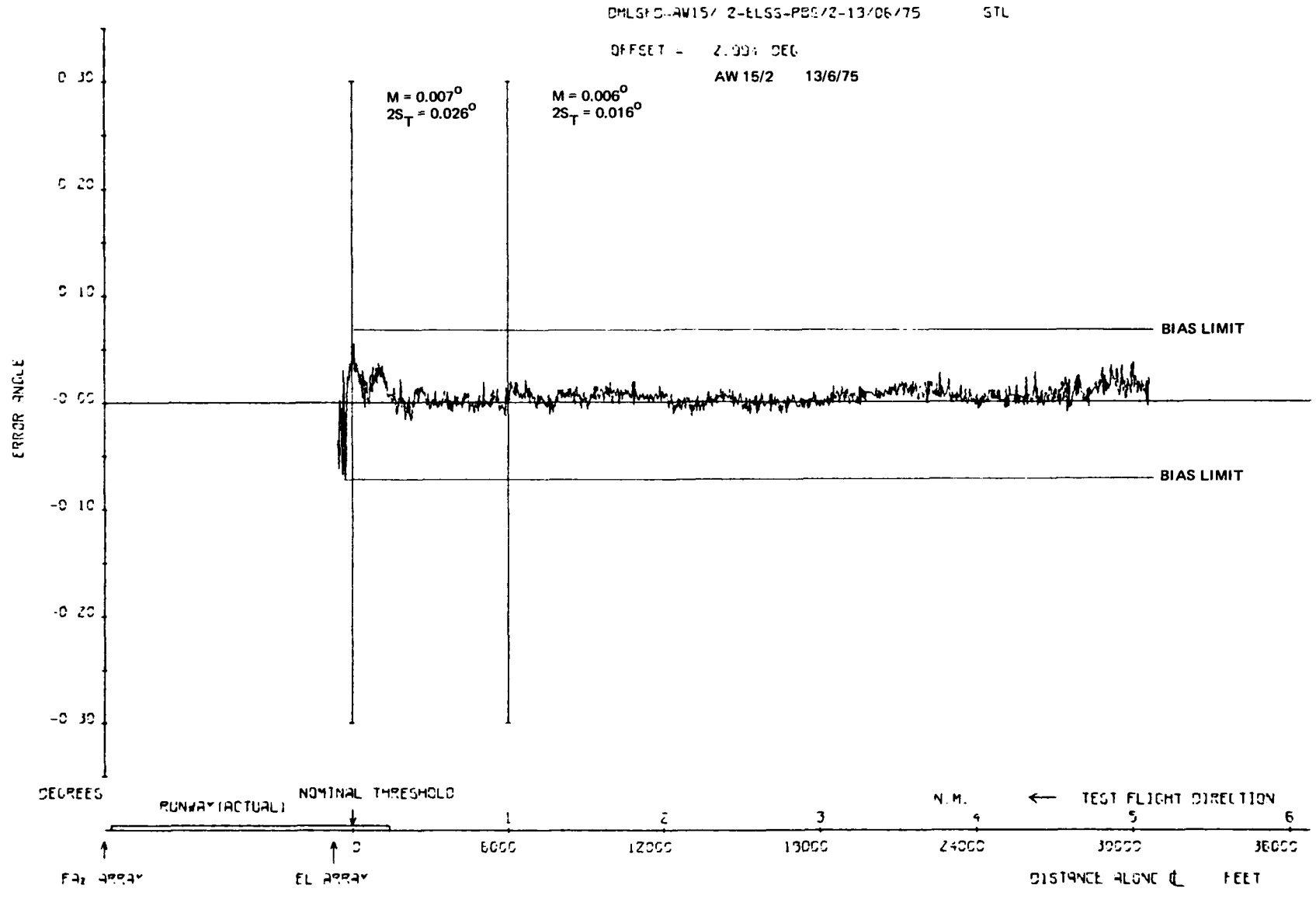

Fig 4.47c Elevation accuracy. 3 degree approach to touchdown

Fig 4.47c

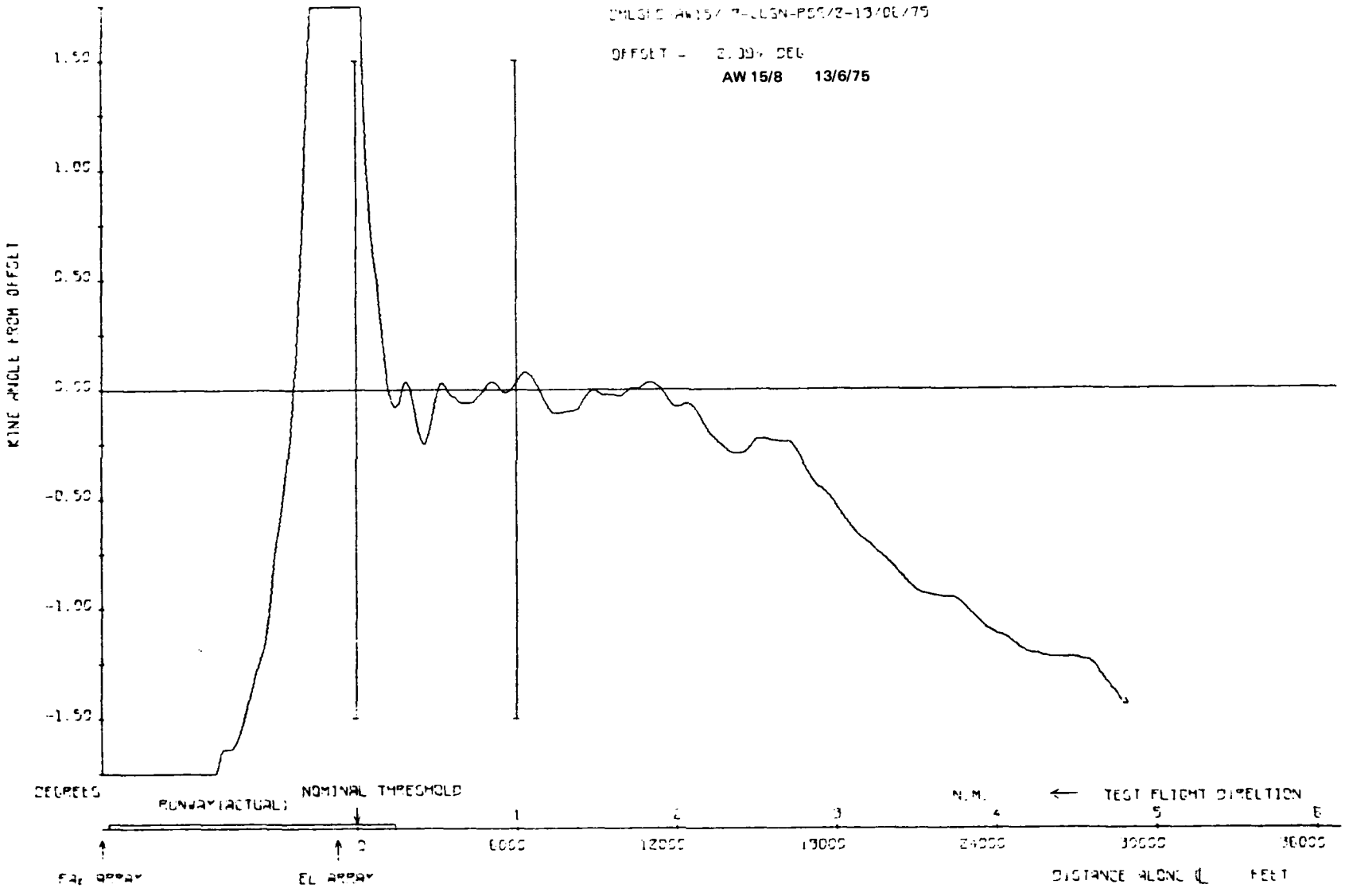

Fig 4.48a

Fig.4.48a Elevation accuracy. 3 degree approach to 100 ft level overfly

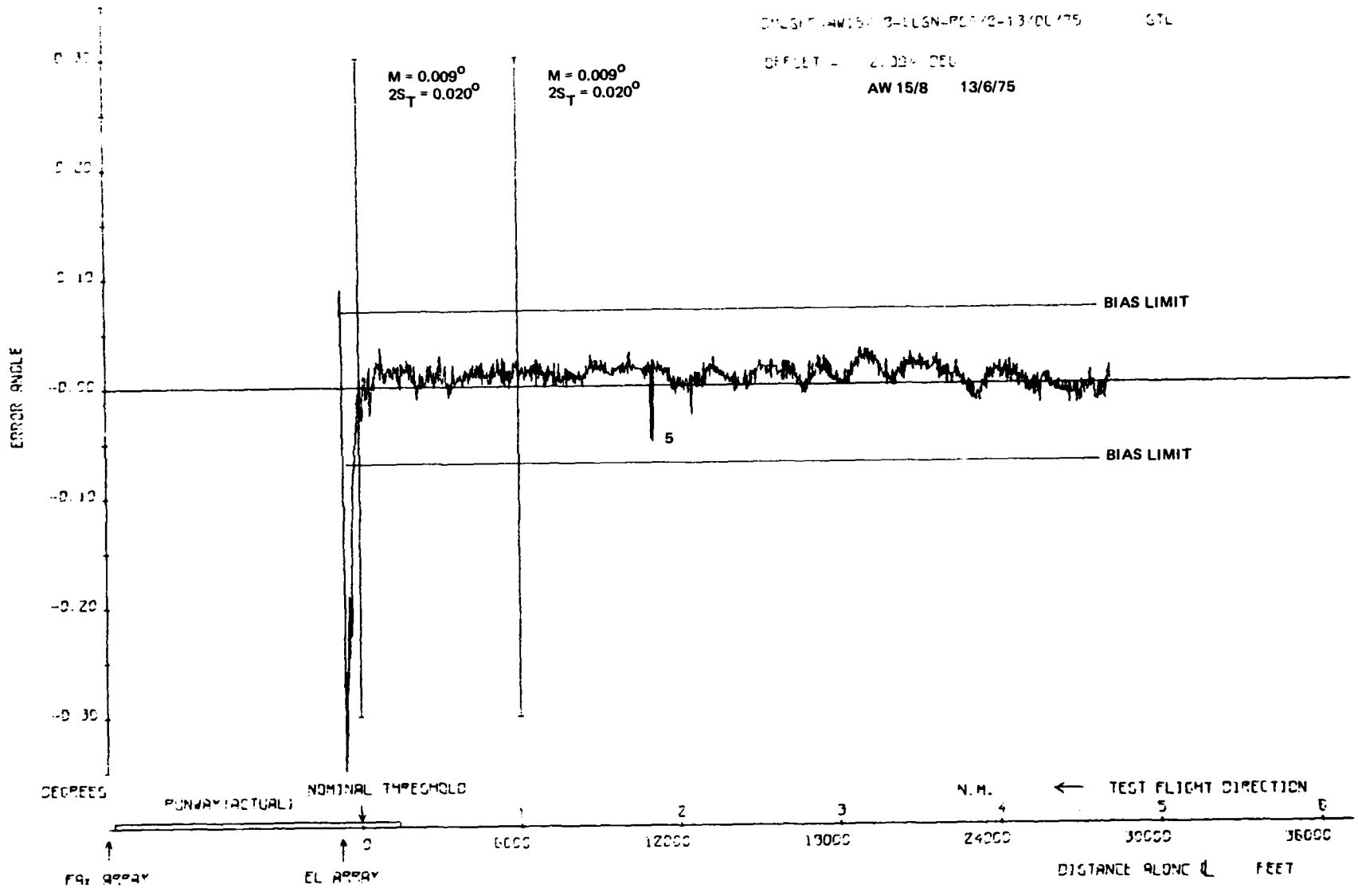

Fig 4.48c Elevation accuracy. 3 degree approach to 100 ft level overfly

Fig 4.48c

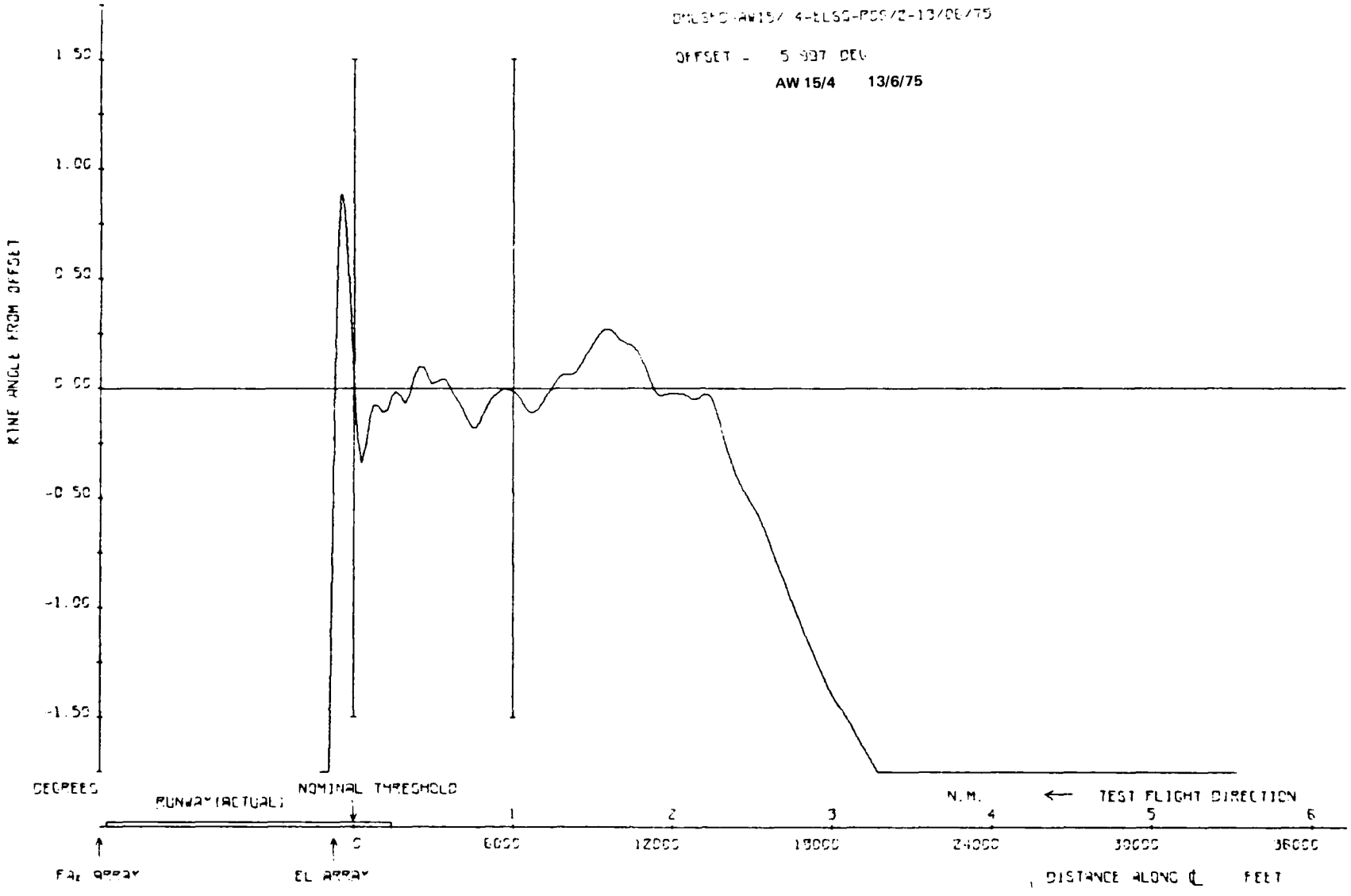

Fig 4.49a

Fig 4.49a Elevation accuracy. 6 degree approach to 50 ft

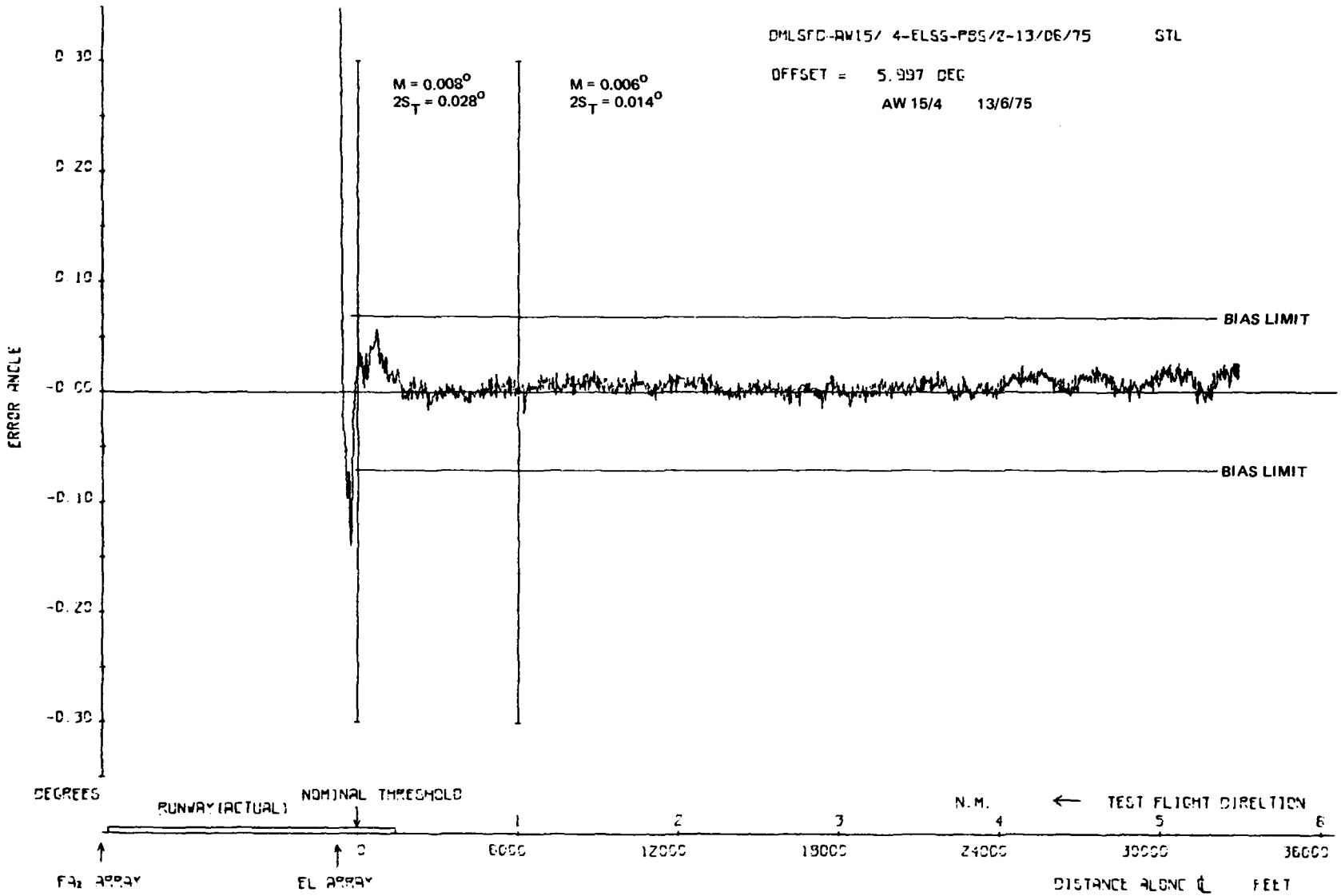

Fig 4.49c

Fig 4.49c Elevation accuracy. 6 degree approach to 50 ft

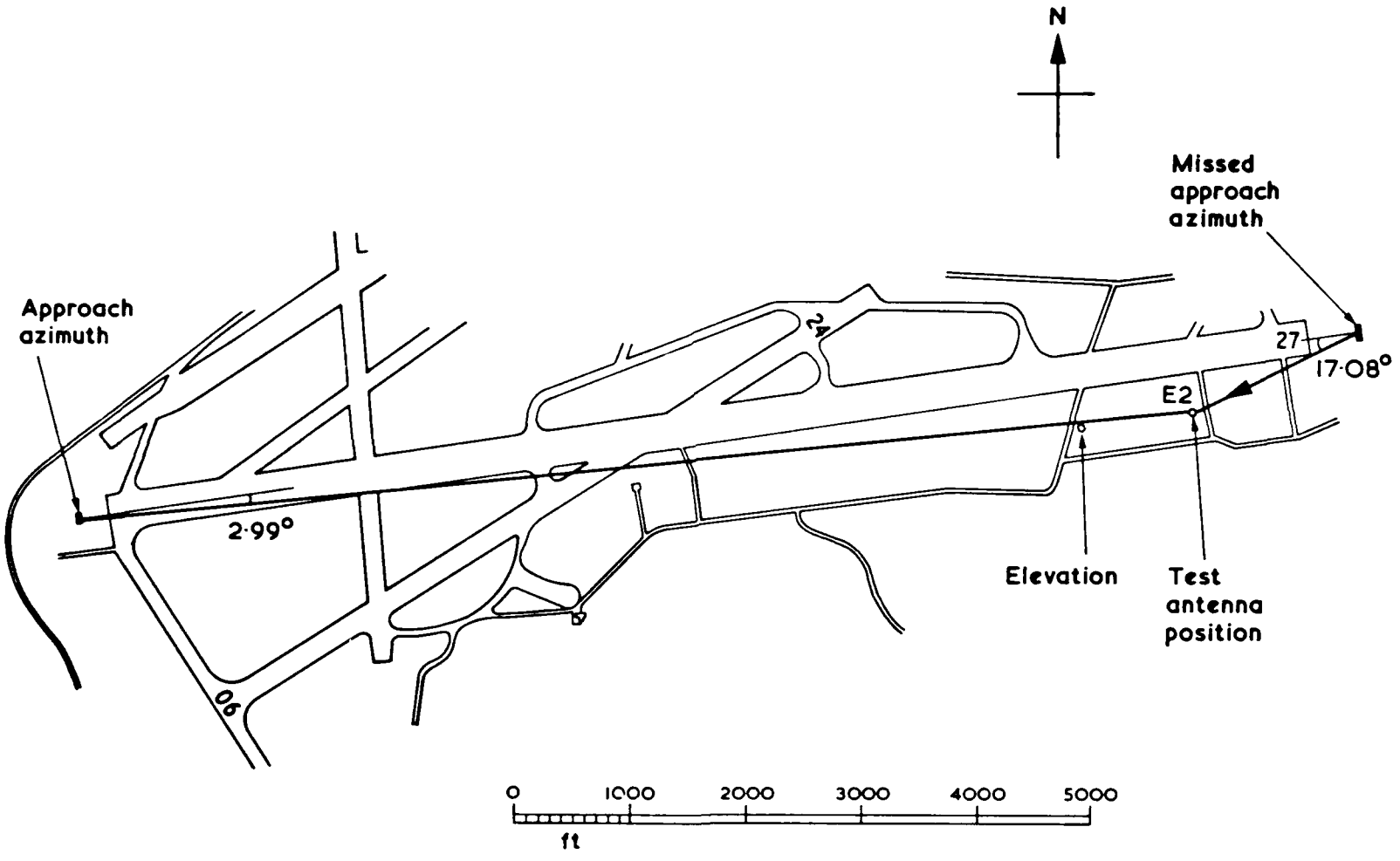

Fig 4.50 Stability test – general site plan Bedford

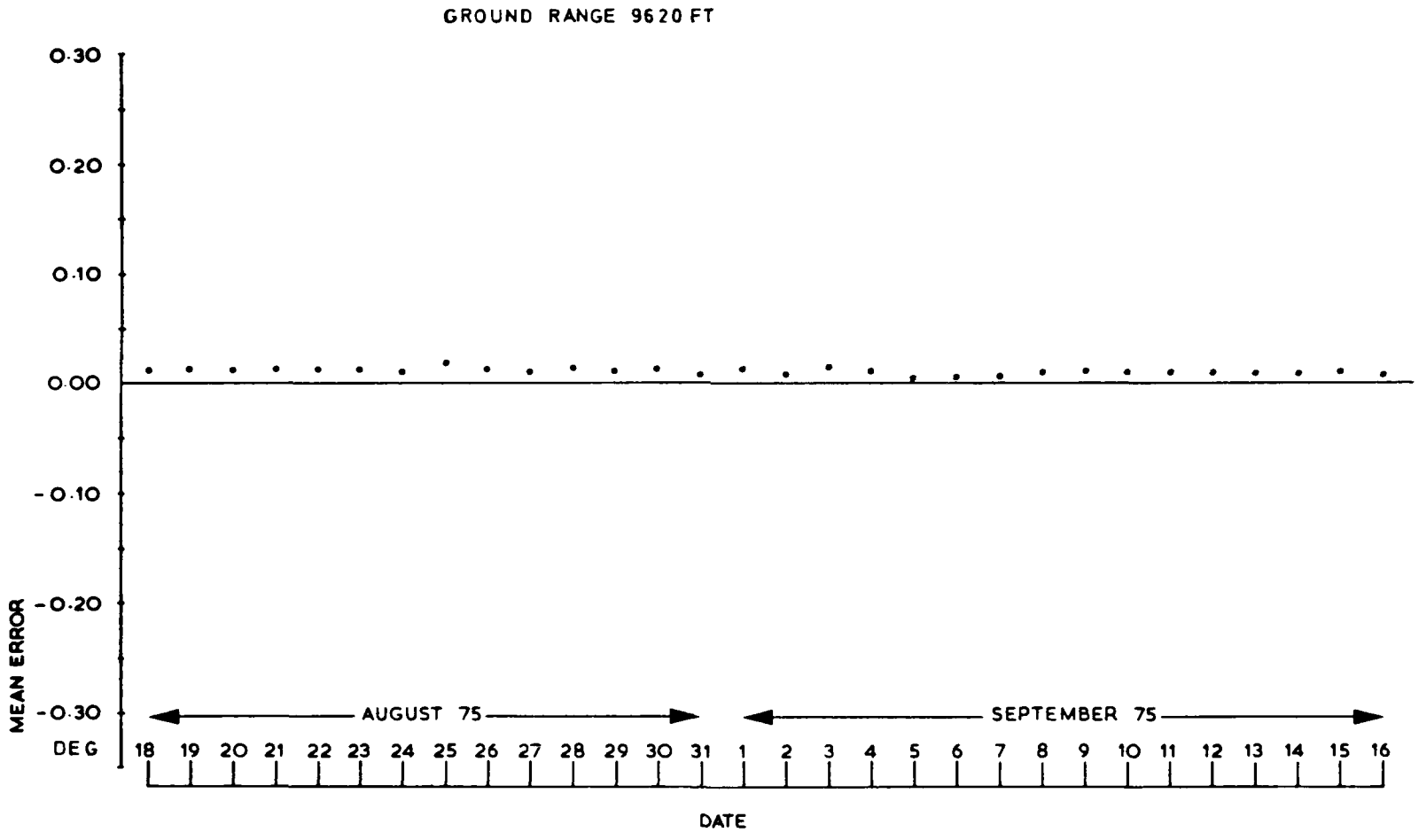

Fig 4.51 Stability test – approach mean error

Fig 4.51

Fig 4.52

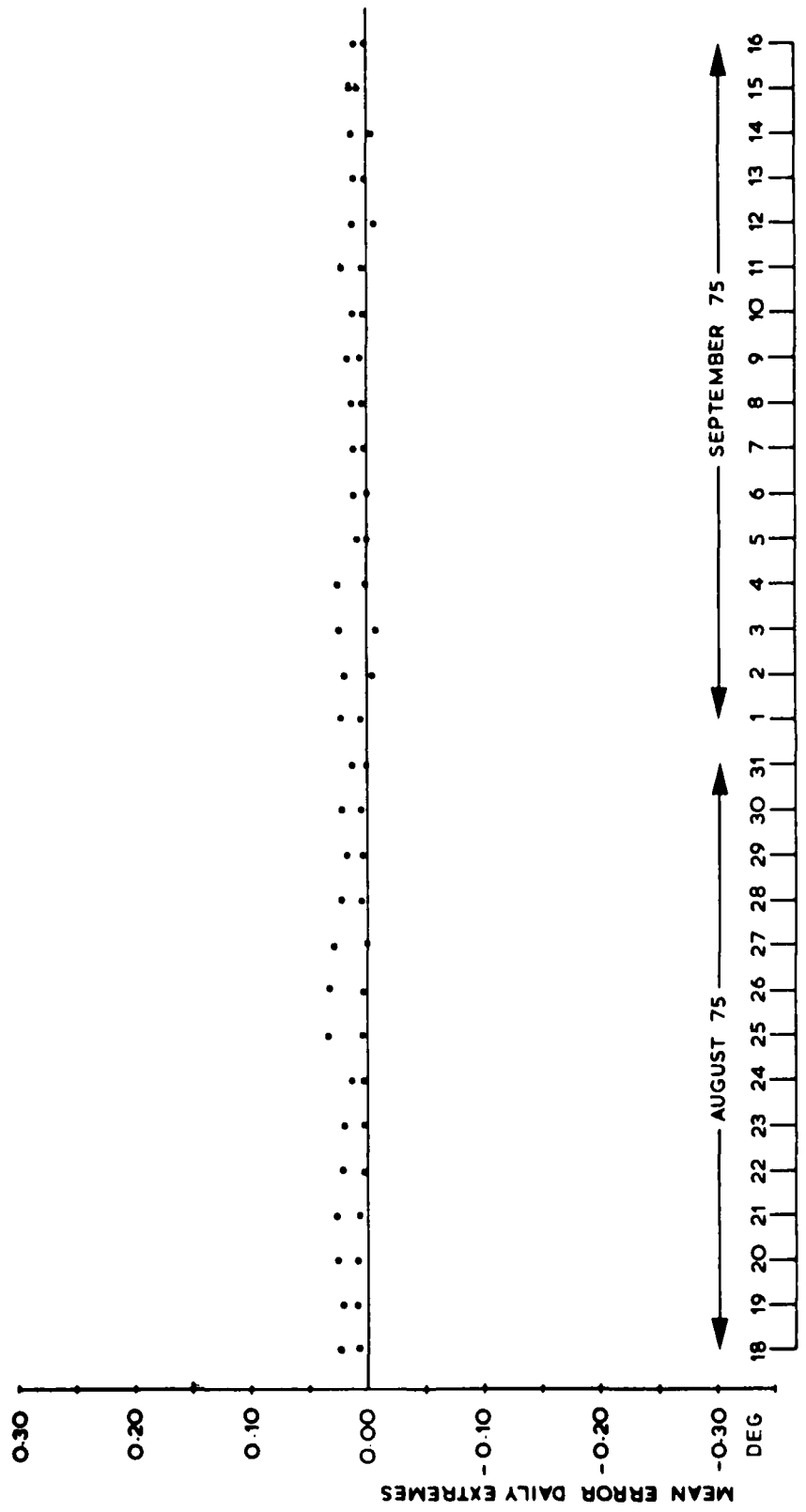

Fig 4.52 Stability test – approach azimuth daily mean error extremes

TR 79052

Fig 4.53

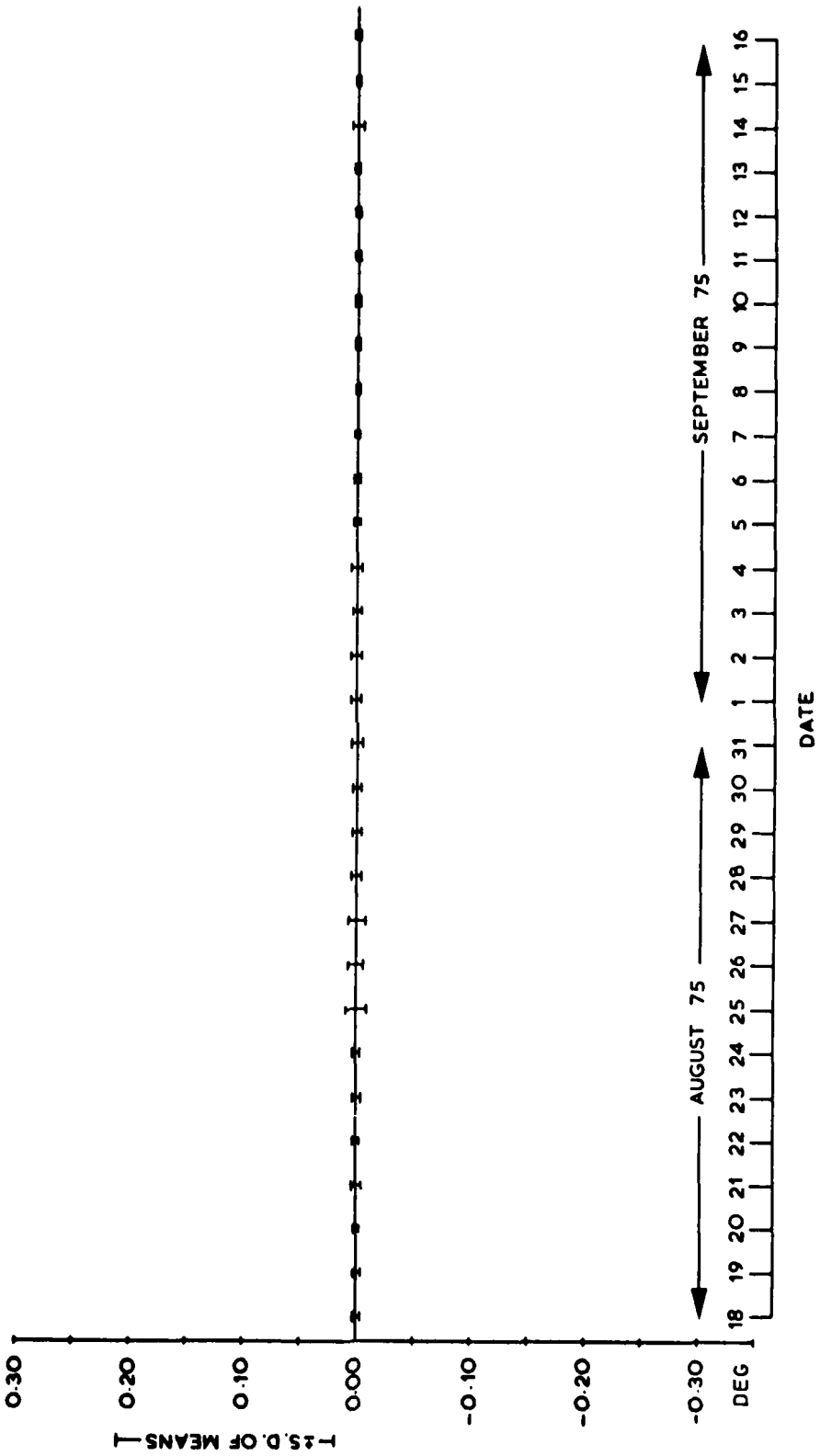

TR 79052

Fig 4.53 Stability test – approach azimuth daily standard deviation of means

Fig 4.54

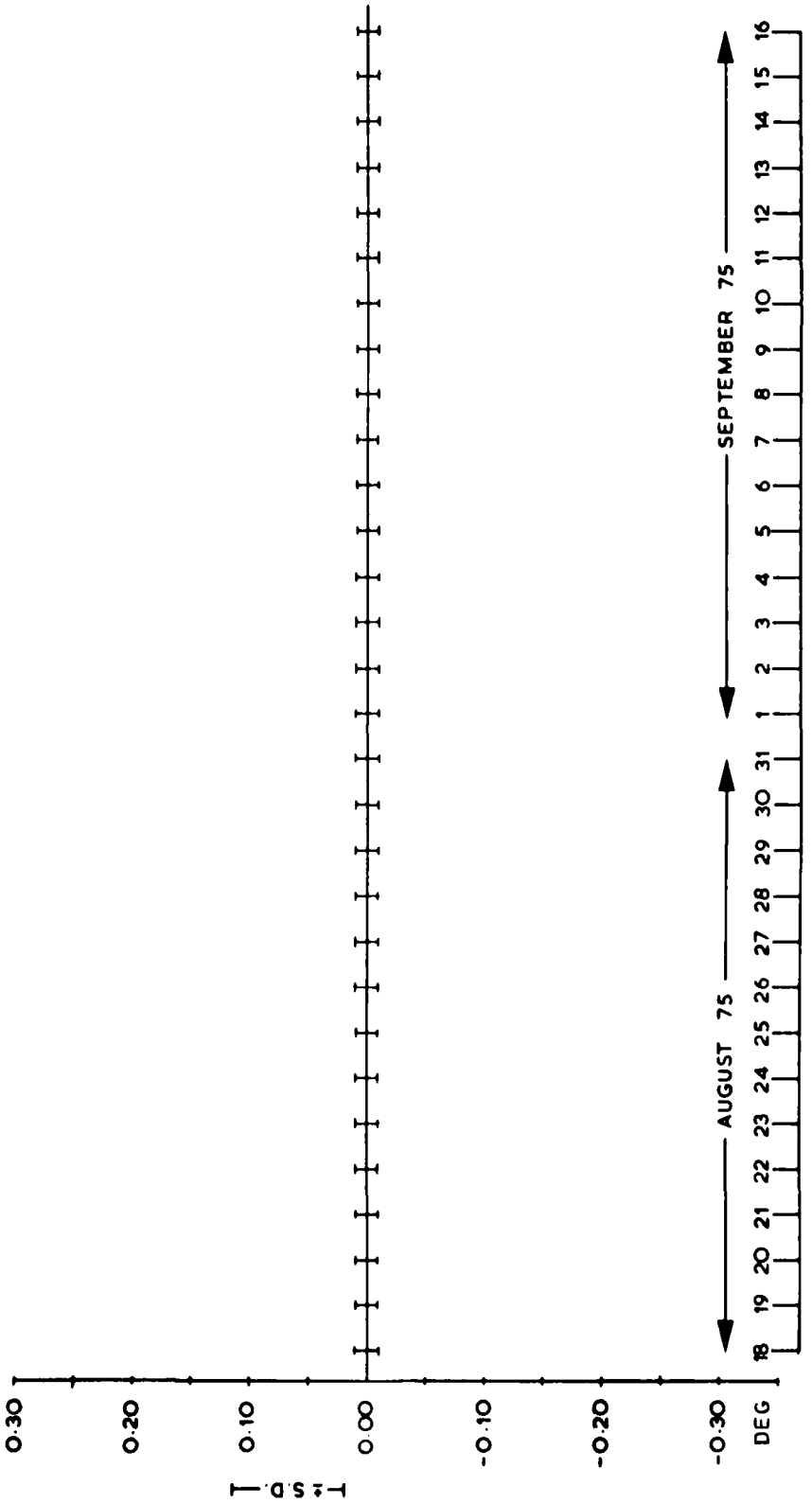

Fig 4.54 Stability test – approach azimuth noise error rms

TR 79052

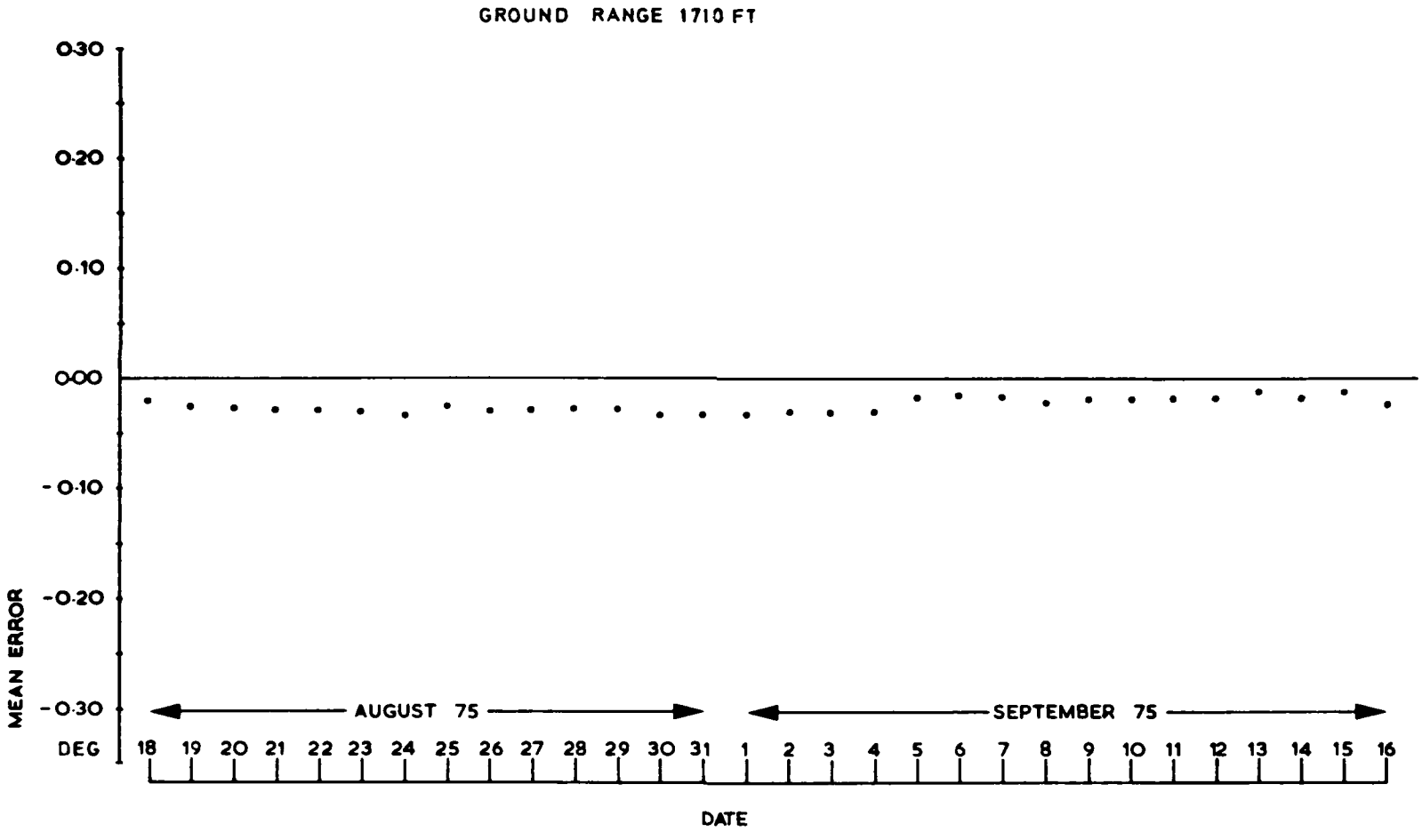

Fig 4.55 Stability test – missed approach azimuth mean error

Fig 4.56

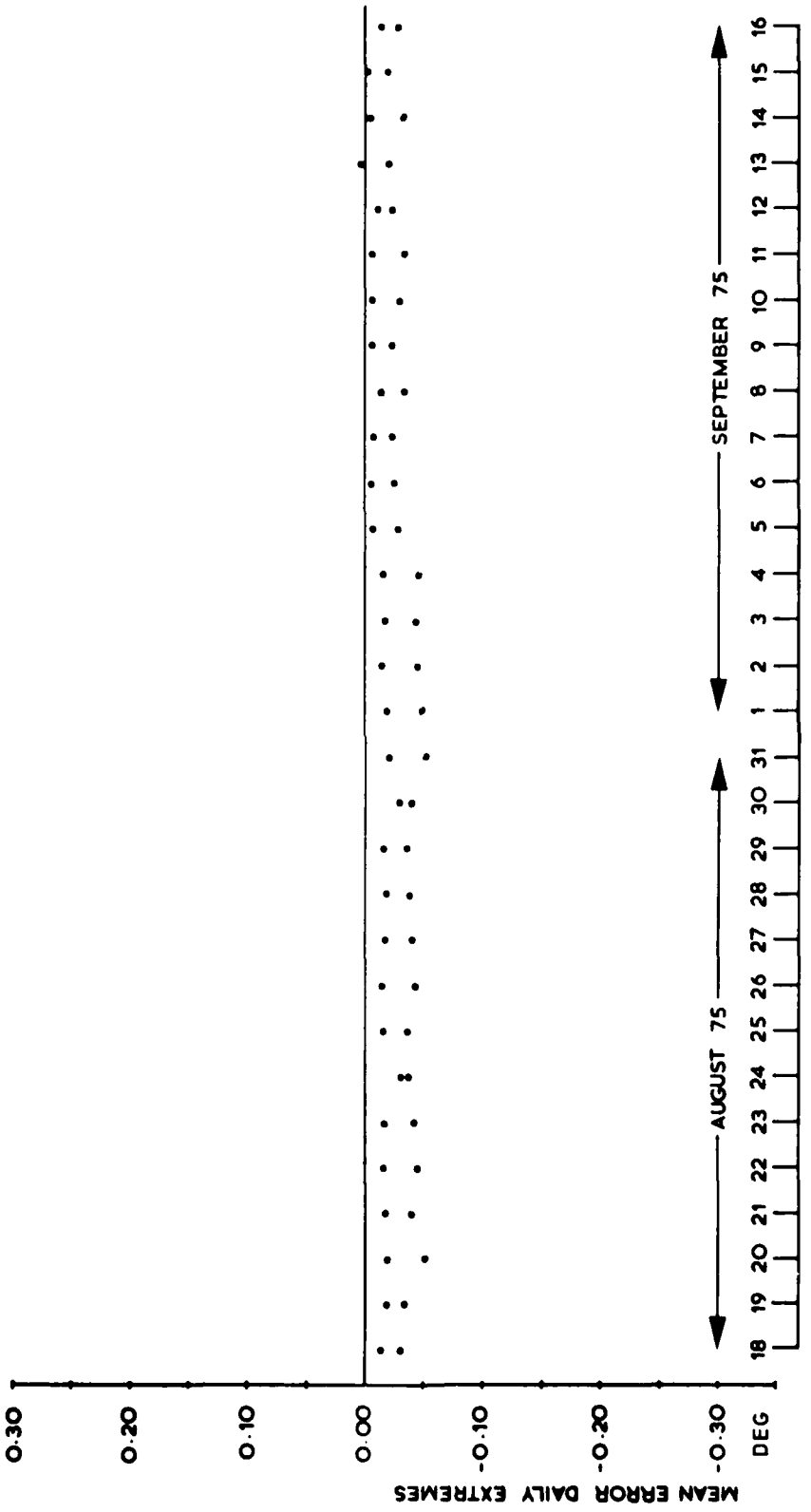

Fig 4.56 Stability test – missed approach azimuth daily mean error extremes

TR 79052

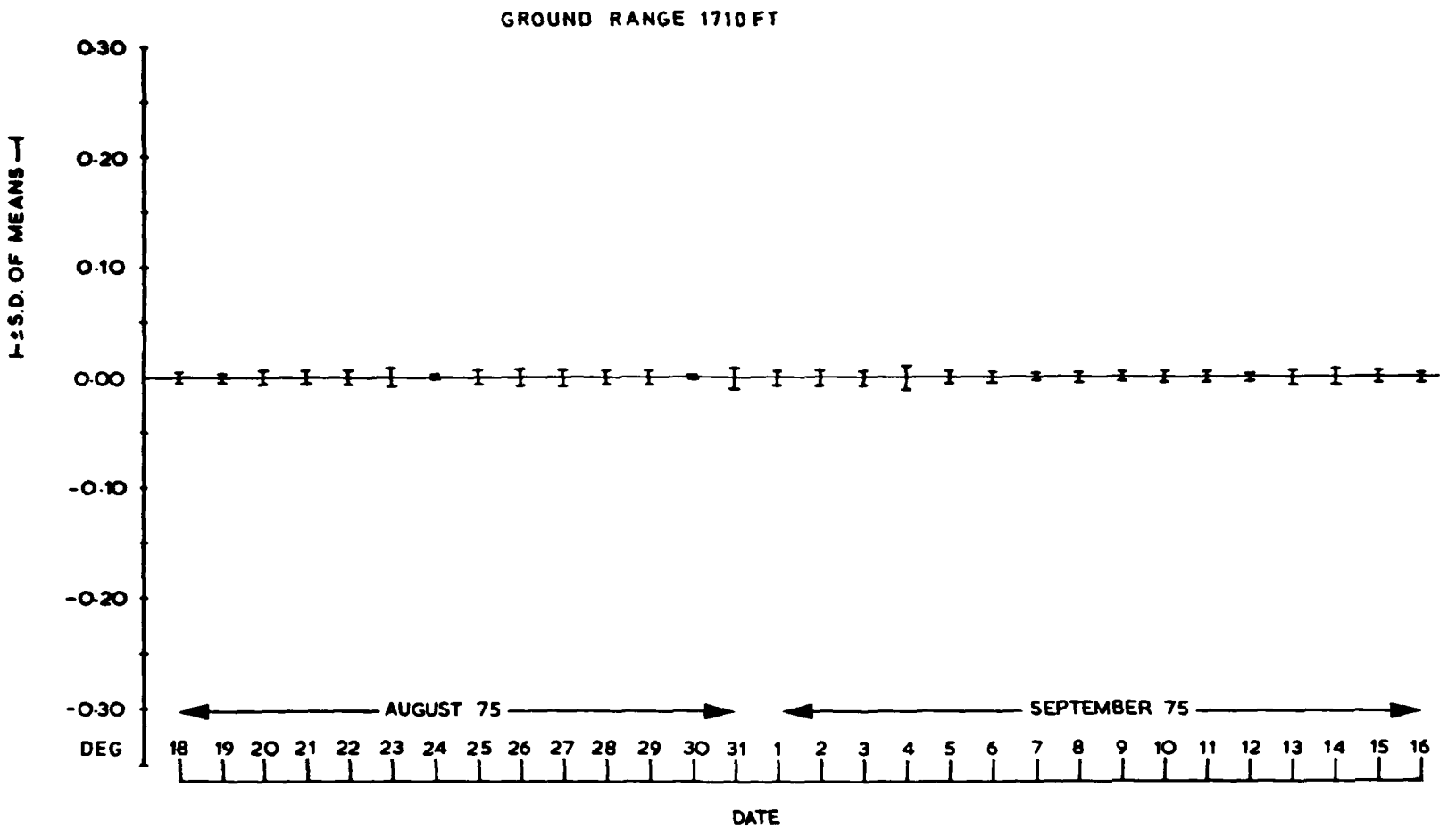

Fig 4.57 Stability test – missed approach azimuth daily standard deviation of means

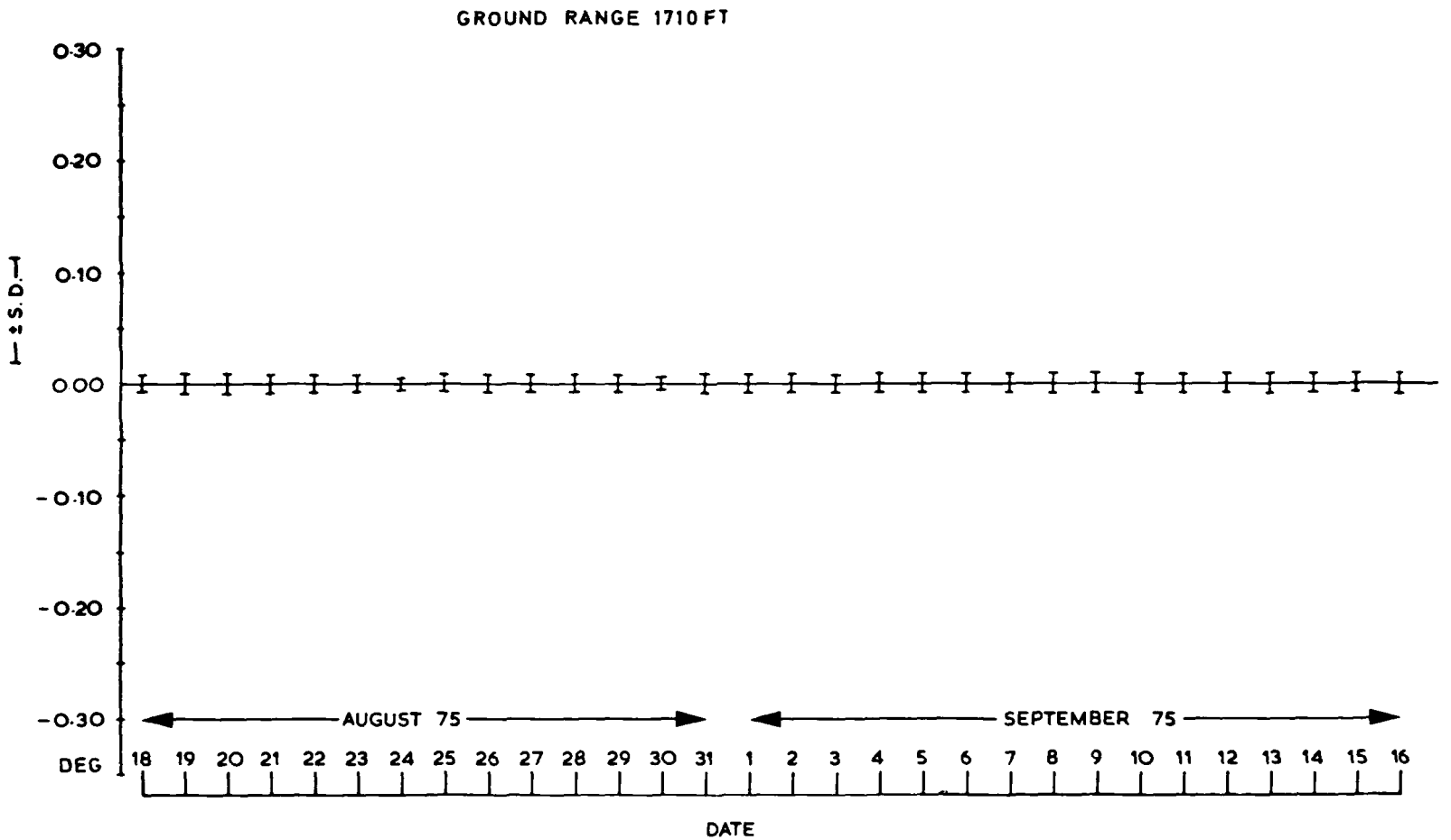

Fig 4.58 Stability test – missed approach azimuth noise error rms

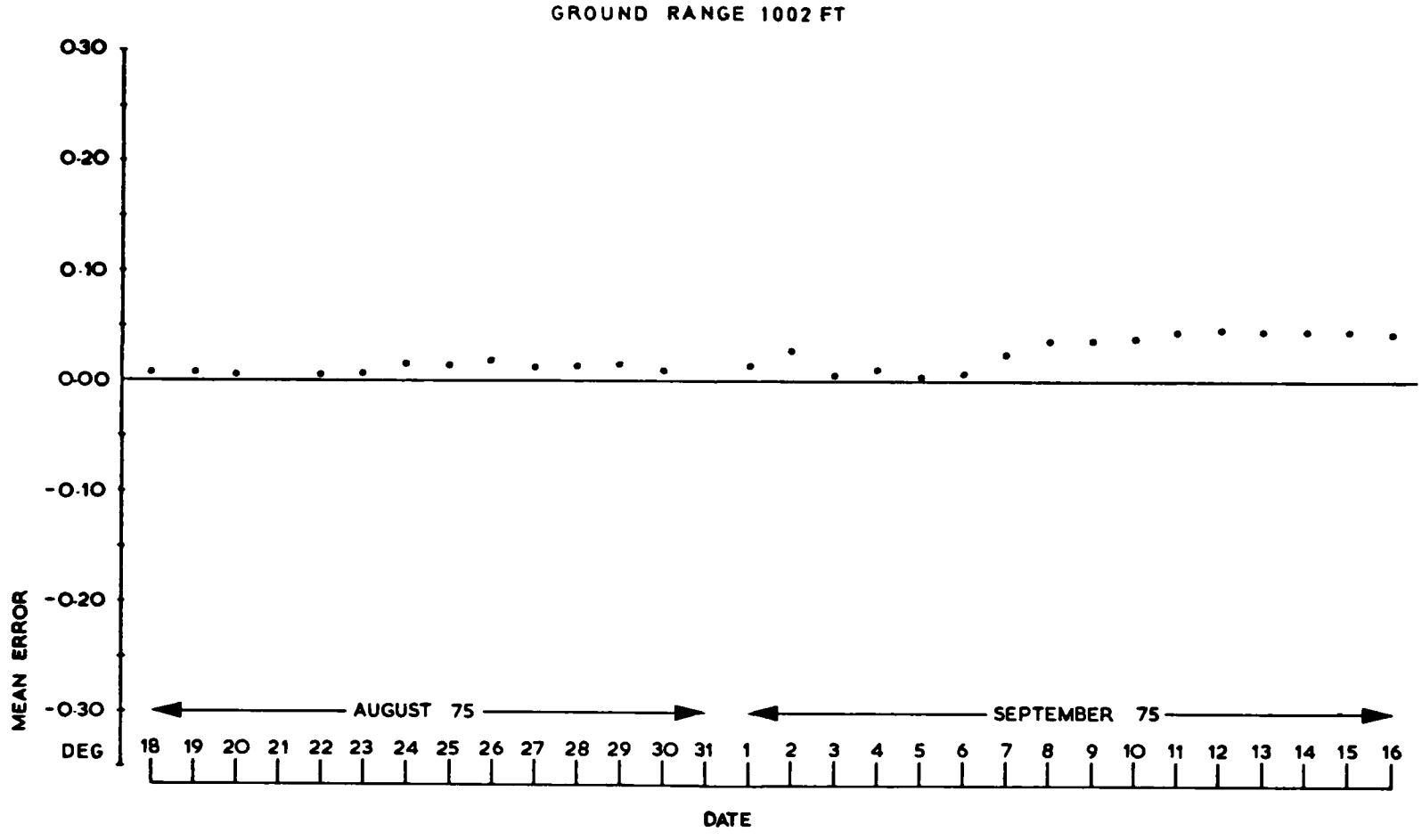

Fig 4.59 Stability test – elevation mean error

Fig 4.60

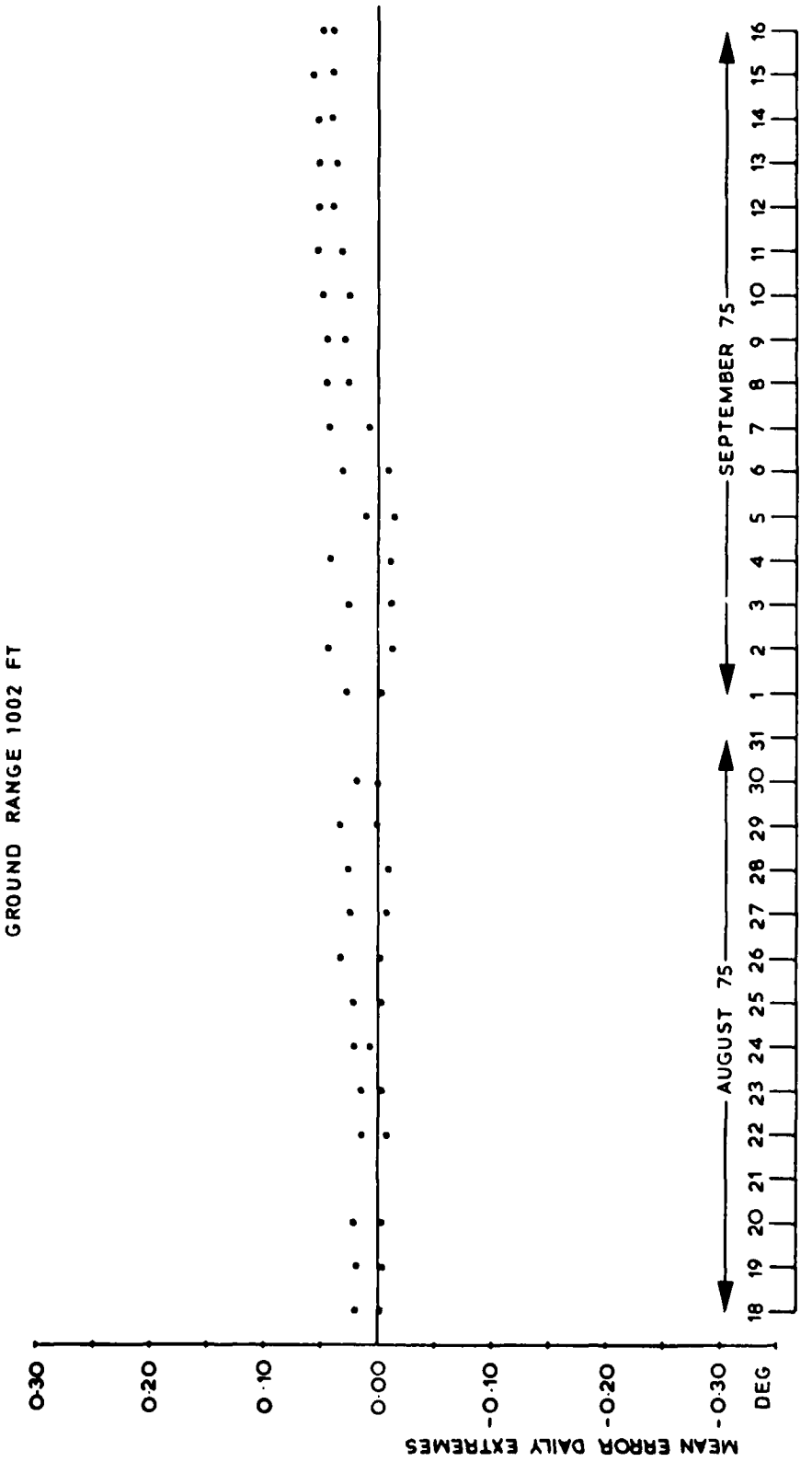

Fig 4.60 Stability test – elevation daily mean error extremes

TR 79052

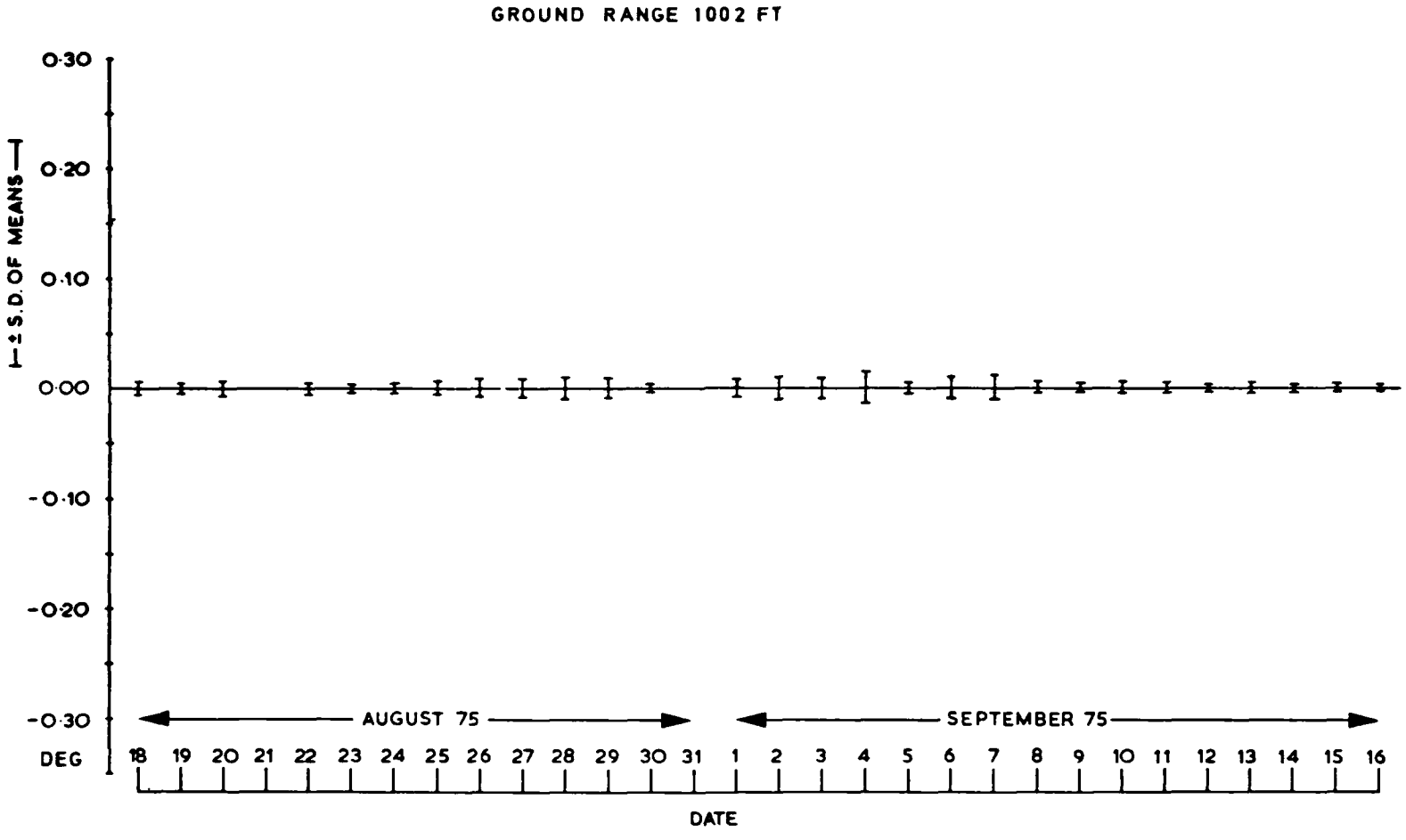

Fig 4.61 Stability test – elevation daily standard deviation of means

Fig 4.61

Fig 4.62

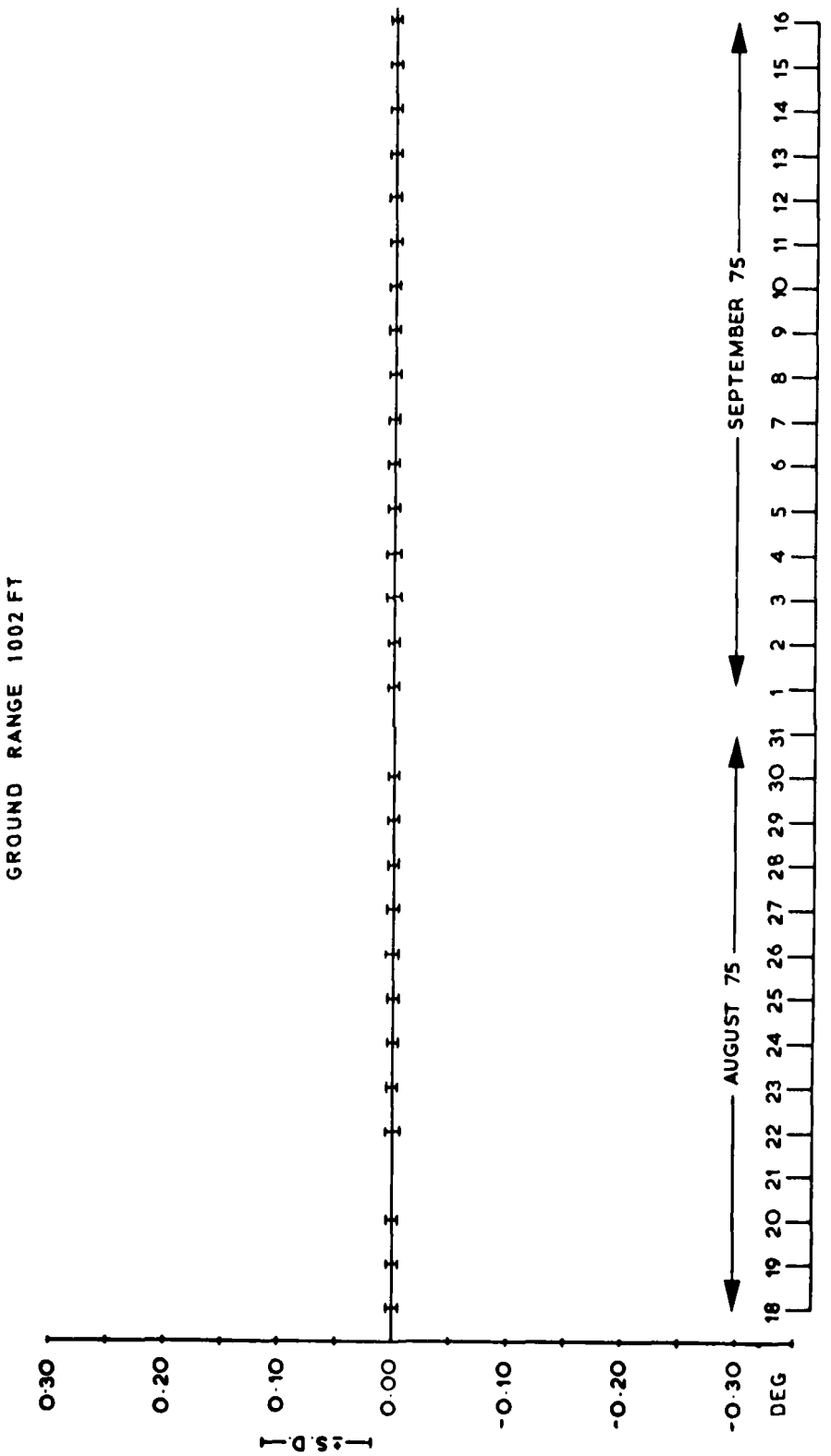

Fig 4.62 Stability test – elevation noise error rms

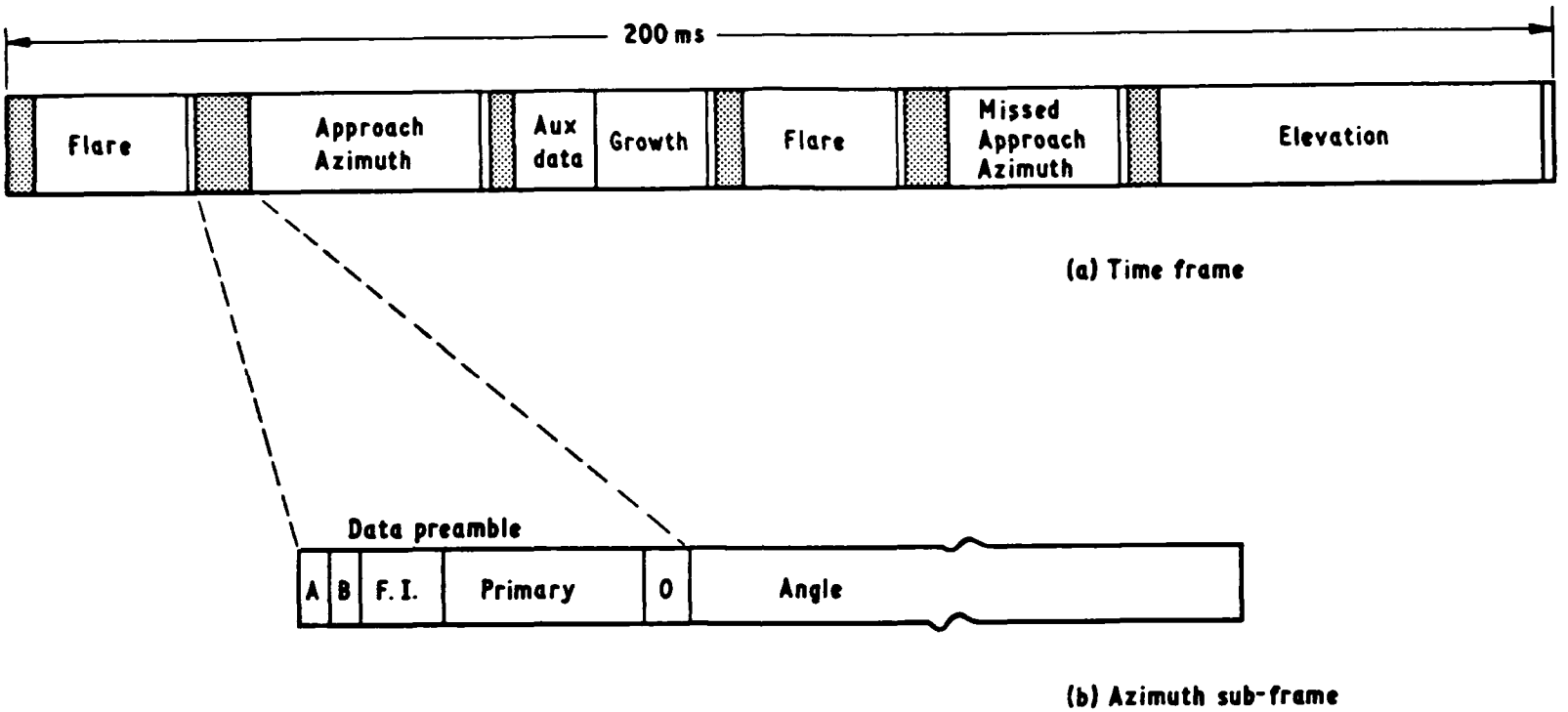

Fig 5.1 TDM signal format

Fig 5.1

Fig 5.2

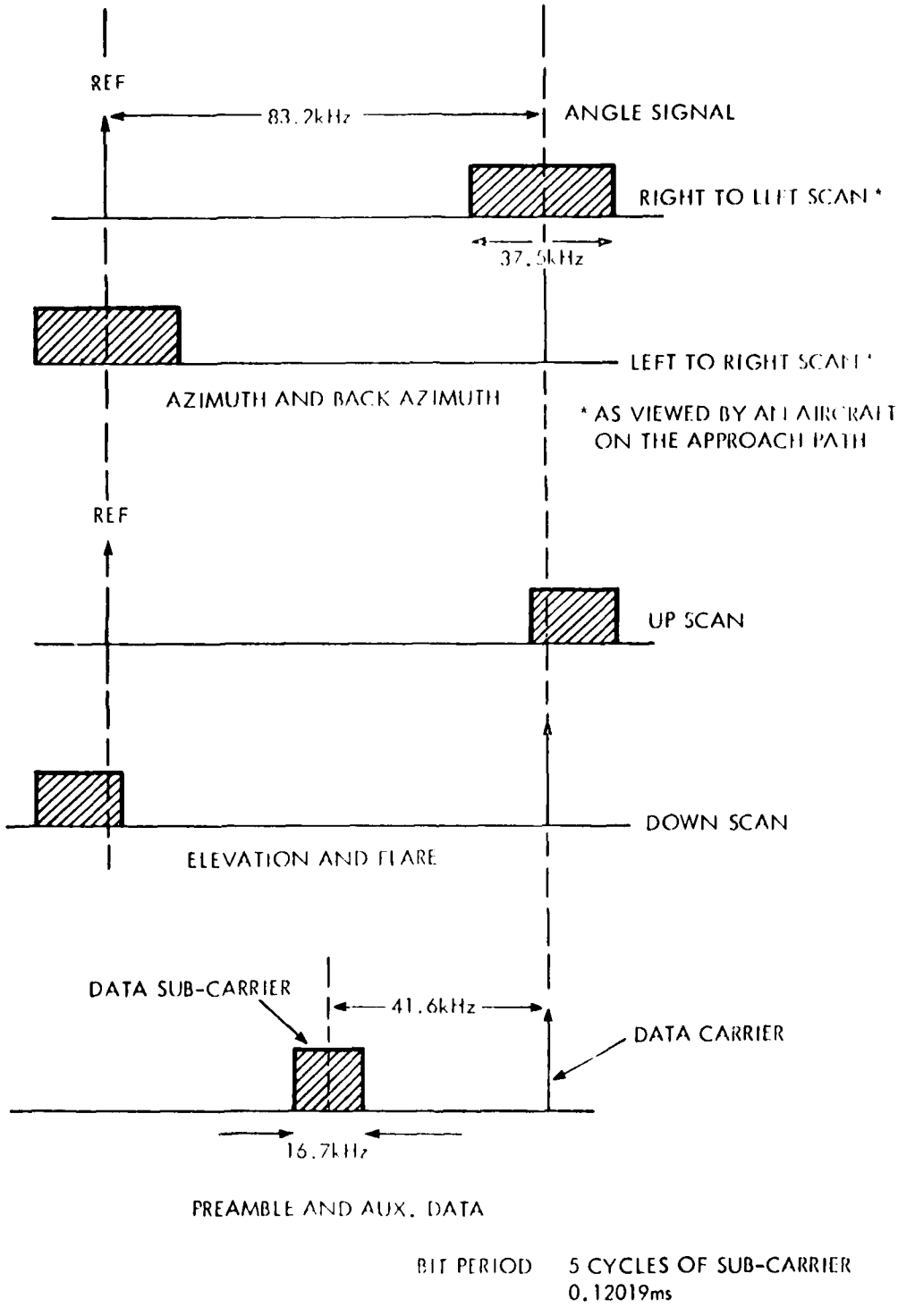

Fig 5.2 Relative frequencies of the angle and data components of the system

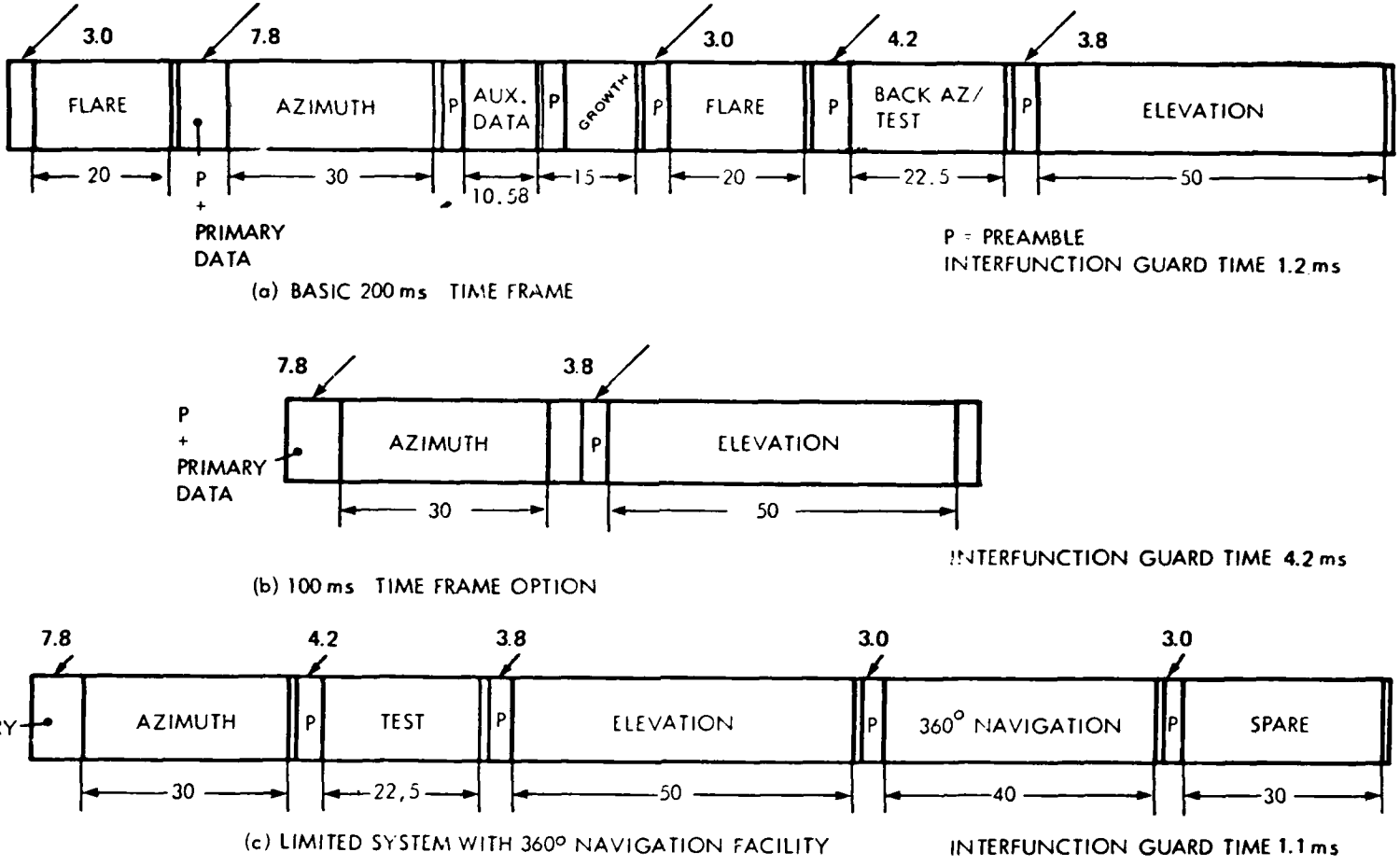

Fig 5.3 Time frame arrangement (major alternatives)

Fig 5.4

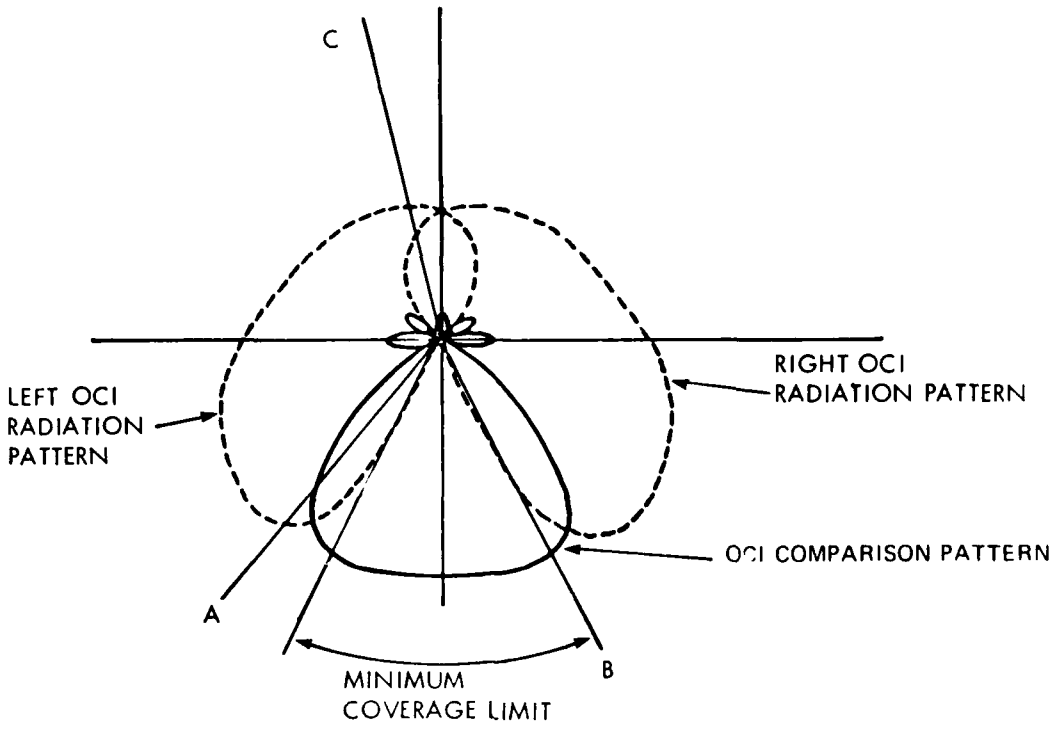

(a) AZIMUTH SYSTEM - AZIMUTH COVERAGE PATTERN

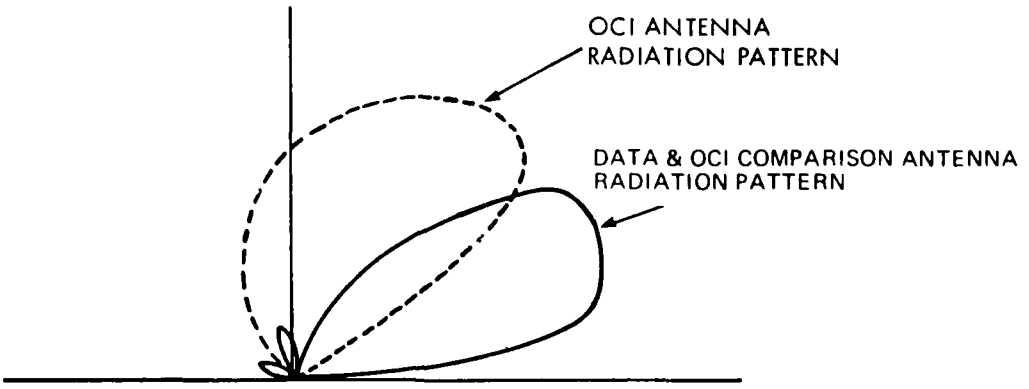

(b) ELEVATION SYSTEM - ELEVATION COVERAGE PATTERN

TR 79052

Fig 5.4 OCI antenna patterns

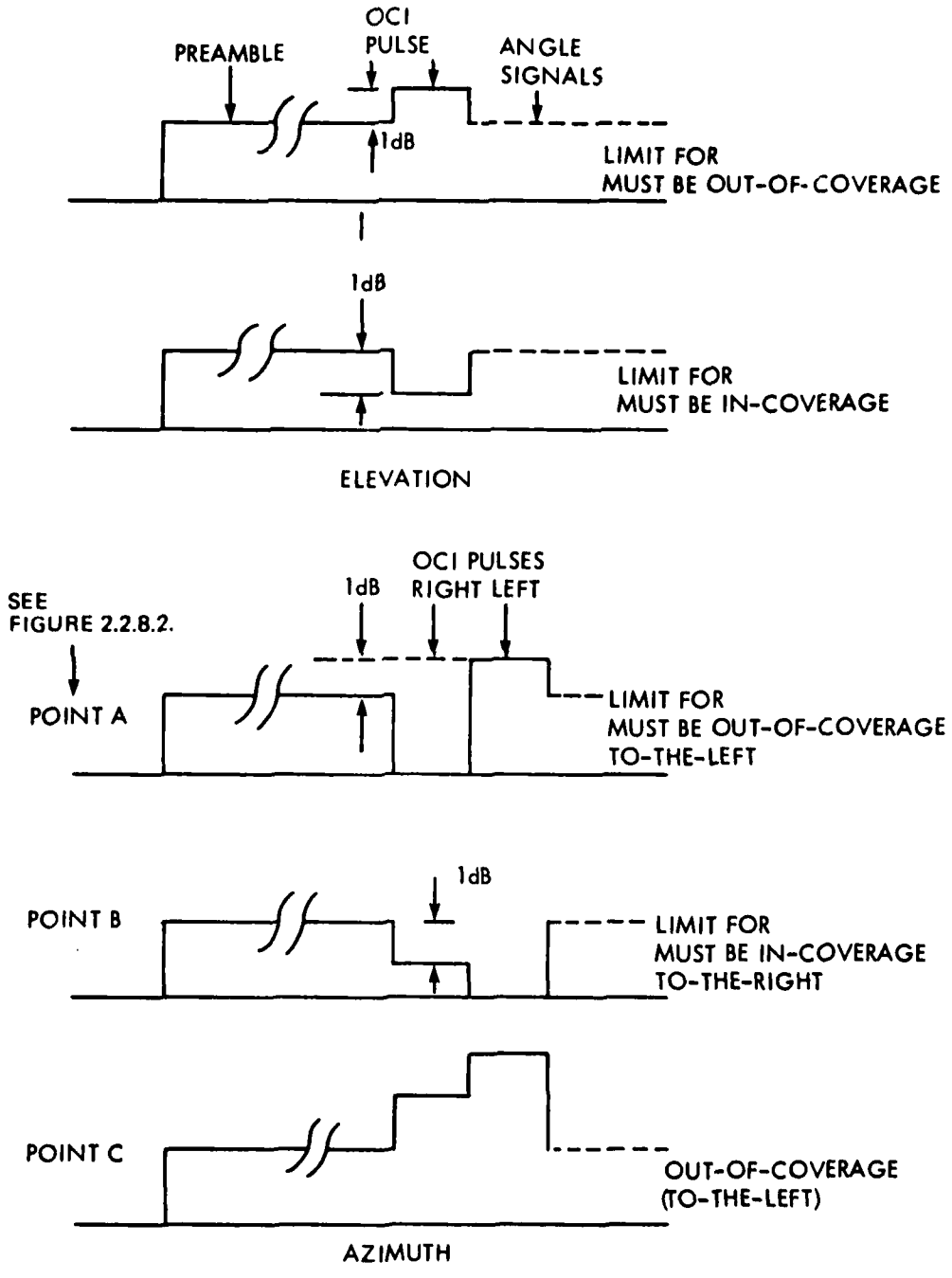

TR 79052

Fig 5.5 OCI limits (as seen by the aircraft)

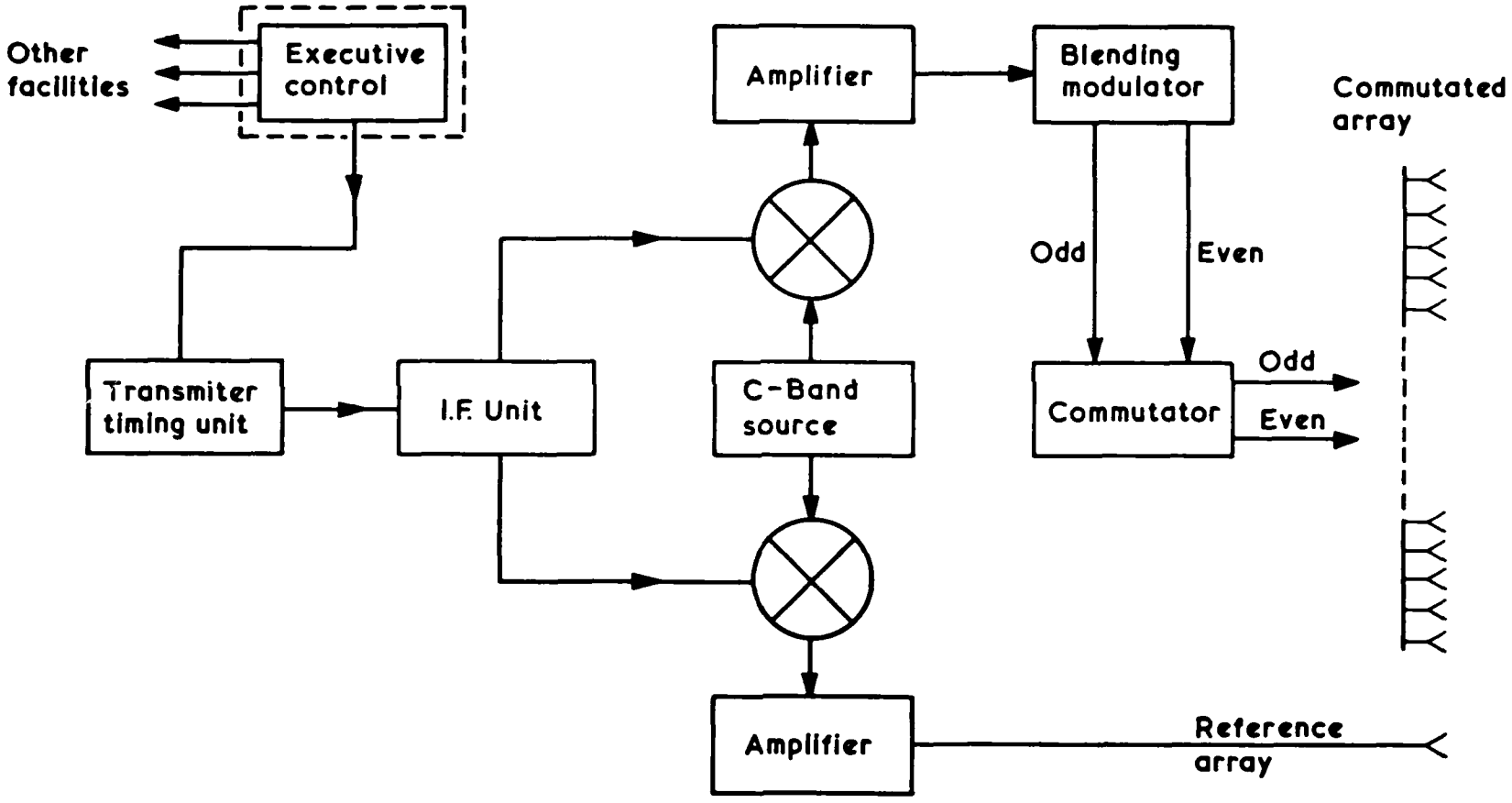

Fig 5.6 Typical ground facility

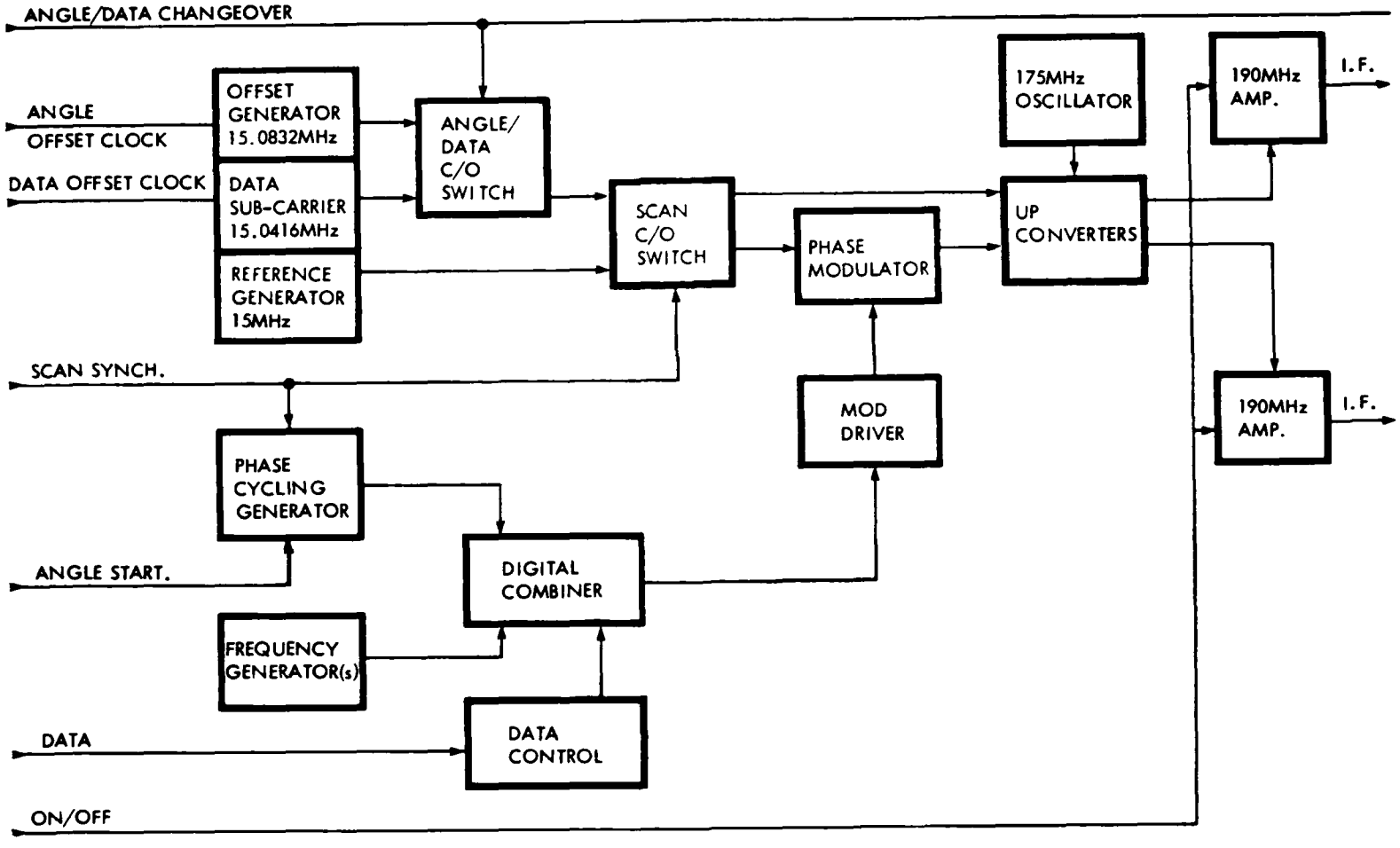

Fig 5.7 Transmitter IF unit

Fig 5.7

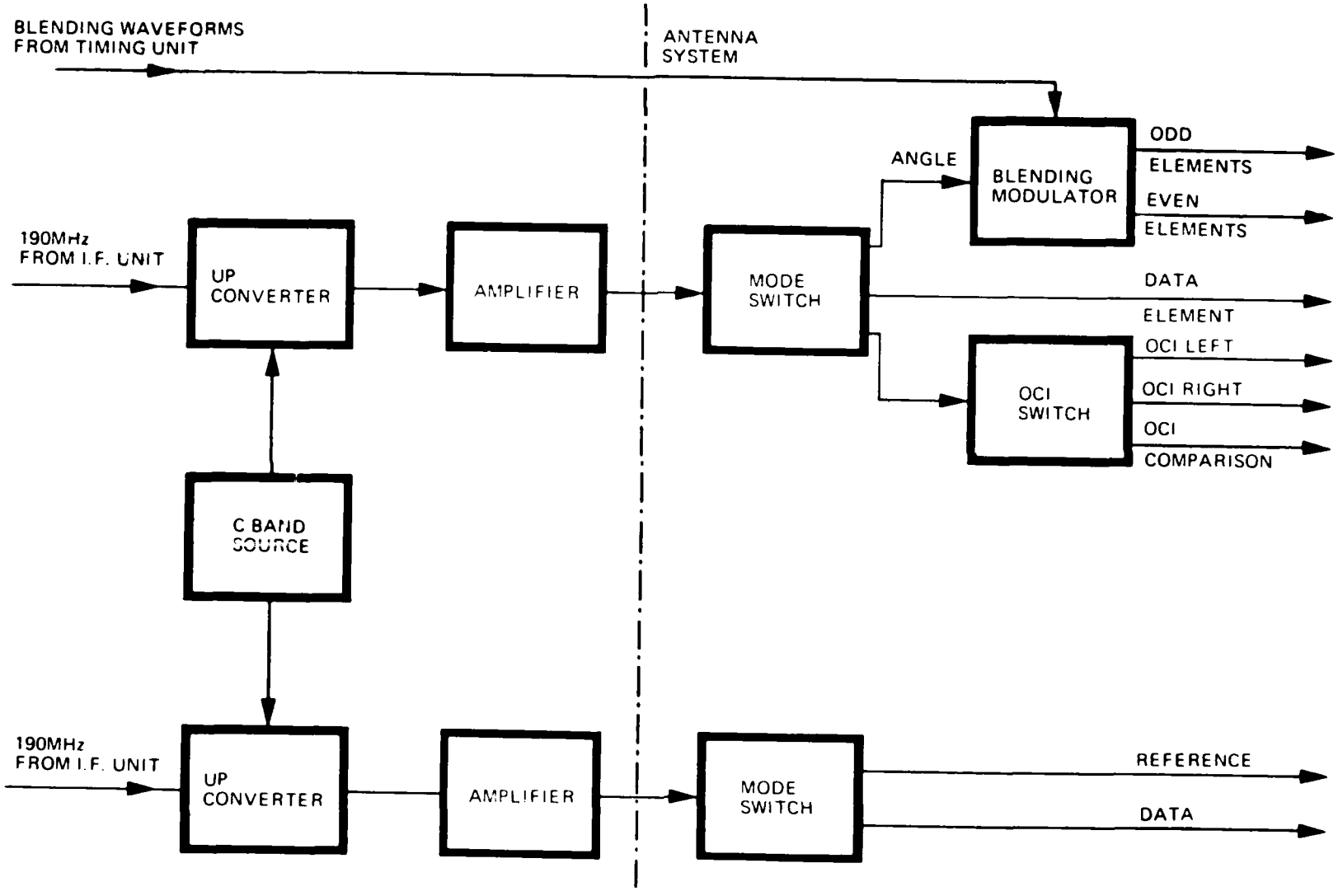

Fig 5.8 Transmitter and antenna RF

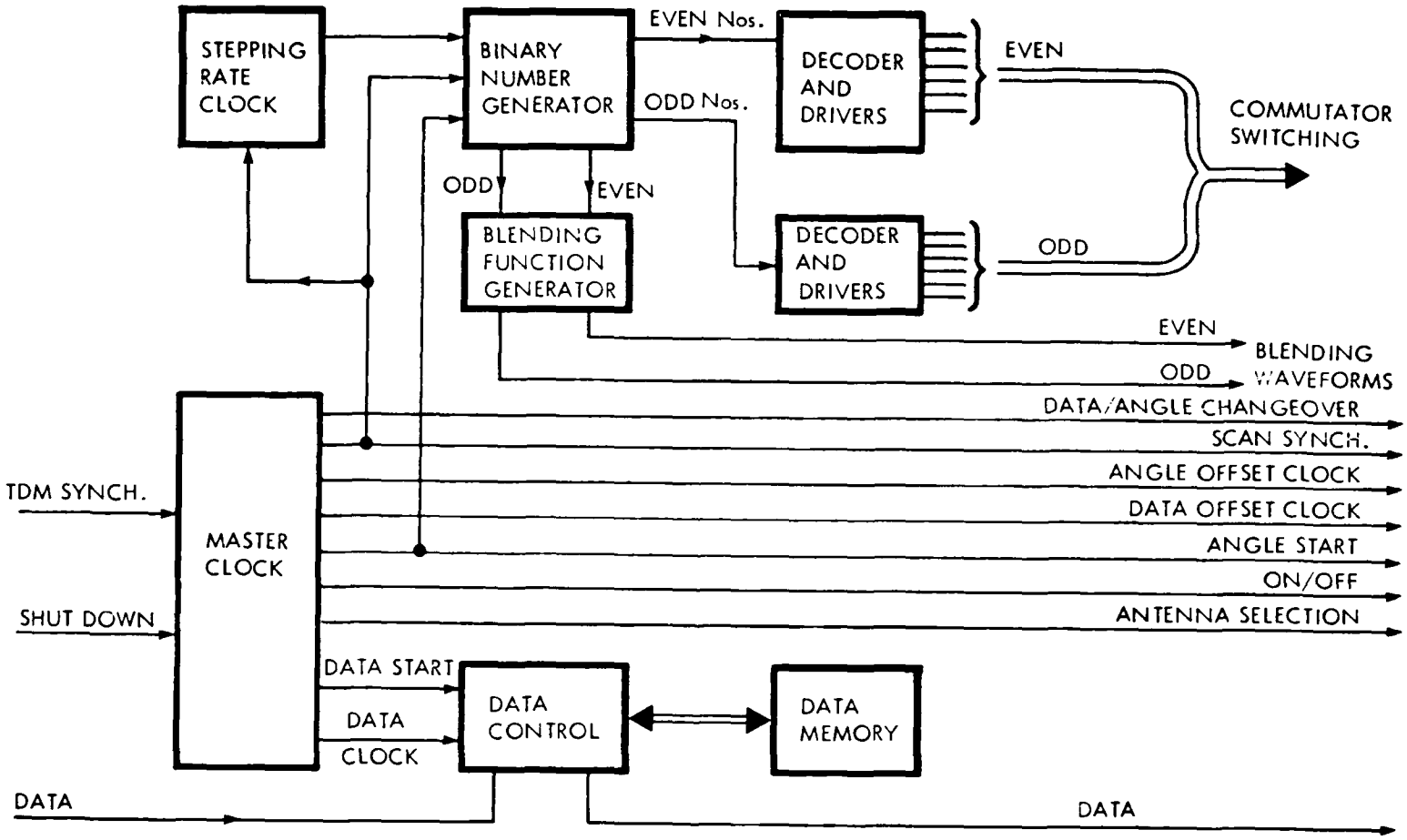

Fig 5.9 Transmitter timing unit

Fig 5.9

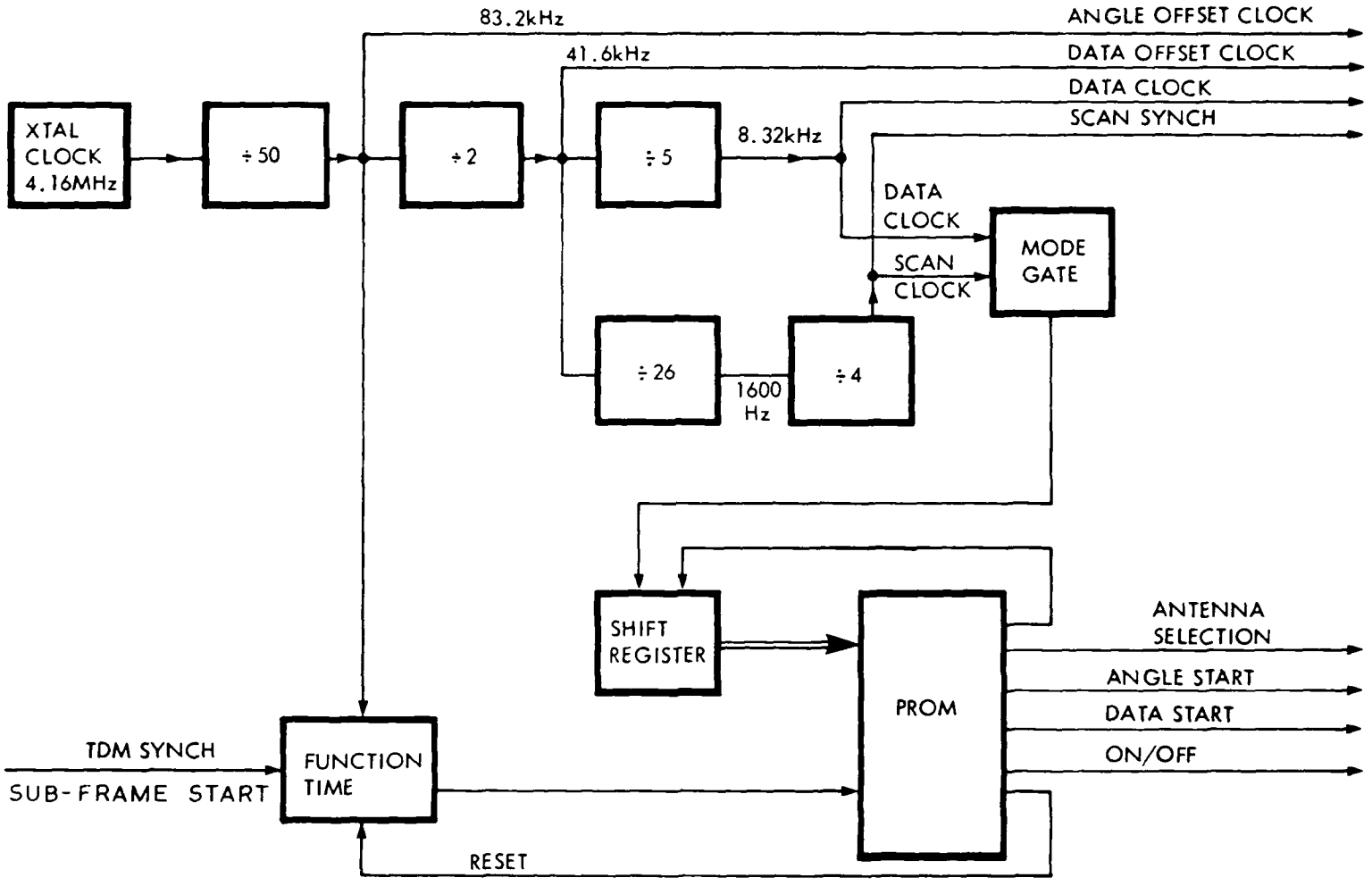

Fig 5.10 Master clock

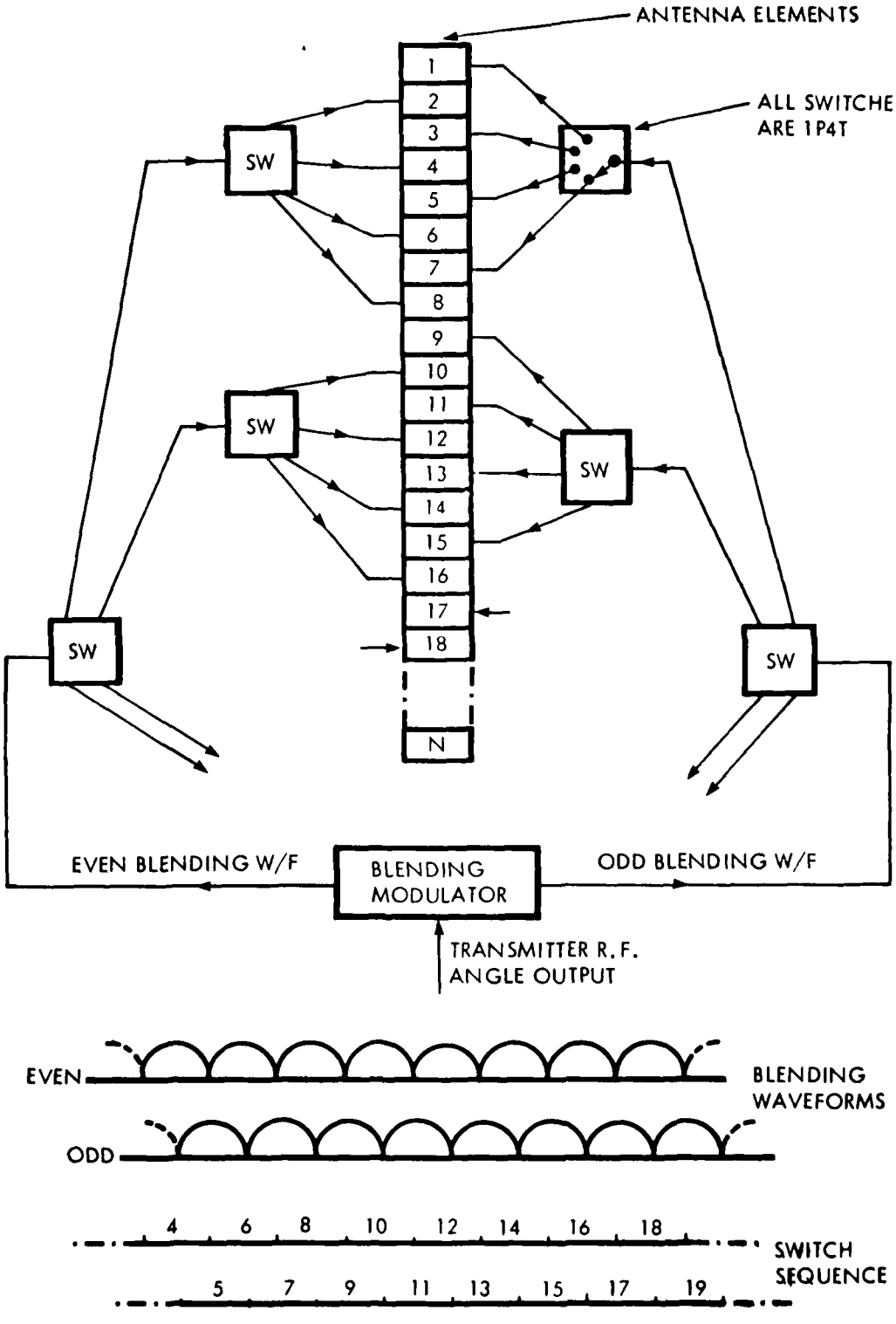

TR 79052

Fig 5.11 Commutator switching

Fig 5.12

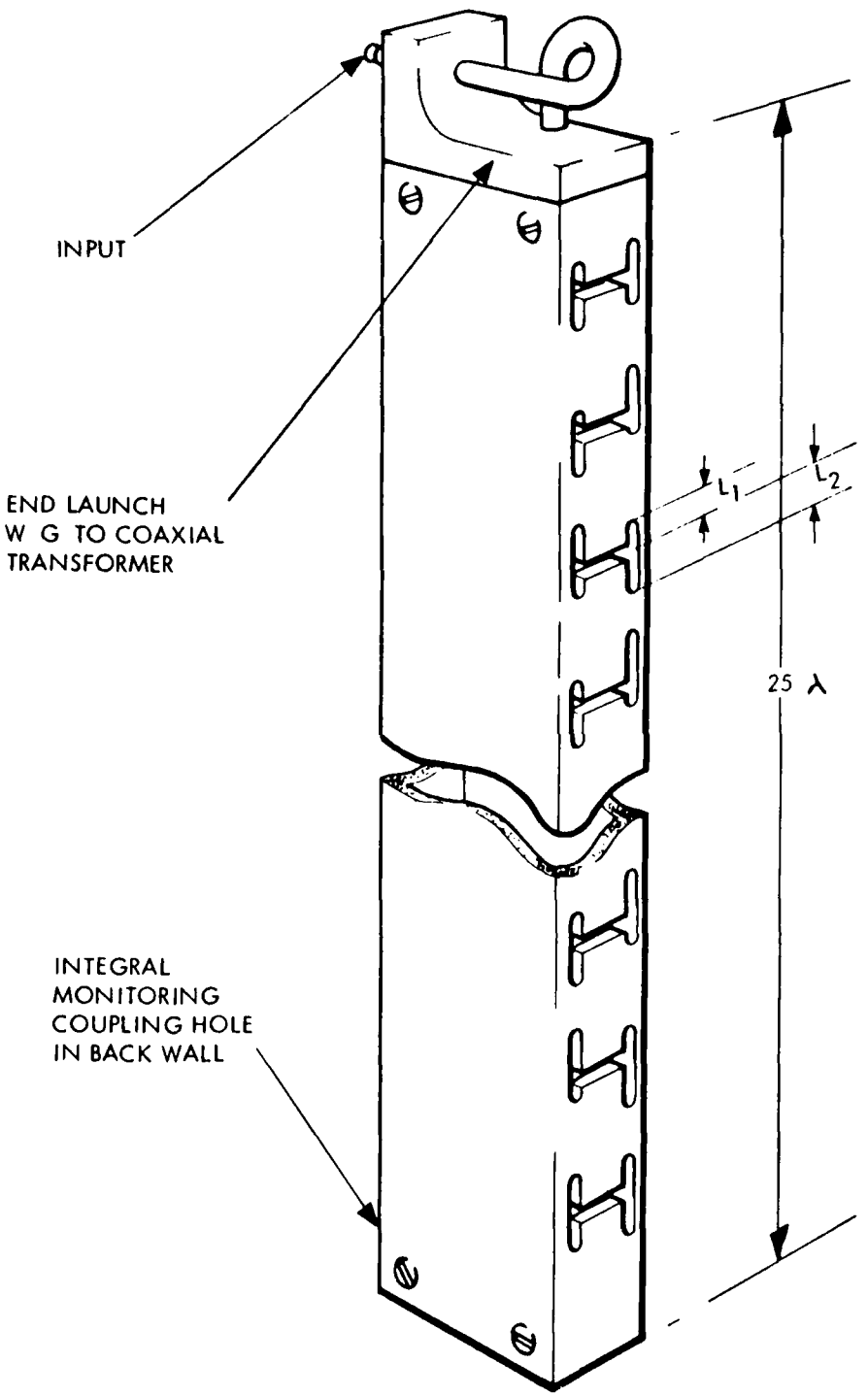

TR 79052

Fig 5.12 Azimuth vertical column element

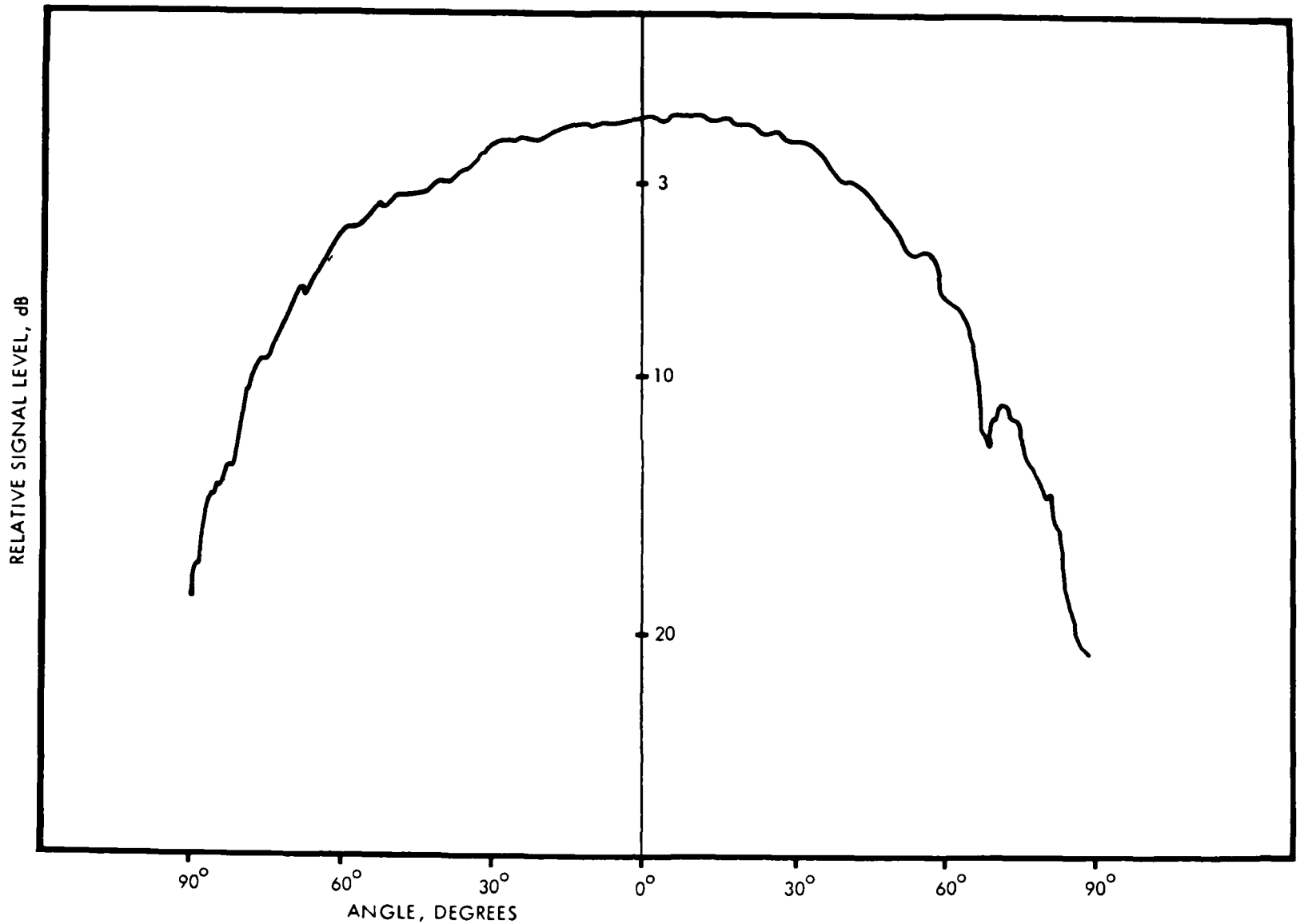

Fig 5.13 Azimuth array — typical azimuth radiation pattern

Fig 5.13

Fig 5.14

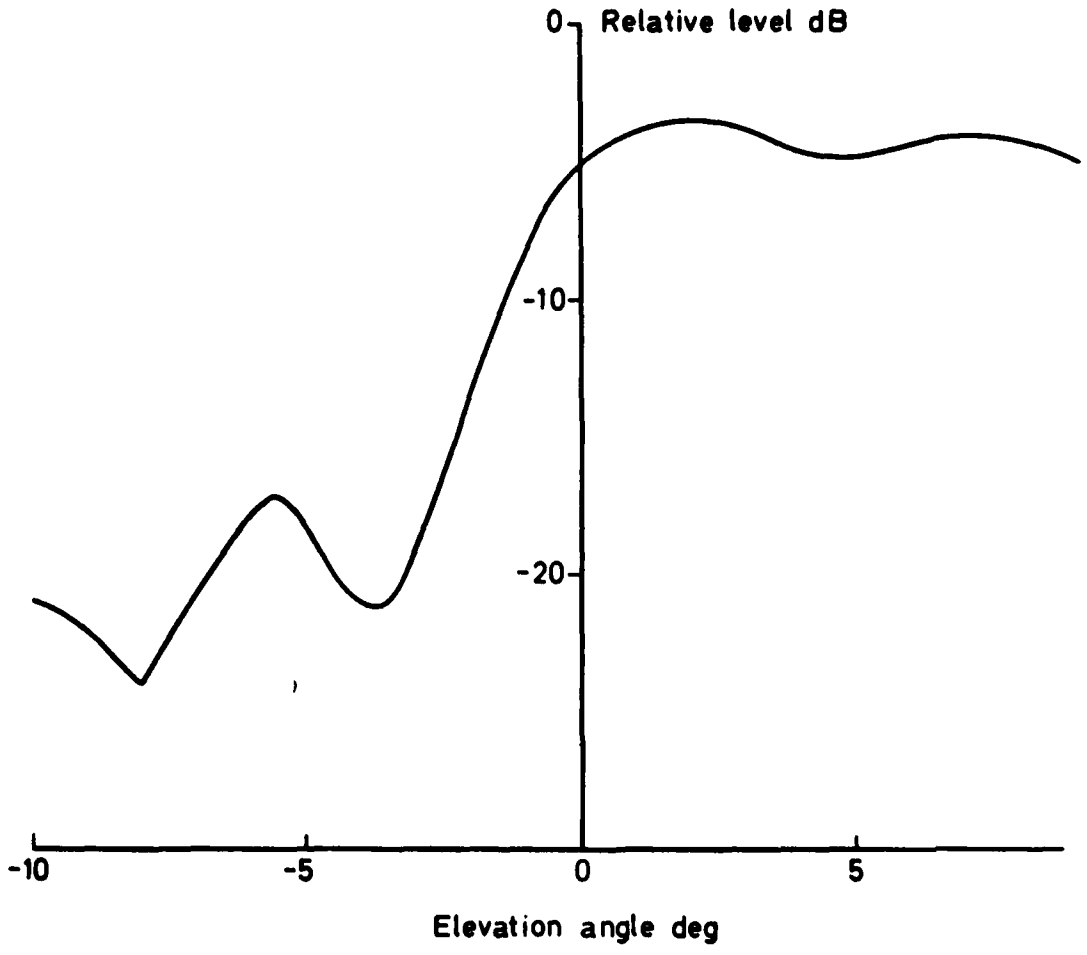

TR 79052

Fig 5.14 Column element typical vertical radiation pattern

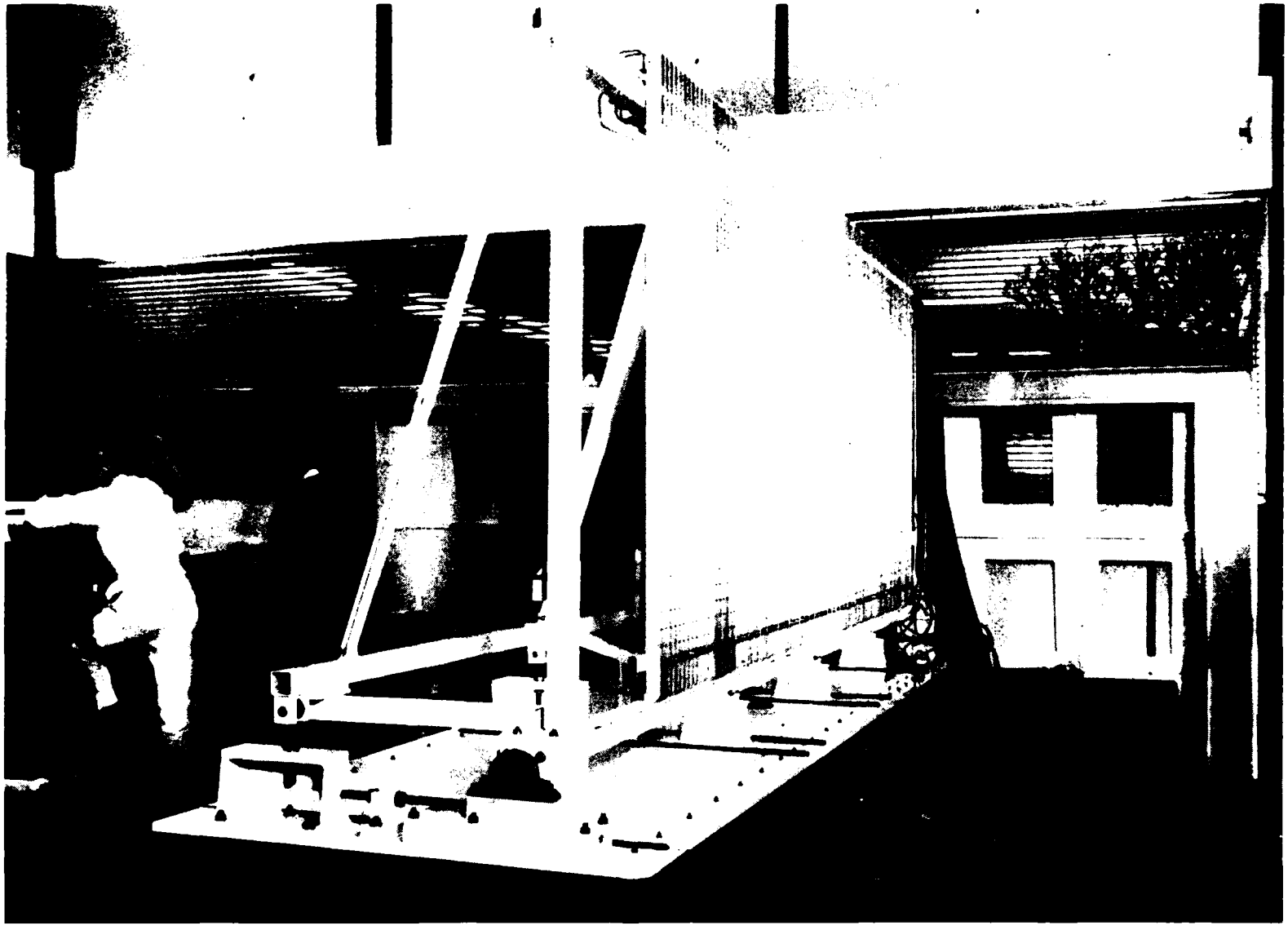

Fig 5.15 Azimuth array showing slotted columns and support frame

Fig 5.15

Fig 5.16

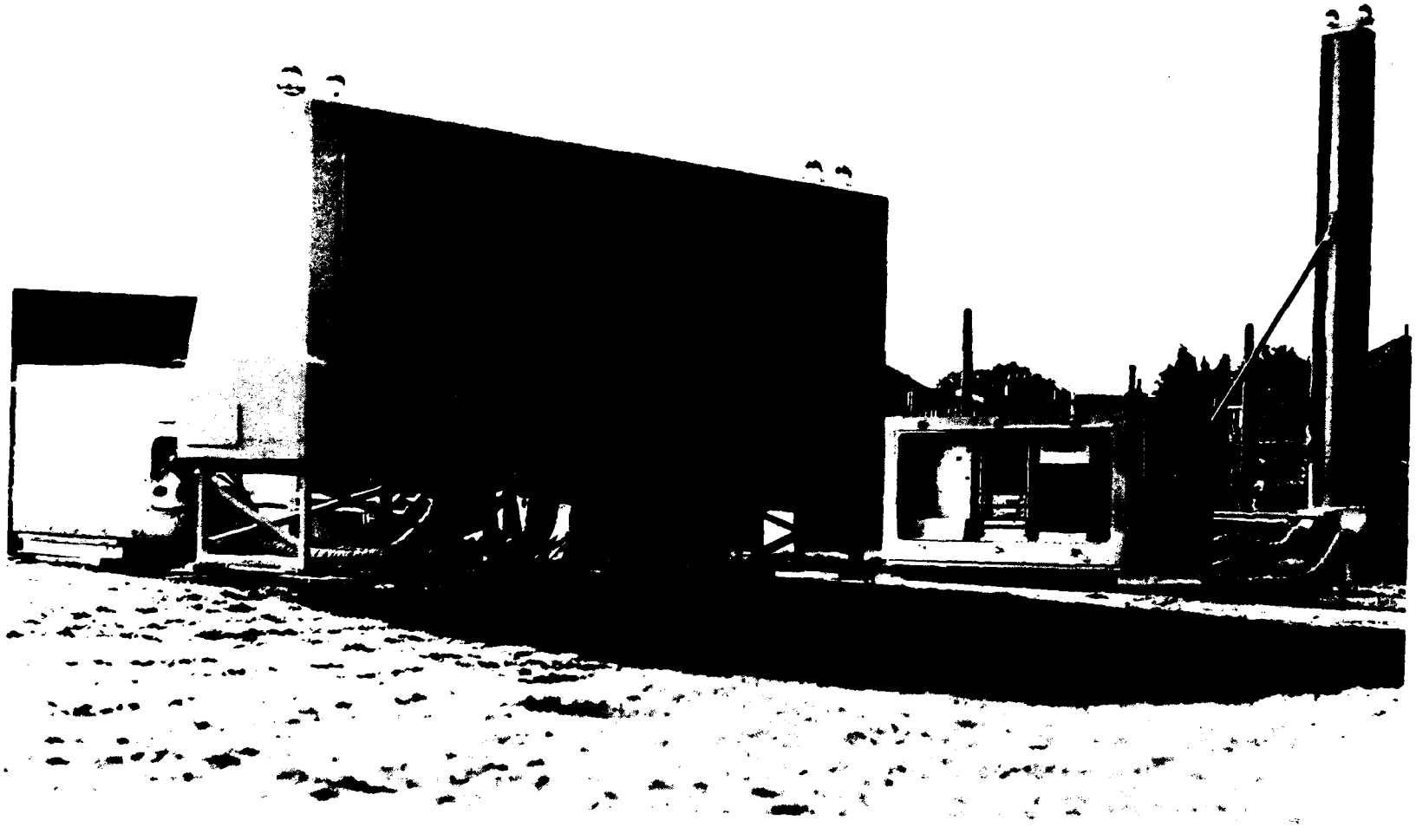

Fig 5.16 Collocated elevation and azimuth arrays

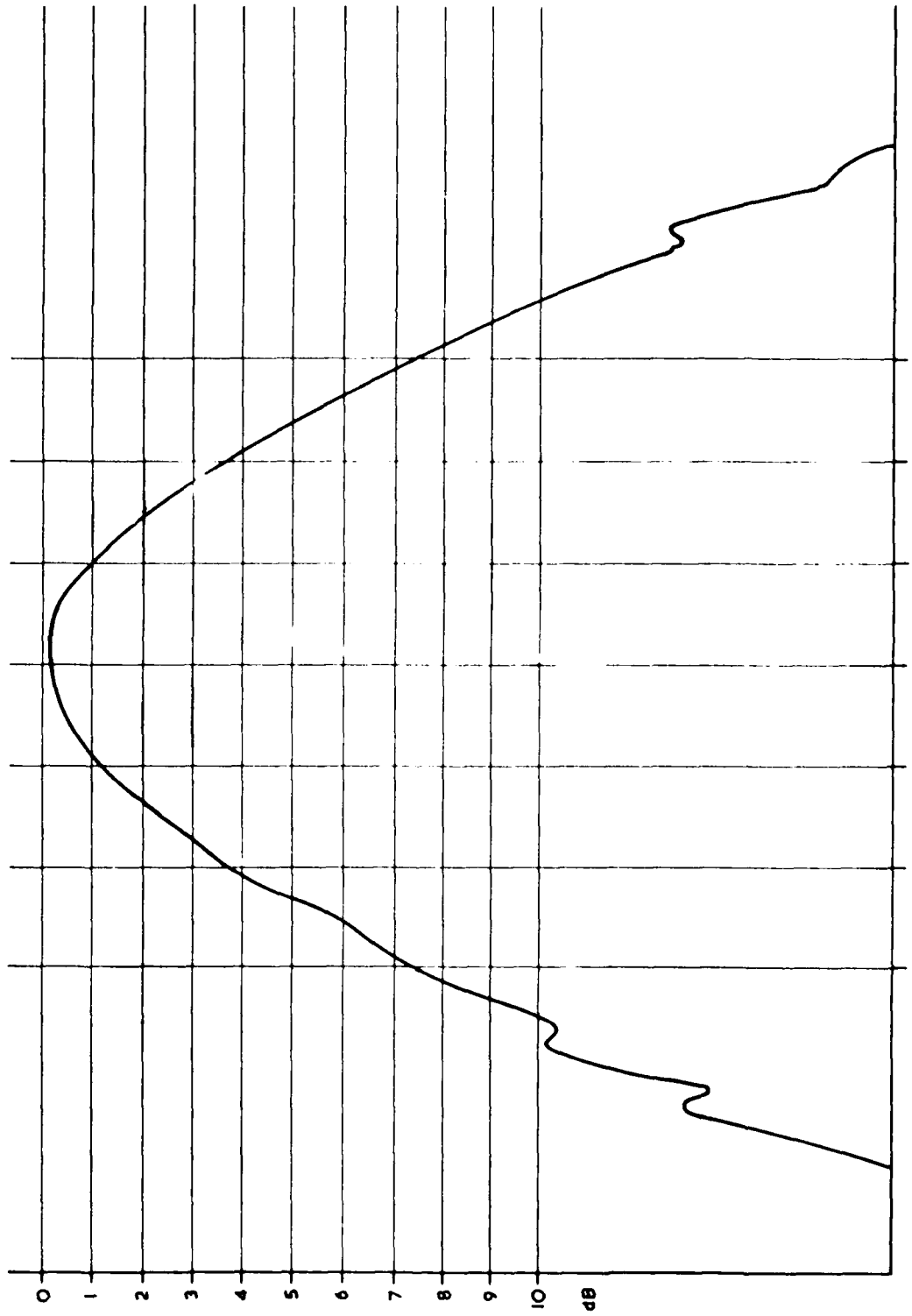

Fig 5.17 Elevation array element – azimuth radiation pattern

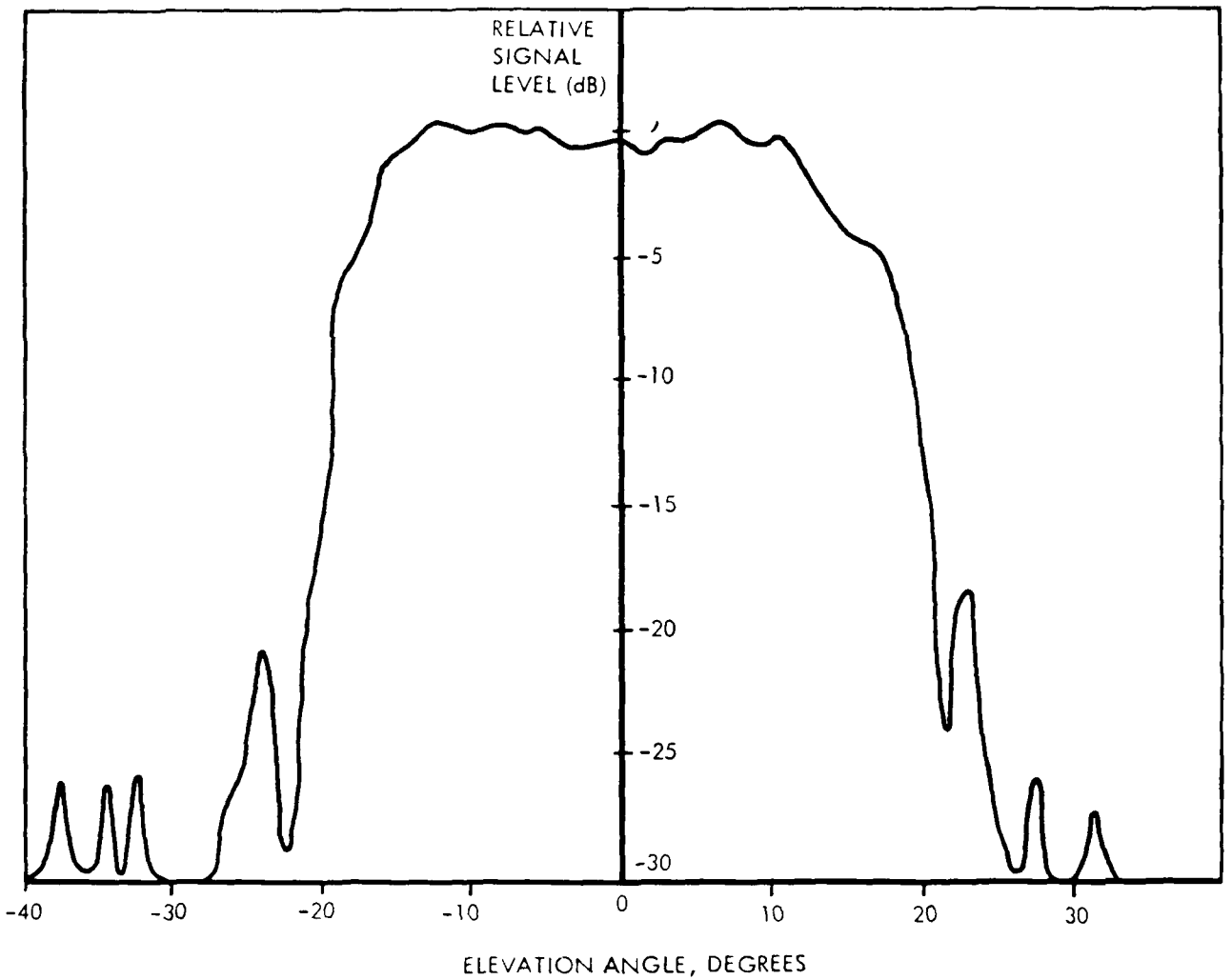

Fig 5.18 Elevation array element – elevation radiation pattern

Fig 5.19 Completed 54 wavelength GRP elevation array

Fig 5.20

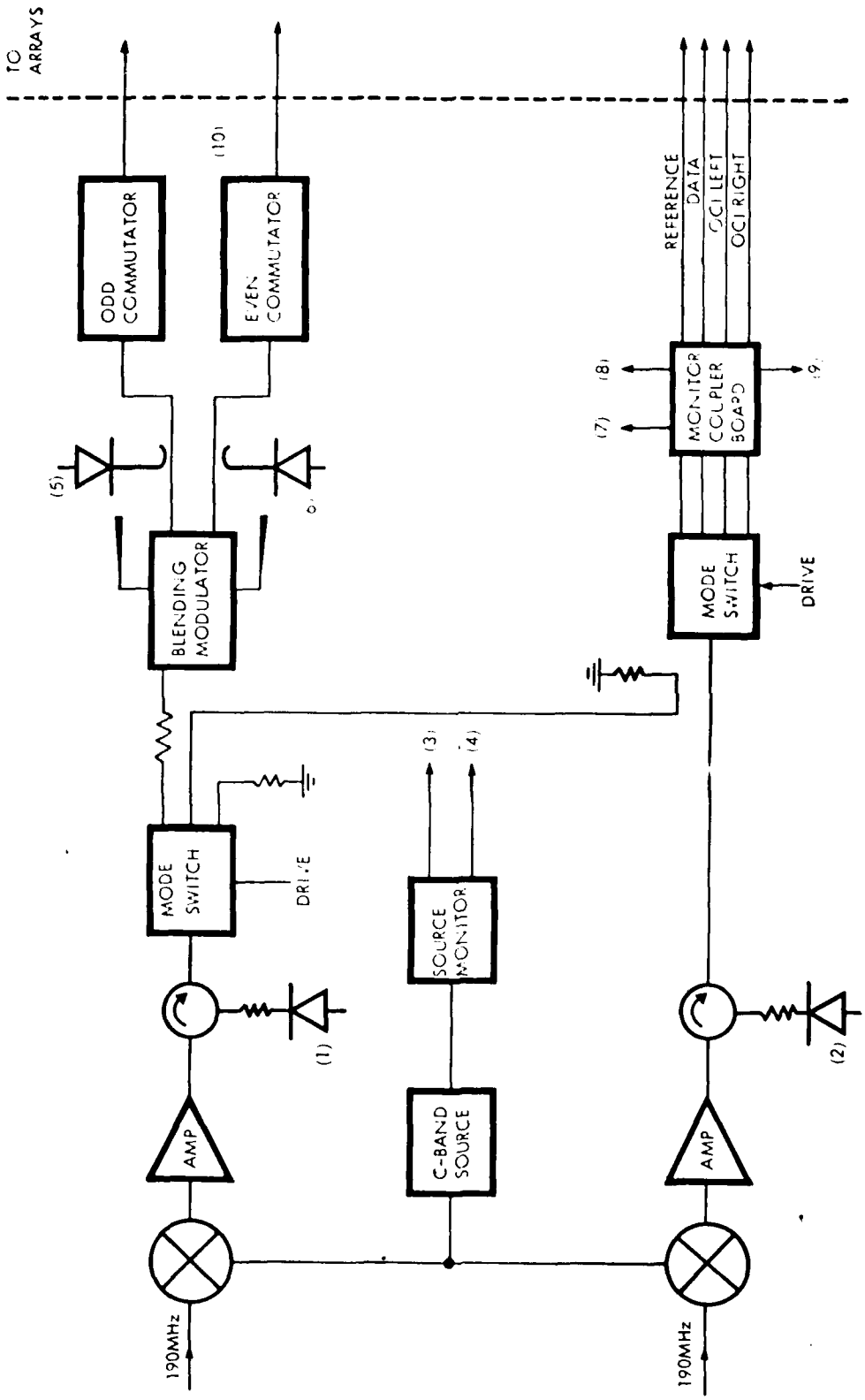

Fig 5.20 Internal monitor – azimuth facility

TR 79052

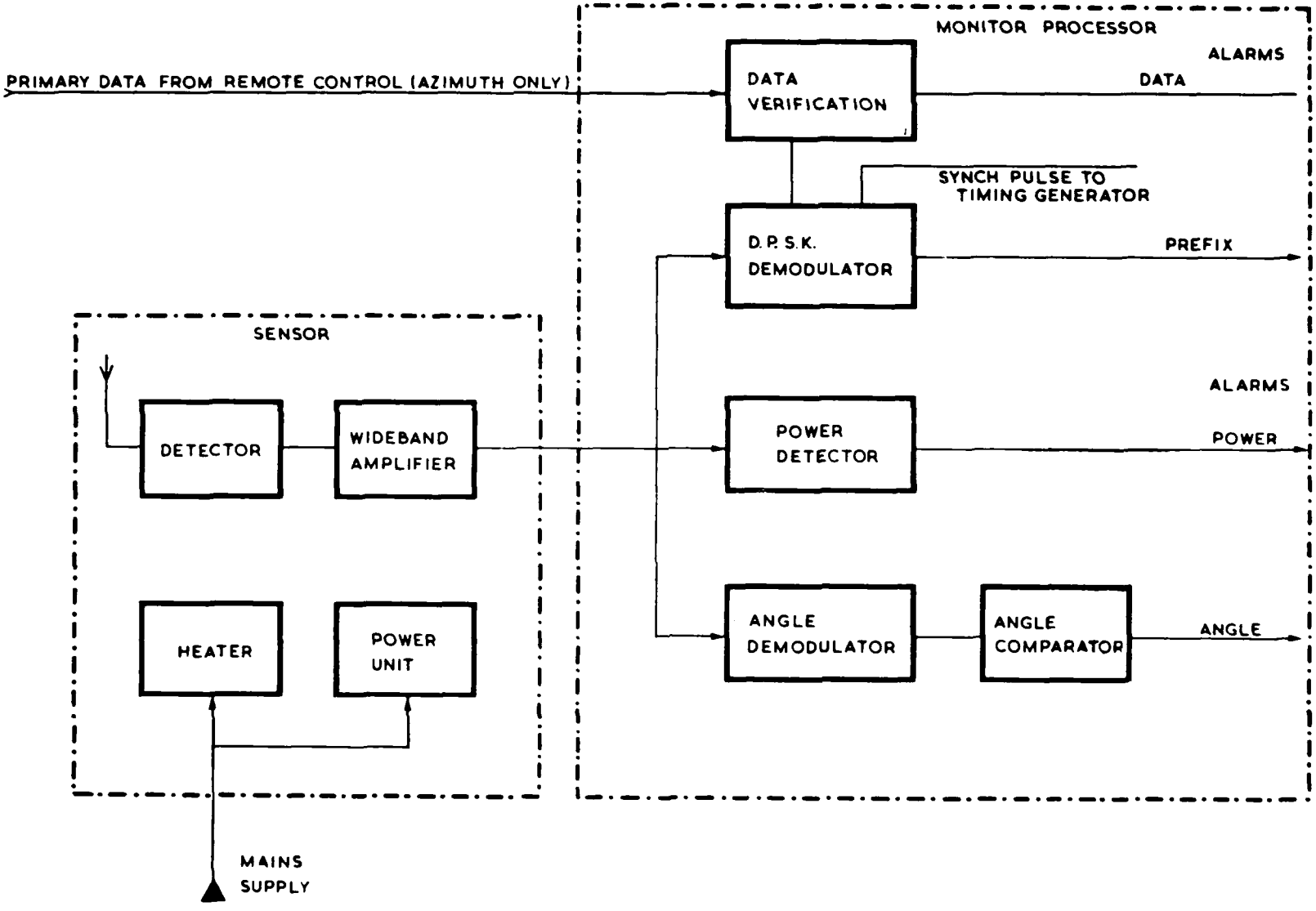

Fig 5.21 Integral monitor

Fig 5.21

Fig 5.22

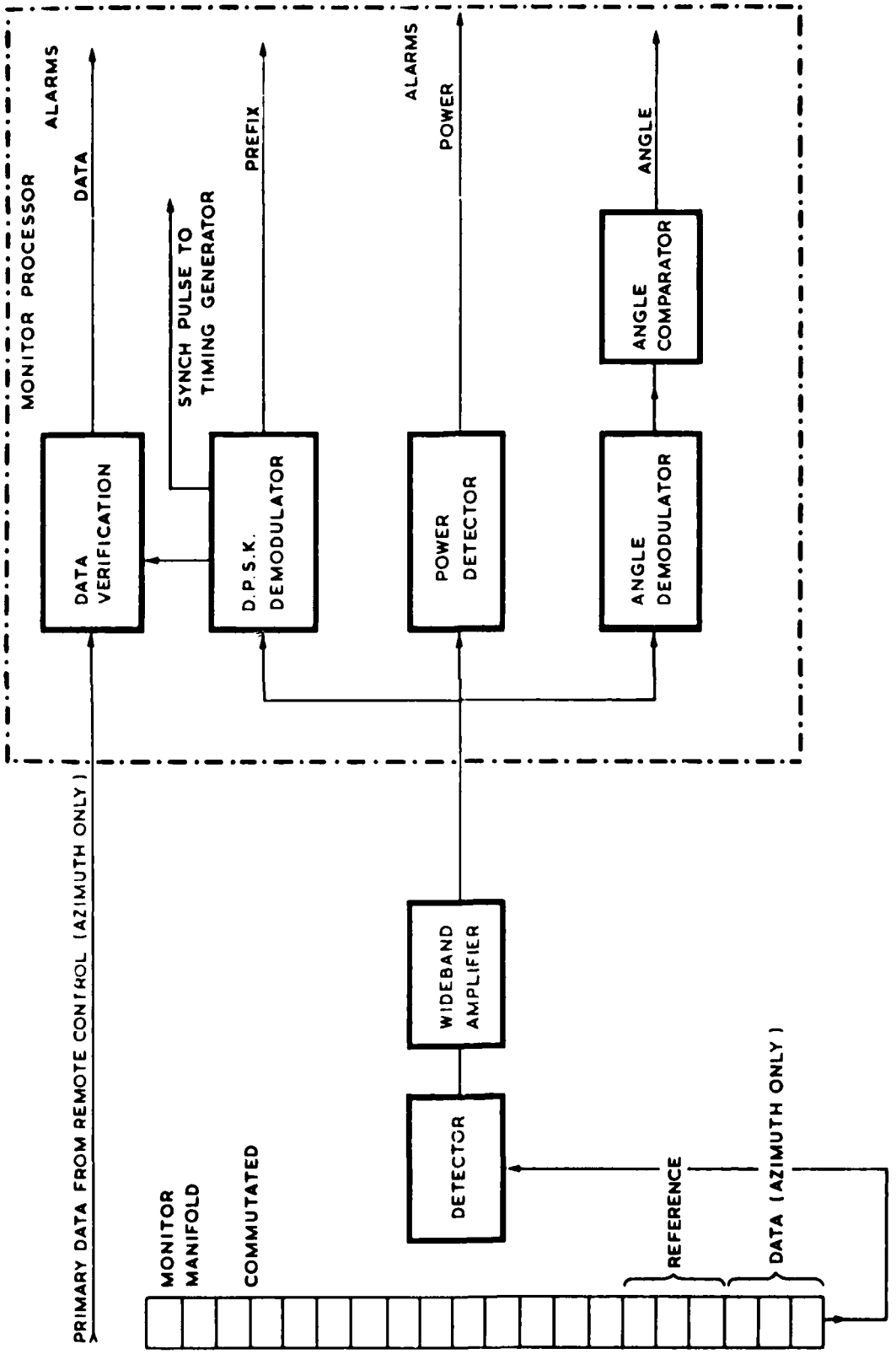

Fig 5.22 Field monitor

TR 79052

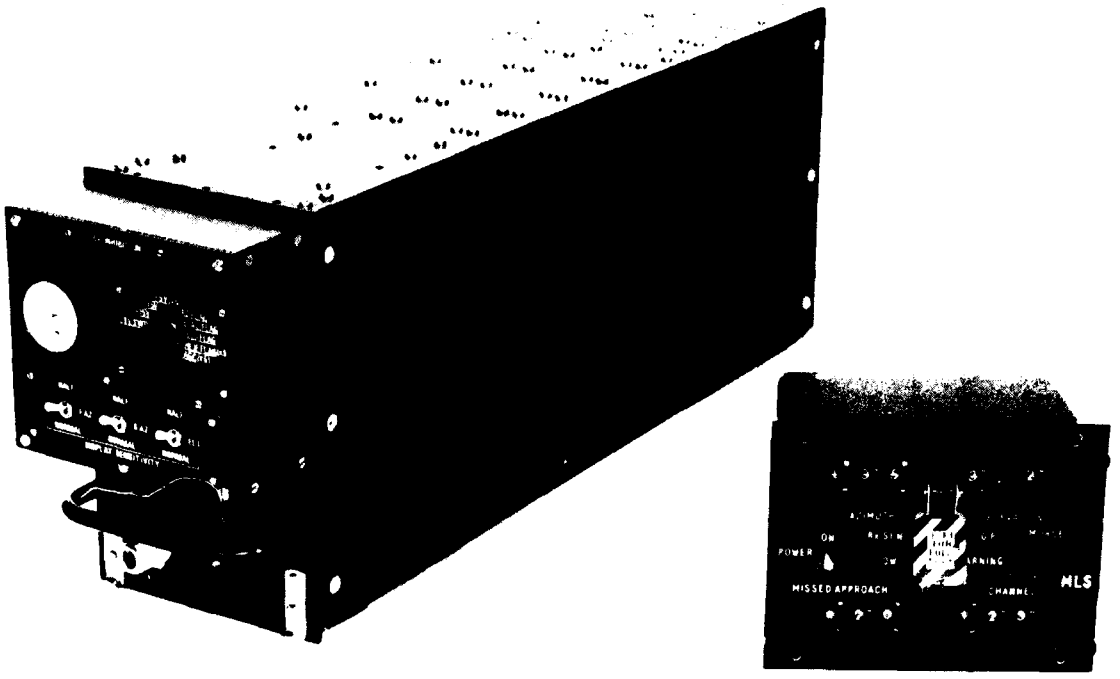

Fig 5.23a Full capability receiver and control unit

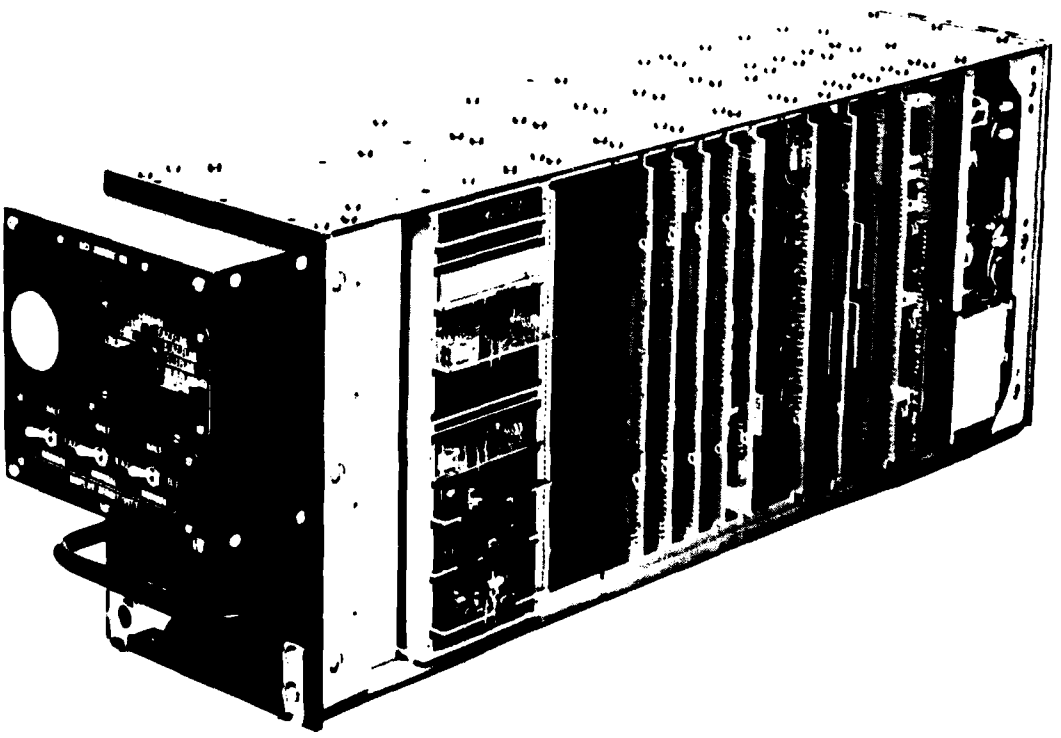

TR 79062 C15534

Fig 5.23b Internal view of receiver

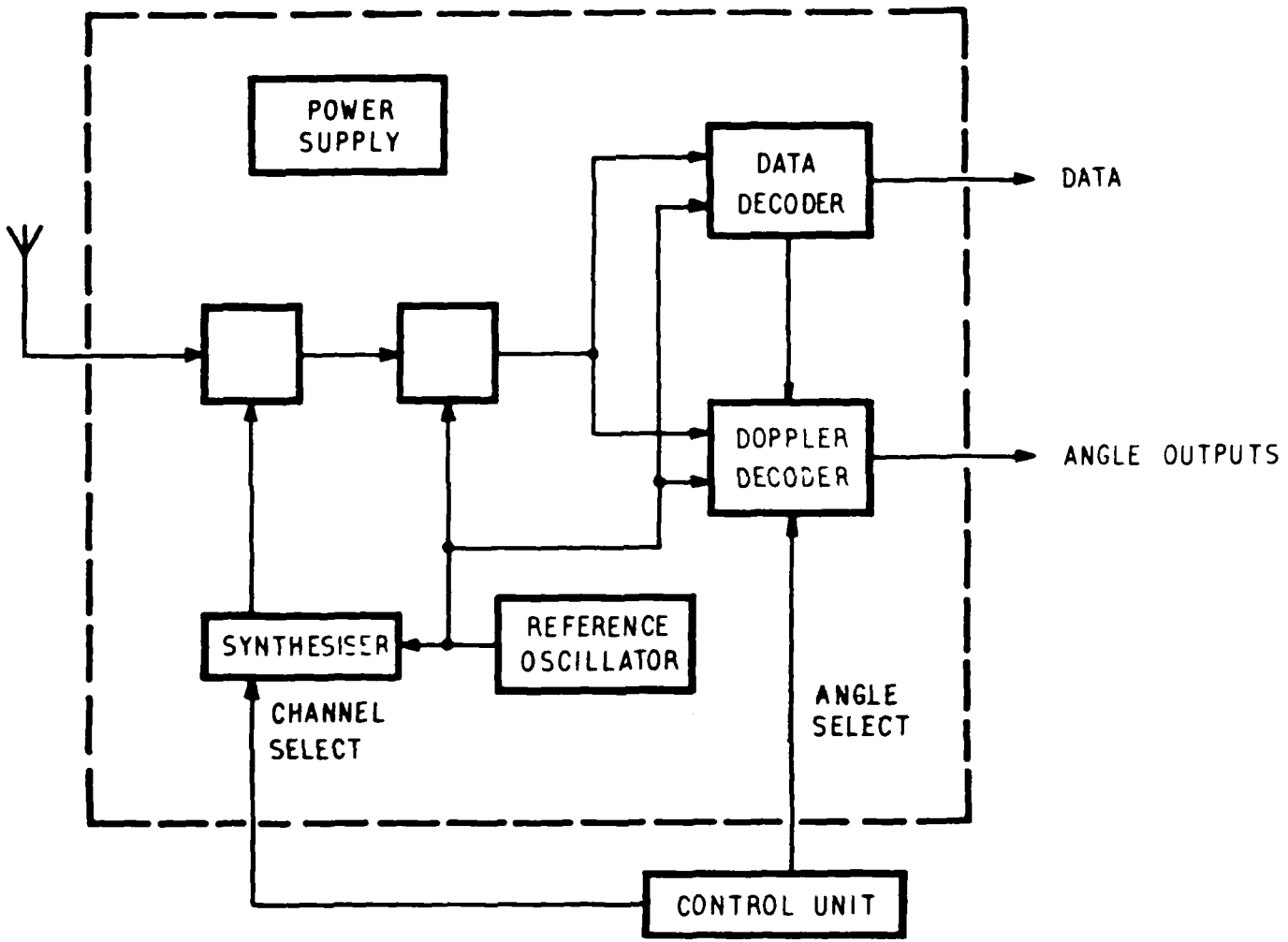

Fig 5.24 Block diagram for TDM receivers

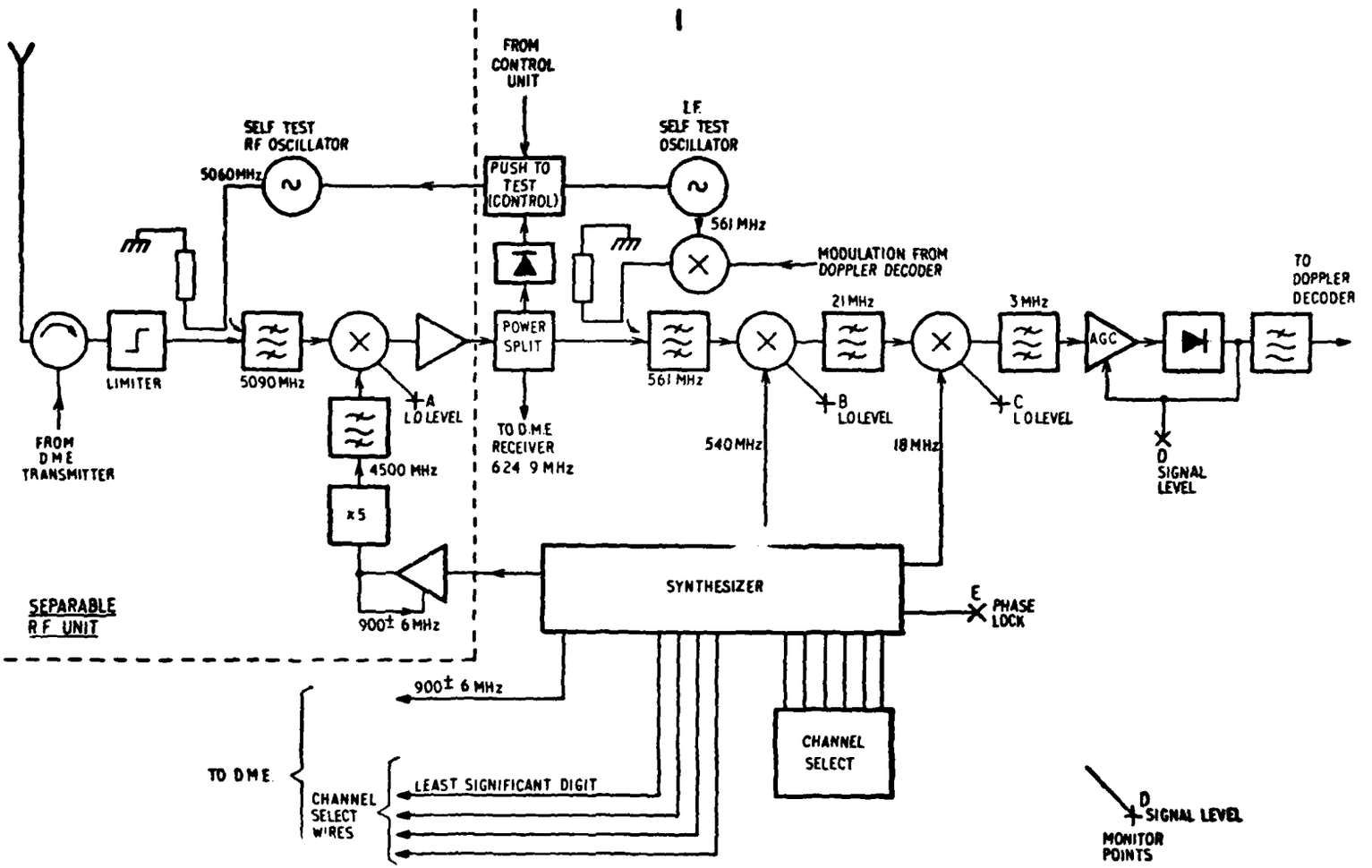

Fig 5.25 Receiver RF/IF circuits

Fig 5.25

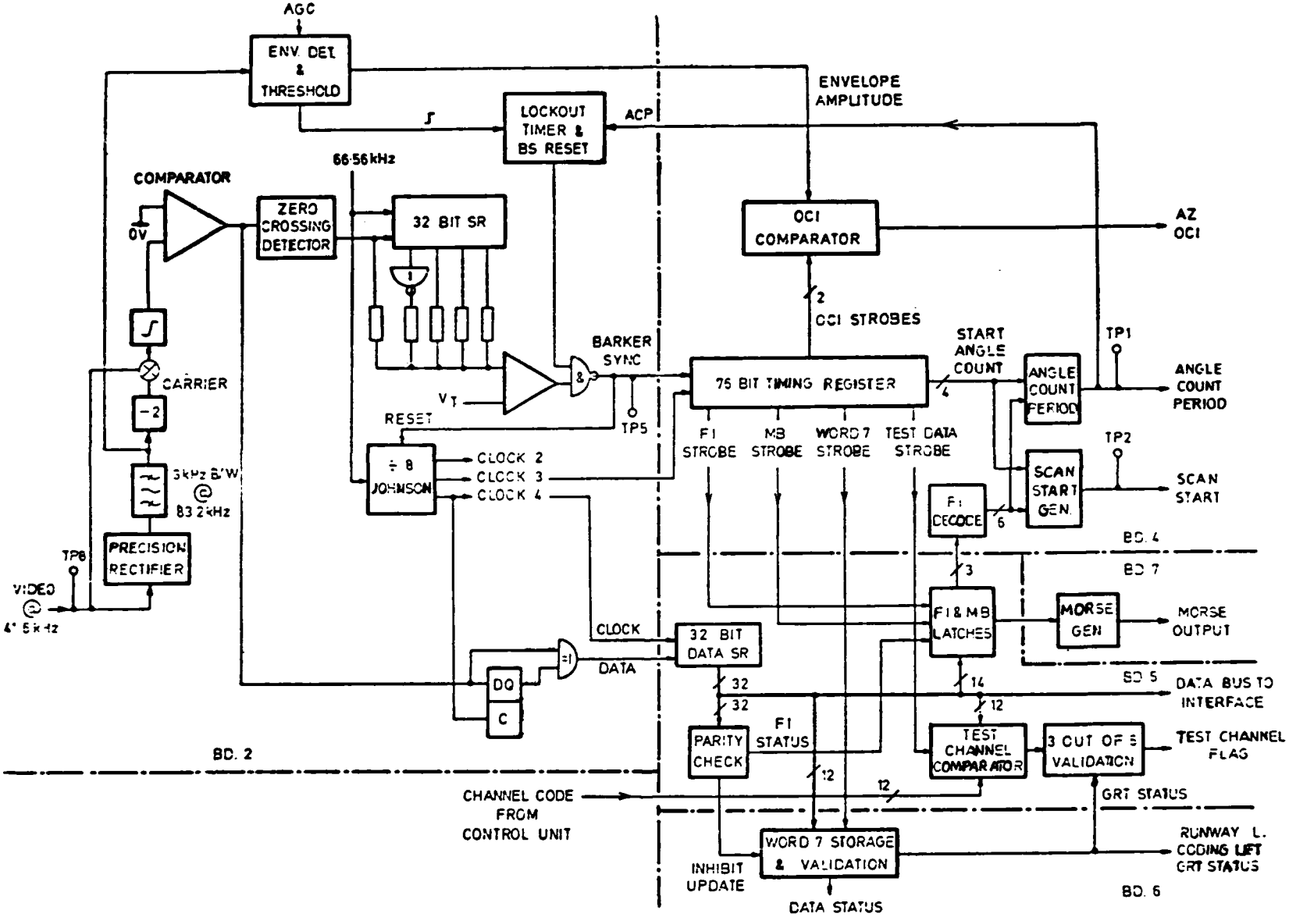

Fig 5.26 Data demodulator and decoder

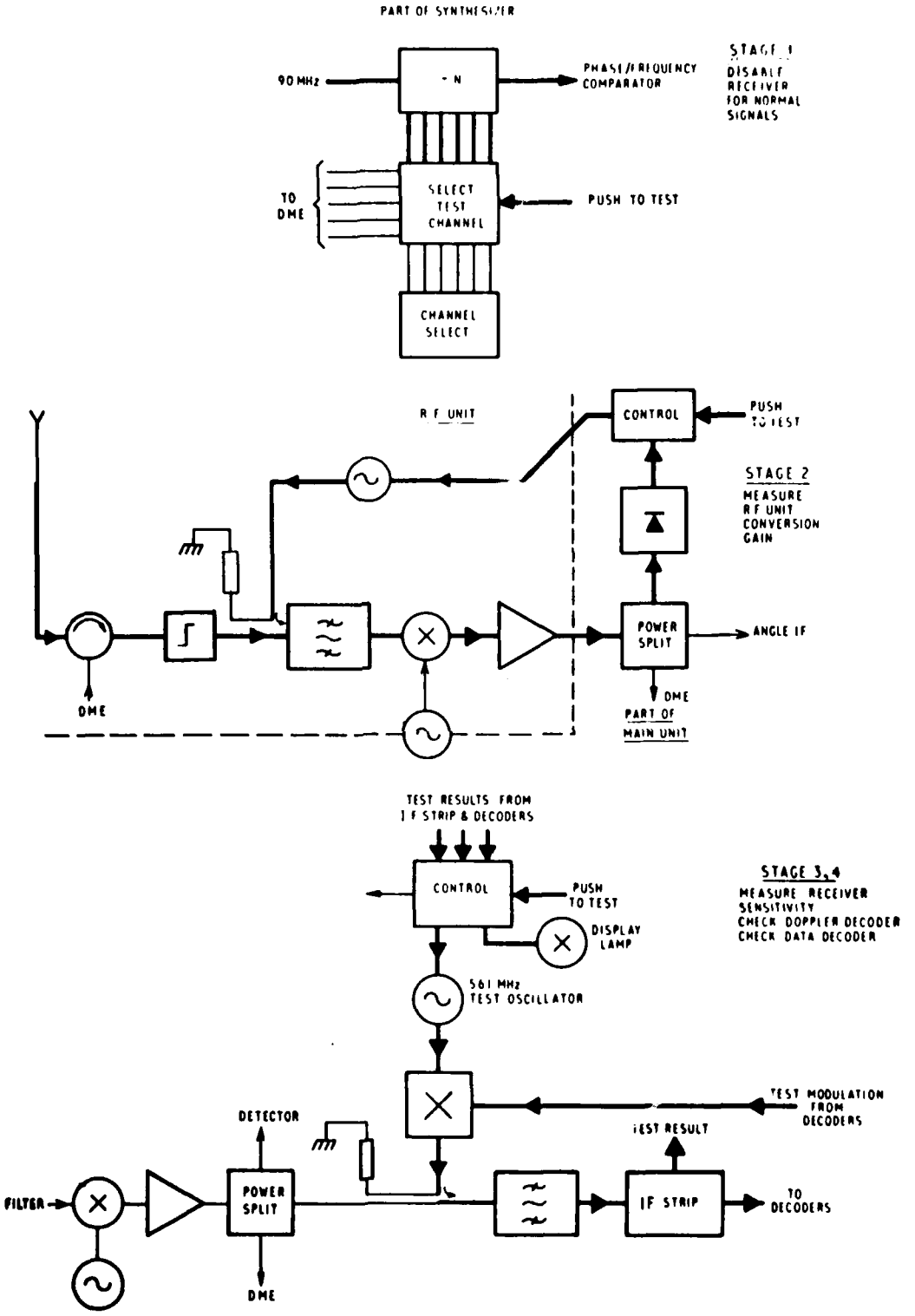

TA 79052

Fig 5.27 RF/IF self test circuit

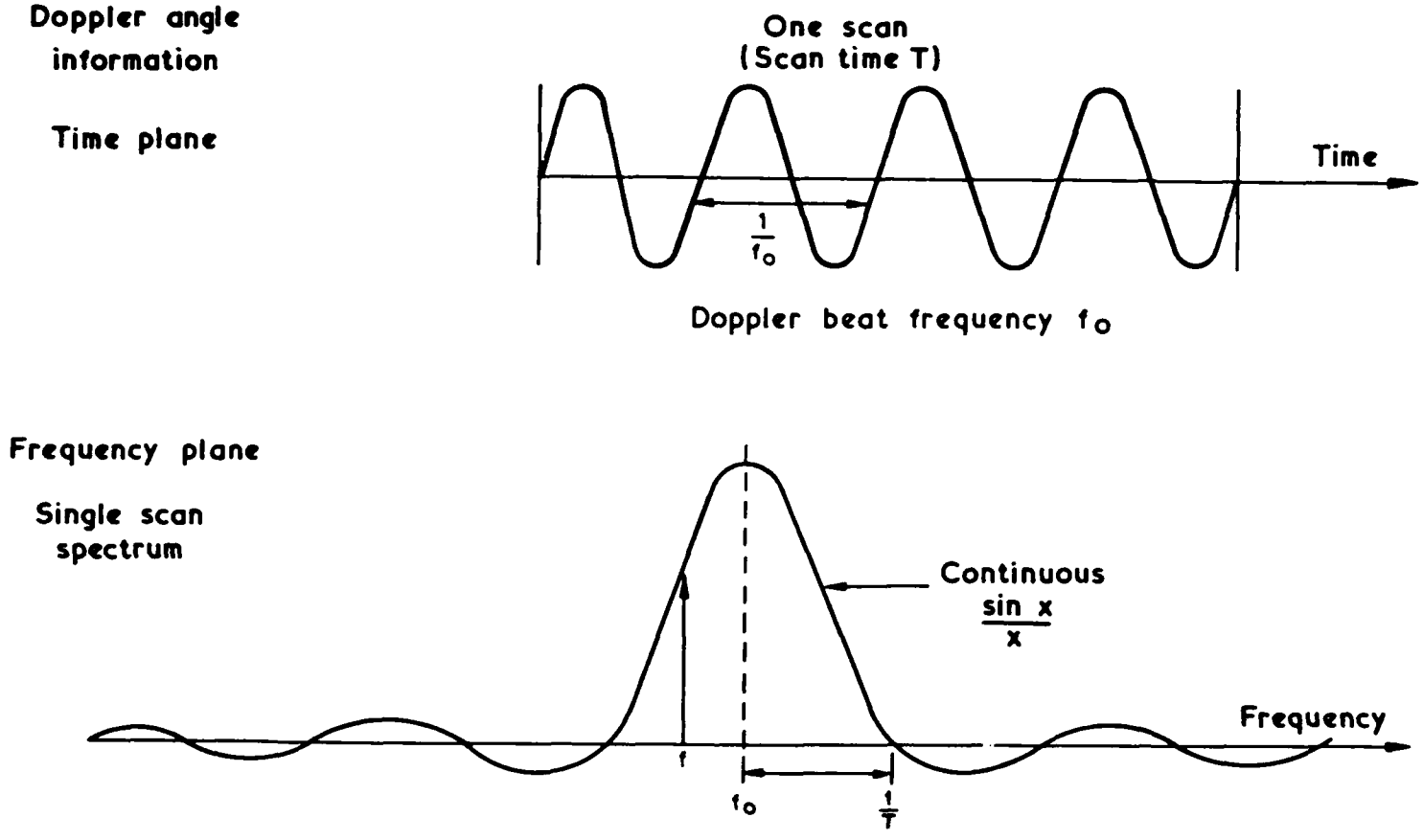

Fig 5.28 The Doppler signal

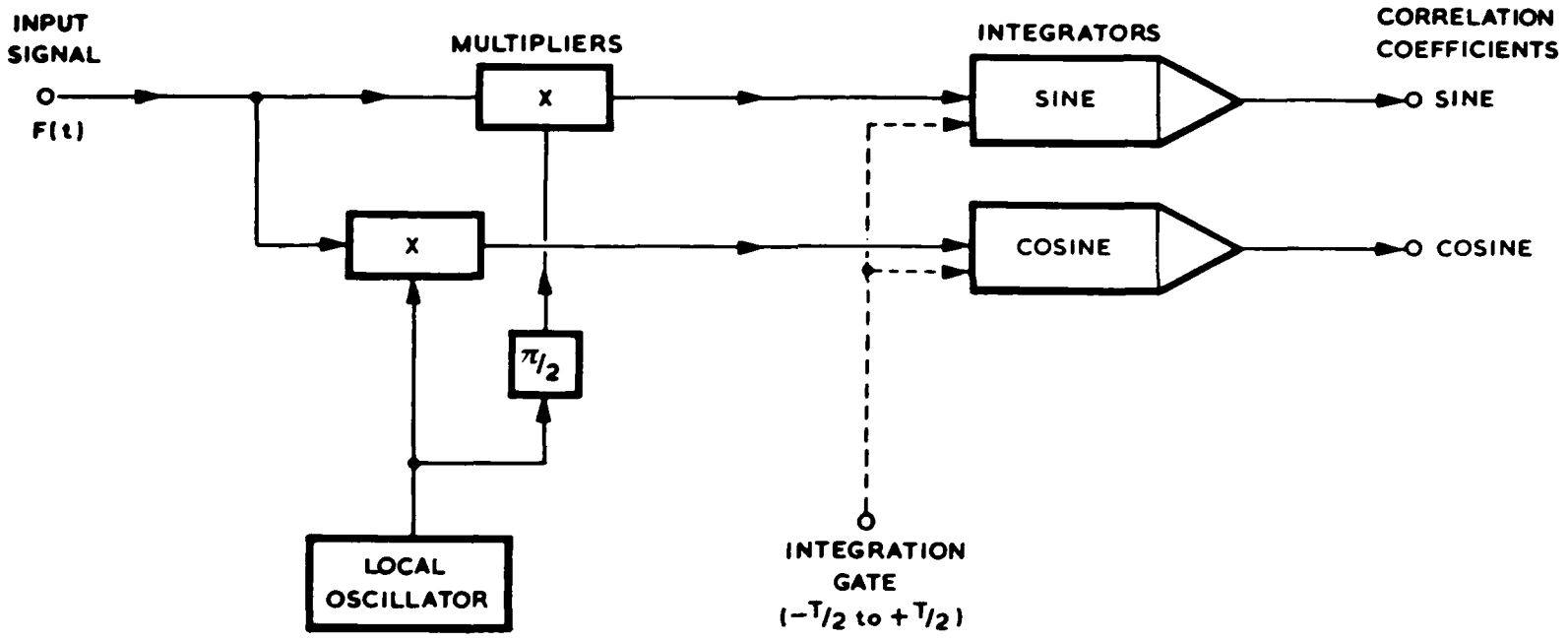

Fig 5.29 Single frequency analogue correlator

Fig 5.29

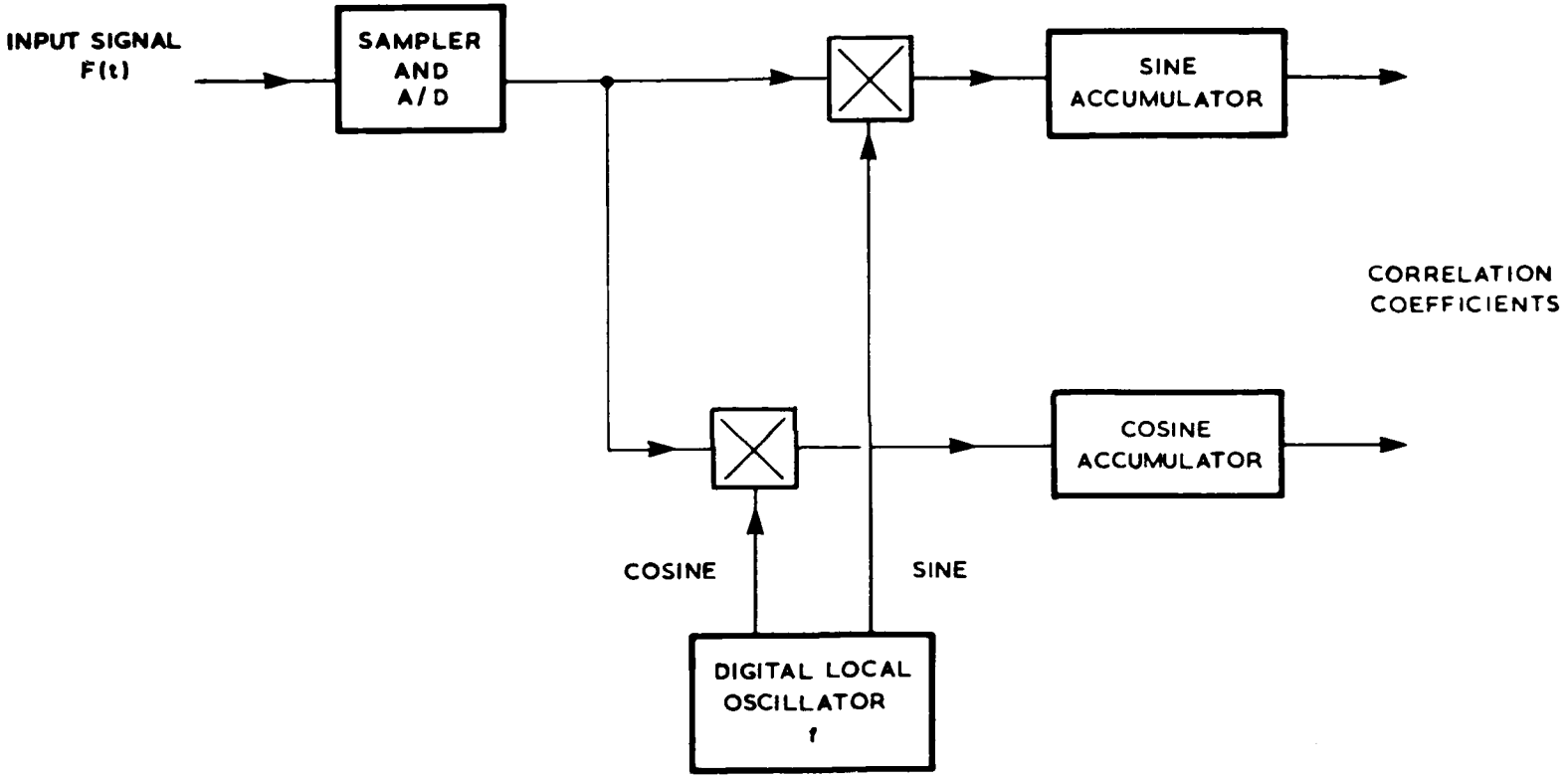

Fig 5.30 Digital frequency correlator

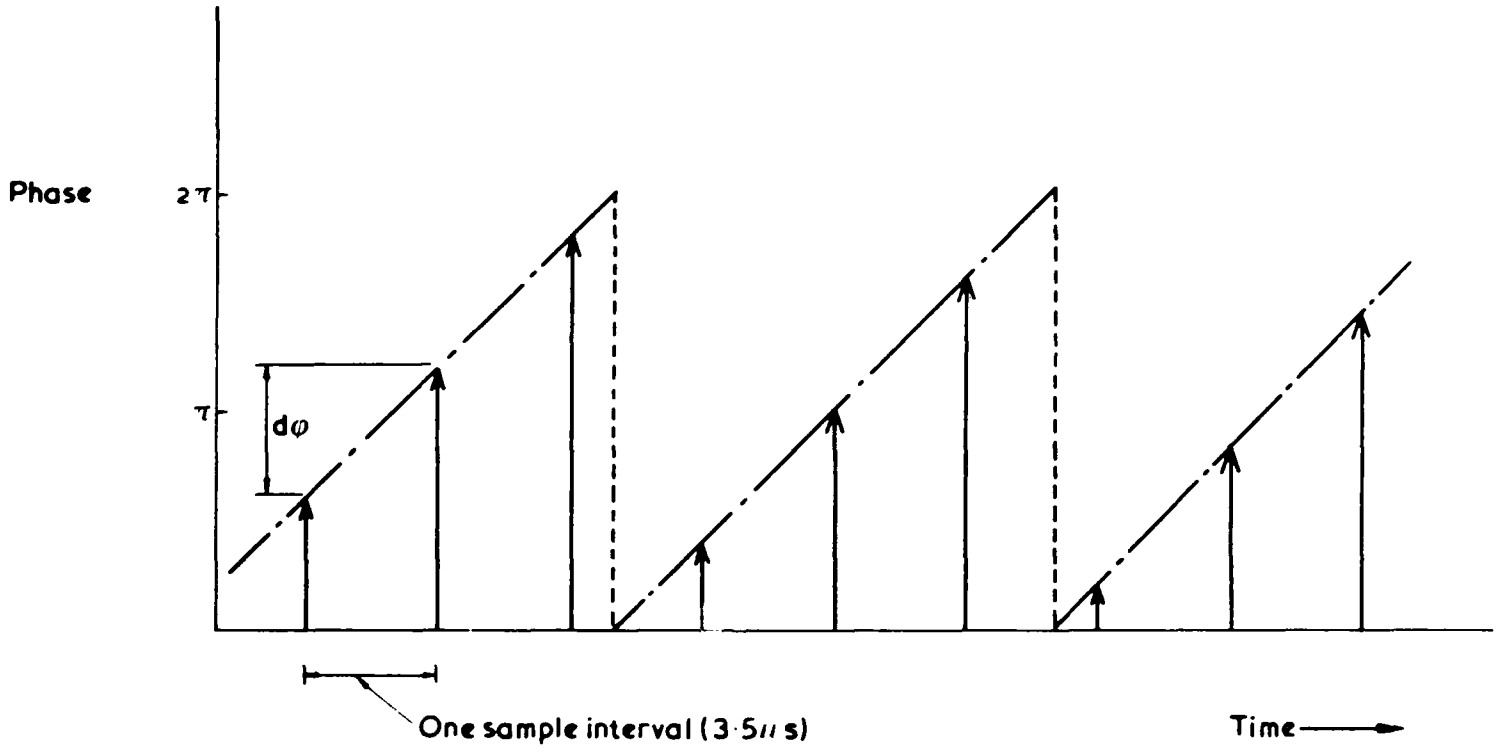

Fig 5.31 Digital frequency generation

Fig 5.31

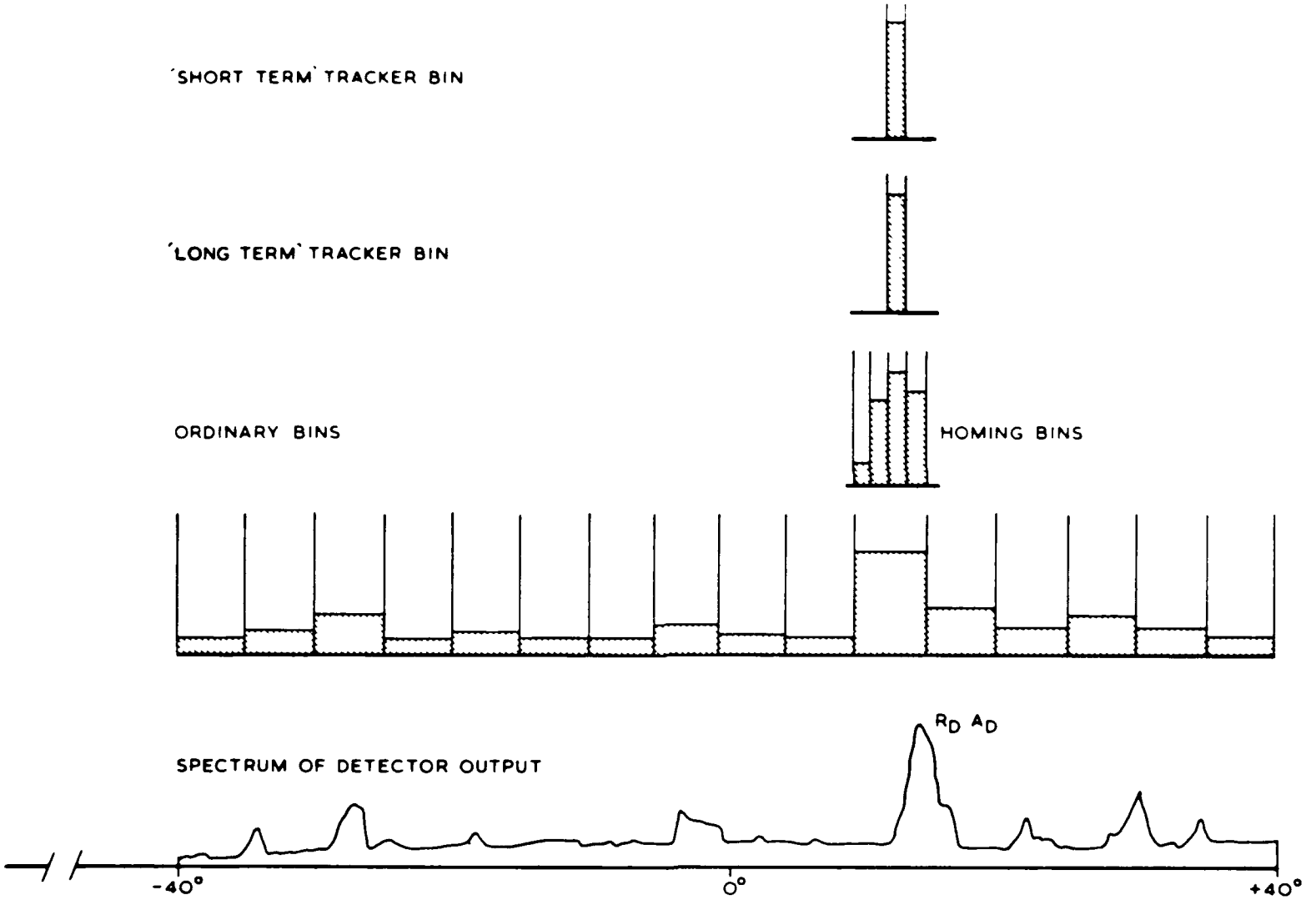

Fig 5.32 Correlator acquisition and validation process

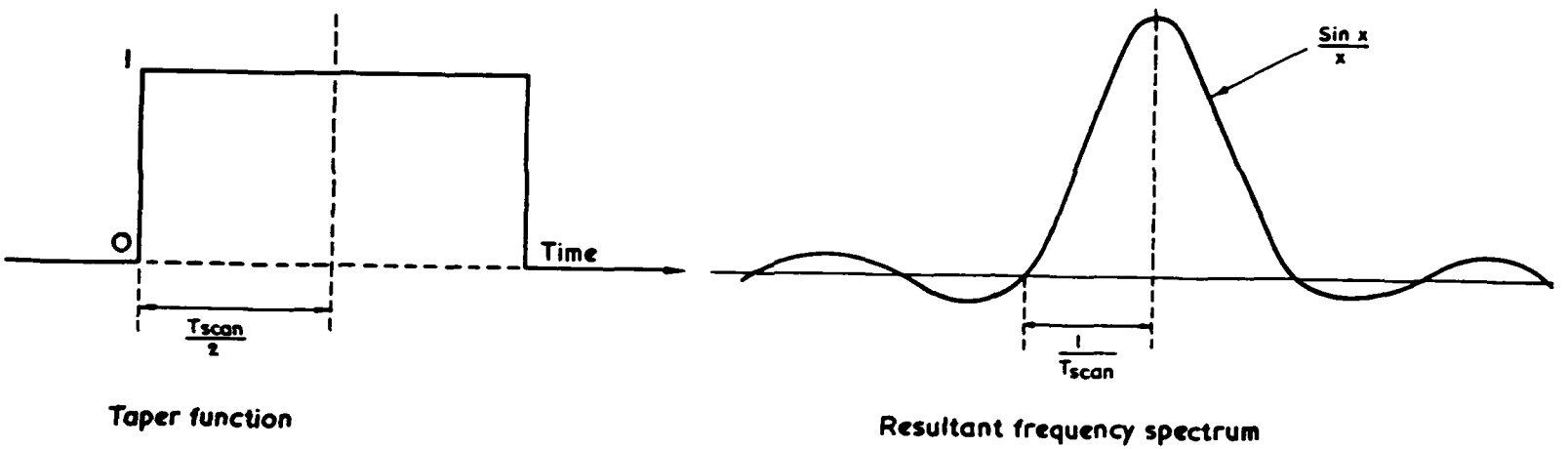

Fig 5.33 The frequency spectrum resulting from the use of a sum taper function

Fig 5.33

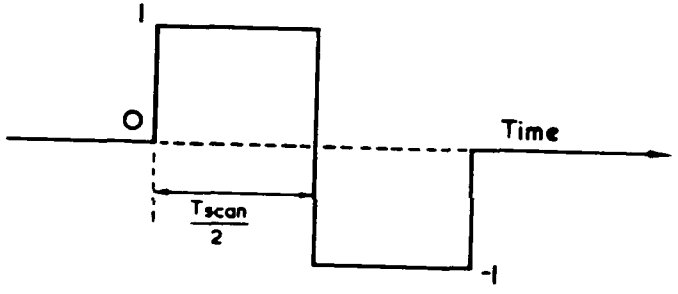

Taper function

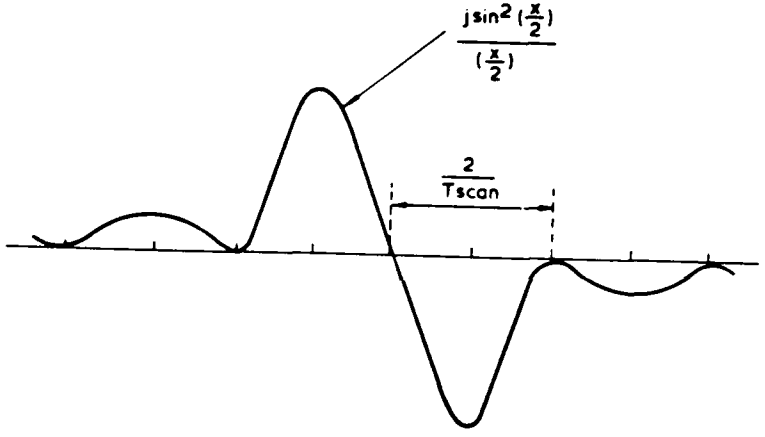

Resultant frequency spectrum

Fig 5.34 The frequency spectrum resulting from the use of a taper function difference

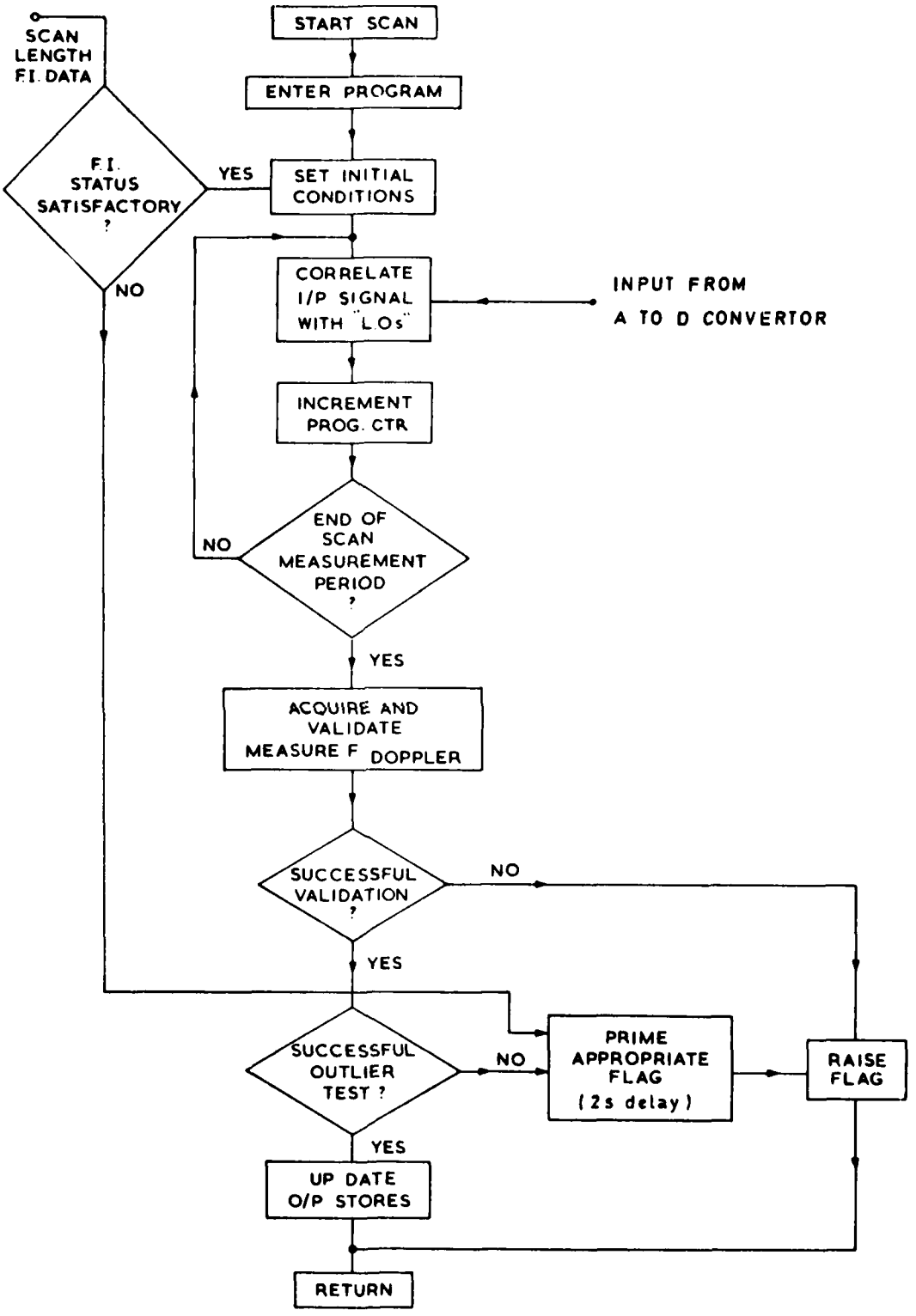

TR 79052

Fig 5.35 Simple correlation system flow diagram


DATE
FILME
7-8